

**MOVEMENT OF NEW NITROGEN THROUGH OCEANIC FOOD
WEBS: A STABLE ISOTOPE APPROACH**

A Dissertation
Presented to
The Academic Faculty

by

Jason Paul Landrum

In Partial Fulfillment
of the Requirements for the Degree
Doctor of Philosophy in the
School of Biology

Georgia Institute of Technology
May 2009

COPYRIGHT © JASON PAUL LANDRUM 2009

MOVEMENT OF NEW NITROGEN THROUGH OCEANIC FOOD WEBS: A STABLE ISOTOPE APPROACH

Approved by:

Dr. Joseph Montoya, Advisor
School of Biology
Georgia Institute of Technology

Dr. Mark Hay
School of Biology
Georgia Institute of Technology

Dr. Marc Weissburg
School of Biology
Georgia Institute of Technology

Dr. Emanuele DiLorenzo
School of Earth and Atmospheric Science
Georgia Institute of Technology

Dr. Ellery Ingall
School of Earth and Atmospheric Science
Georgia Institute of Technology

Date Approved: March 28, 2009

This body of work is dedicated to my family, and especially to my Mom and Dad. Thank you all for the constant love and support, and for helping me develop into the person that I have become.

ACKNOWLEDGEMENTS

Primarily, I wish to thank Joseph Montoya, who has supported me throughout this process, and has consistently guided me towards becoming a patient, thoughtful, and competent oceanographer. I would also like to thank Mark Hay, Marc Weissburg, Manu DiLorenzo, and Ellery Ingall for helpful comments during committee meetings and manuscript revisions. I would also like to thank Anya Waite and Peter Thompson for time spent at sea and valuable conversations about life and oceanography. Thanks should also go to John Collen, David Fields, David Garton, Zachary Hallinan, Carrie Holl, Robert Martinez, Jud Partin, and Brian Woodall for motivation and inspiration. I would like to thank Samantha Allen, Tiffany Andras, Wils Beadle, Ponch Davoodi, Carmen Carrion, Mary Crumley, Alex Engelmann, Kathy Ghanouni, Julia Grosse, Madison Hall, Rachel Horak, Mimi Murad, Viniya Patidar, Connie Rich, Camila Santiago, Rachel Sedlack, Chris Payne, Gauthami Penekalapati, and Beth van Gessel for help in and around the lab. Finally, thanks are due to all of the great friends I've made within and outside of Georgia Tech over the past several years.

TABLE OF CONTENTS

	Page
ACKNOWLEDGEMENTS	iv
LIST OF TABLES	ix
LIST OF FIGURES	xi
LIST OF SYMBOLS AND ABBREVIATIONS	xvii
SUMMARY	xx
<u>CHAPTER</u>	
1 INTRODUCTION	1
1.1 N and C linkages	1
1.2 The oceanic carbon cycle: Interacting pumps and long-term carbon storage	2
1.3 Supply-Side of the oceanic nitrogen cycle: N from above and below	5
1.4 New N in the North Atlantic	7
1.5 Patterns of diazotroph abundance and influence on N cycling	9
1.6 Input of diazotroph N to oceanic food webs: Leaky cells and hungry zooplankton?	13
1.7 Biological pump efficiency: POM export and remineralization	15
1.8 POM sources and fate in the ocean: What causes observed vertical flux profiles?	18
1.9 Stable nitrogen isotope tracers	19
1.9.1 In-situ tracers in the oceans	19
1.9.2 Compound specific isotopic analysis	28
1.10 Research objectives	31

1.10.1	Alteration of elemental and isotopic composition of OM: Microbial and metazoan processing	31
1.10.2	Basin-scale distribution of N isotopes	31
2	TEMPERATURE EFFECTS ON CHANGES IN C:N RATIO, $\delta^{15}\text{N}$, AND $\delta^{13}\text{C}$ OF DECOMPOSING ORGANIC MATTER	33
2.1	Introduction	33
2.2	Materials and Methods	35
2.3	Results	36
2.4	Discussion	41
2.4.1	Changes in elemental composition of OM	41
2.4.2	Changes in $\delta^{15}\text{N}$ of Organic Matter	43
2.4.3	Changes in $\delta^{13}\text{C}$ of Organic Matter	44
2.4.4	Ecological applications	49
2.4.4.1	Alteration of OM $\delta^{15}\text{N}$	49
2.4.4.2	Changes in $\delta^{13}\text{C}$ of OM	51
2.4.4.3	Conclusions	52
3	ORGANIC MATTER PROCESSING BY THE SHRIMP <i>PALAEMONETES</i> SP.: ISOTOPIC AND ELEMENTAL EFFECTS	53
3.1	Introduction	53
3.2	Materials and Methods	54
3.3	Results	56
3.4	Discussion	57
3.4.1	Ecological/Biogeochemical applications	63
4	BASIN-SCALE DISTRIBUTION OF STABLE NITROGEN ISOTOPES IN THE SUBTROPICAL NORTH ATLANTIC: MOVEMENT OF DIAZOTROPH NITROGEN INTO MESOZOOPLANKTON	65

4.1 Introduction	65
4.2 Materials and Methods	68
4.3 Results	71
4.3.1 SJ0005 Leg 1 – Stations 2-10	71
4.3.2 SJ0005 Leg 2 – Stations 10-17	73
4.3.3 SJ0005 Leg 3 – Stations 17-49	78
4.3.4 North-South comparisons between Leg 1 (Stns. 7, 9, 10) & Leg 3 (Stns. 20, 22, 24)	86
4.4 Discussion	88
4.4.1 Trends in $\delta^{15}\text{N}_{\text{SP}}$ and diazotroph N contribution	89
4.4.2 Trophic interactions: Utilization and movement of diazotroph N	90
4.4.3 Trends in $\delta^{15}\text{N}_{\text{ZP}}$ and diazotroph N contribution	92
4.4.4 Mechanisms contributing to new N: Lateral and vertical trends	97
4.4.5 N isotope mass balance in the subtropical North Atlantic	99
5 TOTAL AND DIAZOTROPH-DERIVED SUSPENDED PARTICLE CONCENTRATION AND MESOZOOPLANKTON BIOMASS IN THE SUBTROPICAL NORTH ATLANTIC OCEAN BASIN	105
5.1 Introduction	105
5.2 Materials and Methods	107
5.3 Results	110
5.3.1 SJ0005 Leg 1 – Stations 2-10	110
5.3.2 SJ0005 Leg 2 – Stations 10-17	110
5.3.3 SJ0005 Leg 3 – Stations 17-49	116
5.4 Discussion	122

5.4.1 PN distributions	122
5.4.2 N_{ZOO} biomass distributions	123
5.4.3 N_{ZOO} distributions among size fractions	127
5.4.4 N_{D} contribution to PN	129
5.4.5 N_{D} contribution to N_{ZOO}	132
5.5.5 Mesozooplankton migration	139
5.5.6 Spatial variation in N_{D} trophic transfer efficiency	140
5.5.7 Conclusions	145
6 CONCLUSIONS	147
6.1 General conclusions	147
6.2 Broader implications and future questions for N cycle studies	151
REFERENCES	161
VITA	194

LIST OF TABLES

Table 1.1: Isotopic enrichment factors for various biologically mediated reactions.	25
Table 2.1: Mean changes (± 1 S.D.) in $\delta^{15}\text{N}$, $\delta^{13}\text{C}$, N content, C content, and C:N ratio of shrimp tissue collected at each time point during the 25°C experiment.	38
Table 2.2: Mean changes (± 1 S.D.) in $\delta^{15}\text{N}$, $\delta^{13}\text{C}$, N content, C content, and C:N ratio of shrimp tissue collected at each time point during the 4°C experiment.	39
Table 2.3: ANCOVA results comparing N content (%), C Content (%), $\delta^{15}\text{N}$ (‰), $\delta^{13}\text{C}$ (‰) and $\Delta\text{C:N}$ values of decomposed shrimp tissue at both 4°C and 25°C. For the first four variables, temperature was used as the main effect, and $\Delta\text{C:N}$ was used as the covariate. In the last model ($\Delta\text{C:N}$), temperature was used as the main effect, and time (days) was used as the covariate.	40
Table 3.1: Mean (± 1 S.D.) $\delta^{15}\text{N}$, $\delta^{13}\text{C}$, Nitrogen (N) content, Carbon (C) content, and C:N ratios of flake food exposed to various environments. ‘Dry flake food’ represents flake food that has not been exposed to any experimental factor (negative control). ‘Feces’ represents the fecal material collected during each experiment and the ‘leftovers’ represent the remaining organic matter during those experiments. ‘ASW’ and ‘CASW soak’ values represent dry flake food soaked in incubation media.	58
Table 4.1: Mean reference $\delta^{15}\text{N}$ values (‰) for mesozooplankton collected in both the tropical Atlantic and tropical Pacific Oceans between 3°N and 3°S. Error is represented by ± 1 standard deviation.	72
Table 4.2: Least squares means of $\delta^{15}\text{N}$ (‰) (± 1 S.E.) of mesozooplankton size fractions collected along Leg 3 of cruise track SJ0005, a zonal transect spanning the subtropical North Atlantic Ocean at 32°N.	83
Table 4.3: Least squares means of $\delta^{15}\text{N}$ (‰) of mesozooplankton size fractions collected during the daytime (0600-1800) or nighttime (1800-0600) along Leg 3 of cruise track SJ0005, a zonal transect spanning the subtropical North Atlantic Ocean at 32°N.	84

Table 4.4: Mean $\delta^{15}\text{N}$ (‰) of mesozooplankton collected along two zonal transects that overlap with longitude, but differ in latitude (27°N versus 32°N). Northern stations represent stations where zooplankton were collected at 32°N and southern stations at 27°N. Error is represented by ± 1 standard error. $\Delta\delta^{15}\text{N}$ are differences in mean values for $\delta^{15}\text{N}_{\text{ZP}}$ between North and South stations.	87
Table 5.1: Mean (± 1 SD) integrated areal mesozooplankton biomass within each depth range collected along Leg 2 of cruise track SJ0005, a SE to NW transect in the western subtropical North Atlantic Ocean.	113
Table 5.2: Mean (± 1 SD) integrated areal mesozooplankton biomass of different size fractions collected along Leg 2 of cruise track SJ0005, a SE to NW transect in the western subtropical North Atlantic Ocean.	114
Table 5.3: Mean (± 1 SD) integrated areal mesozooplankton biomass within each depth range collected along Leg 3 of cruise track SJ0005, a zonal transect spanning the subtropical North Atlantic Ocean at 32°N.	120
Table 5.4: Mean (± 1 SD) integrated areal mesozooplankton biomass of different size fractions collected along Leg 3 of cruise track SJ0005, a zonal transect spanning the subtropical North Atlantic Ocean at 32°N.	121

LIST OF FIGURES

	Page
Figure 1.1: Schematic representing a simplified version of the biological pump.	4
Figure 1.2: Color contour plot showing global distribution of N* plotted along the 300m isobath. Figure was prepared using Ocean Data View (Schlitzer 2008).	10
Figure 1.3: Global oceanic sediment trap POC flux with depth (Lutz et al., 2002). Data used in this graph originates from Suess (1980), Martin et al. (1987) and Lutz et al. (2002). Reprinted with permission from American Geophysical Union, from: Lutz M., R. Dunbar, and K. Caldeira (2002), Regional variability in the vertical flux of particulate organic carbon in the ocean interior, <i>Global Biogeochem. Cycles</i> , 16 (3), 1037, doi:10.1029/2000GB001383.	17
Figure 1.4: $\delta^{15}\text{N}$ and $\delta^{13}\text{C}$ (‰) of food sources in a salt marsh food web off the eastern coast of the United States. From Peterson et al. (1986). Reprinted with permission from AAAS.	22
Figure 1.5: Nitrogen oxidation states present in the world's ocean and the biological processes that drive their distributions. Adapted from (Montoya 2008).	24
Figure 1.6: Schematic of the distributions of nitrogen isotopes in particles and mesozooplankton in a typical oceanic food web under strong diazotrophy in the mixed layer. Notice the community-level shift towards lower $\delta^{15}\text{N}$ values than if deep NO_3^- were the dominant N source supporting these communities. Adapted from (Montoya et al. 2002).	27
Figure 1.7: Mean $\delta^{15}\text{N}$ (± 1 S.D.) of both suspended and sinking particles collected from filtered water samples and sediment traps, respectively, at the OFP site off of Bermuda. Reprinted with permission from Macmillan Publishers Ltd: <i>Nature</i> , (Altabet et al. 1991).	29

Figure 2.1: Time course of $\Delta\text{C:N}$, ΔC Content and ΔN of shrimp tissue exposed to microbial decomposition at 4°C and 25°C. $\Delta\text{C:N}$ represents the differences in compositional values for paired shrimp halves ($\Delta\text{C:N} = \text{C:N}_{\text{Decomposed}} - \text{C:N}_{\text{Control}}$) at each removal date. The same calculation was made for N and C content. At least three shrimp halves were collected on each collection time point. Conditioned artificial seawater (CASW) was used as the incubation medium and was collected from aquaria housing live shrimp (*Palaemonetes* sp.). Total incubation time for the 4°C and 25°C assay was 97 days and 34 days, respectively. 42

Figure 2.2: Time course of $\delta^{15}\text{N}$ and $\delta^{13}\text{C}$ of shrimp tissue exposed to microbial decomposition at 4°C and 25°C. $\Delta\delta^{15}\text{N}$ represents the differences in compositional values for paired shrimp halves ($\Delta\delta^{15}\text{N} = \delta^{15}\text{N}_{\text{Decomposed}} - \delta^{15}\text{N}_{\text{Control}}$) at each removal date. The same calculation was made for $\delta^{13}\text{C}$. At least three shrimp halves were collected on each collection time point. Conditioned artificial seawater (CASW) was used as the incubation medium and was collected from aquaria housing live shrimp (*Palaemonetes* sp.). Total incubation time for the 4°C and 25°C assay was 97 days and 34 days, respectively. 45

Figure 2.3: Time course of $\delta^{15}\text{N}$ and $\delta^{13}\text{C}$ of shrimp tissue exposed to microbial decomposition at 4°C and 25°C. $\Delta\delta^{15}\text{N}$ represents the differences in compositional values for paired shrimp halves ($\Delta\delta^{15}\text{N} = \delta^{15}\text{N}_{\text{Decomposed}} - \delta^{15}\text{N}_{\text{Control}}$) at each removal date. The same calculation was made for $\delta^{13}\text{C}$. At least three shrimp halves were collected on each collection time point. Conditioned artificial seawater (CASW) was used as the incubation medium and was collected from aquaria housing live shrimp (*Palaemonetes* sp.). Total incubation time for the 4°C and 25°C assay was 97 days and 34 days, respectively. 46

Figure 2.4: Differences in $\delta^{15}\text{N}$ and $\delta^{13}\text{C}$ between paired shrimp halves ($\Delta\delta^{15}\text{N} = \delta^{15}\text{N}_{\text{Decomposed}} - \delta^{15}\text{N}_{\text{Control}}$) with increasing C:N ratio. C:N ratios of shrimp tissue provide a proxy for the microbial processing of the shrimp tissue, where higher C:N ratios signify more exposure to microbial decomposition. Conditioned artificial seawater (CASW) was used as the incubation medium and was collected from aquaria housing live shrimp (*Palaemonetes* sp.). Total incubation time for the 4°C and 25°C assay was 97 days and 34 days, respectively. 47

Figure 3.1: Mean N and C content (wt-%) of dry flake food, flake food remaining after experiments (leftovers), shrimp fecal pellets (feces), as well as flake food soaked in either ASW or CASW. Mean treatment values represented by different letters are significantly different ($p < 0.01$). Upper letters represent N content comparisons, while lower letters represent C content comparisons. Error bars are set at ± 1 S.D. 59

- Figure 3.2: Mean $\delta^{15}\text{N}$ and $\delta^{13}\text{C}$ (‰) of dry flake food, flake food remaining after experiments (leftovers), shrimp fecal pellets (feces), as well as flake food soaked in either ASW or CASW. Mean treatment values represented by different letters are significantly different ($p < 0.01$). Upper letters represent $\delta^{15}\text{N}$ comparisons, while lower letters represent $\delta^{13}\text{C}$ comparisons. Error bars are set at ± 1 S.D. 60
- Figure 4.1: Chart of cruise track SJ0005 comprised of three Legs: Leg 1 travels from Ft. Pierce, FL eastward towards the center of the North Atlantic gyre, Leg 2 turns northwest towards the Eastern coast of the US, and Leg 3 turns eastward at $\sim 32^\circ\text{N}$ and traverses the basin, terminating eventually in the Canary Islands. Solid circles represent stations where a MOCNESS was deployed and open diamonds represent stations where meter nets were deployed to collect mesozooplankton. 69
- Figure 4.2: Color contour plots showing A) in-situ temperature ($^\circ\text{C}$) and σ_T , and B) Nitrate (μM) and fluorometric measurements taken along Leg 2 of cruise track SJ0005, a SE to NW transect in the western subtropical North Atlantic Ocean. Figure was prepared using Ocean Data View (Schlitzer 2008). 74
- Figure 4.3: Color contour plots showing $\delta^{15}\text{N}$ (‰) and the corresponding diazotroph N contribution to suspended particles collected along Leg 2 of cruise track SJ0005, a SE to NW transect in the western subtropical North Atlantic Ocean. In the top figure, feature A and B are labeled as described in the text. Figure was prepared using Ocean Data View (Schlitzer 2008). 75
- Figure 4.4: Color contour plots showing $\delta^{15}\text{N}$ (‰) and diazotroph N contribution (%) to mesozooplankton communities along Leg 2 of cruise track SJ0005, a SE to NW transect in the western subtropical North Atlantic Ocean. Figure was prepared using Ocean Data View (Schlitzer 2008). 76
- Figure 4.5: Weighted mean $\delta^{15}\text{N}$ (‰) of both suspended particles and mesozooplankton within the upper 500m of the water column along Leg 2 of cruise track SJ0005, a SE to NW transect in the western subtropical North Atlantic Ocean. 77
- Figure 4.6: Color contour plot showing hydrographic data of the water column along Leg 3 of cruise track SJ0005, a zonal transect spanning the subtropical North Atlantic Ocean at 32°N . Panel A shows seawater in-situ temperature ($^\circ\text{C}$) and σ_T in the upper 500m, while Panel B shows both nitrate concentrations (μM) and fluorometric measurements observed along the same transect, but only within the upper 250m. Figure was prepared using Ocean Data View (Schlitzer 2008). 79

- Figure 4.7: Color contour plots showing $\delta^{15}\text{N}$ (‰) and diazotroph N contribution (%) to mesozooplankton communities along Leg 3 of cruise track SJ0005, a zonal transect spanning the subtropical North Atlantic Ocean at 32°N. In the top figure, feature C and D are labeled as described in the text. Figure was prepared using Ocean Data View (Schlitzer 2008). 80
- Figure 4.8: Color contour plots showing $\delta^{15}\text{N}$ (‰) and diazotroph N contribution (%) to mesozooplankton communities along Leg 3 of cruise track SJ0005, a zonal transect spanning the subtropical North Atlantic Ocean at 32°N. Figure was prepared using Ocean Data View (Schlitzer 2008). 82
- Figure 4.9: Weighted mean $\delta^{15}\text{N}$ (‰) of both suspended particles and mesozooplankton within the upper 500m of the water column along Leg 3 of cruise track SJ0005, a zonal transect spanning the subtropical North Atlantic Ocean at 32°N. 85
- Figure 4.10: Mean $\delta^{15}\text{N}$ (‰) of mesozooplankton collected at different depths during daytime and nighttime tows along Leg 3 of cruise track SJ0005, a zonal transect spanning the subtropical North Atlantic Ocean at 32°N. Mesozooplankton were collected at 100m intervals, and the circles are plotted in the middle of these intervals. The circles are also offset along the y-axis to show error bars (± 1 S.D.). 96
- Figure 5.1: Chart of cruise track SJ0005 comprised of three Legs: Leg 1 travels from Ft. Pierce, FL eastward towards the center of the North Atlantic gyre, Leg 2 turns northwest towards the eastern coast of the US, and Leg 3 turns westward at ~32°N and traverses the basin, terminating eventually in the Canary Islands. Solid circles represent stations where a MOCNESS was deployed and open diamonds represent stations where meter nets were deployed to collect mesozooplankton. The gray box represents the surface area used to determine total and diazotroph N biomass for this section of the subtropical North Atlantic. 108
- Figure 5.2: Color contour plot showing PN concentrations ($\mu\text{M N}$) of suspended particles collected in the upper 250m of the water column along Leg 2 of cruise track SJ0005, a SE to NW transect in the western subtropical North Atlantic Ocean. Figure was prepared using Ocean Data View (Schlitzer 2008). 111
- Figure 5.3: Color contour plot showing mesozooplankton N biomass (mg N m^{-3}) (left) and diazotroph N contribution (right) for different size fractions collected in the upper 500m of the water column along Leg 2 of cruise track SJ0005, a SE to NW transect in the western subtropical North Atlantic Ocean. Figure was prepared using Ocean Data View (Schlitzer 2008). 112

Figure 5.4: Color contour plots showing PN concentration ($\mu\text{M N}$) of suspended particles collected in the upper 250m of the water column along Leg 3 of cruise track SJ0005, a zonal transect spanning the subtropical North Atlantic Ocean at 32°N . Figure was prepared using Ocean Data View (Schlitzer 2008).	117
Figure 5.5: Color contour plots showing mesozooplankton N biomass (mg N m^{-3}) (left) and diazotroph N contribution (right) for different size fractions collected in the upper 500m of the water column Leg 3 of cruise track SJ0005, a zonal transect spanning the subtropical North Atlantic Ocean at 32°N . Figure was prepared using Ocean Data View (Schlitzer 2008).	119
Figure 5.6: Total mesozooplankton N biomass (mg N m^{-2}) (all size fractions) collected in the upper 200m and from 200-500m in the water column along Leg 2 of cruise track SJ0005, a SE to NW transect in the western subtropical North Atlantic Ocean.	125
Figure 5.7: Total mesozooplankton N biomass (mg N m^{-2}) (all size fractions) collected in the upper 200m and from 200-500m in the water column along Leg 3 of cruise track SJ0005, a zonal transect spanning the subtropical North Atlantic Ocean at 32°N .	126
Figure 5.8: Total diazotroph N biomass (mg N m^{-2}) of mesozooplankton (all size fractions) collected in the upper 200m and from 200-500m in the water column along Leg 2 of cruise track SJ0005, a SE to NW transect in the western subtropical North Atlantic Ocean.	134
Figure 5.9: Total diazotroph N biomass (mg N m^{-2}) of mesozooplankton of different size fractions in the upper 500m of the water column along Leg 2 of cruise track SJ0005, a SE to NW transect in the western subtropical North Atlantic Ocean.	135
Figure 5.10: Total diazotroph N biomass (mg N m^{-2}) contributed to mesozooplankton (all size fractions) collected in the upper 200m and from 200-500m in the water column along Leg 3 of cruise track SJ0005, a zonal transect spanning the subtropical North Atlantic Ocean at 32°N .	137
Figure 5.11: Total diazotroph N biomass (mg N m^{-2}) contributed to mesozooplankton of different size fractions in the upper 500m of the water column along Leg 3 of cruise track SJ0005, a zonal transect spanning the subtropical North Atlantic Ocean at 32°N .	138

Figure 5.12: Schematic representation of upper ocean trophic scheme of total N of suspended particles and mesozooplankton. Values in each box are represented by the mean (± 1 SD) depth-integrated N biomass for both suspended particles (upper 200m) and mesozooplankton (upper 500m) along Leg 3 of cruise track SJ0005, a zonal transect spanning the subtropical North Atlantic Ocean at 32°N. TTE represents trophic transfer efficiency of N between particles and mesozooplankton. 142

Figure 5.13: Schematic representation of upper ocean trophic scheme of diazotroph N of suspended particles and mesozooplankton. Values in each box are represented by the mean (± 1 SD) depth-integrated diazotroph N biomass for both suspended particles (upper 200m) and mesozooplankton (upper 500m) along Leg 3 of cruise track SJ0005, a zonal transect spanning the subtropical North Atlantic Ocean at 32°N. TTE represents trophic transfer efficiency of N between particles and mesozooplankton. 143

LIST OF SYMBOLS AND ABBREVIATIONS

AMT	Atlantic Meridional Transect
ANCOVA	Analysis of covariance
ANOVA	Analysis of variance
BATS	Bermuda Atlantic Time-series
C	Carbon
°C	Degrees Celsius
CF-IRMS	Continuous flow isotope ratio mass spectrometry
CO ₂	Carbon dioxide
C _T	Total inorganic carbon
CTD	Conductivity temperature depth
DIN	Dissolved inorganic nitrogen
DOM	Dissolved organic matter
DVM	Diel vertical migration
ESTOC	European Station for Time-Series in the Ocean, Canary Islands
Fe	Iron
GF/F	Glass-fiber filter/type F (nominal pore size 0.7 µm)
Gg	Gigagrams (10 ⁹ grams)
Gt	Gigatonnes (10 ¹⁵ grams)
HOT	Hawaii Ocean Time-series
KNO ₃	Potassium nitrate
MOCNESS	Multiple Opening/Closing Net Environmental Sampling System
m	meter

mg	milligrams
mm	millimeters
mmol	millimoles
μM	Micromolar (micromoles L^{-1})
μm	Micrometers
N	Nitrogen
N_2	Dinitrogen
N_D	Diazotroph nitrogen
NO_3^-	Nitrate
NCP	Net community production
NH_4Cl	Ammonium chloride
NPP	Net primary production
NW	Northwest
N_{ZOO}	Mesozooplankton nitrogen
OM	Organic matter
P	Phosphorus
PIC	Particulate inorganic carbon
PN	Particulate nitrogen
PO_4^{3-}	Phosphate
POC	Particulate organic carbon
POM	Particulate organic matter
PON	Particulate organic nitrogen
R/V	Research vessel
σ_T	Density at in-situ temperature and 1 atmosphere
$\pm 1 \text{ SD}$	± 1 Standard deviation

± 1 SE	± 1 Standard error
SE	Southeast
STNA	Subtropical North Atlantic
Tg	Teragrams (10^{12} grams)
TTE	Trophic transfer efficiency
TTE _D	Diazotroph trophic transfer efficiency
yr	Years

SUMMARY

Nitrogen (N) generally limits primary production across large areas of the world's oceans. Allochthonous inputs of N (i.e., “new” N) via N₂-fixing organisms (diazotrophs) are crucial for sustaining primary production and are often associated with net export of organic matter (OM) from surface waters. Diazotroph N (N_D) contribution plays an integral role in supporting oceanic food webs and regulating the flux of OM into and through the oceans (e.g., the biological pump). Stable isotope techniques were used to trace the input and movement of new N through oceanic food webs. Laboratory experiments were performed to determine elemental and isotopic shifts of OM exposed to microbial and metazoan processing. $\delta^{15}\text{N}$ of OM was typically higher when exposed to microbial communities, with no difference in $\delta^{15}\text{N}$ of OM between experiments incubated at different temperatures (4°C and 25°C). In separate experiments, shrimp digestion did not alter the $\delta^{15}\text{N}$ of OM through digestion, but the $\delta^{15}\text{N}$ of macerated OM was enriched in ^{15}N . Both of these experiments provide insight into the mechanisms driving variations in the $\delta^{15}\text{N}$ of OM in the world's oceans. To assess the role of diazotrophs in oceanic food webs, we used the distribution of $\delta^{15}\text{N}$ to quantify the relative N_D contribution to suspended particle N (PN) and mesozooplankton N biomass (N_{ZOOP}) in the subtropical North Atlantic (STNA). Qualitatively, N_D contribution was often high for both PN and N_{ZOOP}, with the highest contributions occurring in the mixed layer. Our results also indicate higher N_D contribution to both PN and N_{ZOOP} in the western portion of the basin than in the east. N_D contribution to larger mesozooplankton at depth further suggests that migrating mesozooplankton transport N_D out of the mixed layer. Quantitatively, N_D trophic transfer efficiency was lower than bulk N trophic transfer efficiency, suggesting low assimilation of N_D by mesozooplankton. Overall, we estimated a N_D pool turnover time on the order of weeks for our region of study. These findings demonstrate that N_D is laterally and vertically variable in the STNA, and that the

N_D pool is sensitive to perturbations on short timescales. We discuss the global implications of our findings and their implications for the N cycle and elemental fluxes through oligotrophic oceans.

CHAPTER 1

INTRODUCTION

1.1 N and C cycle linkages

Photosynthetically-fixed organic matter (OM) provides a source of energy and nutrients for oceanic food webs, and also represents a pathway for CO₂ removal from the atmosphere (e.g., biological pump) over long timescales (100's to 100,000's of years) (Falkowski et al. 2000). Autotrophic C-fixation and growth is often limited by the availability of other essential nutrients (e.g., N, P, Si). Thus, nutrient availability generally sets an upper limit for total community production and the availability of resources for heterotrophs occupying higher trophic levels. N availability limits primary production over large areas of the world's oceans, especially in oligotrophic subtropical/tropical gyres (Falkowski et al. 1998, Zehr & Ward 2002, Davey et al. 2008). Despite nutrient limitation and low production rates, these systems make a major contribution to global OM production and export (Michaels et al. 1996, Emerson et al. 1997, Emerson et al. 2008). An external supply of N (e.g., biological N₂-fixation) is required to balance N export processes (e.g., sinking organic matter) and sustain oceanic food webs in these N-limited ecosystems (Dugdale & Goering 1967, Eppley & Peterson 1979). Thus, external N inputs to N-depleted areas directly influence food web processes, which, in turn, influence C movement into and through the world's oceans.

N₂-fixing organisms (diazotrophs) provide a source of N for oceanic food webs, but the extent of their contribution to higher trophic levels in the oceanic food web remains largely unknown (LaRoche & Breitbarth 2005, Mulholland 2007). Identifying the relative contribution of N sources supporting biological communities is an important first step in elucidating both food web structure and function in N-depleted ecosystems. Food web processes also play a central role in the vertical flux of OM in marine systems

(e.g., mesozooplankton fecal pellet egestion) (Morales 1999, Frangoulis et al. 2005), and may play a larger role in transporting diazotroph C and N out of the mixed layer. Thus, quantifying diazotroph N incorporation into, and movement through various organic pools (e.g., particles and mesozooplankton) provides insight into the role diazotrophs play in influencing the ocean's productivity and its capacity to remove CO₂ from the atmosphere (Michaels et al. 1996, Raven & Falkowski 1999, Capone 2001, Karl et al. 2002, Lipschultz et al. 2002).

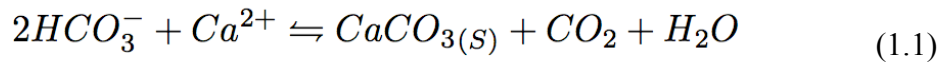
1.2 The oceanic carbon cycle: Interacting pumps and long-term carbon storage

The oceanic carbon cycle is a dynamic system where physical, chemical and biological processes play a critical role in the movement and redistribution of carbon throughout the oceans (Honjo 1996, Battle et al. 2000, Falkowski et al. 2000). Recently, much attention has been paid to the global carbon cycle because of the widely accepted correlation between atmospheric CO₂ concentrations and global temperature (Battle et al. 2000, Falkowski et al. 2000). The ocean represents one of the largest carbon reservoir on earth, containing roughly 38,000 GtC (IPCC 2001, 2007). Atmospheric CO₂ initially dissolves into the ocean and hydrates to form the diprotic acid, carbonic acid (H₂CO₃). H₂CO₃ is then dissociated into bicarbonate (HCO₃⁻) and carbonate ions (CO₃²⁻) as a function of pH. Both the high solubility of CO₂ and the aforementioned dissociation of ions allow the ocean to hold almost 50 times more carbon than what is found in the atmosphere (Figure 1.1). The movement of CO₂ in and out of the oceans depends on the interactions between the solubility, carbonate and biological pumps. The latter two processes play a more substantial role in long-term (i.e., hundreds of thousands of years) carbon sequestration relative to the solubility pump (i.e., ~1500 years) since they ultimately inject atmospheric C into permanent storage (i.e., the rock cycle) via delivery of particulate inorganic carbon (PIC) and particulate organic carbon (POC) into deep-sea sediments. This distinction has stimulated interest in understanding the functioning and

efficiency of the biological and alkalinity pumps in sequestering anthropogenic atmospheric CO₂ (Sabine et al. 2004, Peng 2005).

The biological pump is the movement of biologically produced particulate organic matter (POM) out of the surface oceans and into the deep-sea (Figure 1.1). Specifically, autotrophic phytoplankton and bacteria fix dissolved inorganic carbon (CO₂) into organic matter, which then sinks out of the euphotic zone and into deeper waters, post-mortem. Sinking POM is exposed to heterotrophic organisms while in transit, and only ~0.6% of OM fixed at the surface actually settles to the sea floor. Despite its small magnitude, the export of POM into the interior of the ocean via the biological pump represents a major sink for carbon over long timescales, and is one of the only biologically-driven mechanisms for long-term carbon burial in the sea.

The carbonate pump can also provide a long-term sink for biologically produced inorganic carbon (e.g., CaCO₃), but typically opposes the biological pump in regulating the net movement of CO₂ into and out of the ocean. While the biological pump depletes surface waters of dissolved CO₂, the carbonate pump increases oceanic *p*CO₂ due to the overall release of CO₂ during calcification by certain phytoplankters (e.g., coccolithophorids) and zooplankton (e.g., pteropods), which removes alkalinity from solution:



The efficiency of the biological pump relative to the carbonate pump is reflected in the rain ratio, which is the POM:PIC ratio of sinking particles out of the euphotic zone and into the deep sea (Sarmiento et al. 2002). Despite the usefulness of this ratio in determining net movement of CO₂ into and out of the oceans, it has been difficult to estimate an appropriate global ‘rain ratio’ through both observation-based estimates due to insufficient information concerning the processes influencing respiration of POM in the deep ocean (Honjo 1996, Fujii et al. 2005).

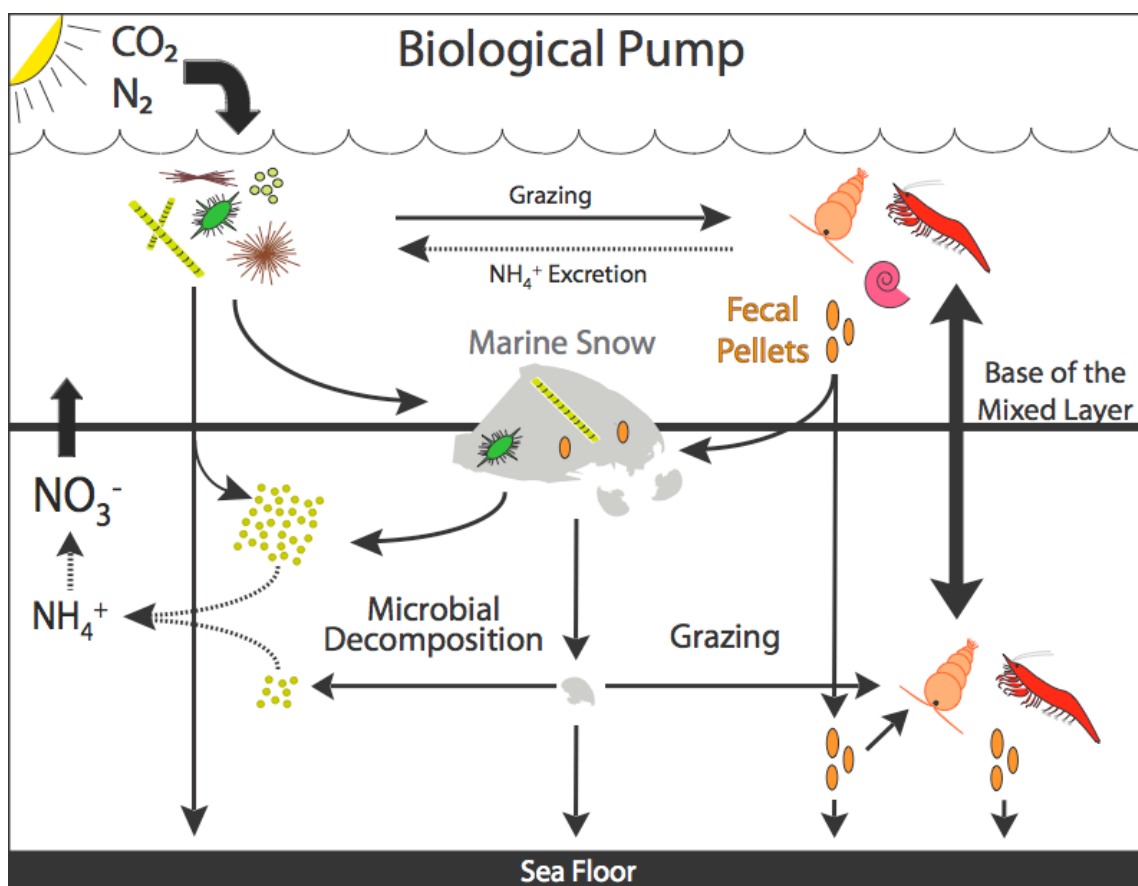


Figure 1.1 Schematic representing a simplified version of the biological pump.

The biological pump is affected by the rate of carbon fixation in surface waters, the amount of surface production exiting the euphotic zone, and the remineralization and/or transformation of POM both throughout the water column and in deep-sea sediments. Global oceanic carbon fixation rates have been estimated to be $\sim 380 \text{ mg-C m}^{-2} \text{ day}^{-1}$, or $\sim 45\text{-}50 \text{ Gt-C per year}$ (Longhurst et al. 1995, Honda 2003, Carr et al. 2006), and are generally limited by the availability of light and nutrients within the euphotic zone. Seasonal changes in insolation have a strong effect on the depth of light penetration within the water column, though biological factors also affect light penetration (e.g., particle absorption and or scattering) and availability. Nutrient distributions within the euphotic zone are often much more spatially and temporally variable, and are influenced by physical, chemical and biological processes.

Areas where canonically limiting nutrients (NO_3^- , PO_4^{3-}) are plentiful often support the greatest C production per unit area (e.g., upwelling zones), though micronutrients (e.g., iron) can sometimes limit primary production in such areas (e.g., high nutrient, low chlorophyll zones). Conversely, the euphotic zone is consistently oligotrophic (i.e., low nutrient) within oceanic gyres, and generally exhibits low areal production rates due to limiting nutrients for phytoplankton growth (Louanchi & Najjar 2000). Although areal production rates are often low in oligotrophic areas, these zones are especially important in global C production because of their large surface area ($>70\%$ of global oceanic surface area) (Poulton et al. 2006). Ultimately, to estimate the ocean's capacity to fix C, it is crucial to estimate the relative magnitudes of mechanisms that introduce nutrients (generally N) that limit production into the euphotic zone of oceanic gyres (Falkowski et al. 1998, Falkowski et al. 2000, Houghton 2007).

1.3 Supply-Side of the oceanic nitrogen cycle: N from above and below

Nitrogen (N) availability limits primary production over vast areas of the world's oceans, especially in the oligotrophic subtropical/tropical areas (Ryther & Dunstan 1971,

Graziano et al. 1996, Moore et al. 2008). Geographically, oligotrophic oceanic gyres represent over 70% of the ocean's surface area, and despite low production rates per unit area, contribute significantly to global oceanic primary production. Deep wintertime mixing occurs in these zones, driving the mixed layer to ~400m, and minimizing surface production. As Spring approaches, greater insolation input, lower wind speeds (shallow mixed layer depth), and abundant surface nutrients typically produce a bloom of phytoplankton within the euphotic zone. The mixed layer is thermally stratified through the summer months, where export of biologically produced OM out of the euphotic zone leads to strong nutrient depletion in the euphotic zone. Regenerated N, or inorganic N that has been recycled through various biological pools in the upper ocean (e.g., NH_4^+ released through decomposition of OM), can support primary production, but new N inputs are required to sustain primary production due to N losses from surface waters (i.e., sinking particles) (Dugdale & Goering 1967, Dugdale 1986). New N is defined as any allochthonous input of N to the mixed layer, and typically originates from three main sources: deep nitrate (NO_3^-), wet and dry surface deposition, and biological N_2 -fixation. Rivers also represent a major source of N (and P) to oceans, but may only impact coastal zones over biological timescales.

Ratios of NO_3^- uptake to total N ($\text{NO}_3^- + \text{NH}_4^+$) produce the “f-ratio” which has been used to estimate the relative proportion of new production within the euphotic zone. Since the upper oceans are assumed to be at steady state on a timescale of years, the input of new N is linked to export of N from the upper ocean (Eppley & Peterson 1979). Although the f-ratio has been shown to be a convenient way to measure new production, other biological processes may confound accurate f-ratio measurements (e.g., euphotic zone nitrification). Nitrification has received attention as a potential source of recycled N (Yool et al. 2007) within the euphotic zone that may produce overestimates of new production based on NO_3^- and NH_4^+ uptake ratios (i.e., f-ratio). However, it is still unclear how extensive nitrification is within the euphotic zone, globally, and if it is a

considerable source of NO_3^- to surface waters, given its light sensitivity. Thus, nitrification is generally thought only to be an important component of deep ocean nitrate production.

1.4 New N in the North Atlantic

The North Atlantic plays a crucial role in global C and N dynamics, especially in terms of the sequestration of anthropogenically introduced C (Peng 2005) and is the most extensively sampled of the ocean basins. Diapycnal mixing was initially thought to be the primary mechanism for new N inputs, but early estimates of diapycnal diffusivities ($K_z = 0.11\text{-}0.37 \text{ cm}^2 \text{ s}^{-1}$) through broad-scale tracer experiments (sulfur hexafluoride - SF_6) suggested low new N vertical flux into the mixed layer (Lewis et al. 1986, Ledwell et al. 1993, 1998). Higher estimates of diapycnal diffusivity constants ($K_z = 0.4\text{-}1.95 \text{ cm}^2 \text{ s}^{-1}$) at higher latitudes within the North Atlantic suggest spatial variation in the magnitude of vertical nitrate flux rates into the euphotic zone, but still may not be applicable to N flux at lower latitudes ($<30^\circ\text{N}$) (Oschlies 2002b, Capone et al. 2005).

Mesoscale eddies have also received attention in their ability to promote primary production through facilitating inputs of deep NO_3^- into the euphotic zone (Mittelstaedt 1987, McGillicuddy & Robinson 1997, Oschlies 2002a, McGillicuddy et al. 2003). Mesoscale eddies are large features (100-250 km in diameter) that frequently occur in the North Atlantic Ocean basin, and influence biogeochemical cycling in the upper ocean (McGillicuddy & Robinson 1997, Martin & Pondaven 2003, McGillicuddy et al. 2003, Benitez-Nelson & McGillicuddy 2008). At least three types of eddies (cyclonic, anticyclonic, and mode-water eddies) roam the waters of the subtropical North Atlantic and influence the local vertical structure of the water column. Cyclonic eddies exhibit cooler internal temperatures because of considerable upwelling of deeper, nutrient-rich water, and anti-cyclonic eddies, which incur the opposite pattern by driving downwelling of surface waters, exhibit warmer cores. Mode-water eddies are identified by doming

seasonal isopycnals and depressed main isopycnals, but produce net upwelling into the euphotic zone. Mesoscale eddies are not homogeneously distributed within the North Atlantic basin, and occur most frequently in the northwestern portion of the basin, often originating from the Gulf Stream and traveling inwards into the gyre. The intensity of mesoscale eddies are also greatest in this zone, producing a basin wide difference in eddy influence between the eastern and western North Atlantic (Mourino-Carballido & Neuer 2008).

N deposition can originate from dry sources, generally originating from aerosols, inorganic N species (e.g., HNO_3) and dust, deposited downstream of the Sahara Desert (Jickells 1999, Mahowald et al. 2005, Baker et al. 2007), and wet sources (e.g., NO_3^- , NH_4^+) that are deposited through precipitation over ocean basins. “Wet” sources of deposited N include NH_3 and NO_3 species that are predominantly generated from both lightning strikes (Shepon et al. 2007), and aerosols emitted as a byproduct of biomass burning (Baker et al. 2003, Baker et al. 2006, Baker et al. 2007). Anthropogenically-induced N deposition rates have also increased globally since the mid-1800s and represent another potentially important source of N to the North Atlantic (Vitousek et al. 2002a, Vitousek et al. 2002b, Duce et al. 2008, Galloway et al. 2008). Although originally thought to be a minor contribution of N to the oceans (Prospero et al. 1996), recent estimates of global rates of N deposition (both dry and wet) suggest that anthropogenic N inputs to oceanic systems contribute up to ~67 Tg N, or ~3% of total new production annually (Duce et al. 2008). These estimates represent a considerable fraction of new N inputs, but are spatially and temporally variable across ocean basins. For example, precipitation is not uniform across the North Atlantic basin, where the highest and most stable inputs occur in northwestern regions heavily influenced by the Gulf Stream (annual oceanic precipitation data sets: TRMM/GIOVANNI). Generally, the low annual precipitation across most of the gyre minimizes the impact of N deposition from upstream sources (e.g., biomass burning from contiguous US). Also,

dust source location, transport mechanisms (e.g., atmospheric conditions), and simultaneous deposition of other limiting elements (e.g., iron) may alter the effects of N deposition on phytoplankton production and community structure (Jickells 1999, Sarthou et al. 2003, Mahowald et al. 2005). Deposition of heterogeneous mixtures composed of limiting nutrients for both non-N₂-fixing phytoplankton (e.g., N) and diazotrophs (e.g., P, Fe, Mo) may shift community structure across the basin (Mills et al. 2004, Baker et al. 2007).

N₂-fixation plays a major role in supporting primary production in many oligotrophic ocean basins (Karl et al. 1997, Karl et al. 2002, Montoya et al. 2002, Galloway et al. 2004, Montoya et al. 2004, Capone et al. 2005, Mahaffey et al. 2005, Karl & Letelier 2008). Global pelagic N₂-fixation has been estimated by extrapolation of shipboard N₂-fixation rate estimates, many of which were made in the North Atlantic (Capone et al. 1997, Capone et al. 2005). Other geochemically-based estimates have also been employed to estimate global N₂-fixation (Gruber & Sarmiento 1997, Mahaffey et al. 2003, Deutsch et al. 2007). For example, Gruber and Sarmiento (1997) formulated a proxy (N*) for net N-input or loss based on departures in nutrient ratios (NO₃⁻ and PO₄³⁻) from Redfield stoichiometry. N* distributions provide a qualitative and quantitative tool to assess the interaction between N₂-fixation and denitrification on a global scale (Figure 1.2). Current estimates of global N₂-fixation rates are around 100-150 Tg N yr⁻¹, but may increase with more improved sampling techniques and/or more complete N₂-fixation rate estimates of newly discovered oceanic diazotrophs (e.g., unicellular diazotrophs) and diazotroph/diatom association (e.g., *Richelia/Hemiaulus*).

1.5 Patterns of diazotroph abundance and influence on N cycling

The best known oceanic diazotrophs belong to the genus *Trichodesmium*, and are non-heterocystous cyanobacteria that form dense blooms, have a broad subtropical and tropical distribution, and can be easily collected and manipulated experimentally. New

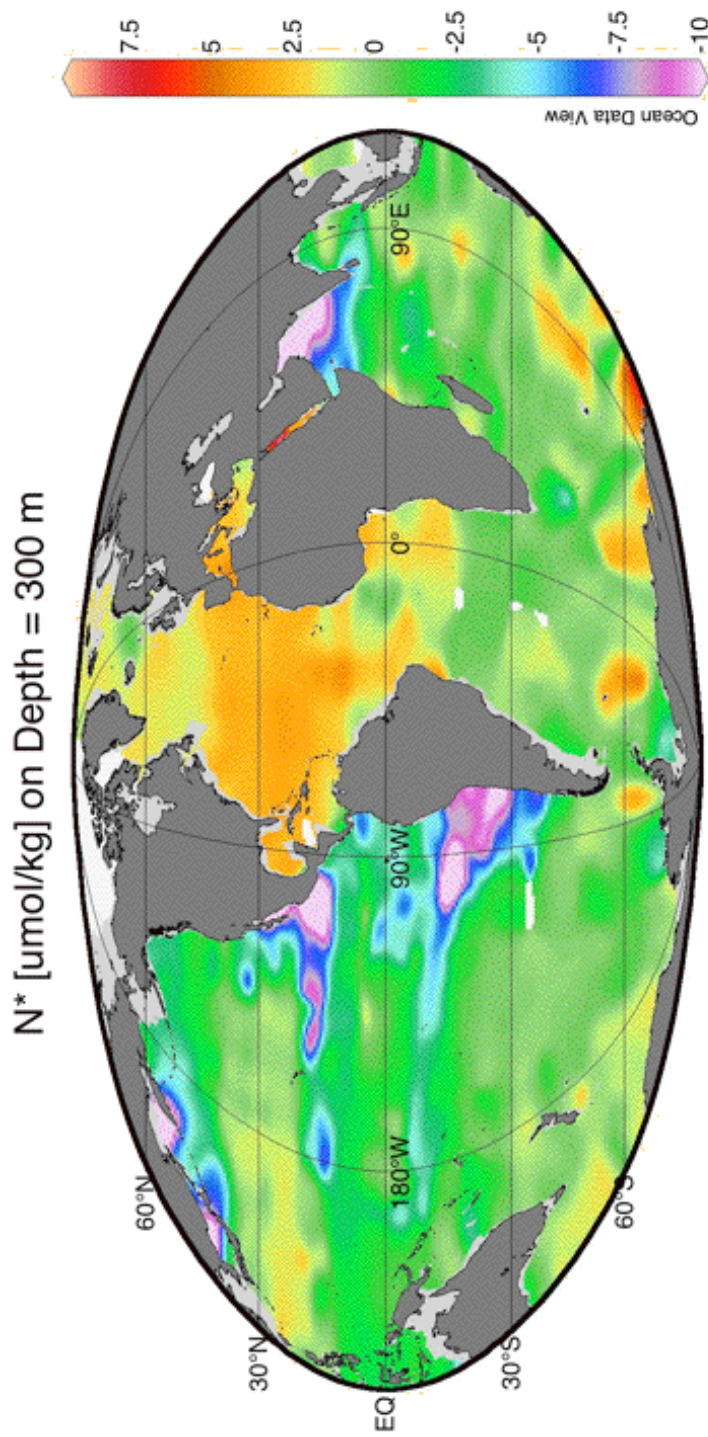


Figure 1.2 - Color contour plot showing global distribution of N^* plotted along the 300m isobath using data from the World Ocean Atlas. Figure was prepared using Ocean Data View (Schlitzer 2008)

satellite approaches have been developed to track the occurrence of *Trichodesmium* blooms globally, and estimate their impact on N cycling (Subramaniam et al. 2002, Westberry et al. 2005, Westberry & Siegel 2006). *Trichodesmium spp.* are estimated to contribute from 60 to 80 TgN yr⁻¹, based on extrapolation of direct rate measurements (Capone et al. 1997, Capone et al. 2005, Mahaffey et al. 2005). These rates only account for 40 to 59% of geochemically derived N₂-fixation for the North Atlantic and Pacific oceans (Mahaffey et al. 2005), but other oceanic N₂ fixing organisms (e.g., *Richelia intracellularis*, unicellular diazotrophs) may contribute significantly to these geochemical estimates. For example, observed N₂-fixation rates and geographical distributions for *R. intracellularis*, an endosymbiotic diazotroph typically associated with diatoms, suggest that these symbiotic associations can produce N inputs as great as, or greater than, *Trichodesmium* in the marine environment (Carpenter et al. 1999). New molecular tools also have revealed a diverse array of unicellular organisms (Zehr et al. 2000, Falcon et al. 2002, Zehr & Ward 2002, Falcon et al. 2004a, Falcon et al. 2004b, Zehr et al. 2007) that may contribute greatly to new N supply in the upper ocean (Montoya et al. 2004).

Few N₂-fixation rates measurements exist for these diazotrophs, but Montoya et al. (2004) found that these unicellular diazotrophs can fix large amounts of N (~4 mmol N m⁻² d⁻¹ in the Arafura Sea; 0.5 mmol N m⁻² d⁻¹ in the Eastern North Pacific gyre) and may contribute up to 10% of global N₂-fixation. Even though these rate measurements represent snapshots in time, gathering more rate measurements over a larger geographical range will allow us to gain a better sense for the impact of unicellular diazotrophs on present global N₂-fixation rate estimates, and provide a more accurate picture of the current marine N budget. There is also a need to focus future experiments towards identifying the proximal factors that influence N₂-fixation rates by unicellular diazotrophs, as well as determine the mechanisms by which new N travels into higher trophic levels.

Diazotrophs can greatly contribute to primary production rates, and at times, form large blooms in the subtropical/tropical oceans. *Trichodesmium* is circumglobally distributed in the subtropics and tropics (Letelier & Karl 1996, Capone et al. 1997, Karl et al. 1997, Letelier & Karl 1998, Zehr et al. 2000, Subramaniam et al. 2002, Capone et al. 2005, Westberry & Siegel 2006), and blooms of *Trichodesmium* can cover large areas (up to 2×10^6 km² – Arabian Sea) (Capone et al. 1998) and fix large quantities of both N and C (Letelier & Karl 1996, Capone et al. 1997, Letelier & Karl 1998, Carpenter et al. 2004, Capone et al. 2005). *Trichodesmium* blooms are generally short (i.e., several weeks) and spatially patchy, but can dominate C-fixation and flux where they occur. Other diazotrophs that live symbiotically with diatoms (e.g., *Richelia/Hemiaulus* diazotroph/diatom assemblages – DDAs) also form blooms that can enhance production within the water column (Carpenter et al. 1999, Subramaniam et al. 2008). Unicellular diazotrophs have the potential to affect N input in oligotrophic areas (Falcon et al. 2004a, Montoya et al. 2004), however, the broad-scale contribution of these diazotrophs to both C- and N-fixation in the world's oceans have yet to be determined. Diazotrophs can also stimulate primary production of other phytoplankton through release of newly fixed NH₄⁺ and DON (Mulholland et al. 2004, Mulholland et al. 2006) and/or through microbial and/or metazoan degradation. Thus, diazotrophs may also indirectly increase C and N export by stimulating production of other phytoplankton that subsequently die, or are consumed and exported out of the surface ocean. Although diazotroph blooms can enhance primary productivity in certain regions, few studies document export of diazotrophs into deeper water as collected by shallow (<500m) sediment traps (Karl et al. 1997, Voss et al. 2001). Thus, although diazotrophs like can drive CO₂ uptake in surface waters, the quantity of diazotroph POM exported out of the mixed layer remains largely unknown.

Biological N₂-fixation plays a prominent role in global biogeochemical cycling, but we are limited in our knowledge of the mechanisms and the extent by which new N

enters and supports both primary (i.e., non-diazotroph phytoplankton) and secondary production in oceanic food webs. Although much attention has been paid to N release by *Trichodesmium* (Mulholland et al. 2004, Mulholland et al. 2006, Mulholland 2007), the extent to which diazotrophs release biologically usable N into surface waters and how much non-diazotrophic primary production can be attributed to this new N remain unclear. Also, few studies have traced the movement of new N into higher trophic levels, such as zooplankton communities (Montoya et al. 2002, McClelland et al. 2003, Holl et al. 2007). Understanding the extent to which diazotroph N supports both primary and secondary production is paramount to elucidating the function of oceanic food webs in areas where diazotrophs often dominate N inputs.

1.6 Input of diazotroph N to oceanic food webs:

Leaky cells and hungry zooplankton?

Diazotrophs can support primary production by other phytoplankton through release of newly fixed N. N_2 -fixation is an energetically expensive process, requiring up to 16 ATP to reduce N_2 to NH_4^+ (LaRoche & Breitbarth 2005), so any such losses of fixed N are costly to the diazotroph and could promote the growth of competitors. Nonetheless, several studies have documented significant N release by *Trichodesmium* sp. (Mulholland et al. 2004, Mulholland et al. 2006) For example, Mulholland et al. (2004) found increasing NH_4^+ , DON (e.g., amino acids), and dissolved free amino acids (DFAA) in culture media taken from batch cultures of *Trichodesmium* grown in N-free medium. Comparisons of gross and net rates of N_2 -fixation by field collected and laboratory cultures of *Trichodesmium* also suggest significant release of fixed N (Mulholland et al. 2006, Mulholland 2007). The low $\delta^{15}N$ of suspended particles (Montoya et al. 2002, Holl et al. 2007, Reynolds et al. 2007) in regions with significant *Trichodesmium* populations also suggests that newly fixed N is passed from

Trichodesmium to other primary producers, though the mechanisms and pathways are not well understood.

Newly fixed N can move into higher trophic levels by direct ingestion and assimilation of diazotrophs or other phytoplankton that grow on diazotrophically fixed N. To date, efforts to quantify the movement of newly fixed N into food webs have largely focused on trophic relationships between *Trichodesmium* and only a few copepod species (e.g., *Miracia* sp., *Oculosetella* sp., *Macrosetella* sp., and *Microsetella* sp.). A harpacticoid copepod, (*Macrosetella gracilis*) is known to use *Trichodesmium* as both a physical and nutritional substrate (Oneil et al. 1996, O'Neil 1998), but very few other zooplankton have been observed to consume *Trichodesmium*. Although some zooplankton can consume and live on *Trichodesmium*, these zooplankton do not always appear to consume *Trichodesmium* in nature. For example, Eberl and Carpenter (2007) present stable isotope data that suggest that *Macrosetella gracilis* do not always exclusively consume *Trichodesmium*, but may only use colonies as habitat for reproduction while consuming other *Trichodesmium*-associated microorganisms. Other studies have also observed sparse adult zooplankton colonization of *Trichodesmium* colonies in field-collected colonies, and suggest that the metazoan microcommunity of *Trichodesmium* colonies might predominantly include larval stages (e.g., nauplii) (Sheridan et al. 2002). Aside from these studies on zooplanktivorous consumption of *Trichodesmium* colonies, no studies to date have documented zooplankton consumption of unicellular diazotrophs, and these connections require more attention. Although there is little consensus on the main mechanisms by which new N enters higher trophic levels, other studies have shown the contribution of diazotroph N into higher trophic levels (Montoya et al. 1992, McClelland & Montoya 2002, McClelland et al. 2003, Holl et al. 2007). Thus, new N seems to enter food webs and support secondary production, especially in oligotrophic subtropical and tropical waters. Along with supporting both primary and secondary production, new production that is consumed and exported from

the surface oceans represents a crucial component for both sustaining deeper biological communities and also as a regulator for the global C cycle through the biological pump.

1.7 Biological pump efficiency: POM export and remineralization

Only about a third ($\sim 10\text{-}16\text{ Gt-C}$) of the POM produced in the euphotic zone actually sinks into deeper waters (Falkowski et al. 1998, Falkowski et al. 2000), while only $3\text{ mg C m}^{-2}\text{ day}^{-1}$ or 0.34 Gt-C yr^{-1} of this sinking POM ($\sim 0.5\text{-}0.7\%$) reaches below 2000m and settles on the sea floor (Lampitt and Antia, 1997) (Figure 1.3). In order to measure sinking flux at various depths, sediment traps have typically been deployed to capture and preserve sinking POM as it travels through the water column. Despite design disagreements, various forms of sediment traps have been used for collecting sinking POM since the 1970's, and have provided critical insight into the fate of POM as it traverses the ocean depths. These devices collect sedimenting particles over various spatial and temporal scales, allowing characterization of the flux and composition of POM at various depths within the water column. Biological productivity at the surface of the open ocean influences the flux of dissolved and particulate matter to the deep-sea, which decreases with depth (Deuser & Ross 1980, Deuser et al. 1981, Asper et al. 1992, Wefer & Fischer 1993, Deuser et al. 1995, Lampitt & Antia 1997, Boyd et al. 1999, Francois et al. 2002). Nutrient abundance and flux in the euphotic zone (e.g., N, P, Fe, Si, sunlight, etc.) typically sets the upper limits for primary production rates, and thus directly affect the gross OM available for export (Deuser & Ross 1980, Deuser et al. 1981, Altabet et al. 1991, Voss et al. 1996, Gruber & Sarmiento 1997, Altabet 2001). In areas where nutrients are limiting, new sources of nutrients (e.g., nitrogen) control the export of POM from the euphotic zone (i.e., “new” versus “recycled” nutrients *sensu* (Dugdale & Goering 1967, Eppley & Peterson 1979). Although the overall amount of POM available for export is an important boundary condition, heterotrophic

decomposition within the water column also influences the amount and composition of POM reaching the ocean floor.

Decreasing fluxes of POM with depth suggest that the world's oceans not only support surface production of POM, but also act as huge heterotrophic digesters where planktonic organisms remineralize and/or repackage the sinking organic matter (OM) that is produced in the surface waters (Berelson 2002, del Giorgio & Duarte 2002, Francois et al. 2002, Andersson et al. 2004). POM entering the mesopelagic layer is subject to rapid degradation via both macro and microbial heterotrophic organisms. Roughly 95-99% of surface production becomes remineralized and recycled within the upper ~1000m of the ocean and can be returned to the atmosphere over short time scales (i.e., seasonal timescales). Despite rapid remineralization of POM in the upper ocean, POM does in fact reach the sea floor where it is either remineralized or buried in sediments for long time periods (i.e., thousands of years).

Regional differences of biological pump efficiency are evident in data from long-term field stations (e.g., BATS and ESTOC) (Neuer et al. 2002). For example, Neuer and colleagues (2002) found a significantly lower e-ratio (i.e., C_{org} Flux:PP ratio) between the BATS (0.078) and ESTOC (0.016) sites from 1996-1998, highlighting observed contrasts in both overall productivity and export of POM between the western and eastern parts of the subtropical North Atlantic. Furthermore, they hypothesized that considerable N_2 -fixation in the western end of the basin could account for the differences in both overall production and vertical flux. Latitudinal comparisons of biological pump efficiency have also been made between long-term sites that exhibit very different seasonal variability in physical and biological processes (Oligotrophic: ALOHA; Mesotrophic: K2). Marked differences in overall primary production (2-3 times higher at K2) and OM export provide for interesting comparisons in the physical and biological mechanisms influencing the biological pump efficiency at these sites. Higher e-ratios (50%) for

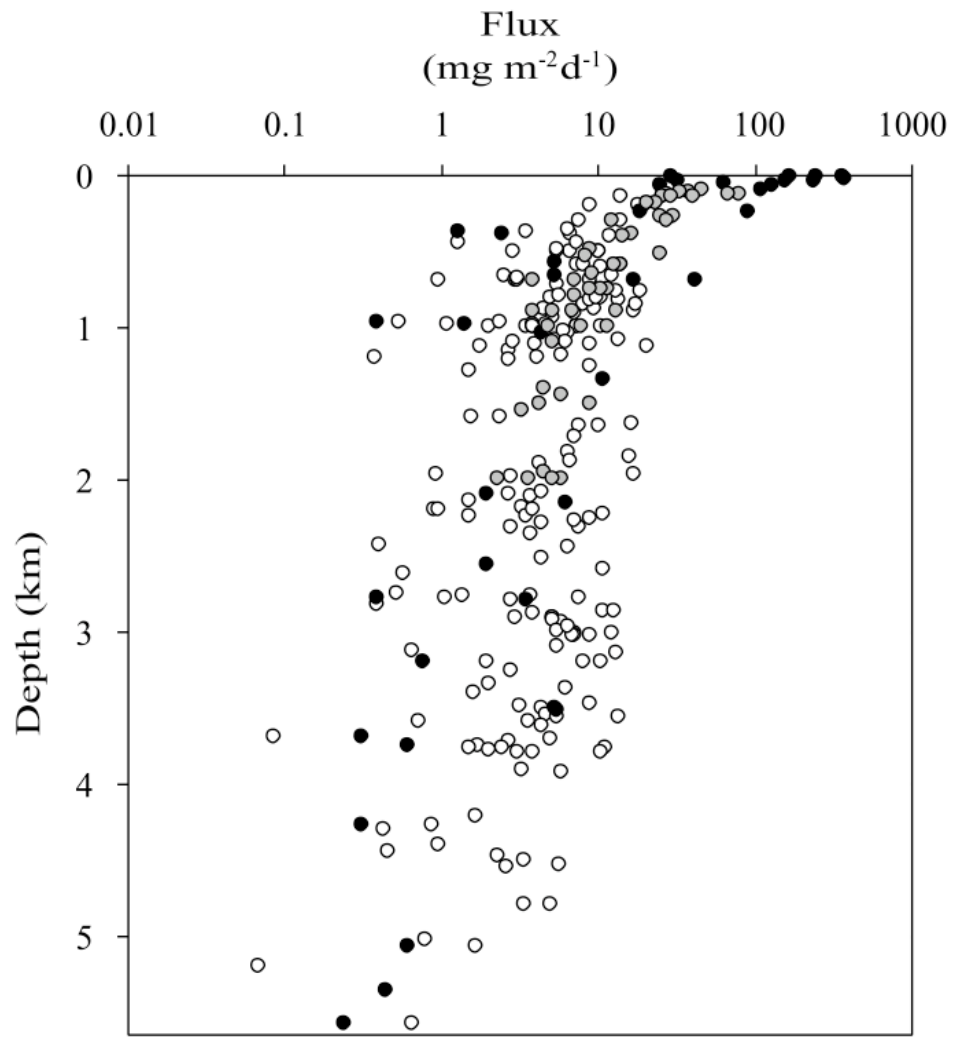


Figure 1.3 – Global oceanic sediment trap POC flux with depth (Lutz et al., 2002). Data used in this graph originates from Suess (1980), Martin et al. (1987) and Lutz et al. (2002). Reprinted with permission from American Geophysical Union from: Lutz M., R. Dunbar, and K. Caldeira (2002), Regional variability in the vertical flux of particulate organic carbon in the ocean interior, *Global Biogeochem. Cycles*, 16 (3), 1037, doi:10.1029/2000GB001383.

shallow flux (150 m) were found at the K2 site with respect to station ALOHA (20%), which was attributed to higher abundances, and C_{org} flux, of dense diatom populations at the K2 site. Also, higher abundances of diel vertical migrating zooplankton at the K2 site facilitated flux through excreted fecal pellets, and through zooplankton mortality. Given these results, C_{org} flux depends on the phytoplankton and zooplankton communities within the water column, and may be applicable to food web comparisons elsewhere, where different types of diazotrophs (diazotroph/diatom assemblages vs. *Trichodesmium*) dominate N inputs and flux out of the euphotic zone (Carpenter et al. 1999, Montoya et al. 2002, Montoya et al. 2007, Subramaniam et al. 2008).

1.8 POM sources and fate in the ocean: What causes observed vertical flux profiles?

POM sinking out of the euphotic zone can originate from direct sinking of senescent or dead phytoplankton cells (Gowing et al. 2001), marine snow (Alldredge et al. 1990), rapidly sinking forms such as aggregates of cells (Alldredge & Gotschalk 1988, Alldredge & Silver 1988) or fecal pellets (Urrere & Knauer 1981, Dagg et al. 1982, Small et al. 1983, Small et al. 1987, Turner 2002, Dagg et al. 2003, Suzuki et al. 2003, Thor et al. 2003). Of these sinking particles, fecal pellets have generally been viewed as the dominant form of sinking organic material in the water column, because they typically sink more rapidly than other particles in the ocean and they are often distinguishable (and quantifiable) components of POM collected from sediment traps.

Sinking POM is often heterogeneous, originating from different sources (i.e., fecal pellets, marine snow, algal cells, etc.), it is difficult to trace the origin and fate of that organic matter as it traverses the water column. Qualitative differences in sinking POM can provide insight into the dominant mechanisms influencing POM remineralization and/or repackaging in the water column. For example, changes in specific lipid biomarkers in POM samples collected in sediment traps reflect both the source and diagenetic alteration of POM in the water column and in sediments

(Wakeham 1995, Wakeham et al. 1997, Wakeham et al. 2002). NMR spectroscopy also provides information on the abundance of specific components of sinking POM (e.g., amino acids, carbohydrates and fats). For example, Hedges et al. (1999) used NMR spectra, to show that the chemical composition of sedimenting particles changed very little with depth in the Equatorial North Pacific, despite extensive overall remineralization of this sinking organic matter. Other studies, however, suggest that POM does not always show non-selective preservation. Lee et al. (2001) compared the composition and concentrations of individual amino acids (AAs) of sinking POM and found that the molar ratios of AAs exhibited different behavior with depth. In their analysis, they observed several AAs that were preferentially removed from POM while other AAs were preferentially incorporated/sequestered into POM. They attributed these patterns to the differential utilization of AAs by microbes (e.g., bacteria) and macrofauna (e.g., deep-dwelling copepods).

Surface production and heterotrophic processes in the water column clearly influence particle flux, but the origin of sinking POM (euphotic zone versus marine snow) and the dominant mechanisms driving transformation of this POM (microbial versus macrofaunal) in the water column remain poorly understood. Isotopic techniques can potentially provide more specific information about the origin of the POM and the processes influencing its degradation in the water column.

1.9 Stable nitrogen isotope tracers

1.9.1 In-situ tracers in the oceans

Isotopes, by definition, are atoms of an element with the same number of protons, but different numbers of neutrons, and thus different masses. Nitrogen has two stable isotopes (^{14}N and ^{15}N) in the natural environment, where ^{14}N is more abundant (99.634% by atoms) than ^{15}N . Despite their large difference in natural abundance, the relative

proportions of both nitrogen isotopes can be measured and compared among various inorganic and organic pools. Since measuring absolute concentrations of these isotopes is difficult, isotopic ratios are measured and expressed as per mil (‰) deviations from the isotope ratio in a known standard (Tropospheric N₂) using the delta convention:

$$\delta^{15}\text{N} = \left(\frac{R_{\text{sample}}}{R_{\text{standard}}} - 1 \right) \times 1000 \quad (1.2)$$

where $R = {}^{15}\text{N} / {}^{14}\text{N}$.

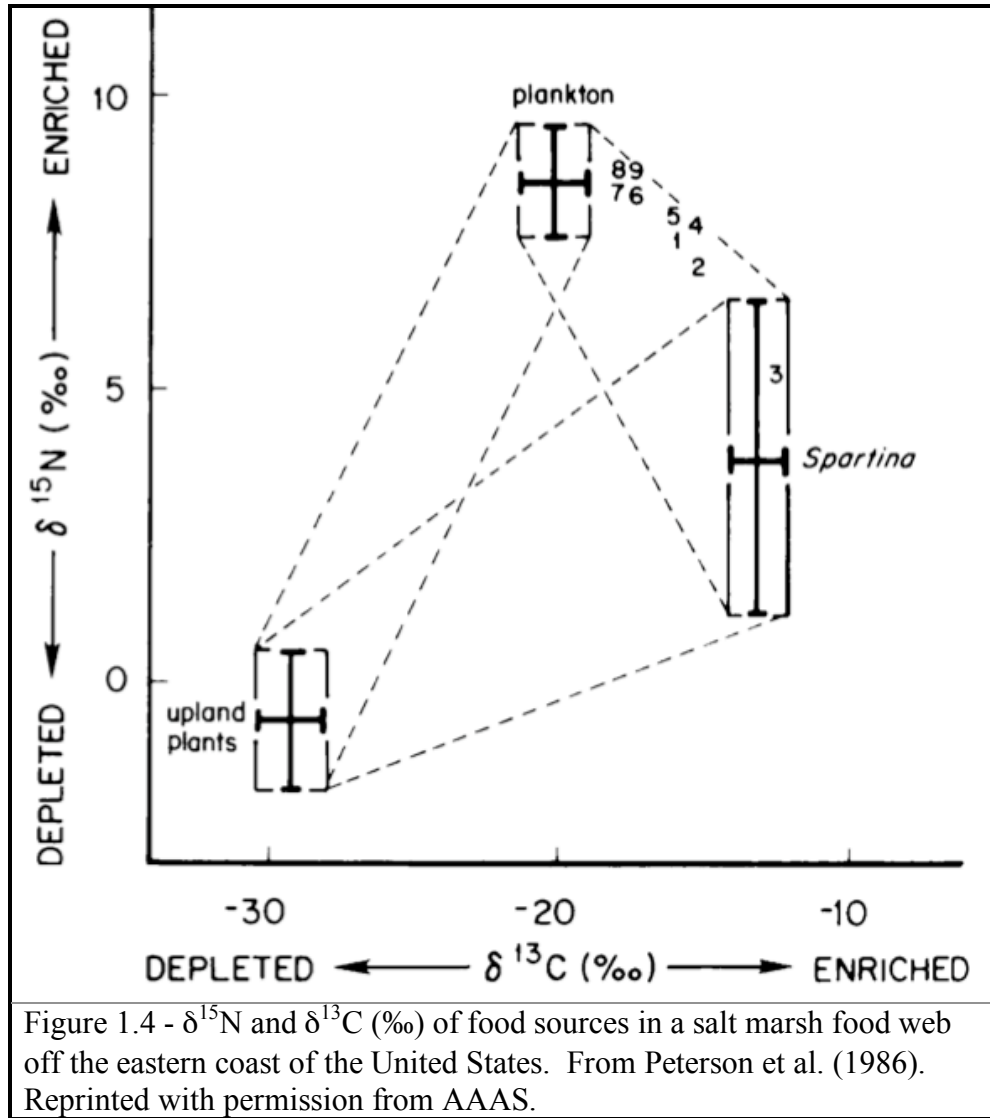
Stable isotopes of biologically active elements (i.e., N, C, O, H, and S) provide a powerful tool for studying biogeochemical cycles, as well as the structure and dynamics of ecological communities. Stable isotopes are especially useful in ecosystem level studies, since mass-dependent discrimination between isotopes provides information on the biological transformations of elements within food webs. For example, isotopic fractionation occurs during biochemical reactions associated with the uptake of nutrients (e.g., NO₃⁻) by phytoplankton within the water column since covalent bonds associated with lighter isotopes are more reactive than bonds associated with heavier isotopes (Montoya & McCarthy 1995).

Stable isotope analysis of higher organisms also yields information concerning the movement of those nutrients through food webs. For example, DeNiro and Epstein (1981) determined that organisms generally show little isotopic fractionation of C isotopes through consumption and metabolism, while organisms generally retain more ¹⁵N relative to their diets. Given these observations, many studies have used stable isotope ratios from bulk biological material to link consumers within food webs (Peterson & Fry 1987, Peterson 1999, Post 2002), to trace movements of nutrients between different habitats (Voss et al. 1996, Altabet 2001), to follow animal migrations (Hansson et al. 1997, Cerling et al. 2006), as well as to assess the physiological condition of animals (Hobson et al. 1993, Gannes et al. 1997, Adams & Sterner 2000). Studies have mainly focused on using natural abundance of stable isotopes ratios of certain organisms

and/or trophic positions in order to trace the flow of energy and nutrients within ecosystems. For example, Peterson et al. (1986) used the natural distributions of N and C isotopes in plant and animal communities to reconstruct a Georgia (USA) salt marsh food web (Figure 1.4).

Given isotopically distinct sources, an isotope mass balance approach can be used to quantify the relative contribution of C and/or N sources to primary and secondary production (Montoya et al. 2002, Sommer et al. 2006, Reynolds et al. 2007). Isotopic mass balance models are most accurate when few distinct baseline isotopic end-members exist (N isotopes can resolve $N + 1$ distinct sources) within the system and when the important isotopic fractionation factors are known. The biochemical complexity of organisms can make interpreting stable isotope distributions difficult.

N exhibits a wide range of oxidation states in food webs, driven primarily by biological processes (Figure 1.5). Enzymatic reactions often produce kinetic isotope fractionations that alter the $\delta^{15}\text{N}$ within and between both inorganic and organic N pools (Table 1.1). For example, kinetic fractionation can occur as N moves between various inorganic and organic pools of N, such as fractionation associated with DIN uptake (Montoya & McCarthy 1995, Needoba et al. 2003, Needoba et al. 2004), zooplankton consumption (Checkley & Entzeroth 1985, Checkley & Miller 1989), and microbial decomposition of OM (Macko & Estep 1984, Macaulay et al. 1995). Thus, isotope mass balance model also requires an understanding the kinetic fractionations driving shifts in the relative abundance of ^{15}N between multiple pools. Despite the dynamic nature of N in marine systems, N stable isotopes can be used to trace the origin and transformation of N in the water column of oligotrophic areas, where the sources of N are well delineated. In tropical and subtropical regions of oceanic gyres, thermal stratification during the summertime reduces vertical nutrient exchange. Nutrients inputs via eddy diffusion and mixing providing a source of new N available to support production in the upper ocean.



Deep NO_3^- injected into the surface waters may contribute significantly to upper ocean productivity, but this input is spatially and temporally variable in the North Atlantic (Lewis et al. 1986, Ledwell et al. 1993, Capone et al. 2005). Biological N_2 -fixation is often a dominant input of new N to the euphotic zone of the North Atlantic (Capone 2001, Lipschultz et al. 2002, Zehr & Ward 2002, Montoya et al. 2004, Capone et al. 2005, Mahaffey et al. 2005, Montoya et al. 2007), but the impact of diazotroph N on higher trophic levels deserves more attention.

N_2 -fixation rates are generally measured in short shipboard incubations at stations along a cruise track, making it difficult to scale up these rates to a basin scale. The distribution of nitrogen stable isotopes in organic pools of N can provide a longer time- and space-integrated measure of new N inputs via diazotrophic activity. In the central North Atlantic gyre, the two major sources of new N are isotopically distinct: deep $\delta^{15}\text{NO}_3^-$ values range from 4.5 to 6‰ while PON produced by biological N_2 -fixation ranges from $\delta^{15}\text{N}_{\text{POM}} = -2$ to 0‰ (Montoya et al. 2002). This isotopic contrast allows us to quantify the relative importance of biological versus physical supply of N to both primary and secondary production in the surface oceans (Montoya et al. 2002, Mahaffey et al. 2003, Holl et al. 2007, Reynolds et al. 2007) (Figure 1.6). For example, Montoya et al. (2002) found that diazotrophs can contribute up to 100% and 50% of the N used by phytoplankton and zooplankton, respectively, in the mixed layer of the North Atlantic. Similarly, Reynolds et al. (2007) found that diazotrophs contributed significantly to phytoplankton biomass in the North Atlantic, but their data also showed an interesting decline in diazotroph N contribution with increasing latitude northward, at least in the Central North Atlantic. Several other studies have documented low $\delta^{15}\text{N}$ values of zooplankton biomass in regions with significant N_2 -fixation, suggesting that zooplankton derive a sizeable portion of their N from diazotrophs.

Given that zooplankton (and presumably higher consumers) consume and

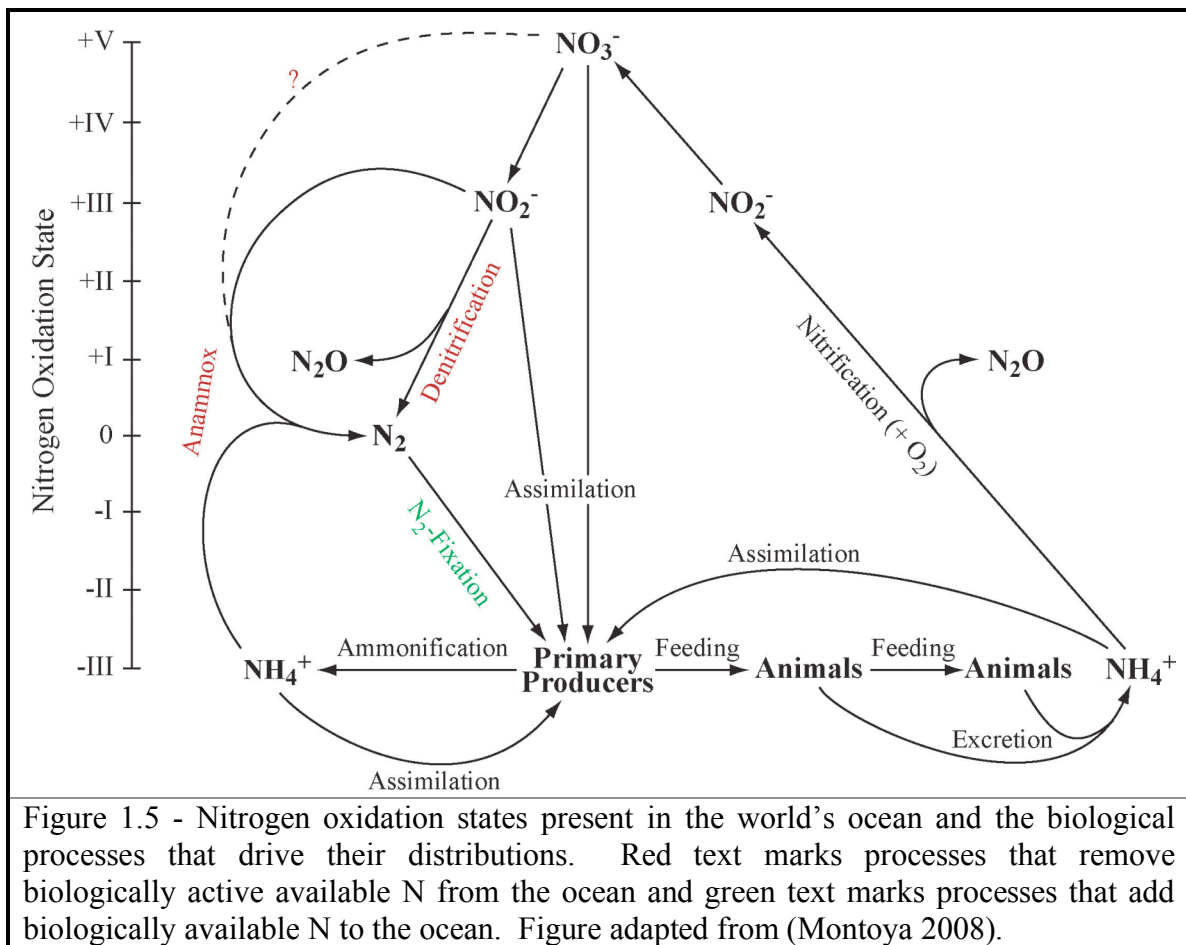


Table 1.1 – Isotopic enrichment factors for various biologically mediated reactions.

Biological Process	Chemical Reaction	Enrichment Factor (ε)	Location
Nitrification	$(\text{NH}_4^+ \rightarrow \text{NO}_3^-)$	15‰ 14-38‰	Chesapeake Bay ^a Nitrifying bacterial strains ^b
Denitrification	$(\text{NO}_3^- \rightarrow \text{N}_2)$	20 - 40‰ 22 -27‰ 25‰	ETNP ^c Arabian Sea ^d Gulf of California ^e
Nitrogen fixation	$(\text{N}_2 \rightarrow \text{N}_{\text{org}})$	-1.08 to -2.15‰ -2‰ -1.24‰ -0.38‰	North Atlantic <i>Tricho</i> colonies ^f Gulf of Mexico <i>Tricho</i> colonies ^g North Atlantic <i>Richelia/Hemiaulus</i> ^f Western Tropical North Pacific ^h
Ammonia assimilation	$(\text{NH}_4^+ \rightarrow \text{N}_{\text{org}})$	6.5 - 8‰ 9.1‰ 5 - 20‰	Chesapeake Bay ^a Delaware Estuary ⁱ Bacterial assemblage ^j
Nitrate assimilation	$(\text{NO}_3^- \rightarrow \text{N}_{\text{org}})$	5 – 10‰ 4 - 6‰ 5‰ 5‰ 5‰	Phytoplankton cultures ^k Southern Ocean ^l Subarctic Pacific ^m Equatorial Pacific ⁿ Eastern North Pacific ^e

Citations: ^aHorrigan et al. (1990); ^bCasciotti et al. (2003); ^cVoss et al. (2001); ^dBrandes et al. (1998); ^eAltabet et al. (1999b); ^fCarpenter et al. (1999); ^gHoll et al. (2007); ^hMariotti et al. (1981); ⁱKarl et al. (1997); ^jCifuentes et al. (1989); ^kHoch et al. (1994); ^lMontoya and McCarthy (1995); ^mSigman et al. (1999a); ⁿWu et al. (1997); ^oAltabet (2001); ^pAltabet et al. (1999b).

incorporate N that is derived from diazotrophs, it is also important to consider their contribution to the export of new production from the upper ocean, particularly since zooplankton play a critical role in mediating N export from the upper ocean to depth (Urrere & Knauer 1981, Lampitt et al. 1990, Lampitt & Antia 1997, Lee 2002). We can further use stable isotope ratios to trace the movement and processing of POM flux out of the surface ocean, through the deep ocean and eventually into deep-sea sediments.

Vertical profiles of $\delta^{15}\text{N}$ and $\delta^{13}\text{C}$ of suspended, sinking and sediment POM have been used to address several questions concerning POM transport and transformation within the water column and in deep-sea sediments: (1) What are the origins of POM (vertical v. lateral advection); (2) How do surface nutrient conditions affect the flux of POM exiting the euphotic zone; (3) What processes and organisms dominate remineralization of POM within the water column; (4) What is the trophic structure of the deep sea, where sinking OM generally represents the base of the food chain; (5) Does information extracted from sediment cores provide an accurate account of past climates and elemental inventories? (Altabet et al. 1991, Altabet & Francois 1994, Voss et al. 1996, Nakatsuka et al. 1997, Wu et al. 1999a, Altabet 2001, Freudenthal et al. 2001, Altabet et al. 2002, Lourey et al. 2003, Lourey et al. 2004, Gaye-Haake et al. 2005). Stable isotopic analysis of POM has been quite useful in addressing the questions above, but observed vertical trends in $\delta^{15}\text{N}$ of POM have produced somewhat ambiguous results.

Many studies have documented an enrichment of $\delta^{15}\text{N}$ of the POM exposed to decomposition in the water column (Saino & Hattori 1987, Altabet et al. 1991, Wu et al. 1999a), however, other studies reveal a decrease in $\delta^{15}\text{N}$ values of POM with depth. The variation in $\delta^{15}\text{N}$ is related to the type of particles found (i.e., suspended v. sinking), their exposure time to heterotrophic decomposition and the removal or addition of nitrogenous components (e.g., proteins, amino acids, nucleic acids) depleted or enriched in ^{15}N (Altabet et al. 1991, Voss et al. 1996, Nakatsuka et al. 1997). For example, Altabet et

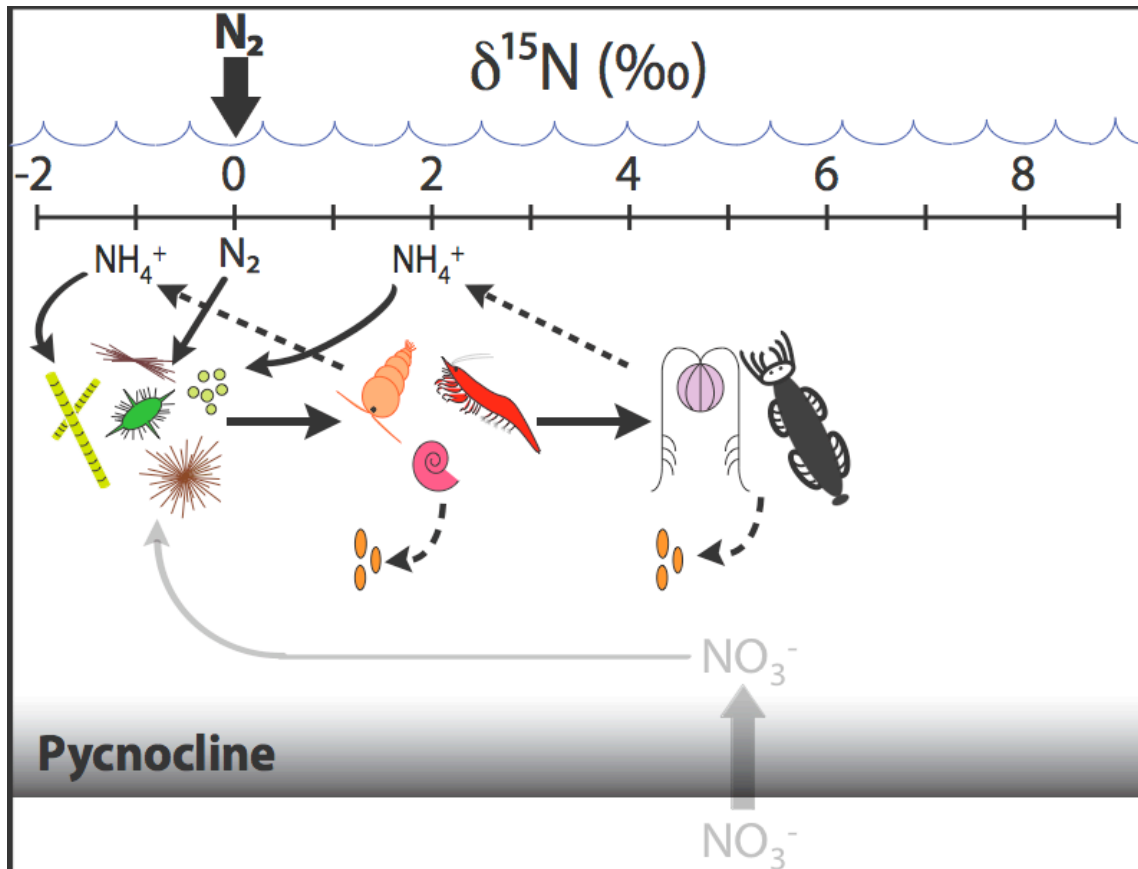


Figure 1.6 – Schematic of the distributions of nitrogen isotopes in particles and mesozooplankton in a typical oceanic food web under strong diazotrophy in the mixed layer. Notice the community-level shift towards lower $\delta^{15}\text{N}$ values than if deep NO_3^- were the dominant N source supporting these communities. Adapted from (Montoya et al. 2002).

al. (1991) found that suspended particles exhibited higher $\delta^{15}\text{N}$ values than that of sinking particles in POM collected from the OFP-site near Bermuda (Figure 1.7). They concluded that the observed divergent $\delta^{15}\text{N}$ patterns of the two types of particles suggest that sinking particles are subjected to biological remineralization and/or repackaging processes different from those acting on suspended particles (Altabet et al. 1991). However, in this example, as well as other studies revealing similar patterns (cited above), bulk $\delta^{15}\text{N}$ values limit our ability to determine the source of the POM while also limiting our ability to distinguish between specific biological processes influencing the transformation of particles in the ocean. The use of compound-specific (eg., AAs) isotopic composition of POM will reduce the limitations of bulk isotopic values in determining the source and fate of POM traversing the water column.

1.9.2 Compound specific isotopic analysis

Stable isotope ratios of whole organisms or tissues have been used to trace the flow of biologically essential elements between different pools and determine trophic relationships between organisms in food webs. Nitrogen isotopic ratios and their changes relative to food web processes can be extremely useful in tracing sinking organic matter in the ocean. $\delta^{15}\text{N}$ values are known to increase by roughly 3.4‰ with each trophic transfer, and thus can be useful in determining the trophic position of organisms within a community (Deniro & Epstein 1981, Minagawa & Wada 1984). This information can be used to determine the food sources of organisms within the water column, as well as the fate of that material after digestion and excretion (i.e., fecal pellets). Although stable isotope ratios of bulk samples have been helpful in ecosystem studies, they are limited in their ability to reveal multiple food sources of consumers (i.e., there are often more food sources than available isotope ratios) as well as the biochemical and/or physiological underpinnings of the observed stable isotopic ratios (Gannes et al. 1997, McClelland & Montoya 2002).

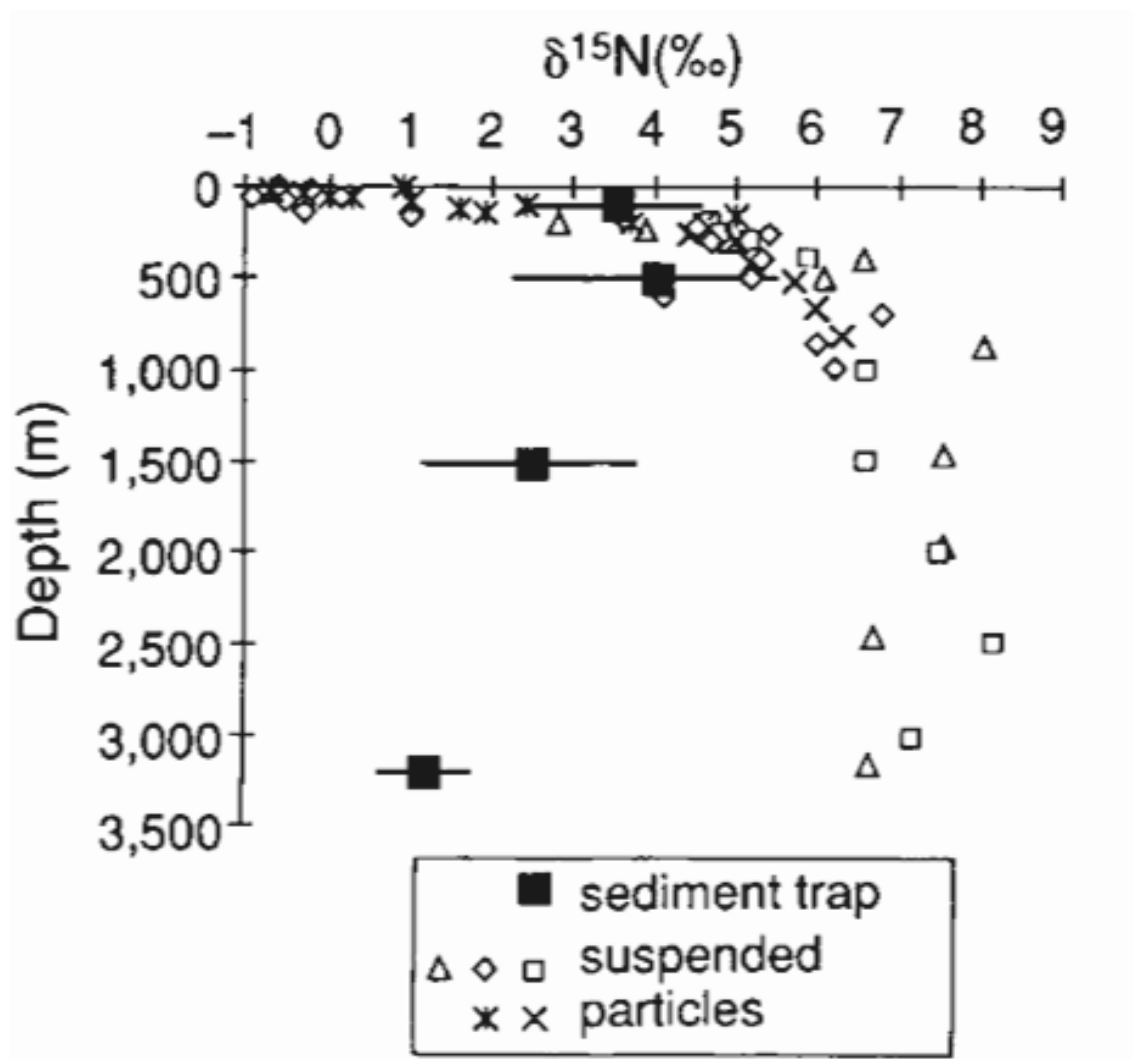


Figure 1.7 - Mean $\delta^{15}\text{N}$ (± 1 S.D.) of both suspended and sinking particles collected from filtered water samples and sediment traps, respectively, at the OFP site off of Bermuda. Reprinted with permission from Macmillan Publishers Ltd: *Nature*, (Altabet et al. 1991).

To avoid these constraints, recent work has focused on analyzing the isotopic composition of specific compounds isolated from bulk tissues (e.g., lipids and AAs) in order to provide information about the source of energy and nutrients to these organisms (Hare et al. 1991, Fantle et al. 1999, McClelland & Montoya 2002, McCarthy et al. 2003, McCarthy et al. 2004, McCarthy et al. 2007). The distribution of nitrogen isotopes among individual AAs in an organism provide detailed information on its trophic position as well as the sources of N supporting the primary producers at the base of the food web. Specifically, Montoya and McClelland (2002) have shown that certain AAs (e.g., phenylalanine) do not change in $\delta^{15}\text{N}$ between trophic levels, while other AAs (e.g., glutamic acid) show large $\delta^{15}\text{N}$ changes between trophic levels. This information allowed them to quantify the number of trophic transfers within the food web by simply subtracting the $\delta^{15}\text{N}$ values of glutamic acid and phenylalanine ($\delta^{15}\text{N}_{\text{glu}} - \delta^{15}\text{N}_{\text{phen}}$) (McClelland & Montoya 2002, McClelland et al. 2003).

McCarthy et al. (2007) used a similar approach to characterize the trophic structure of organic matter in the equatorial Pacific Ocean. They used vertical patterns in the $\delta^{15}\text{N}$ of individual AAs to provide information on the processing and degradation of sinking POM in the water column. McCarthy et al. (2007) extended the trophic measure of McClelland and Montoya (2002) by using multiple AAs to quantify trophic shifts with depth in the water column. By subtracting mean $\delta^{15}\text{N}$ values of enriching AAs (e.g., glutamic acid, aspartic acid) from the mean $\delta^{15}\text{N}$ values of non-enriching AAs (e.g., phenylalanine, threonine), they could determine the number of trophic transfers (via macrofaunal consumption) organic matter undergoes as it sinks through the water column. Despite these promising results, the isotopic fractionations associated with both eukaryotic and prokaryotic heterotrophy (i.e., this dissertation) remain poorly quantified.

1.10 Research objectives

1.10.1 Alteration of elemental and isotopic composition of OM:

Microbial and metazoan processing

Understanding the isotopic fractionation associated with biological transformation of POM can help elucidate the origin of particles from the surface ocean (i.e., trophic level indicators) as well as the dominant repackaging/remineralizing mechanisms transforming sinking particles over various spatial and temporal scales. My main research objectives are:

- 1) Determine the alteration of elemental and isotopic composition of OM digested by crustaceans.
- 2) Determine the temperature effects on the elemental and isotopic composition of OM exposed to microbial decomposition

1.10.2 Basin-scale distribution of N isotopes

As previously stated, new N inputs into aquatic systems have been, and continue to be, quantified using several methods (acetylene reduction and $^{15}\text{N}_2$ uptake). However, fewer studies have directly addressed how and to what extent newly fixed N supports higher trophic levels in oceanic food webs. In order to address this directly, I use the $\delta^{15}\text{N}$ of both suspended particles and zooplankton collected along a cruise that spans the subtropical North Atlantic to characterize the food web and trace the movement of new N into those food webs. My main research objectives are:

- 1) Analyze oceanic food web structure by using natural distributions of stable isotope ratios between various different organic pools that exist in the water column (namely suspended particles and zooplankton).

- 2) Determine the relative contribution of new N by N₂-fixing organisms to secondary production, by examining both vertical and horizontal structure of zooplankton and particle stable isotope ratios.
- 3) Assess the relative efficiency of N into zooplankton between diazotroph N and other N sources (e.g., deep NO₃⁻).

CHAPTER 2

TEMPERATURE EFFECTS ON CHANGES IN C:N RATIO, $\delta^{15}\text{N}$, AND $\delta^{13}\text{C}$ OF DECOMPOSING ORGANIC MATTER

2.1 Introduction

The biological pump plays a critical role in transporting organic matter downward in the world's oceans (Falkowski et al. 1998, Battle et al. 2000, Falkowski et al. 2000, Hedges et al. 2001). Understanding the origin and fate of organic matter is essential in determining the influence of marine biological processes on global atmospheric CO_2 concentrations (Honjo 1996, Lampitt & Antia 1997, Raven & Falkowski 1999, Falkowski et al. 2000) while also providing potential proxies for reconstructing past climates and biogeochemical inventories (Altabet & Francois 1994, Altabet et al. 1995, Altabet et al. 1999a, Altabet et al. 2002, Ganeshram et al. 2002, Liu et al. 2005).

Sinking organic matter originates from many sources in the euphotic zone, including dead phytoplankton cells, marine snow, dead zooplankton, and fecal pellets (Turner 2002). Particles are continually exposed to decomposition by heterotrophs while sinking through the water column (Lee et al. 1987, Lee & Fisher 1992, 1994, Azam 1998, Boyd & Newton 1999, Azam & Worden 2004, Frangoulis et al. 2005), leading to a decrease in mass flux with depth (Lampitt & Antia 1997, Boyd et al. 1999, Antia et al. 2001, Lutz et al. 2002, Andersson et al. 2004). Most of the organic matter produced in the euphotic zone is rapidly remineralized by heterotrophic organisms, though rapidly-sinking organic matter, including fecal pellets, zooplankton carcasses, and aggregates, may avoid complete decomposition within the water column and reach the seafloor (Deuser & Ross 1980, Deuser et al. 1981, Asper et al. 1992, Lampitt & Antia 1997, Hedges et al. 2001, Berelson 2002, Francois et al. 2002).

Vertical profiles of the isotopic composition of both suspended and sinking particles can provide information on their origin and the diagenetic processes acting on them (Altabet et al. 1991, Altabet & Francois 1994, Voss et al. 1996, Nakatsuka et al. 1997, Wu et al. 1999b, Altabet 2001, Freudenthal et al. 2001, Altabet et al. 2002, Lourey et al. 2003, Lourey et al. 2004, Gaye-Haake et al. 2005). For example, Altabet et al. (1991) and Voss et al. (1996) used the isotopic composition of surface nitrate, suspended particles and sinking organic matter to trace the movement of N from surface waters into the deep sea. Vertical trends of $\delta^{15}\text{N}$ and $\delta^{13}\text{C}$ in sediment cores can also be useful in reconstructing past climates and oceanic biogeochemical inventories (Altabet & Francois 1994, Altabet et al. 1995, Altabet et al. 1999a, Altabet et al. 2002, Ganeshram et al. 2002, Liu et al. 2005). However, accurately interpreting these robust patterns requires a clear understanding of the ways that biological processes (e.g., microbial decomposition) influence the isotopic composition of organic matter, which remains poorly understood. Thus, despite the potential use of $\delta^{15}\text{N}$ and $\delta^{13}\text{C}$ measurements to determine the origin and diagenesis of organic matter, it is essential to first determine how microbial degradation shapes the isotopic composition of OM.

Previous laboratory studies have assessed the impact of microbial processes on the isotopic composition of organic matter in both marine (Wada 1980, Ziemann et al. 1984, Macko et al. 1994), and fresh-water (Lehmann et al. 2002) environments. Decomposed OM is generally enriched in ^{15}N , most likely as a result of deamination reactions, which have been shown to strongly discriminate against ^{15}N *in vitro* (Macko et al. 1986, Bada et al. 1989). However, all experiments to date have been performed at temperatures characteristic of surface waters in tropical and sub-tropical oceans (i.e., 19 - 25°C) rather than temperatures relevant to particles traversing the deep ocean (i.e., 2-4°C). Temperature differences can potentially affect the isotopic alteration of organic matter during decomposition, ultimately changing the $\delta^{15}\text{N}$ and $\delta^{13}\text{C}$ of organic matter collected in the water column and in sediments (Galimov 1981). Here, we report on a set

of experiments designed to characterize isotopic alterations associated with microbial degradation of organic matter by incubating shrimp tissue in seawater at both 4°C and 25°C.

2.2 Materials and Methods

Decomposition assays were performed in 25-L polycarbonate containers held at constant temperature (4°C and 25°C) in environmental chambers at Georgia Institute of Technology. The 25°C assay ran from January 15, 2005 to February 19, 2005 and the 4°C assays ran from February 12, 2005 to May 20, 2005. Twenty-five frozen whole white shrimp were used in the experiments. Initially, whole shrimp were thawed and sliced in half (dorso-ventrally) to provide control and experimental samples. Control halves were immediately dried at 60°C and stored over desiccant until prepared for isotopic analysis. Experimental shrimp halves were placed in separate 50mL polyethylene Falcon™ tubes with holes and submerged in Instant Ocean® artificial seawater (ASW) (total volume: 18L) inoculated with 100mL of water collected from aquaria housing live shrimp (*Palaemonetes sp.*). ASW salinity ranged from 18-25‰ throughout the experiment. Conditioned ASW (CASW) used in the 4°C assays was initially placed in the 4°C environmental chamber for 3 days prior to experimentation in order to drop the water temperature before the experiment began. Shrimp halves were then collected at various times throughout the duration of the experiment. At each sampling, a minimum of three shrimp halves were haphazardly collected and removed from the CASW and immediately transferred to a 60°C drying oven. After drying, the experimental halves were ground and prepped for isotopic analysis in the same fashion as the control halves (Montoya et al. 2002).

All measurements were performed using a Micromass Optima mass spectrometer system interfaced to a Carlo-Erba NA2500 elemental analyzer for continuous-flow isotope-ratio mass spectrometry (CF-IRMS). All isotope abundances are expressed in per

mil units (‰) and are calculated relative to either tropospheric N₂ ($\delta^{15}\text{N}$) or Pee Dee Belemnite ($\delta^{13}\text{C}$) standards. The analytical error associated with our bulk isotope measurements was typically $\pm 0.15\text{‰}$.

Each experimental sample was compared to its control tissue sample in order to minimize the impact of natural compositional and isotopic differences between individual shrimp. All elemental and isotopic composition values are presented as the mean of the three samples ± 1 standard deviation. We calculated the change in C:N ratio ($\Delta\text{C:N} = \text{C:N}_{\text{decomposed}} - \text{C:N}_{\text{control}}$) to provide an index to the degree of decomposition during the experiment. Q_{10} values were also calculated for both C and N decreases in both experiments:

$$Q_{10} = (R_2/R_1)^{(10/T_2-T_1)} \quad (2.1)$$

where R_1 and R_2 represent the decomposition rate of either C or N, and T_1 and T_2 represent experimental temperature of 4°C and 25°C, respectively.

All statistical comparisons were made with a full-factorial ANCOVA, with temperature (4°C or 25°C) as the fixed variable and $\Delta\text{C:N}$ ratio as the continuous covariate. Since none of the interaction terms (e.g., Temperature * $\Delta\text{C:N}$ ratio) differed significantly ($p > 0.05$), these terms were removed and a reduced ANCOVA was used in analyzing our data.

2.3 Results

Shrimp tissue C:N increased linearly with time regardless of temperature, and thus, decomposition rates (Figure 2.1; Tables 2.1 & 2.2). Shrimp tissue decomposed significantly faster in the 25°C experiment ($m_{25^\circ\text{C regression}} = 0.17 \text{ d}^{-1}$) relative to the 4°C experiment ($m_{4^\circ\text{C regression}} = 0.018 \text{ d}^{-1}$) (Table 3). Increases in C:N were driven by preferential removal of N relative to C from the shrimp tissue throughout the experiment (Tables 2.1 & 2.2). Shrimp tissue N and C content decreased over time in both experiments, however, the C content of shrimp tissue did not change with time in the 4°C

experiment (Table 2.3). Given that C:N was a good indicator of the state of decomposition of the shrimp tissue in our experiments, and N was preferentially removed relative to C (Figure 2.1), we used the change in C:N (Δ C:N) to relate our elemental and isotopic data to the state of decomposition of shrimp tissue.

Shrimp tissue N content decreased linearly and tissue C:N ratio increased with time at both temperatures, but shrimp tissue C content showed more variability (Figure 2.3). Decreases in N content were significantly influenced by the state of decomposition of the shrimp tissue (i.e., Δ C:N), with no significant influence of temperature (Table 2.3). Shrimp tissue C content decreased linearly with increasing C:N in the 25°C experiment, but showed no clear trend in the 4°C experiment (Figure 2.3). As with N content, the decreases we observed in C content were related to the state of decomposition of the shrimp tissue rather than to temperature (Table 2.2). Overall, mean C content decreased in the 25°C experiment, but changed only slightly in the 4°C experiment (Tables 2.1 & 2.2).

The $\delta^{15}\text{N}$ of shrimp tissue showed little change in the 4°C experiment and increased considerably with time in the 25°C experiment (Figure 2.2). Shrimp tissue mean $\delta^{15}\text{N}$ generally increased ($\sim 2\text{-}3\text{‰}$) with increasing C:N in the 25°C experiment, but showed little alteration ($\sim 0.5\text{‰}$) in the 4°C experiment (Figure 2.4, Tables 2.1 & 2.2). However, temperature alone did not account for a significant portion of the variation in shrimp tissue $\delta^{15}\text{N}$ between the two experiments, while decreases in $\Delta\delta^{15}\text{N}$ could be explained by the degree of decomposition of the shrimp tissue (Table 2.3).

The $\delta^{13}\text{C}$ of shrimp tissue became more negative with time, and was influenced by temperature differences between the two experiments (Tables 2.1 & 2.2; Figure 2.2). The $\delta^{13}\text{C}$ of shrimp tissue also tended to become more negative with increasing C:N at both temperatures (Figure 2.3). An ANCOVA revealed that the shrimp tissue exhibited

Table 2.1 - Mean changes (± 1 S.D.) in $\delta^{15}\text{N}$, $\delta^{13}\text{C}$, N content, C content, and C:N ratio of shrimp tissue collected at each time point during the 25°C experiment.

<u>Incubation Days</u>	<u>$\delta^{15}\text{N}$ (‰)</u>	<u>$\delta^{13}\text{C}$ (‰)</u>	<u>N Content (%)</u>	<u>C Content (%)</u>	<u>C:N</u>
0 - Control	5.8 ± 0.2	-21.5 ± 1.7	11.2 ± 1.5	40.6 ± 3.2	4.3 ± 0.4
3	6.7 ± 0.2	-23.1 ± 0.3	10.0 ± 0.2	41.9 ± 0.7	4.9 ± 0.1
6	6.7 ± 0.7	-23.0 ± 1.1	8.3 ± 0.3	40.0 ± 0.9	5.6 ± 0.1
10	6.0 ± 0.3	-24.2 ± 0.5	7.2 ± 0.4	42.6 ± 2.1	6.9 ± 0.7
13	5.2 ± 3.3	-23.6 ± 0.04	6.7 ± 0.9	35.3 ± 4.2	6.1 ± 0.1
18	6.3 ± 0.8	-23.8 ± 0.3	5.7 ± 0.8	35.5 ± 4.5	7.2 ± 0.3
20	6.2 ± 1.2	-24.4 ± 0.6	4.7 ± 1.1	33.9 ± 4.8	8.4 ± 0.7
23	7.7 ± 0.9	-24.4 ± 0.2	5.1 ± 0.4	39.4 ± 3.1	9.0 ± 0.2
34	7.8 ± 0.6	-24.3 ± 0.1	3.1 ± 0.7	25.8 ± 4.9	9.7 ± 0.9

Table 2.2 - Mean changes (± 1 S.D.) in $\delta^{15}\text{N}$, $\delta^{13}\text{C}$, N content, C content, and C:N ratio of shrimp tissue collected at each time point during the 4°C experiment.

<u>Incubation Days</u>	<u>$\delta^{15}\text{N}$ (‰)</u>	<u>$\delta^{13}\text{C}$ (‰)</u>	<u>N Content (%)</u>	<u>C Content (%)</u>	<u>C:N</u>
0 - Control	6.1 ± 0.5	-22.6 ± 0.6	11.8 ± 0.5	40.0 ± 1.7	4.0 ± 0.1
3	6.7 ± 0.2	-22.0 ± 0.2	11.3 ± 0.5	39.8 ± 1.7	4.1 ± 0.1
7	6.3 ± 0.5	-22.4 ± 0.3	11.6 ± 0.3	39.8 ± 1.7	4.1 ± 0.1
16	6.1 ± 0.9	-21.9 ± 0.6	10.0 ± 2.4	35.7 ± 7.9	4.2 ± 0.1
22	6.1 ± 0.7	-22.3 ± 0.2	10.8 ± 1.1	39.3 ± 2.7	4.2 ± 0.2
29	6.7 ± 0.6	-22.4 ± 0.2	9.8 ± 2.2	35.4 ± 7.3	4.2 ± 0.1
33	6.6 ± 0.6	-22.2 ± 0.5	10.3 ± 0.3	38.3 ± 0.3	4.3 ± 0.2
62	6.3 ± 0.2	-23.1 ± 0.3	9.7 ± 0.8	39.4 ± 0.9	4.7 ± 0.3
97	6.6 ± 0.5	-23.9 ± 0.8	8.1 ± 1.5	39.2 ± 1.6	5.8 ± 0.9

Table 2.3 - ANCOVA results comparing N content (%), C Content (%), $\delta^{15}\text{N}$ (‰), $\delta^{13}\text{C}$ (‰) and $\Delta\text{C:N}$ values of decomposed shrimp tissue at both 4°C and 25°C. For the first four variables, temperature was used as the main effect, and $\Delta\text{C:N}$ was used as the covariate. In the last model ($\Delta\text{C:N}$), temperature was used as the main effect, and time (days) was used as the covariate

Variable	Source	DF	Sum of Squares	F-Ratio	P-value
<u>N Content (%)</u>	Model	2	311.10	93.22	<0.0001
	Temperature	1	0.00038	0.0002	0.98
	$\Delta\text{C:N}$	1	177.55	106.41	<0.0001
	Error	46	76.75	-	-
	Total	48	387.85	-	-
<u>C Content (%)</u>	Model	2	295.94	6.43	0.0034
	Temperature	1	3.70	0.16	0.69
	$\Delta\text{C:N}$	1	200.61	8.72	0.0049
	Error	46	1057.87	-	-
	Total	48	1353.81	-	-
<u>$\delta^{15}\text{N}$</u>	Model	2	26.02	11.28	0.0001
	Temperature	1	3.56	3.09	0.086
	$\Delta\text{C:N}$	1	23.18	20.10	<0.0001
	Error	46	53.03	1.15	-
	Total	48	79.04	-	-
<u>$\delta^{13}\text{C}$</u>	Model	2	89.57	23.71	<0.0001
	Temperature	1	13.67	7.24	0.0099
	$\Delta\text{C:N}$	1	17.23	9.12	0.0041
	Error	46	86.87	1.89	-
	Total	48	176.45	-	-
<u>$\Delta\text{C:N}$</u>	Model	3	157.92	152.58	<0.0001
	Temperature	1	147.82	428.46	<0.0001
	Time (Days)	1	83.27	241.34	<0.0001
	Temp*Time	1	53.64	155.47	<0.0001
	Error	45	15.53	-	-
	Total	48	173.45	-	-

more negative $\delta^{13}\text{C}$ values in the 25°C experiment relative to the 4°C experiment, while the slopes of both regressions did not differ significantly (Table 2.3, Figure 2.4).

2.4 Discussion

Particulate organic matter represents a major sink of carbon in the world's oceans and plays a significant role in global biogeochemical cycling. Although numerous studies have described compositional changes of POM in the water column, questions still remain concerning the processing of this POM, especially in the deeper ocean (<1000m). Thus, it is crucial to identify the source(s) of this organic matter and characterize the biological alterations it undergoes as it traverses the water column. Our efforts here focused on determining the compositional and isotopic alterations of organic matter associated with microbial activity in order to better explain vertical water column trends observed in the field.

2.4.1 Changes in elemental composition of OM

In our experiments, microbes preferentially remineralized nitrogen relative to carbon, a pattern consistent with the common observation that N_{org} is preferentially remineralized with respect to C_{org} in suspended and sinking particles in the deep ocean (Knauer et al. 1979, Hedges et al. 2001, Lee 2002). Our data suggest a preferential utilization of nitrogen-rich biomolecules (e.g., proteins), but our experiments did not explicitly test the potential importance of physical leaching as a pathway for loss of shrimp organic matter. However, the large Q_{10} values for both N (2.5) and C (9.0) content in our experiments both suggest that microbes are directly involved in decomposing shrimp tissue since biological processes typically show a large temperature effect (i.e., $Q_{10} > 2$). Our results also suggest that temperature does not significantly influence relative elemental composition changes in OM, despite significant differences in decomposition rate.

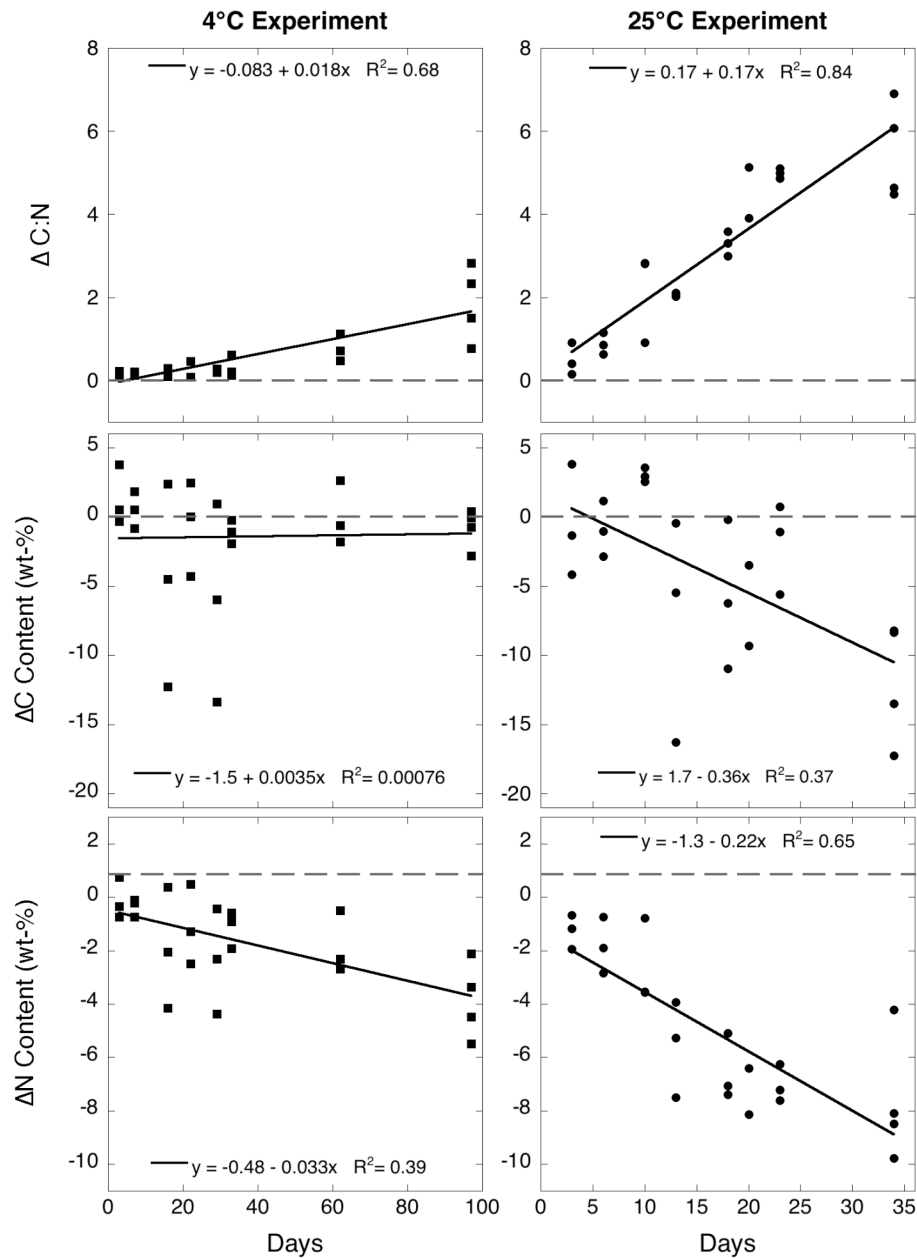


Figure 2.1 - Time course of $\Delta C:N$, ΔC Content and ΔN of shrimp tissue exposed to microbial decomposition at 4°C and 25°C. $\Delta C:N$ represents the differences in compositional values for paired shrimp halves ($\Delta C:N = C:N_{\text{Decomposed}} - C:N_{\text{Control}}$) at each removal date. The same calculation was made for N and C content. At least three shrimp halves were collected on each collection time point. Conditioned artificial seawater (CASW) was used as the incubation medium and was collected from aquaria housing live shrimp (*Palaemonetes* sp.). Total incubation time for the 4°C and 25°C assay was 97 days and 34 days, respectively.

2.4.2 Changes in $\delta^{15}\text{N}$ of OM

Previous studies documenting isotopic alteration of decomposing organic matter have been carried out at temperatures similar to those in surface waters (19-25°C) (Wada 1980, Zieman et al. 1984, Macko et al. 1994, Lehmann et al. 2002) and have not addressed decomposition under conditions typical of deeper, colder waters (2-4°C). Our results are consistent with previous studies that found increasing $\delta^{15}\text{N}$ of decomposing organic matter with time (Macko et al. 1994, Lehmann et al. 2002). For example, Macko et al. (1994) found higher $\delta^{15}\text{N}$ (+2.3‰) of powdered seagrass and sediment slurries incubated in anaerobic Winogradsky columns. Lehmann et al. (2002) found a ~3‰ increase in $\delta^{15}\text{N}$ of particulate organic matter decomposed over a similar time period in an oxic environment at 25°C, while we observed a 2‰ increase in shrimp tissue $\delta^{15}\text{N}$ in our 25°C experiment (oxic) over a similar time period (Fig. 2 & 4). Interestingly, Lehmann et al. (2002) saw a much smaller increase in C:N ratio in their oxic experiments ($\Delta\text{C:N}=2.5$) than we did ($\Delta\text{C:N}=5.4$), suggesting that the shrimp tissue used in our experiments was degraded more substantially than the POM used in Lehmann's experiments. Furthermore, Lehmann's results showed greater isotopic alteration per unit change in C:N ratio ($\Delta\delta^{15}\text{N}/\Delta\text{C:N} = 1.2\text{‰}$) than our data, despite the more extensive OM degradation we attained in our experiments ($\Delta\delta^{15}\text{N}/\Delta\text{C:N} = 0.4\text{‰}$). While these contrasts may reflect specific differences in experimental conditions (e.g., the microbial assemblages and composition of the organic matter used), the general pattern of $\delta^{15}\text{N}$ increasing with C:N ratio during aerobic decomposition appears to be robust. Despite differences in decomposition rate between our 4°C and 25°C experiments (Figure 1), we did not find any significant effect of temperature on the rate of change in the $\delta^{15}\text{N}$ of decomposing shrimp tissue, which suggests that similar biological processes altered shrimp tissue $\delta^{15}\text{N}$ regardless of decomposition rate.

Diagenetic processes may alter $\delta^{15}\text{N}$ of organic matter via release/loss of biomolecules with a distinctive $\delta^{15}\text{N}$, kinetic isotopic fractionation of proteins and amino acids through peptide bond hydrolysis and/or deamination, and/or the preferential addition of microbial biomass with a distinctive $\delta^{15}\text{N}$. All of these factors seem feasible given that: 1) amino acids exhibit different $\delta^{15}\text{N}$ values (Macko et al. 1987, McClelland & Montoya 2002, McCarthy et al. 2003, McClelland et al. 2003), 2) heterotrophic microbes are generally enriched in ^{15}N with respect to their substrate (Macko & Estep 1984, Macko et al. 1987), and 3) deamination reactions discriminate significantly against ^{15}N (Macko et al., 1986, Bada et al., 1989). Bulk isotopic analysis cannot distinguish the specific processes leading to ^{15}N enrichment of shrimp tissue in our experiments, but compound-specific analyses may help to elucidate these processes.

2.4.3 Changes in $\delta^{13}\text{C}$ of OM

In contrast with our results for $\delta^{15}\text{N}$, shrimp tissue exhibited significantly lower $\delta^{13}\text{C}$ as decomposition proceeded ($\Delta\text{C:N}$ increased) in both experiments. Low shrimp tissue $\delta^{13}\text{C}$ values in our 25°C experiment are consistent with other lab-based studies that document decreasing $\delta^{13}\text{C}$ of organic matter with time (Macko & Estep 1984, Macko et al. 1994, Lehmann et al. 2002). Decreasing $\delta^{13}\text{C}$ values could reflect either preferential addition of ^{13}C -depleted microbial biomass, preferential removal of organic molecules enriched in ^{13}C , or kinetic isotopic fractionation during decomposition. The first argument seems unlikely since microbes are generally enriched in ^{13}C with respect to their substrate (Macko & Estep 1984, Macko et al. 1987, Piao et al. 2006). The second process seems feasible, since preferential removal of relatively enriched organic molecules (e.g., proteins, nucleic acids) could have contributed to lower $\delta^{13}\text{C}$ values in the residual shrimp tissue. As noted above, increases in the C:N ratio of shrimp tissue were

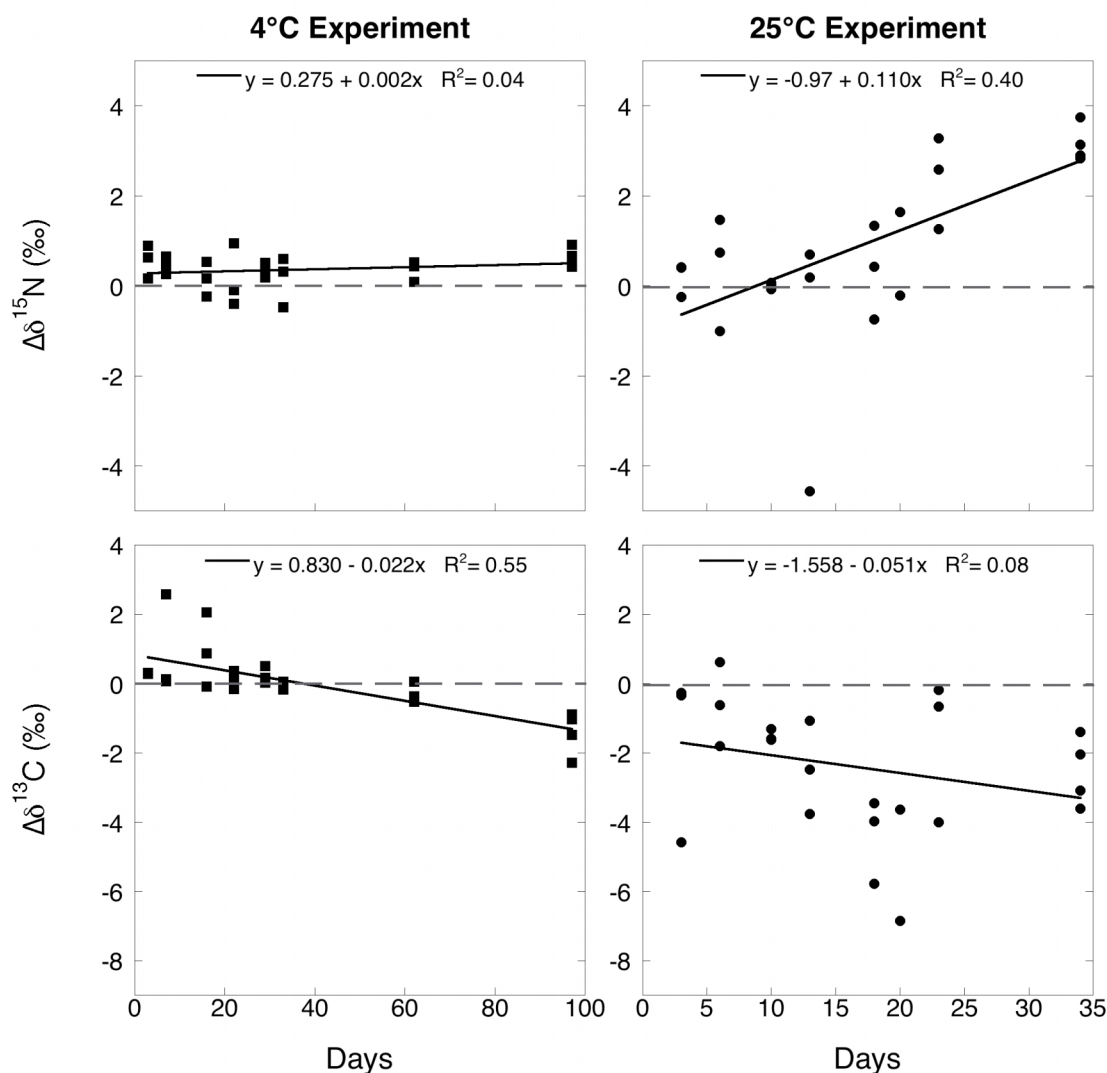


Figure 2.2 - Time course of $\delta^{15}\text{N}$ and $\delta^{13}\text{C}$ of shrimp tissue exposed to microbial decomposition at 4°C and 25°C. $\Delta\delta^{15}\text{N}$ represents the differences in compositional values for paired shrimp halves ($\Delta\delta^{15}\text{N} = \delta^{15}\text{N}_{\text{Decomposed}} - \delta^{15}\text{N}_{\text{Control}}$) at each removal date. The same calculation was made for $\delta^{13}\text{C}$. At least three shrimp halves were collected on each collection time point. Conditioned artificial seawater (CASW) was used as the incubation medium and was collected from aquaria housing live shrimp (*Palaemonetes* sp.). Total incubation time for the 4°C and 25°C assay was 97 days and 34 days, respectively.

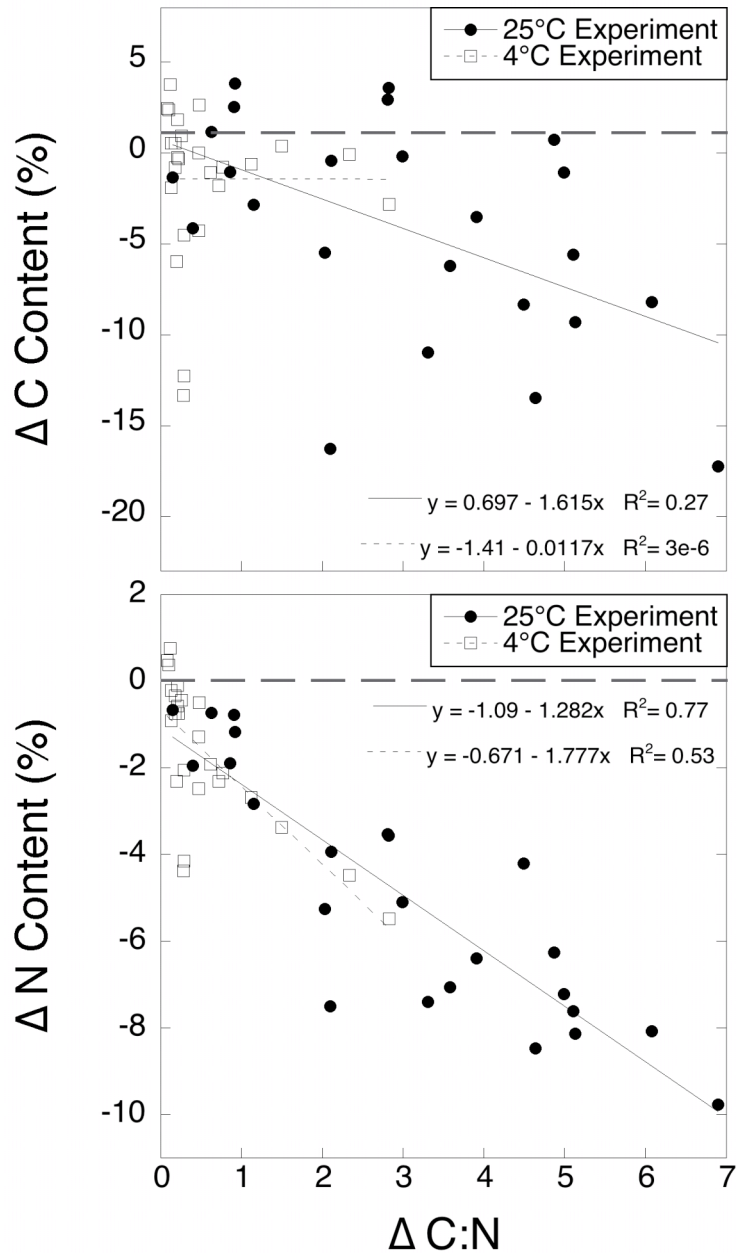


Figure 2.3 - Time course of $\delta^{15}\text{N}$ and $\delta^{13}\text{C}$ of shrimp tissue exposed to microbial decomposition at 4°C and 25°C. $\Delta\delta^{15}\text{N}$ represents the differences in compositional values for paired shrimp halves ($\Delta\delta^{15}\text{N} = \delta^{15}\text{N}_{\text{Decomposed}} - \delta^{15}\text{N}_{\text{Control}}$) at each removal date. The same calculation was made for $\delta^{13}\text{C}$. At least three shrimp halves were collected on each collection time point. Conditioned artificial seawater (CASW) was used as the incubation medium and was collected from aquaria housing live shrimp (*Palaemonetes* sp.). Total incubation time for the 4°C and 25°C assay was 97 days and 34 days, respectively.

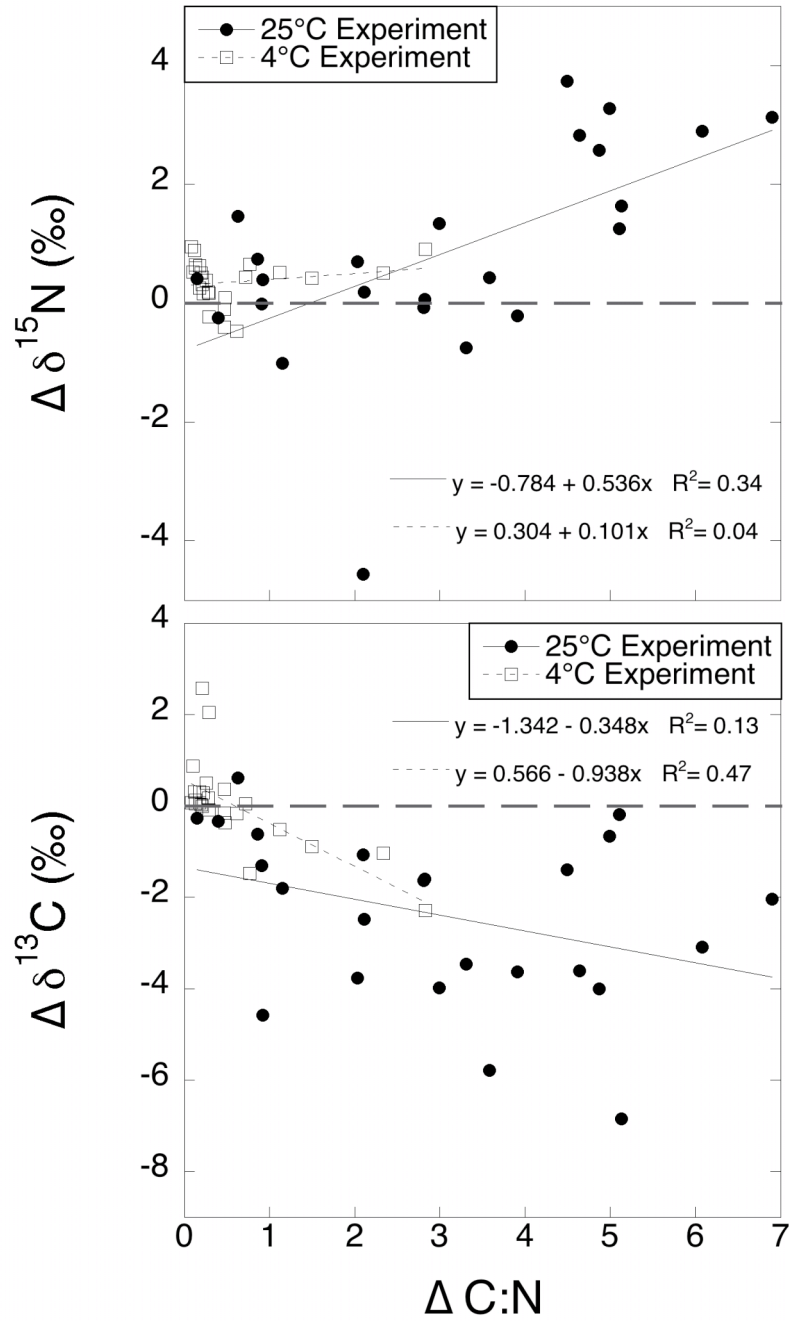


Figure 2.4 - Differences in $\delta^{15}N$ and $\delta^{13}C$ between paired shrimp halves ($\Delta\delta^{15}N = \delta^{15}N_{\text{Decomposed}} - \delta^{15}N_{\text{Control}}$) with increasing C:N ratio. C:N ratios of shrimp tissue provide a proxy for the microbial processing of the shrimp tissue, where higher C:N ratios signify more exposure to microbial decomposition. Conditioned artificial seawater (CASW) was used as the incubation medium and was collected from aquaria housing live shrimp (*Palaemonetes* sp.). Total incubation time for the 4°C and 25°C assay was 97 days and 34 days, respectively.

primarily driven by the removal of nitrogen, suggesting that nitrogenous components (e.g., proteins, nucleic acids) of the shrimp tissue were preferentially utilized and removed during decomposition. The minimal loss in C during the incubations, rising C:N ratios, and decreasing $\delta^{13}\text{C}$ of shrimp tissue all suggest that nitrogen-poor biomolecules, such as lipids, were conserved during the incubations.

C:N ratios are often used as an indicator of the state of OM, since increasing C:N ratios often represent OM with higher carbohydrate and lipid content with respect to proteins (Deniro and Epstein, 1978, Focken and Becker, 1998, Bodin et al., 2007). Our isotopic data suggest that lipids were conserved during our experiments, since proteins and carbohydrates are typically enriched in ^{13}C with respect to lipids (Deniro & Epstein 1977, Galimov 1981, Post et al. 2007). Other studies also suggest that proteins and carbohydrates are preferentially removed from phytoplankton during decomposition, leaving behind lipid-rich residual organic matter (Harvey et al. 1995).

Aside from the growing literature documenting both bulk and compound specific $\delta^{13}\text{C}$ of decomposing OM and/or associated biomolecules (Harvey & Johnston 1995, Harvey et al. 1995, Harvey & Macko 1997, Nguyen & Harvey 1997, Meckenstock et al. 1999, Lehmann et al. 2002, Lehmann et al. 2004, Sun et al. 2004, Dai et al. 2005, Ding & Sun 2005), few studies have focused on the mechanisms producing changes in $\delta^{13}\text{C}$ during decomposition. Several prior studies have documented clear changes in bulk $\delta^{13}\text{C}$ during decomposition. For example, both Macko et al. (1994) and Lehmann et al. (2002) found decreasing bulk $\delta^{13}\text{C}$ ($\Delta\delta^{13}\text{C} = -2.8\text{‰}$ and -1.8‰ , respectively) with decomposition of OM, but only the former experiment were consistent with the $\Delta\delta^{13}\text{C}$ of shrimp tissue in our experiments. These earlier experiments were conducted at 25°C , but our results show a clear effect of temperature on $\delta^{13}\text{C}$ alteration during decomposition. The higher $\delta^{13}\text{C}$ in our 4°C experiment relative to our 25°C experiment could be due to several factors, such as temperature-dependent kinetic isotopic fractionation effect (Galimov 1981, Silfer et al.

1992), OM exposure to different microbial communities, and differential selection and decomposition of isotopically distinct biomolecules (Harvey & Johnston 1995, Harvey et al. 1995, Harvey & Macko 1997, Nguyen & Harvey 1997, Ding & Sun 2005). Since kinetic fractionation varies with absolute temperature, the small relative temperature difference (298K vs 277K) between our experiments most likely did not dominate the isotopic changes we observed. Although our data clearly show the impact of biological processes on the isotopic composition of shrimp tissue, a more thorough analysis of the isotopic composition of individual components of the organic matter and the microbes reworking that OM will be required to resolve the mechanisms at work.

2.4.4 Ecological applications

2.4.4.1 Alteration of OM $\delta^{15}\text{N}$

Although this study does not directly address the isotopic alteration of POM associated with consumption by different heterotrophs (macrofaunal v. microbial), it does provide context for evaluating the potential mechanisms for isotopic transformation of both suspended and sinking particles in the ocean. Variation in the $\delta^{15}\text{N}$ of field-collected POM is generally attributed to differences in the type of particles collected (i.e., suspended v. sinking) and their exposure time to heterotrophic reworking (Altabet 1988, Altabet et al. 1991, Voss et al. 1996, Nakatsuka et al. 1997). For example, suspended POM at the Ocean Flux Program (OFP) site, south of Bermuda, became increasingly enriched in ^{15}N with depth while the $\delta^{15}\text{N}$ of sinking POM revealed the opposite pattern (Altabet et al. 1991). Altabet et al. (1991) hypothesized that the observed differences could be microbially-mediated, with suspended particles becoming more enriched in ^{15}N due to microbial hydrolysis and deamination reactions, while the $\delta^{15}\text{N}$ of sinking particles reflects microbial processes that preferentially remove ^{15}N or add ^{14}N . Sinking particles also tend to undergo compositional changes during transport as amino acids and proteins

are preferentially metabolized relative to lipids and carbohydrates, leading to C:N ratios increasing with depth). These compositional changes could lead to isotopic alteration independently of any kinetic fractionation during decomposition. Our results are consistent with previous studies that document an increase in the $\delta^{15}\text{N}$ of suspended POM with depth (Saino & Hattori 1980, Altabet et al. 1991, Saino 1992, Altabet & Francois 1994, Nakatsuka et al. 1997, Wu et al. 1999b), but contrast with observed vertical trends of decreasing $\delta^{15}\text{N}$ values of sinking particles with depth (Altabet et al. 1991, Voss et al. 1996, Wu et al. 1999b).

In both of our experiments, shrimp tissue was enriched in ^{15}N with increasing $\Delta\text{C:N}$, a proxy for the extent of decomposition. Our results suggest that microbes alone can drive significant decomposition of OM while simultaneously increasing the $\delta^{15}\text{N}$ of the residual OM via hydrolysis and deamination of nitrogenous components, regardless of decomposition rate. Thus, observed vertical profiles of suspended POM $\delta^{15}\text{N}$ in oceanic water columns may be explained by microbial heterotrophic reworking. However, if $\delta^{15}\text{N}$ is to be used as a tracer for N in suspended POM, further work (e.g., compound-specific analysis) is required to isolate the biochemical underpinnings leading to microbially-mediated isotopic fractionation (McClelland & Montoya 2002, McCarthy et al. 2003, McClelland et al. 2003). Despite these limitations, our results do provide an initial empirical index to the extent of OM decomposition/reworking (e.g., $\Delta\text{C:N}$ ratio) as a function of depth in the water column, which may help determine the extent of decomposition of POM in the water column as well as its trophic state (via stable isotope analysis).

There is little empirical evidence for decreases in the $\delta^{15}\text{N}$ of OM associated with microbial heterotrophy (Wada 1980, Macko & Estep 1984, Lehmann et al. 2002). Zieman et al. (1984) did observe considerable decreases in $\delta^{15}\text{N}$ of decomposing mangrove leaves, but the mechanisms driving this large isotopic alteration ($\sim 10\%$) have

yet to be determined, although N₂-fixation or dissolved nitrogen uptake (DIN) could have potentially driven these changes. Our results suggest that microbial decomposition alone does not contribute to the decrease in the $\delta^{15}\text{N}$ values of sinking particles observed in various ocean basins.

Vertical gradients in the $\delta^{15}\text{N}$ of suspended POM are generally stronger in surface waters (<500m) than in deeper, colder waters (>500m). This suggests that temperature could influence shifts in $\delta^{15}\text{N}$ of suspended POM, potentially through increased microbial activity at higher temperatures. However, our data show that microbial alteration of OM $\delta^{15}\text{N}$ is not significantly influenced by temperature, despite significant differences in decomposition rate. This suggests that similar diagenetic processes alter POM $\delta^{15}\text{N}$ regardless of temperature differences within the water column (warm surface waters vs. cold deep waters) and that the time of suspension within the water column is the primary factor controlling the extent of decomposition of OM as well as its isotopic composition. We expect that if we ran our 4°C experiment for a significantly longer time period, we would observe isotopic shifts similar to those we observed in the 25°C experiment. This further implies that decomposition experiments performed at 25°C can provide insight into processes under deep-sea temperature conditions.

2.4.4.2 Changes in $\delta^{13}\text{C}$ of OM

Vertical profiles of the $\delta^{13}\text{C}$ of both suspended and sinking POM show significant variation (Nakatsuka et al. 1997, Nakanishi & Minagawa 2003, Lourey et al. 2004). Several factors may influence $\delta^{13}\text{C}_{\text{POM}}$ in the water column, including compositional and isotopic alteration driven by microbial degradation (Qian et al. 1996, Harvey & Macko 1997, Megens et al. 1998, Hall et al. 1999, Meckenstock et al. 1999, Mazeas et al. 2002, McCarthy et al. 2004, Sun et al. 2004) and/or macrofaunal consumption and excretion (Small et al. 1987, Altabet & Small 1990, Montoya et al. 1992, Breteler et al. 2002, Turner 2002, Tamelander et al. 2006). Our results suggest that microbial decomposition

causes OM to become depleted in ^{13}C , which occurs due to either compositional alteration and/or kinetic fractionation of carbon isotopes during microbial decomposition. Other lab and field studies support our findings, yet vertical profiles of $\delta^{13}\text{C}_{\text{POM}}$ do not always show a decrease with depth (Nakatsuka et al. 1997, Lourey et al. 2004, Nakanishi & Minagawa 2003). However, several other lab studies suggest that fecal pellets produced by zooplankton are often depleted in ^{13}C relative to their food source, perhaps reflecting the presence of a peritrophic membrane around the pellet (Breteler et al. 2002, Tamelander et al. 2006). Thus, it may be more difficult to identify the processes that are influencing POM transformation in the water column through measurement of the bulk stable isotopic composition of POM. Further separation and analysis of the individual components of POM (i.e., amino acids, sterols, fatty acids) are required to discriminate between microbial and macrofauna processing.

2.4.4.3 Conclusions

Tracing the origin and transformation of POM within the world's oceans provides crucial information regarding present and past global biogeochemical cycles. However, we must first understand the proximate mechanisms for both elemental and isotopic alterations via biological activity before we can use isotopic distributions to characterize decompositional processes in nature. Our study focused on microbial decomposition, one of the major biological influences on POM abundance and composition in the oceans. Our results showed that N is preferentially utilized with respect to C, and that OM $\delta^{15}\text{N}$ increases with decomposition, but is not affected by incubation temperature. This implies that similar microbial processes drive elemental and isotopic changes in OM, and that decomposition experiments performed at higher temperatures are relevant for processes occurring in the deep ocean. This further suggests that vertical profiles of $\delta^{15}\text{N}$ can be interpreted without concern for fractionation effects caused by temperature differences.

CHAPTER 3

ORGANIC MATTER PROCESSING BY THE SHRIMP

PALAEEMONETES SP.: ISOTOPIC AND ELEMENTAL EFFECTS

3.1 Introduction

Fecal material plays an important role in particulate organic matter (POM) flux and nutrient cycling in aquatic ecosystems (Wotton & Malmqvist 2001). Fecal material can dominate the vertical flux of organic matter in pelagic environments, and is a critical component of the biological pump transporting C and N downward through the water column (Emerson & Roff 1987, Lampitt et al. 1990, Voss 1991, Dam et al. 1995, Le Fevre et al. 1998, Sarnelle 1999, Wassmann et al. 2000, Werner 2000, Dubischar & Bathmann 2002, Turner 2002, Dagg et al. 2003, Frangoulis et al. 2005). However, despite their importance for both regional and global C_{org} and N_{org} fluxes, the fate of fecal pellets sinking out of the surface ocean is still not well understood. A number of workers (Wakeham 1995, Burns et al. 2003, Stubing & Hagen 2003, Burns et al. 2004) have used sterols and fatty acids as biomarkers to determine the type of heterotrophy responsible for reworking sinking POM, but have typically found it difficult to separate the effects of reprocessing by larger grazers (e.g., copepods) and microbes. Other investigators (Wada & Hattori 1976, Altabet & McCarthy 1986, Altabet et al. 1991, Voss et al. 1996, Hernes et al. 2001, Schneider et al. 2003) have focused on vertical trends in the chemical and isotopic composition of POM as markers of its origin and fate. However, despite some success in characterizing organic matter transformation, few studies have actually determined the isotopic alteration associated with crustacean digestion of organic matter (Turner 1987, Checkley & Miller 1989, Sato et al. 2002, Turner 2002). The impact of macrocrustaceans on organic matter transformation and/or remineralization is critical to understanding the impact of these trophic processes on the efficiency of the biological

pump in pelagic ecosystems (Honda 2003, Andersson et al. 2004, Mackenzie et al. 2004). Here we present results from a lab-based study assessing the effects of feeding processes (e.g., “sloppy feeding”) and digestion on the isotopic and elemental composition of marine organic matter.

Stable isotopes of nitrogen and carbon have proved useful in tracing biologically-mediated input (Capone 2001, Montoya et al. 2002), transformation (Montoya et al. 1992, Nakatsuka et al. 1997, Peterson 1999, Breteler et al. 2002, Lehmann et al. 2002, Mackenzie et al. 2004), and export (Wada & Hattori 1976, Altabet 1988, Altabet et al. 1991, Altabet & Francois 1994, Voss et al. 1996, Wu et al. 1997, Peterson 1999, Smith et al. 2002, Lourey et al. 2003, Lourey et al. 2004) of these elements in marine ecosystems. Various studies have focused on the isotopic fractionation associated with the movement of carbon and nitrogen through individual organisms and/or food webs (Deniro & Epstein 1981, Peterson & Fry 1987, Wada et al. 1987, Kling et al. 1992, Montoya et al. 1992, Montoya et al. 2002), while other studies have addressed the potential for isotopic alteration of organic matter as a result of processing by individual organisms within those food webs (Checkley & Miller 1989, Altabet & Small 1990, Hasegawa et al. 2001, Breteler et al. 2002, Schmidt et al. 2003, Tamelander et al. 2006). However, despite this progress, questions still remain concerning the isotopic alteration of organic matter (OM) associated with crustacean digestion. Determining the isotopic impact of food handling and processing by animals will facilitate efforts to trace the flow and transformation of organic matter within ecosystems (Gannes et al. 1997, Peterson 1999).

3.2 Materials and Methods

Shrimp (*Palaemonetes* sp.) were housed in a 50-gallon aquarium filled with artificial seawater (ASW, Instant Ocean brand) mixed to a salinity of 18-20 PSU. The aquarium was maintained at 25°C in an environmental chamber. ASW was filtered internally by both a large sponge filter and a Whistler™ water recirculation filter pump.

Experiments were run twice daily, involving all shrimp living in the aquarium. During each experiment, shrimp were fed Tetramin™ fish food (flakes), and were allowed between 10-12 hours to consume the flakes and produce fecal pellets. At the end of each experiment, all solid organic matter (i.e., fecal pellets, leftover flakes) was removed from the aquarium and placed in a clean 1-L beaker for further separation and preparation for isotopic analysis. After organic matter collection, the shrimp were then fed after 1-2 hours to begin the next experiment. After the organic matter was collected, fecal pellets were carefully isolated using pre-combusted (450°C for 4 hours) Pasteur pipettes, placed on small weighing boats, and dried in an oven at 60°C. Fecal pellets were long, cylindrical particles (~3-7mm long, ~0.5-1 mm diameter) that were easily seen with the naked eye. Further examination with a dissecting microscope was necessary at times to distinguish between fecal pellets and unconsumed food. The remaining flake material ('leftovers') was also collected and dried.

Before beginning a new experiment, shrimp were visually inspected for flake food remaining in their guts in order to prevent carryover of fecal material from one experiment to the next. Fecal matter released by shrimp after the initial collection and before the next feeding was discarded. Shrimp were not obviously underfed since some uneaten flakes always remained in the aquarium. Incubations in which shrimp died were excluded from our analysis since consumption of carcasses/molts could affect the isotopic composition of the collected organic matter.

In order to determine the isotopic alteration of flake food due to prolonged exposure to ASW, dry flake food was placed into small, autoclaved flasks and submerged in 200mL of either freshly prepared ASW or conditioned artificial seawater (CASW) collected from the aquarium housing shrimp. This experiment was run twice, and 7-10 individual replicate flasks were used in each experiment. The dry flake food was soaked for at least 12 hours in either ASW or CASW and then collected from the flask and dried.

All bulk isotopic measurements were performed using a Micromass Optima continuous-flow isotope-ratio mass spectrometer (CF-IRMS) system. The mass spectrometer was interfaced to a Carlo-Erba NA2500 elemental analyzer used for combustion and purification of sample nitrogen and carbon. Solid samples were dried at 60°C, then ground with mortar and pestle, and stored in pre-combusted glass vials from which sub-samples were taken for isotopic analysis. All isotope abundances are expressed as δ values relative to either tropospheric N₂ ($\delta^{15}\text{N}$) or Pee Dee Belemnite ($\delta^{13}\text{C}$). Analytical error associated with bulk isotope measurements was typically better than $\pm 0.1\text{‰}$ for standards similar in size to our samples.

3.3 Results

As expected, fecal pellets showed declines in both N and C content with respect to the flake food while both ASW and CASW controls showed little change (Table 3.1). A one-way ANOVA revealed that C:N ratios of flake food differed significantly as a function of exposure to the shrimp in our aquarium ($F(4, 90) = 60.5$, $p < 0.0001$). A Tukey-Kramer HSD post-hoc test further showed that C:N ratios of fecal pellets (8.62 ± 1.2) were significantly ($p < 0.05$) greater than C:N ratios of dry flake food (6.61 ± 0.2). Both N and C content of fecal pellets differed significantly (**N content**: $F(4, 90) = 223.9$, $p < 0.0001$; **C content**: $F(4, 90) = 140.1$, $p < 0.0001$) with respect to the dry food source (Table 3.1, Figure 3.1). Pair-wise comparisons revealed a significantly lower C content after digestion by shrimp, with no other significant changes in the controls or leftover flakes. The N content of the fecal pellets were also significantly lower than in the dry flake food, while leftover flakes (including both macerated and unaltered flakes) also had a significantly lower N content than the dry flake food (Tukey's post-hoc test, $p < 0.05$). There were no other significant changes in either N or C content of the dry flake food.

Flake food did change significantly during our experiments ($F(4, 90) = 11.36$, $p < 0.0001$), but these changes were driven primarily by shrimp activity rather than digestion.

Fecal material showed no significant changes in $\delta^{15}\text{N}$ or $\delta^{13}\text{C}$ relative to either dry or soaked flake food (Tukey-Kramer HSD post-hoc test, $p < 0.01$). However, flake food $\delta^{15}\text{N}$ differed significantly as a result of exposure to feeding shrimp. The $\delta^{15}\text{N}$ of remaining flakes was 0.8‰ higher than the dry flake food and submerged flake food controls (Tukey-Kramer HSD, $p < 0.01$), while $\delta^{13}\text{C}$ remained unchanged throughout both the fecal pellet extraction experiments, and in the control ASW and CASW submersion experiments ($F(4, 90) = 1.46$, $p = 0.22$). There were no significant isotopic changes in either ASW or CASW control experiments (Tukey-Kramer HSD, $p < 0.01$).

3.4 Discussion

Our results suggest that organic matter consumed by shrimp does not undergo significant isotopic change despite clear decreases in both N and C content during gut passage. After shrimp digestion, the mean N and C content of the flake food dropped from 8.2% to 2.0% and from 47% to 14% by weight, respectively. However, despite considerable utilization of the flake food, we did not find any evidence for isotopic change of flake food associated with shrimp digestion. Our results are consistent with the minimal alteration of $\delta^{15}\text{N}$ with crustacean digestion observed in lab-based studies (Breteler et al. 2002, Tamelander et al. 2006), while contrasting with results from a number of field-based studies that have documented either higher (Altabet & Small 1990, Montoya et al. 1992, Small & Ellis 1992) or lower (Montoya et al. 1992, Schmidt et al. 2003, Tamelander et al. 2006) $\delta^{15}\text{N}$ values for crustacean-derived fecal pellets relative to the food source. Our results also contrast with the more negative fecal pellet $\delta^{13}\text{C}$ values observed in these studies (Breteler et al. 2002, Tamelander et al. 2006).

The varied outcomes in these experiments could be influenced by a number of factors including the incorporation of components other than fecal pellets (e.g., eggs) into the isotopic analysis (Breteler et al. 2002, Tamelander et al. 2006), selective feeding by

Table 3.1 - Mean (± 1 S.D.) $\delta^{15}\text{N}$, $\delta^{13}\text{C}$, Nitrogen (N) content, Carbon (C) content, and C:N ratios of flake food exposed to various environments. ‘Dry flake food’ represents flake food that has not been exposed to any experimental factor (negative control). ‘Feces’ represents the fecal material collected during each experiment and the ‘leftovers’ represent the remaining organic matter during those experiments. ‘ASW’ and ‘CASW soak’ values represent dry flake food soaked in incubation media.

<u>Source</u>	<u>$\delta^{15}\text{N}$ (‰)</u>	<u>$\delta^{13}\text{C}$ (‰)</u>	<u>N Content</u> <u>(wt-%)</u>	<u>C Content</u> <u>(wt-%)</u>	<u>C:N</u>
Dry Flake Food	5.5 ± 0.2	-23.1 ± 0.2	8.2 ± 0.2	46.7 ± 1.3	6.6 ± 0.2
Feces	5.5 ± 0.5	-23.0 ± 1.2	2.0 ± 0.9	14.3 ± 1.0	8.6 ± 1.2
Leftovers	6.3 ± 0.6	-22.5 ± 1.0	6.1 ± 0.9	31.6 ± 1.2	6.0 ± 0.4
ASW Soak	5.6 ± 0.3	-23.1 ± 0.3	7.8 ± 1.0	43.0 ± 1.3	6.4 ± 0.2
CASW Soak	5.8 ± 0.1	-23.0 ± 0.2	7.9 ± 0.9	41.3 ± 1.3	6.1 ± 0.1

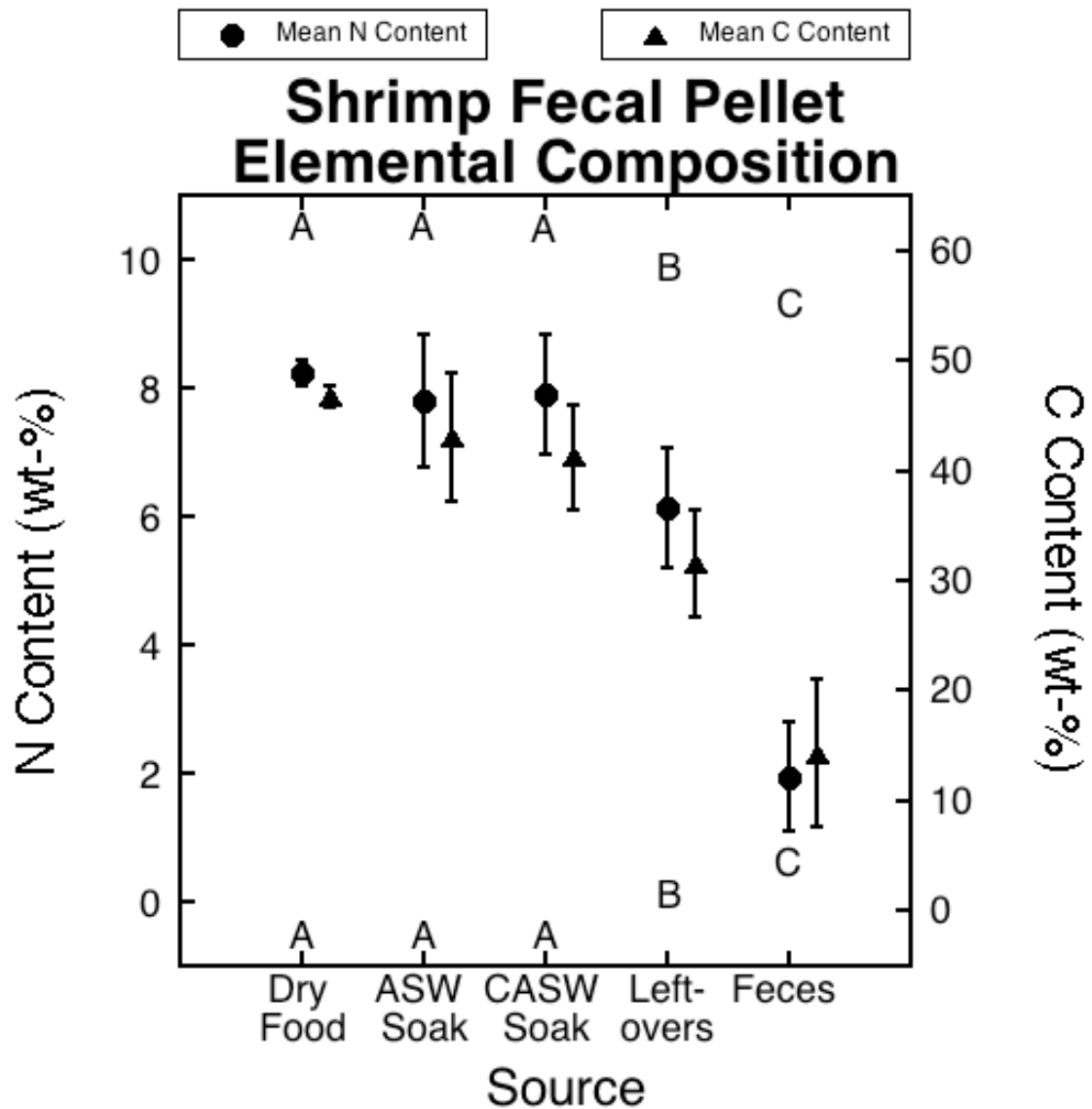


Figure 3.1 - Mean N and C content (wt-%) of dry flake food, flake food remaining after experiments (leftovers), shrimp fecal pellets (feces), as well as flake food soaked in either ASW or CASW. Mean treatment values represented by different letters are significantly different ($p < 0.01$). Upper letters represent N content comparisons, while lower letters represent C content comparisons. Error bars are set at ± 1 S.D.

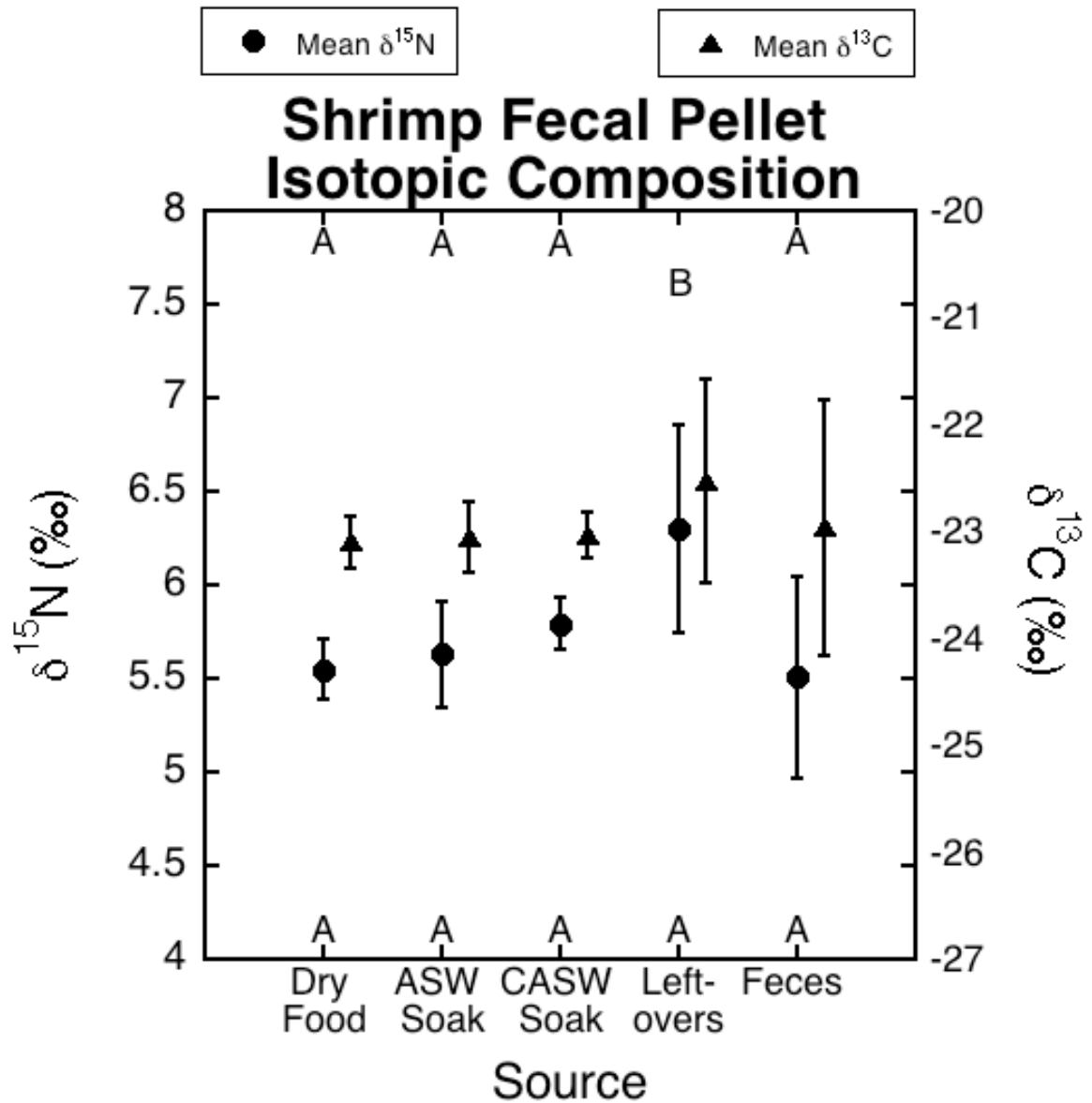


Figure 3.2 - Mean $\delta^{13}\text{C}$ and $\delta^{15}\text{N}$ (‰) of dry flake food, flake food remaining after experiments (leftovers), shrimp fecal pellets (feces), as well as flake food soaked in either ASW or CASW. Mean treatment values represented by different letters are significantly different ($p < 0.01$). Upper letters represent $\delta^{15}\text{N}$ comparisons, while lower letters represent $\delta^{13}\text{C}$ comparisons. Error bars are set at ± 1 S.D.

crustaceans from a mixed food supply (Checkley & Entzeroth 1985, Altabet & Small 1990, Montoya et al. 1992), or the type of organism observed (e.g., euphausiids (Schmidt et al. 2003) versus shrimp). Since our shrimp were provided an isotopically homogeneous food source, we reduced potential isotopic contamination via introduction of other sources (e.g., eggs, macerated, undigested flake food) during fecal pellet collection. Our results also provide a clearer understanding of the isotopic alteration of organic matter in the course of crustacean digestion. In particular, our data suggest that fecal pellets originating from decapods, like shrimp, will retain the isotopic signature of the shrimp's food sources (Lampitt et al. 1990, Wassmann et al. 2000, Werner 2000, Wotton & Malmqvist 2001, Turner 2002).

The absence of significant isotopic alteration of organic matter during crustacean digestion suggests that there is neither significant kinetic fractionation, nor preferential utilization of isotopically distinct classes of biochemicals (i.e., proteins vs. lipids) or specific biomolecules (i.e., amino acids) during gut passage and digestion in these shrimp. Proteins, carbohydrates and lipids generally differ in both $\delta^{15}\text{N}$ and $\delta^{13}\text{C}$ (Galimov, 1981) while there is also considerable variability in the $\delta^{15}\text{N}$ and $\delta^{13}\text{C}$ of individual amino acids and fatty acids (McClelland & Montoya 2002, McCarthy et al. 2003, McCarthy et al. 2004). We would expect a change in the isotopic composition of organic matter if the proportions of these biochemical fractions or biomolecules changed appreciably during crustacean digestion of organic matter. However, we see no isotopic evidence that supports preferential utilization of specific biomolecules of organic matter, despite considerable and differential loss of N and C. We recognize that the digestive processes of *Palamonetes* sp. may not widely represent all crustaceans. Despite this restriction, our data provide an initial assessment of OM isotopic and elemental alteration associated with crustacean digestive processes, which has received minimal attention to date.

Our data also suggest that larger crustaceans can influence both the elemental and the isotopic composition of organic matter without actually ingesting that organic matter. Many larger organisms play a critical role in energy transfer and recycling in aquatic ecosystems simply by their daily function within that ecosystem (Graca 2001, Goldthwait et al. 2004, Goldthwait et al. 2005). For example, euphausiids have been shown to disaggregate larger particles by both particle entrainment and their swimming movement (via beating pleopods) (Dilling & Alldredge 2000, Goldthwait et al. 2004, Goldthwait et al. 2005). However, little is known about how larger organisms, like euphausiids, may indirectly affect the elemental and isotopic composition of organic matter via non-consumptive activities.

Like many decapod crustaceans, shrimp are ‘sloppy’ feeders, macerating food and shedding pieces that are not consumed (Dilling & Alldredge 2000, Graca 2001, Goldthwait et al. 2004, Goldthwait et al. 2005, Ferreira et al. 2006). In our experiments, shredded food was altered in both elemental and isotopic composition relative to both dry and soaked flake food. The mean N and C content of macerated flake food decreased from 8.2% to 6.1% and 47% to 32% by weight, respectively. The mean N content of macerated food was significantly different than any of our controls (i.e., dry flake food, flakes soaked in ASW or CASW), while differences between our controls were not significant. We obtained slightly different results for changes in C content of food with exposure to shrimp. Although the mean C content of the macerated food was significantly different than both of our controls, the mean C content of CASW soaked food was also significantly different than the dry food. Our results suggest that shrimp maceration facilitates either increased microbial decomposition and/or C leaching of organic matter.

Shrimp maceration also influenced the isotopic composition of flake food. The $\delta^{15}\text{N}$ of macerated food was 0.8‰ higher than the $\delta^{15}\text{N}$ of the dry flake food. In contrast, $\delta^{13}\text{C}$ did not change significantly after shrimp maceration. Parallel experiments also did

not show any significant isotopic change of the flake food when soaked in either ASW or CASW in the absence of animals, suggesting that larger consumers link $\delta^{15}\text{N}$ changes to maceration. The higher $\delta^{15}\text{N}$ of macerated food suggests preferential removal of biomolecules with lower $\delta^{15}\text{N}$ via leaching and/or microbial remineralization. Since larger organisms often facilitate microbial reprocessing of organic matter in aquatic systems (Graca 2001, Goldthwait et al. 2005), accelerated microbial decomposition and/or physical leaching of nitrogenous components due to maceration seems to be the two likely explanations for our observations. Separating the effects of microbial processing and physical leaching of the macerated organic matter, thus, deserves future examination.

3.4.1 Ecological/Biogeochemical applications

Our results provide an interesting comparison with other studies aimed at determining the isotopic composition of zooplankton fecal material in two ways: 1) our experimental design allowed us to relate fecal material directly to the food source by using an isotopically homogeneous food source and minimizing contamination, and 2) our experimental design allowed us to investigate the potential isotopic alterations occurring as a result of feeding activity, but not directly associated with digestion (i.e., sloppy feeding). Our results add to the growing knowledge of elemental and isotopic alteration through zooplankton processing, and are relevant to observed vertical trends of suspended and sinking $\delta^{15}\text{N}_{\text{POM}}$ in the world's oceans.

The $\delta^{15}\text{N}$ of sinking POM caught in sediment traps typically decreases with depth, a trend that may reflect reprocessing and coprophagy by deep-dwelling zooplankton (Altabet et al. 1991, Voss et al. 1996, Nakatsuka et al. 1997). Our results suggest that crustacean feeding activities alone may not lead to a decrease in $\delta^{15}\text{N}$ of sinking POM, though other studies have documented decreases in $\delta^{15}\text{N}$ of organic matter associated with crustacean digestion (Schmidt et al. 2003, Tamelander et al. 2006). These mixed

results likely reflect factors such as food choice, crustacean taxon (i.e., copepods vs. decapods), life stage, reproductive status of the organisms (e.g., egg production), and animal size (Checkley & Miller 1989, Altabet & Small 1990, Montoya et al. 1992, Schmidt et al. 2003, Tamelander et al. 2006). Additional studies focused on the influence of metazoans on vertical trends in the $\delta^{15}\text{N}$ and $\delta^{13}\text{C}$ of POM in the ocean may help resolve these uncertainties.

Crustaceans can disaggregate marine snow within the water column, and thus directly influence particle size and flux (Dilling et al. 1998, Dilling & Alldredge 2000, Dilling & Brzezinski 2004, Goldthwait et al. 2005). Our results suggest that this disaggregation may also influence the elemental and isotopic composition of organic matter within the water column, since maceration alone had a clear effect on both the N content and $\delta^{15}\text{N}$ of organic matter in our experiments. In oceanic systems, this animal-mediated disaggregation may contribute to vertical changes in both POM flux and isotopic distributions. Future studies should include in-situ experiments to determine the direct (i.e., consumptive) and indirect (i.e., non-consumptive) influence of zooplankton on particle size, flux, and composition (both isotopic and elemental) while also observing other consequences such as DOM release and utilization by other organisms within these systems.

CHAPTER 4

BASIN-SCALE DISTRIBUTIONS OF STABLE NITROGEN

ISOTOPES IN THE SUBTROPICAL NORTH ATLANTIC OCEAN:

MOVEMENT OF DIAZOTROPH NITROGEN INTO

MESOOZOOPLANKTON

4.1 Introduction

Nitrogen (N) typically limits marine primary production over large areas of the world's oceans on biological timescales (Ryther & Dunstan 1971, Graziano et al. 1996, Moore et al. 2008). Regenerated nitrogen, or inorganic nutrients that have been recycled through various biological pathways in the upper ocean (e.g., NH_4^+ released through decomposition of OM), can support a large fraction of total primary production, but “new” N inputs are required to sustain primary production due to N losses from surface waters (i.e., sinking particles). New N, defined as unrecycled, allochthonous N (e.g., deep NO_3^-) (Dugdale & Goering 1967), can enter the euphotic zone via diapycnal mixing (Lewis et al. 1986), upwelling and/or eddy diffusion (McGillicuddy et al. 1998), atmospheric deposition (Duce et al. 2008), or through N_2 -fixation (Capone et al. 2005, Mahaffey et al. 2005, Karl & Letelier 2008). New N sustains primary production in the upper ocean and acts as a regulator on global oceanic and atmospheric carbon sequestration via the biological pump. At steady state, new production has been linked to export flux out of surface waters, and thus, the inputs of new N dictate the ability of the biological pump to produce and move organic C through the oceans (Eppley & Peterson 1979).

Biological N_2 -fixation provides a crucial source of new N to the world's oceans, especially in oligotrophic oceanic gyres (Capone et al. 1997, Capone et al. 2005,

Montoya et al. 2007). Shipboard N₂-fixation rate measurements have shown considerable N inputs via diazotrophs (Carpenter et al. 1999, Falcon et al. 2004a, Montoya et al. 2004, Capone et al. 2005, Montoya et al. 2007, Zehr et al. 2007). Other methods have been employed to estimate diazotroph activity in the world's oceans, by comparing global nutrient distributions that deviate from Redfield ratios (e.g., N*) (Gruber & Sarmiento 1997), and by tracking the global occurrence and production of important N₂-fixers via satellite (e.g., *Trichodesmium* spp.) (Subramaniam et al. 2002, Westberry et al. 2005, Westberry & Siegel 2006). Despite our heightened appreciation for biological N₂-fixation and its role as a crucial process driving new production in the world's oceans, relatively little is known about the extent to which new N influences production of higher trophic levels, such as mesozooplankton (LaRoche & Breitbarth 2005, Brandes et al. 2007).

For decades, ecologists and oceanographers have used the natural distribution of stable isotopes to trace the inputs and fate of N in ecosystems (Deniro & Epstein 1981, Altabet et al. 1991, Post 2002, West et al. 2006). This approach requires isotopically distinct end members, as well as information concerning the isotopic alteration between separate organic pools, in order to accurately describe both the source and transformation of N within oceanic systems via the natural distribution of stable isotopes. Basin-scale nitrogen isotope mapping provides information on spatial variation of “new” N inputs and movement through these food webs (Montoya et al. 1992, Waser et al. 2000, Dore et al. 2002, Mino et al. 2002, Montoya et al. 2002), and can further provide a rough estimate of the standing stock of exportable POM out of the euphotic zone (Eppley & Peterson 1979).

The North Atlantic Ocean is the best sampled oceanic basin, and high N₂-fixation rates in the basin have been measured from both shipboard experiments and geochemical approaches (Mahaffey et al. 2005). Strong vertical thermal stratification is constant in the tropical North Atlantic (south of 25°N), and most pronounced during the summer

months in the subtropics. In the subtropics, deep convective mixing occurs during the winter months, deepening the mixed layer to ~300m. With the coming spring, greater light penetration, a shallower mixed layer depth, and abundant nutrients from winter mixing facilitates a phytoplankton bloom that lasts several weeks to a month. Biological production and subsequent export of OM out of the mixed layer quickly removes N from this zone. The mixed layer remains N-depleted throughout the summer months, and recycling and allochthonous N inputs stimulate primary production. External N inputs originate from infusion of deep NO_3^- through upwelling, diapycnal mixing and eddy diffusion, or from N inputs via N_2 -fixing organisms. The two dominant N sources (i.e., deep NO_3^- and N_2 -fixation) have distinct isotopic signatures (4.5‰ versus -2‰, respectively), providing a suitable environment to model the isotopic mass balance of nitrogen isotopes within the mixed layer. Our isotope mass balance model allows us to trace biologically mediated input, transformation and export of organic N through the mixed layer and into deeper waters.

Previous studies have used stable N isotopes to determine the relative contribution of N_2 -fixation to suspended particles (Waser et al. 2000, Mino et al. 2002, Montoya et al. 2002, Reynolds et al. 2007) and mesozooplankton (Montoya et al. 2002). However, to our knowledge, no study has assessed basin-wide lateral and vertical (below the mixed layer) variation in $\delta^{15}\text{N}$ of both suspended particles and mesozooplankton in the STNA. Finer spatial and vertical resolution of $\delta^{15}\text{N}$ distributions helps constrain the geographical and vertical N_D contribution to oceanic food webs in the STNA. Here we report on N stable isotope measurements of a basin-scale set of vertically resolved samples of suspended particles and mesozooplankton). We separated mesozooplankton by size, providing insight into the movement of N into and through oceanic food webs of oligotrophic systems. The depth-integrated isotopic composition of both particles and zooplankton provides a platform for discussing the importance of biologically mediated input, transformation and export of new N in oceanic gyres.

4.2 Materials and Methods

Seawater and plankton samples were collected on R/V Seward Johnson cruise SJ0005 (April 25 – May 24 2000), from Ft. Pierce, FL to the Canary Islands (Figure 4.1). Water samples were collected using a CTD -rosette system, equipped with a fluorometer. Suspended particles were collected by gentle pressure filtration of 1.5-18 liters of seawater through pre-combusted (450°C for 2 h) 45-mm GF/F filters that were dried at 60°C and stored over desiccant for analysis ashore. For isotopic and elemental analysis, filters containing particle samples were trimmed to remove the particle-free edge, then cut into quadrants or halves that were pelletized in tin capsules. Seawater nutrient analysis was performed at sea using a Lachat QuickChem 8000 FIA nutrient analyzer.

Mesozooplankton were collected either in diagonal tows of a meter net (333- μ m mesh) through the upper 100m of the water column or with a 1-meter MOCNESS (333- μ m mesh size) deployed to sample zooplankton within 100-m vertical depth increments through the upper 500m of the water column. The MOCNESS flowmeter was used to calculate the total volume of seawater filtered through each net, but the volume of seawater filtered through the meter net was not measured. Animals were separated into size fractions by passage through a set of graded Nitex sieves (4000 μ m, 2000 μ m, 1000 μ m, 500 μ m, 250 μ m) and then immediately frozen. Once ashore, zooplankton samples were dried at 60°C and ground into a fine powder, which was then sub-sampled and pelletized in tin capsules for isotopic analysis. All zooplankton size fractions were weighed after drying to obtain total dry weight (mg) of the zooplankton collected at each station.

All natural abundance N isotope measurements were made by continuous-flow isotope-ratio mass spectrometry (CF-IRMS) using one of two instruments: a Micromass Optima at Georgia Tech, or either a Finnigan MAT-251 or Micromass Isoprime at UMass-Dartmouth. Each mass spectrometer was interfaced to an elemental analyzer for online combustion and purification of sample nitrogen and carbon. Carbon isotope data

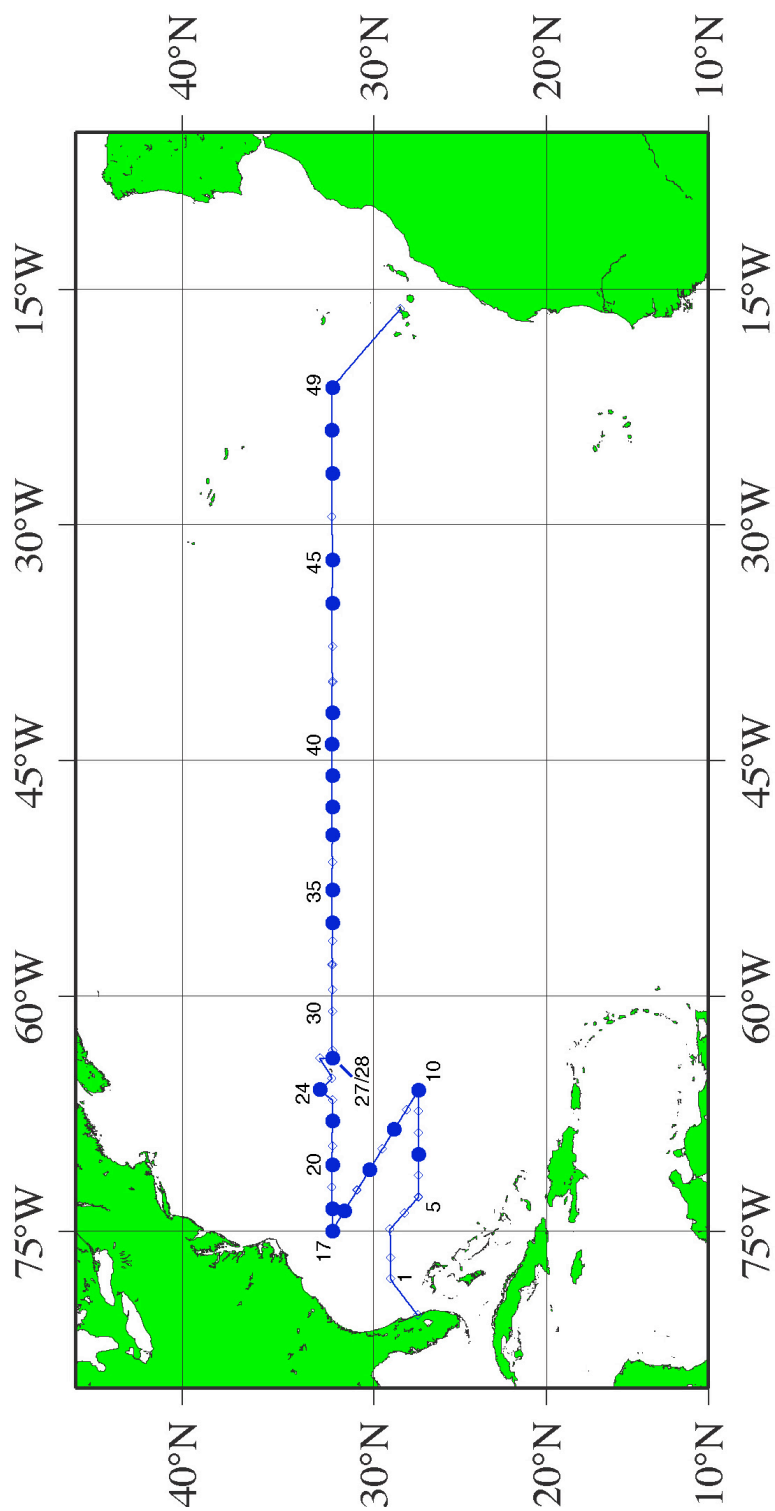


Figure 4.1 - Chart of cruise track SJ0005 comprised of three Legs: Leg 1 travels from Ft. Pierce, FL eastward towards the center of the North Atlantic gyre, Leg 2 turns northwest towards the eastern coast of the US, and Leg 3 turns westward at $\sim 32^{\circ}\text{N}$ and traverses the basin, terminating eventually in the Canary Islands. Solid circles represent stations where a MOCNESS was deployed and open diamonds represent stations where meter nets were deployed to collect mesozooplankton.

will be presented elsewhere. The CF-IRMS systems used were intercalibrated by running a variety of isotopically characterized organic (peptone, acetanilide, methionine, histidine, and glycine) and inorganic (KNO_3 and NH_4Cl) standards. All nitrogen isotope abundances are reported as $\delta^{15}\text{N}$ values relative to atmospheric N_2 . Each analytical run included a size series of elemental (acetanilide or methionine) and isotopic (peptone) standards, which provided a check on the stability of the instrument and allowed us to remove the contribution of any analytical blank from our isotopic measurements (Montoya 2008). In almost all cases, the blank was trivially small relative to the samples run and a blank correction was unnecessary. We conservatively estimate that the overall analytical precision of our isotopic measurements is better than $\pm 0.1\%$.

Diazotrophic N contribution was calculated for both particles and zooplankton using the isotope mass balance approach of Montoya et al. (2002). However, reference values for zooplankton were updated to include $\delta^{15}\text{N}$ values obtained from zooplankton collected on more recent cruises in both the North Atlantic and the South Pacific (Table 4.1). Reference values included zooplankton that were collected in the upper 100m of the water column between 3°N and 3°S of both the Atlantic and Pacific Oceans, a region where surface processes should be dominated by deep NO_3^- inputs via equatorial upwelling.

The mean $\delta^{15}\text{N}$ of particulate nitrogen (PN) in the upper water column was calculated by trapezoidal integration as a function of depth:

$$\text{Weighted Mean } \delta^{15}\text{N}_{SP} = \frac{\sum (PN_i \times \Delta z_i \times \delta^{15}\text{N}_i)}{\sum (PN_i \times \Delta z_i)} \quad (4.1)$$

where PN_i represents the PON concentration (μM), $\delta^{15}\text{N}_i$ represents the isotopic composition of suspended particles, and Δz_i is the depth interval (m) represented by sample (i) (Montoya et al. 1992). Similarly, we calculated the mean depth- and biomass-integrated $\delta^{15}\text{N}$ for individual mesozooplankton size fractions as:

$$\text{Weighted Mean } \delta^{15}N_{ZP} = \frac{\sum (B_{ij} \times \Delta z_i \times \delta^{15}N_{ij})}{\sum (B_{ij} \times \Delta z_i)} \quad (4.2)$$

where B_{ij} and $\delta^{15}N_{ij}$ are the biomass and $\delta^{15}N$, respectively, of zooplankton in size class (j) in interval (i) of thickness Δz_i .

Spatial variation in $\delta^{15}N$ of suspended particles ($\delta^{15}N_{SP}$) was evaluated using 2-way ANOVA with both depth and longitude as independent variables. Alternatively, $\delta^{15}N$ values of mesozooplankton ($\delta^{15}N_{ZP}$) were compared using a general linear model (GLM), which included two fixed variables, size fraction and time of collection (Day or Night), while treating depth and longitude as covariates. Daytime (0600-1800), local time) and nighttime (1800-0600) categories were used to evaluate the isotopic variation associated with diel vertical migration through the water column. A full factorial design was used in all analyses in order to determine interactions between variables. All non-significant variables and interactions ($p > 0.05$) were removed in a follow-up reduced model to increase the statistical power of our GLMs.

Latitudinal comparisons of $\delta^{15}N_{ZP}$ values were performed using an ANCOVA that compared mean $\delta^{15}N_{ZP}$ at southern stations (Leg 1 – stations 7, 9, 10) that overlapped with more northern stations (Leg 3 – stations 20, 22, 24), where latitude (North or South) and size fraction were fixed variables, and depth and longitude were included as covariates. All non-significant variables and interactions ($p > 0.05$) were removed from our analysis. In all statistical tests, p-values < 0.05 were considered significant.

4.3 Results

4.3.1 SJ0005 Leg 1 – Stations 2-10

Leg 1 extended from station 2 (29°3.6'N, 76°42.6'W) eastward to station 3 (29°4.8'N, 74°N51.6'W), southwest to station 5 (27°30'N, 72°49.8'W), and finally due east to station 10 (27°29'N, 66°0.3'W). We do not focus on Leg 1, due to spatial gaps in

Table 4.1 - Mean reference $\delta^{15}\text{N}$ values (‰) for mesozooplankton collected in both the northern tropical Atlantic and southern tropical Pacific Oceans between 3°N and 3°S. Error is represented by ± 1 standard deviation.

Mean Reference Zooplankton $\delta^{15}\text{N}$ Values (‰)				
<u>Size Fraction</u>	<u>SJ0609 – Atlantic Ocean</u>	<u>SJ9603 – Atlantic Ocean</u>	<u>KM0704 – Pacific Ocean</u>	<u>All Cruises</u>
>4000	4.5 \pm 1.3	N/A	5.0 \pm 0.6	4.7 \pm 1.2
2000-4000	5.4 \pm 0.8	6.9 \pm 0.7	5.6 \pm 0.5	5.8 \pm 0.9
1000-2000	4.1 \pm 0.5	6.1 \pm 0.7	5.6 \pm 0.3	5.1 \pm 1.0
500-1000	4.0 \pm 0.9	5.5 \pm 0.8	3.0 \pm 0.4	4.3 \pm 1.2
250-500	3.2 \pm 0.9	4.5 \pm 1.0	4.2 \pm 0.4	3.7 \pm 0.9

$\delta^{15}\text{N}_{\text{SP}}$ and $\delta^{15}\text{N}_{\text{ZP}}$ data, and only use the data acquired along this transect for latitudinal comparisons for stations that overlap in longitude with Leg 3.

4.3.2 SJ0005 Leg 2 – Stations 10-17

Leg 2 extended northwestward from Station 10 (27°29'N, 66°0.3'W) to station 17 (32°16'N, 75°W) (Figure 4.1). In the upper 500m of the water column, temperatures ranged from 16-22°C, coinciding with σ_t values that ranged from 25-26.5 (Figure 4.2A). Both temperature and salinity shoaled west of 70-75°W. The 1- μM NO_3^- contour ranged between 75-200m along Leg 2, with considerable spatial variation (Figure 4.2B). Our fluorometric measurements show a clear pigment maximum around the base of the mixed layer, with an average depth of 75m west of 71°W and deepening to ~125m east of 71°W (Figure 4.2B).

$\delta^{15}\text{N}_{\text{SP}}$ values differed significantly with depth (GLM, F-ratio = 13.68, dF = 1, $p < 0.001$) exhibiting higher $\delta^{15}\text{N}_{\text{SP}}$ values below the mixed layer (4-8‰) than in the upper 100m (0-4‰). $\delta^{15}\text{N}_{\text{SP}}$ values did not differ significantly with longitude along this transect (GLM, F-ratio = 1.41, dF = 1, $p = 0.24$) (Figure 4.3). Higher $\delta^{15}\text{N}_{\text{SP}}$ values also occurred below 125m at stations located on the western (74°30'W-75°W) and eastern ends (66°W-68°W) of Leg 2, where $\delta^{15}\text{N}_{\text{SP}}$ ranged between 6-8‰. Two features (Labeled A & B in Figure 4.3) of lower $\delta^{15}\text{N}_{\text{SP}}$ values (0-2‰) occurred along this transect: the westernmost between 72°W-74°30'W and the easternmost between 71°W-67°30'W. These zones were distinctly different in their vertical structure. The western feature occupied the uppermost 25-125m of the water column, while the eastern feature spanned the entire upper 250m of the water column, with the lowest isotopic values in the upper 75 m. In these two regions, diazotrophs contributed up to 80% of the N in the suspended particles.

$\delta^{15}\text{N}_{\text{ZP}}$ values ranged from 1-7‰ along this transect, with lower values tending to occur in the upper 200m of the southeastern end of the transect (Figure 4.4).

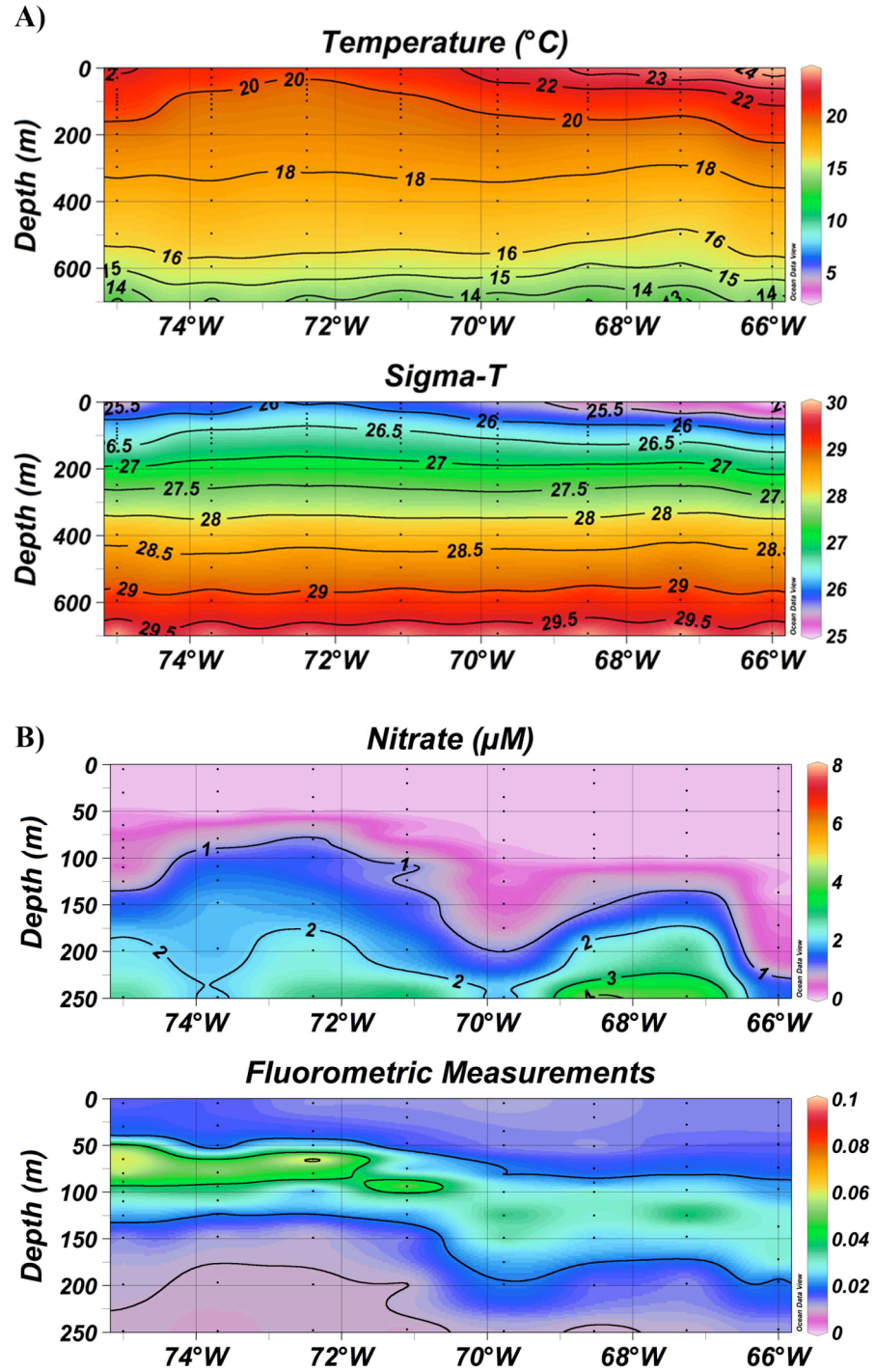


Figure 4.2 - Color contour plots showing A) in-situ temperature (°C) and σ_T , and B) Nitrate (μM) and fluorometric measurements taken along Leg 2 of cruise track SJ0005, a SE to NW transect in the western subtropical North Atlantic Ocean. Figure was prepared using Ocean Data View (Schlitzer 2008).

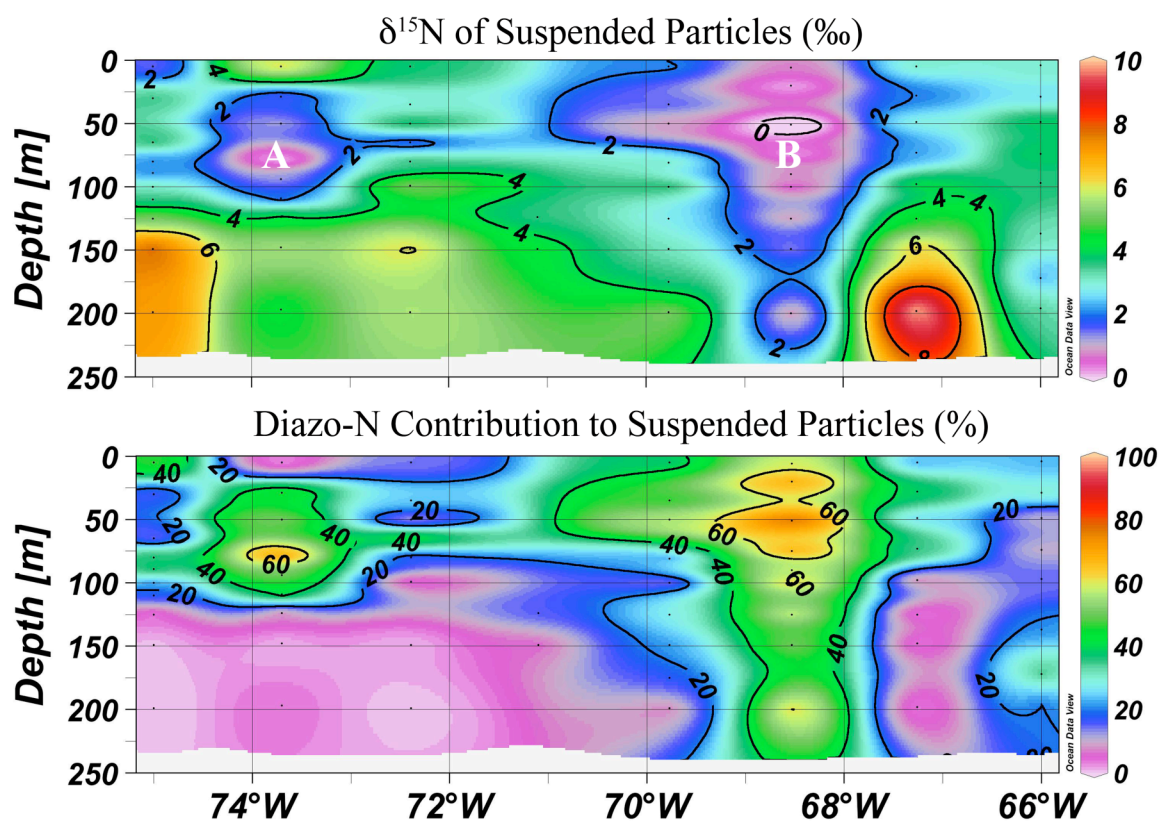


Figure 4.3 – Color contour plots showing $\delta^{15}\text{N}$ (‰) and the corresponding diazotroph N contribution to suspended particles collected along Leg 2 of cruise track SJ0005, a SE to NW transect in the western subtropical North Atlantic Ocean. In the top figure, feature A and B are labeled as described in the text. Figure was prepared using Ocean Data View (Schlitzer 2008).

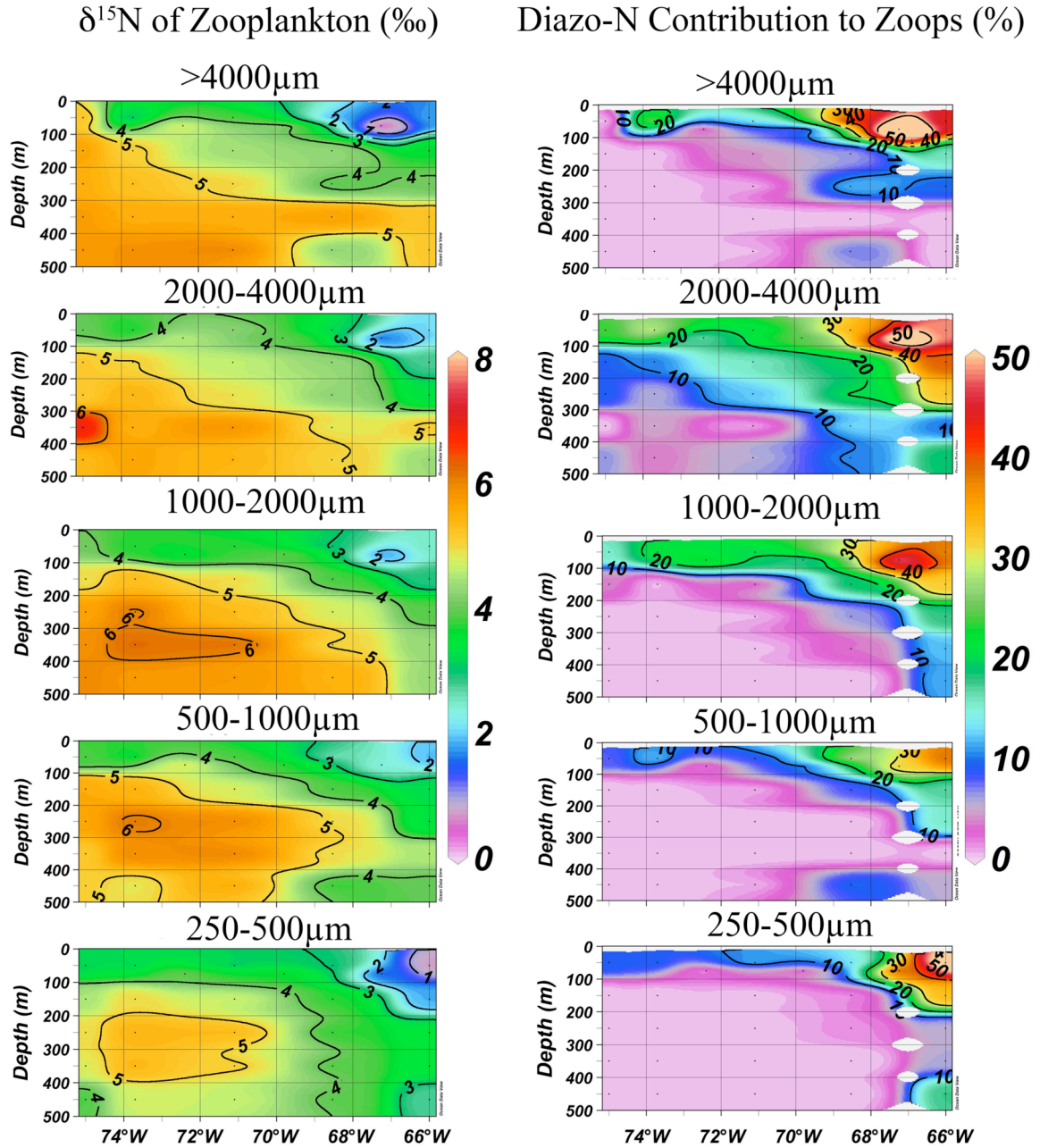


Figure 4.4 – Color contour plots showing $\delta^{15}\text{N}$ (‰) and diazotroph N contribution (%) to mesozooplankton communities along Leg 2 of cruise track SJ0005, a SE to NW transect in the western subtropical North Atlantic Ocean. Figure was prepared using Ocean Data View (Schlitzer 2008).

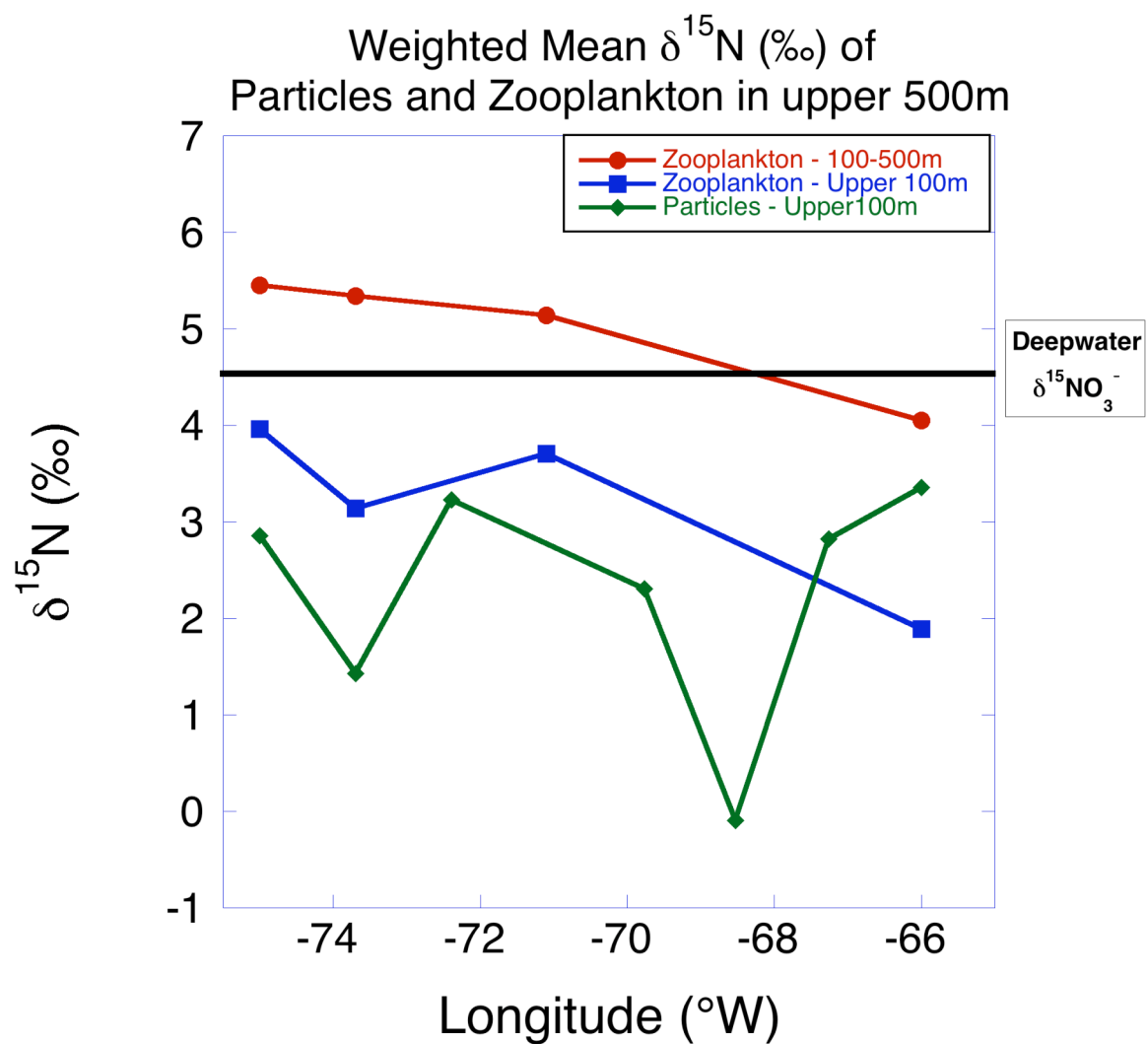


Figure 4.5 - Weighted mean $\delta^{15}\text{N}$ (‰) of both suspended particles and mesozooplankton within the upper 500m of the water column along Leg 2 of cruise track SJ0005, a SE to NW transect in the western subtropical North Atlantic Ocean.

$\delta^{15}\text{N}_{\text{ZP}}$ values did not differ significantly between mesozooplankton size classes (GLM, F-ratio = 0.72, dF = 4, $p = 0.3$), but were significantly different with time of collection (day versus night) (GLM, F-ratio = 4.49, dF = 1, $p < 0.001$), depth (GLM, F-ratio = 97.17, dF = 1, $p < 0.001$), and longitude (GLM, F-ratio = 114.0, dF = 1, $p < 0.001$). We did not observe any significant interaction effects between factors in this model. Also, $\delta^{15}\text{N}_{\text{ZP}}$ generally increased with depth in the water column (Figure 4.4). Finally, $\delta^{15}\text{N}_{\text{ZP}}$ values ranged from 1-3‰ in the upper 200m of the water column at the southeastern end of leg 2 (east of 68°W), but ranged between 4-5‰ west of 68°W. We estimate that mesozooplankton communities east of 68°W derived a considerable amount of their N from diazotrophs, ranging from 20-50% in the upper 200m and 10-20% between 200-500m of the water column.

Weighted mean $\delta^{15}\text{N}$ varied from -0.09-4.0‰ for suspended particles, 1.9-3.7‰ in mesozooplankton caught in the upper 100m, and 2.8-4.7‰ in zooplankton caught below 100m (Figure 4.5). Weighted mean $\delta^{15}\text{N}$ for both suspended particles and mesozooplankton caught in the upper 100m fell below typical values for deepwater NO_3^- (~4.5‰), but weighted mean $\delta^{15}\text{N}$ for mesozooplankton captured below 100m were predominantly higher (Figure 4.5).

Suspended particles exhibited lower weighted mean $\delta^{15}\text{N}$ values than mesozooplankton at all stations except for Station 10, located at the southeastern end of Leg 2. Overall, there was no significant correlation between suspended particle and mesozooplankton $\delta^{15}\text{N}$ (<100m: Pearson's Correlation: $r = -0.36$, $p = 0.8$; 100m-500m: $r = -0.26$, $p = 0.8$), but there was a significant correlation between $\delta^{15}\text{N}$ of zooplankton caught above and below 100m ($r = 0.99$, $p = 0.01$)

4.3.3 SJ0005 Leg 3 – Stations 17-49

The third leg of SJ0005 spanned the subtropical North Atlantic from station 17 (32°16'N, 75°W) to station 49 (32°16'N, 21°16'W) (Figure 4.1). Temperature ranged

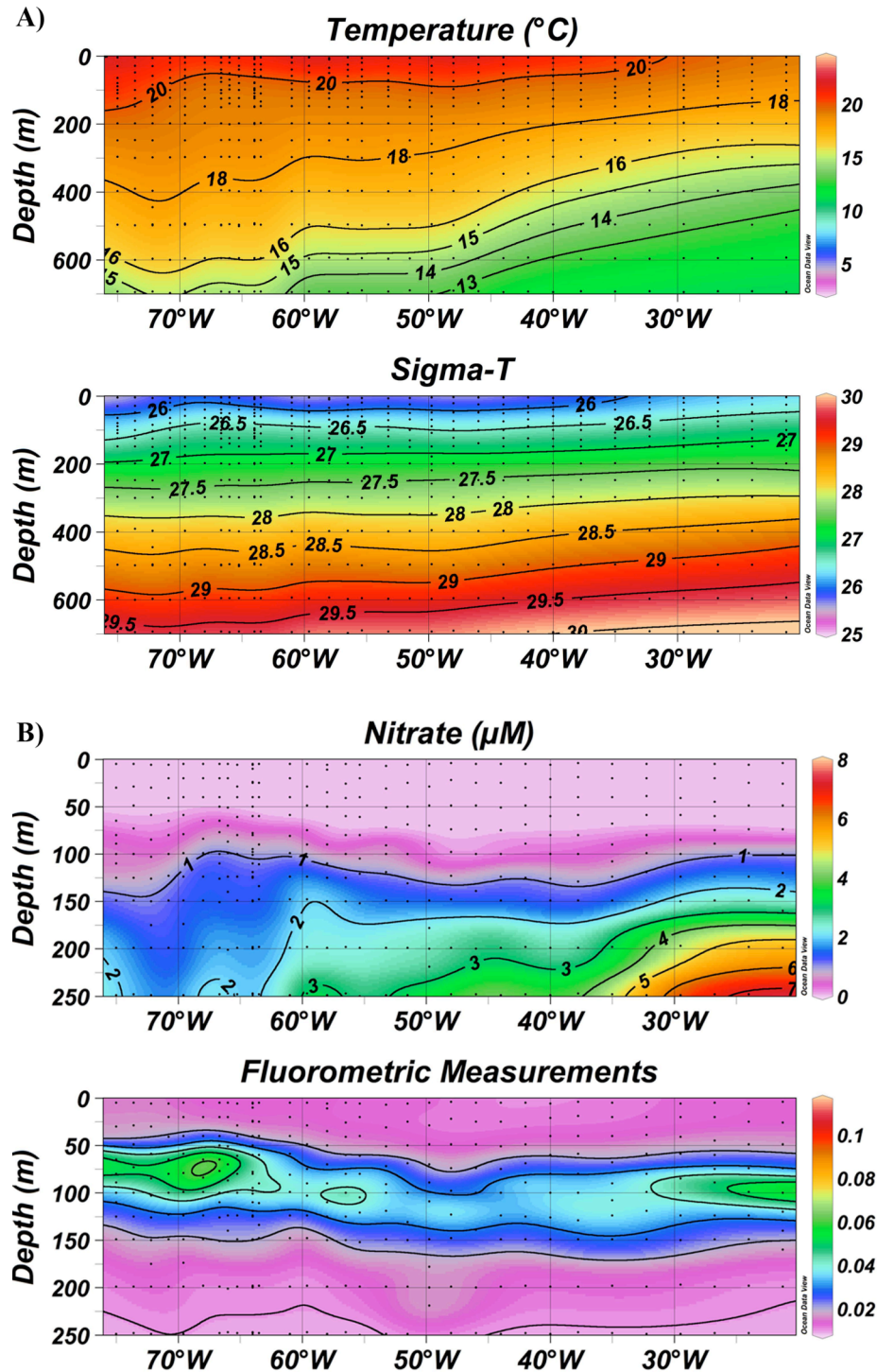


Figure 4.6 - Color contour plots showing hydrographic data of the water column along Leg 3 of cruise track SJ0005, a zonal transect spanning the subtropical North Atlantic Ocean at 32°N . Panel A shows seawater in-situ temperature ($^{\circ}\text{C}$) and σ_T in the upper 500m, while Panel B shows both nitrate concentrations (μM) and fluorometric measurements observed along the same transect, but only within the upper 250m. Figure was prepared using Ocean Data View (Schlitzer 2008).

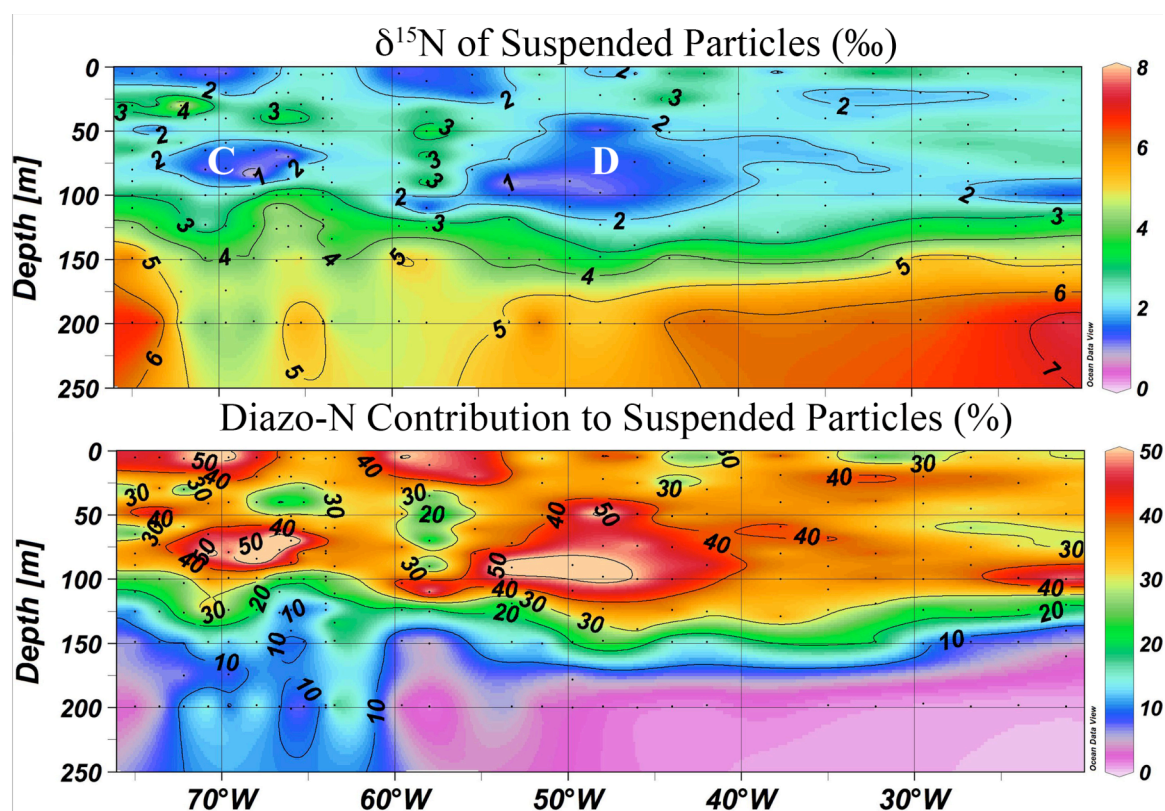


Figure 4.7 - Color contour plots showing $\delta^{15}\text{N}$ (‰) and diazotroph N contribution (%) to zooplankton communities along Leg 3 of cruise track SJ0005, a zonal transect spanning the subtropical North Atlantic Ocean at 32°N. In the top figure, feature C and D are labeled as described in the text. Figure was prepared using Ocean Data View (Schlitzer 2008).

from 14-22°C in the upper 500m of the water column, with cooler water shoaling eastward (Figure 4.6A). σ_T values ranged from 25.5 to 28, and isopycnals shoaled towards the east, converging on a value of 27 in the upper 200m of the water column. As with Leg 2, NO_3^- values were below the limits of detection in surface waters (<50m), and the depth of the 1 μM contour ranged from 100-150m across the transect, deepening steadily from 100m to 150m east of 60°W until rebounding back to 100m at the end of the transect (Figure 4.6B). Fluorometric measurements taken across this transect showed a clear pigment maximum 75-100m across most of the basin, but deepening to between 100-125m in the central North Atlantic between 35-50°W (Figure 4.6B).

$\delta^{15}\text{N}_{\text{SP}}$ values differed significantly with depth (GLM, F-ratio = 103.12, dF = 1, $p < 0.001$), ranging from 1-4‰ in the mixed layer, and increasing with depth (range: 4-7‰) below 100m (Figure 4.7). $\delta^{15}\text{N}_{\text{SP}}$ values did not vary significantly with longitude (GLM, F-ratio = 0.078, dF = 1, $p = 0.8$) and we found no significant interaction between depth and longitude (GLM, F-ratio = 0.24, dF = 1, $p = 0.6$). $\delta^{15}\text{N}_{\text{SP}}$ values of the upper water column and deeper waters differed significantly, as shown by the 3‰ and 4‰ contours that span the basin at 100-125m and 125-150m, respectively. Below these contours, $\delta^{15}\text{N}_{\text{SP}}$ values ranged from 5-7‰, with the greatest values on the eastern and western ends of Leg 3. At depths from 150-250m, $\delta^{15}\text{N}_{\text{SP}}$ values were lower in the region between 55-75°W (3.5-5‰) than at any other station east of 75°W. Although there were no statistically significant differences in $\delta^{15}\text{N}_{\text{SP}}$ values with longitude, several features with pronounced low $\delta^{15}\text{N}_{\text{SP}}$ values appeared in the upper 125m of the water column. Specifically, two very large regions (Labeled C & D – Figure 4.7) containing particles with a $\delta^{15}\text{N}$ ranging between 1-2‰ (the lowest $\delta^{15}\text{N}_{\text{SP}}$ values reported along this transect) occurred between 65-75°W and 30-60°W.

$\delta^{15}\text{N}_{\text{ZP}}$ values increased significantly with increasing size (GLM, F-ratio = 12.23, dF = 1, $p < 0.001$), greater depth (GLM, F-ratio = 258.99, dF = 1, $p < 0.001$) and toward

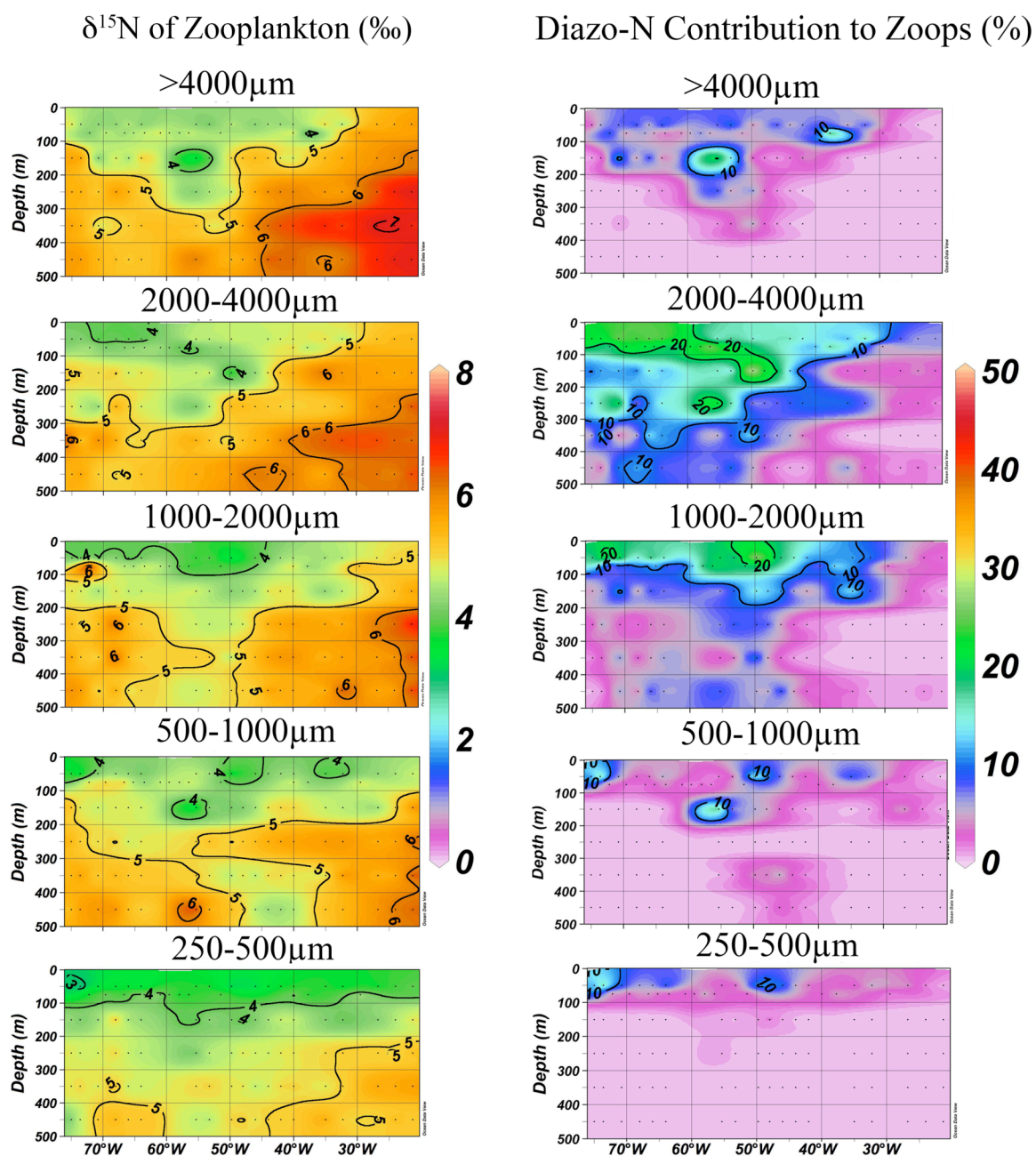


Figure 4.8 - Color contour plots showing $\delta^{15}\text{N}$ (‰) and diazotroph N contribution (%) to mesozooplankton communities along Leg 3 of cruise track SJ0005, a zonal transect spanning the subtropical North Atlantic Ocean at 32°N. Figure was prepared using Ocean Data View (Schlitzer 2008).

Table 4.2 - Least squares means of $\delta^{15}\text{N}$ (‰) (± 1 S.E.) of mesozooplankton size fractions collected along Leg 3 of cruise track SJ0005, a zonal transect spanning the subtropical North Atlantic Ocean at 32°N.

Size Fraction (μm)	Mean $\delta^{15}\text{N}$ (‰)
250-500	4.4 \pm 0.07
500-1000	4.9 \pm 0.07
1000-2000	5.0 \pm 0.07
2000-4000	5.0 \pm 0.07
>4000	5.3 \pm 0.07

Table 4.3 – Least squares means of $\delta^{15}\text{N}$ (‰) of mesozooplankton size fractions collected during the daytime (0600-1800) or nighttime (1800-0600) along Leg 3 of cruise track SJ0005, a zonal transect spanning the subtropical North Atlantic Ocean at 32°N.

Size Fraction (μm)	$\delta^{15}\text{N}$ (‰)	
	Daytime	Nighttime
250-500	4.38 ± 0.08	4.53 ± 0.12
500-1000	4.69 ± 0.08	5.27 ± 0.12
1000-2000	4.72 ± 0.08	5.52 ± 0.12
2000-4000	4.97 ± 0.08	5.29 ± 0.12
>4000	5.05 ± 0.08	5.71 ± 0.12

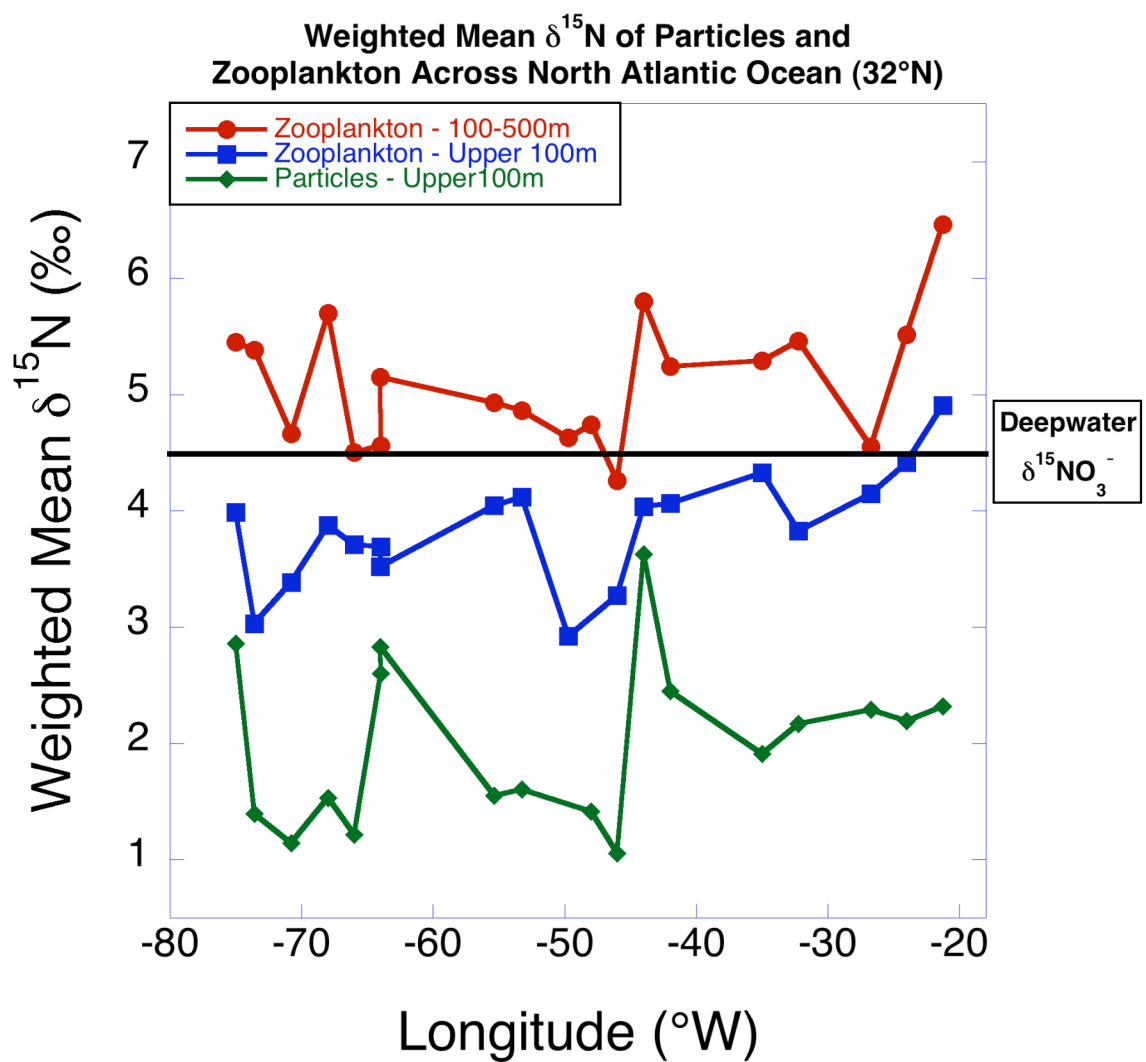


Figure 4.9 - Weighted mean $\delta^{15}\text{N}$ (‰) of both suspended particles and mesozooplankton within the upper 500m of the water column along Leg 3 of cruise track SJ0005, a zonal transect spanning the subtropical North Atlantic Ocean at 32°N.

the east (GLM, F-ratio = 94.97, dF = 1, $p < 0.001$) along this zonal transect (Figure 4.8). The smallest zooplankton (250-500 μ m) exhibited the lowest mean $\delta^{15}\text{N}$ values (Table 4.2). For all size fractions, $\delta^{15}\text{N}_{\text{ZP}}$ values remained between 3-4‰ in the upper 200m and increased to 5-7‰ below 200m. While values ranged from as high as 4-5‰ in the upper 500m of the water column west of 50°W, $\delta^{15}\text{N}_{\text{ZP}}$ values ranged from 5-7‰ east of 50°W. Finally, we observed significantly higher $\delta^{15}\text{N}_{\text{ZP}}$ values for all mesozooplankton (i.e., all size fractions) collected at night (Mean = $4.40\text{‰} \pm 0.06$ ($\pm 1\text{SE}$)) versus zooplankton collected during the daytime (Mean = 3.86 ± 0.24 ($\pm 1\text{SE}$)) (GLM, F-ratio = 58.99, dF = 1, $p < 0.001$). Zooplankton size class also influenced differences in $\delta^{15}\text{N}_{\text{ZP}}$ values (Interaction effect: Size*Time of Collection - GLM, F-ratio = 3.31, dF = 1, $p = 0.01$), where all zooplankton size classes, except for the smallest size fraction, exhibited significantly higher $\delta^{15}\text{N}_{\text{ZP}}$ values in night tows (Table 4.3).

The overall biomass weighted mean of $\delta^{15}\text{N}_{\text{SP}}$ and $\delta^{15}\text{N}_{\text{ZP}}$ in the upper 100m of the water column were 2.0 ± 0.7 and 3.8 ± 0.5 , respectively, while average $\delta^{15}\text{N}_{\text{ZP}}$ below the mixed layer (100-500m) was 4.7 ± 0.5 (Figure 4.9). These means differed significantly (ANOVA with Tukey's post-hoc test, $p < 0.001$). The weighted mean $\delta^{15}\text{N}_{\text{SP}}$ was positively correlated with the $\delta^{15}\text{N}_{\text{ZP}}$ caught in the upper 100m (Pearson's correlation: $r = 0.51$, $p = 0.03$).

4.3.4 North-South comparisons: Leg 1 (Stns. 7, 9, 10) & Leg 3 (Stns. 20, 22, 24)

Mean $\delta^{15}\text{N}_{\text{ZP}}$ values of all zooplankton collected in the upper 500m were significantly lower in the southern stations ($M = 3.34\text{‰}$, $\text{SE} = \pm 0.08$) than in the northern stations ($M = 4.79\text{‰}$, $\text{SE} = \pm 0.08$) (GLM, F-ratio = 152.46, dF = 1, $p < 0.001$) in the western Atlantic. $\delta^{15}\text{N}_{\text{ZP}}$ values also differed significantly between size fractions (GLM, F-ratio = 5.66, dF = 4, $p < 0.001$), where $\delta^{15}\text{N}_{\text{ZP}}$ values were lowest for the smallest (250-500 μ m) mesozooplankton ($3.6\text{‰} \pm 0.13$) and highest for the largest (>4000 μ m) zooplankton ($4.5\text{‰} \pm 0.13$, respectively). $\delta^{15}\text{N}_{\text{ZP}}$ values of other size classes

Table 4.4 – Mean $\delta^{15}\text{N}$ (‰) of zooplankton collected along two zonal transects that overlap with longitude, but differ in latitude (27°N versus 32°N). Northern stations represent stations where zooplankton were collected at 32°N and southern stations at 27°N. Error is represented by ± 1 standard error. $\Delta\delta^{15}\text{N}$ are differences in mean values for $\delta^{15}\text{N}_{\text{ZP}}$ between North and South stations.

Size Fraction (μm)	North Stations	South Stations	$\Delta\delta^{15}\text{N}$ (North-South)
250-500	4.55 ± 0.18	2.69 ± 0.18	1.87
500-1000	4.89 ± 0.18	3.16 ± 0.18	1.73
1000-2000	4.87 ± 0.18	3.38 ± 0.18	1.49
2000-4000	4.79 ± 0.18	3.32 ± 0.18	1.47
>4000	4.83 ± 0.18	4.18 ± 0.18	0.65

(500-4000 μ m) were $\sim 4\text{‰} \pm 0.13$. Further analysis also showed that $\delta^{15}\text{N}_{\text{ZP}}$ values differed significantly between northern and southern stations among different size fractions (Interaction effect: Latitude*Size). The smallest zooplankton exhibited the greatest difference in $\delta^{15}\text{N}$ between North and South stations, while differences between locations declined with increasing zooplankton size (Table 4.4). Finally, mean $\delta^{15}\text{N}_{\text{ZP}}$ values of all zooplankton differed significantly with depth in the water column (GLM, F-ratio = 76.41, dF = 1, $p < 0.001$).

4.4 Discussion

Distributions of N isotopes can reveal the major N sources supporting primary production in oligotrophic oceans, while also providing information on the structure and function of oceanic food webs. Depth and mass integrated $\delta^{15}\text{N}$ values for both suspended particles and mesozooplankton are crucial components in evaluating the extent to which N_2 -fixation supports both primary and secondary producers, and the movement of that N into higher trophic levels. Our data extend the existing body of stable isotope measurements documenting the importance of N_2 -fixation not only to primary producers, but also to mesozooplankton (Montoya et al. 1992, Dore et al. 2002, McClelland & Montoya 2002, Montoya et al. 2002, Montoya et al. 2004, Holl et al. 2007, Reynolds et al. 2007). Overall, along Leg 2 and 3, both $\delta^{15}\text{N}_{\text{SP}}$ and $\delta^{15}\text{N}_{\text{ZP}}$ observed in the mixed layer were significantly lower than mean deepwater $\delta^{15}\text{NO}_3^-$, suggesting considerable inputs of N by N_2 -fixing organisms. $\delta^{15}\text{N}_{\text{SP}}$ values were consistently low (0-4‰) in the upper 100m, but reveal several lower $\delta^{15}\text{N}_{\text{SP}}$ features (-2 to 0‰) spanning hundreds to thousands of kilometers. These features represent areas of more intense N inputs via diazotrophs. Given these isotopic trends, we estimate that diazotrophs contributed up to 80% and 100% of suspended particle N along Leg 2 and 3, respectively.

Low $\delta^{15}\text{N}_{\text{ZP}}$ values also suggest that mesozooplankton are actively incorporating diazotroph N, and although spatially variable, diazotrophs contributed up to 65% and

30% of zooplankton N along Leg 2 and 3, respectively. Our isotope data suggest that smaller zooplankton (<1000 μ m) remained in the upper 200m of the water column, but larger zooplankton tended to move more extensively throughout the upper 500m. Higher $\delta^{15}\text{N}$ values of mesozooplankton collected at night between 100 and 200m suggest that migrants rely less on diazotroph N than animals that remain in the mixed layer throughout the day. This may reflect greater carnivory among migrants and/or active feeding at depth during the day.

$\delta^{15}\text{N}_{\text{ZP}}$ were generally higher for all size fractions at the easternmost 2 stations. Higher $\delta^{15}\text{N}_{\text{ZP}}$ values and consistently low $\delta^{15}\text{N}_{\text{SP}}$ further suggests that diazotroph N is available, but not readily assimilated by mesozooplankton relative to food webs in the western North Atlantic.

4.4.1 Trends in $\delta^{15}\text{N}_{\text{SP}}$ and diazotroph N contribution

Along both Leg 2 and Leg 3, lower $\delta^{15}\text{N}_{\text{SP}}$ values above the base of the mixed layer suggest considerable diazotroph N contribution to suspended particles. Higher diazotroph N contribution in the mixed layer is not surprising, given that diazotrophs and diatom/diazotroph assemblages (DDAs) are often found at high abundance in the uppermost regions (<75m) of the mixed layer (Letelier & Karl 1996, 1998, Carpenter et al. 1999, Carpenter et al. 2004, Davis & McGillicuddy 2006, Foster et al. 2007). Fewer studies have mapped the vertical distribution of unicellular diazotrophs, but recent molecular studies suggest that these organisms are distributed throughout the mixed layer (Church et al. 2005, Langlois et al. 2008). Increasing $\delta^{15}\text{N}_{\text{SP}}$ values with depth below the mixed layer suggests increased remineralization of POM, and thus, enrichment of those particles in ^{15}N , which is typically mediated by microbial decomposition of POM (Macko et al. 1994, Lehmann et al. 2002).

We also observed lateral variation in $\delta^{15}\text{N}$ of suspended particles within the mixed layer. On the northwesterly transect (e.g., Leg 2), two features with low suspended

particles $\delta^{15}\text{N}$ values in surface waters were evident. The first feature occurred in the upper 100m, close to the northwestern corner of the track at Station 17. The second feature is much larger both laterally and vertically in the water column, spanning Stations 11-14 (67°W to 71°W) and reaching depths up to 200m at Station 12 (29°N , $68^\circ30'\text{W}$) (Figure 4.2). Low $\delta^{15}\text{N}_{\text{SP}}$ values in both features suggest that diazotrophs are very active in these areas, contributing 74% and 80% of particle N at the core of the features, respectively. Diazotroph N contribution to suspended particle pools decreases with distance away from the center of each feature (20-50% of the particle biomass). Although we have no floristic or satellite evidence of diazotroph bloom conditions during these two features, large diazotroph blooms can have a major influence on the stable N isotope compositions of suspended particles within the water column (Capone et al. 1998, Carpenter et al. 1999).

Leg 3 also contains several low $\delta^{15}\text{N}_{\text{SP}}$ features in the upper 100m (Figure 4.7), between Stations 17-23 (75°W to $66^\circ40.2'\text{W}$), Stations 28-31 ($63^\circ59.89'\text{W}$ to $59^\circ36.23'\text{W}$), and Stations 37-38 ($49^\circ45.05'\text{W}$ to $47^\circ59.96'\text{W}$), where diazotrophs contributed up to 100% of suspended particles N content. The lowest $\delta^{15}\text{N}_{\text{SP}}$ values, though, occur at depths between 50-100m between Stations 17-26 (74°W - 64°W) and Stations 34-45 (55°W - 21°W) (Figure 4.7). Suspended particles within these two features derived up to 100% and 70% of their N from diazotrophs, respectively.

4.4.2 Trophic interactions: Utilization and movement of diazotroph N

Depth and mass integrated mean $\delta^{15}\text{N}$ can reveal overall diazotroph N contribution to the food web, while also revealing spatial and vertical trends in N movement between the suspended particle N pool and mesozooplankton community. Along both Leg 2 and 3, low weighted mean $\delta^{15}\text{N}_{\text{ZP}}$ within the mixed layer suggest that diazotrophs contribute a significant amount of N to mesozooplankton community biomass. Longer lifetimes, and therefore longer N turnover times, of mesozooplankton

(e.g., weeks to months) relative to phytoplankton (e.g., days) suggest that diazotrophs have been contributing N to these communities over longer timescales than the average turnover time of particles.

Along Leg 2, positive correlations between weighted mean $\delta^{15}\text{N}_{\text{ZP}}$ values within and below the mixed layer suggest that shallow and deeper mesozooplankton are coupled, despite overall higher $\delta^{15}\text{N}$ for mesozooplankton caught at greater depths (Figure 4.5). Minimal overlap in data between weighted mean $\delta^{15}\text{N}_{\text{SP}}$ and $\delta^{15}\text{N}_{\text{ZP}}$ make similar comparisons between these two organic pools difficult (Figure 4.5). However, similar isotopic shifts between particles and mesozooplankton from station 16 to 17 (northwesternmost stations) suggest that particles and mesozooplankton are also closely correlated. Higher weighted mean $\delta^{15}\text{N}_{\text{SP}}$ values relative to $\delta^{15}\text{N}_{\text{ZP}}$ values at the southeasternmost station could have been driven by a recent intermittent influx of N from another source other than via diazotrophs (e.g., vertical advection of deep NO_3^-), but had not been integrated into mesozooplankton biomass.

Along Leg 3, significant positive correlations between the weighted mean of $\delta^{15}\text{N}_{\text{SP}}$ and $\delta^{15}\text{N}_{\text{ZP}}$ for zooplankton within and below the mixed layer, suggest tight coupling between surface particles and zooplankton throughout the water column. Mean $\Delta\delta^{15}\text{N}$ between suspended particles and mixed layer mesozooplankton caught in the upper 100m was $1.6\text{‰} \pm 0.6$, and $1.9\text{‰} \pm 0.7$ along Leg 2 and Leg 3, respectively (Figure 4.5 & 4.9). Overall these $\Delta\delta^{15}\text{N}_{\text{ZP-SP}}$ values equate to about half the typical 3.4‰ fractionation between consumer and food source (Deniro & Epstein 1981, Minagawa & Wada 1984), and suggest that mesozooplankton have heterogeneous diets from food sources that are most likely influenced by microbial community N dynamics. We also observed similar isotopic shifts between shallow and deep mesozooplankton communities. Mean $\Delta\delta^{15}\text{N}$ between shallow and deep mesozooplankton ($\Delta\delta^{15}\text{N}_{\text{ZP},\Delta\text{Z}} = \delta^{15}\text{N}_{\text{ZP-100-500m}} - \delta^{15}\text{N}_{\text{ZP-upper100}}$) was $1.7\text{‰} \pm 0.3$ and $1.5\text{‰} \pm 0.9$ along Leg 2 and 3,

respectively, again suggesting that mesozooplankton caught below the mixed layer were ~0.5 trophic steps removed from mesozooplankton caught in the mixed layer. These $\delta^{15}\text{N}_{\text{ZP},\Delta\text{Z}}$ values suggest that deeper mesozooplankton are incorporating particles from deeper waters (with higher $\delta^{15}\text{N}$), or they are consuming a higher proportion of surface mesozooplankton (i.e., carnivory) relative to surface particles.

4.4.3 Trends in $\delta^{15}\text{N}_{\text{ZP}}$ and diazotroph N contribution

The $\delta^{15}\text{N}$ of zooplankton reflects the N sources supporting secondary production in these waters. Although many species of mesozooplankton were present in our collections, marine mesozooplankton community structure is often strongly size-dependent, and pooling these organisms provides an estimate of aggregate mean utilization and transfer efficiency of N between food source and consumer. Our observations are consistent with previous studies that show modest increases in $\delta^{15}\text{N}$ of marine mesozooplankton with increasing size class (Minagawa & Wada 1984, Montoya et al. 1992, Fry & Quinones 1994, Montoya et al. 2002). ^{15}N content often increases with trophic position because of preferential metabolic losses of ^{14}N in the food web (Deniro & Epstein 1981, Minagawa & Wada 1984, Post 2002). Along Leg 2, $\delta^{15}\text{N}_{\text{ZP}}$ increased slightly with increasing zooplankton size, but $\delta^{15}\text{N}_{\text{ZP}}$ values were not significantly different from one another ($\sim 4.1\text{--}4.7 \pm 0.21\text{‰}$). Along Leg 3, $\delta^{15}\text{N}_{\text{ZP}}$ increases with increasing zooplankton size, which is consistent with a general scaling of $\delta^{15}\text{N}$ with trophic position (Deniro & Epstein 1981, Minagawa & Wada 1984, Montoya et al. 1990, Montoya et al. 1992, Fry & Quinones 1994, Montoya et al. 2002) (Table 4.2). However, $\delta^{15}\text{N}_{\text{ZP}}$ values between the size fractions from 500 μm –4000 μm did not differ significantly (Table 4.2), suggesting minimal ^{15}N enrichment with size in this size range.

Along Leg 2, $\delta^{15}\text{N}$ of the smallest zooplankton showed little $\delta^{15}\text{N}$ variation with depth, especially above the base of the mixed layer ($\sim 3\text{--}4\text{‰}$). Our results suggest that small zooplankton (250–1000 μm) do not incorporate much diazotroph N ($<10\%$) within

the mixed layer, instead deriving a larger portion of their biomass from non-diazotroph particles (e.g., detritus). However, low $\delta^{15}\text{N}$ values of small zooplankton in the mixed layer at the southeastern end of Leg 2 (stations 10 - 14) suggested considerably higher diazotroph N contribution (10-60%) to these mesozooplankton, with a peak contribution at station 11 (Figure 4.4). Low $\delta^{15}\text{N}_{\text{ZP}}$ observed for all other size fractions from stations 10-14 suggests efficient diazotroph N transfer (upwards of 65%) to the entire mesozooplankton community both within the euphotic zone, and deeper in the water column (Figure 4.4). Diazotroph N contribution to mesozooplankton communities decreases northwest of these stations, and was consistently higher in larger mesozooplankton ($>1000\mu\text{m}$), reaching up to 29% in the euphotic zone at station 16. There was little diazotroph N contribution to mesozooplankton below the mixed layer northeast of station 14. Diazotrophs contributed up to 20% of the N for larger zooplankton ($>1000\mu\text{m}$) caught in the upper 200m of the water column, but contributed $<10\%$ N to mesozooplankton caught below 200m. However, the 2000-4000 μm mesozooplankton caught between 100-300m depth incorporated considerable fraction of diazotroph N (10-20%). Zooplankton within the 2000-4000 μm size fraction derived the highest percentages of their N from diazotrophs with respect to the other size classes, both spatially along the transect, and vertically within the water column.

We observed somewhat different vertical and lateral trends in diazotroph N contribution to mesozooplankton along Leg 3. $\delta^{15}\text{N}$ of the smallest zooplankton showed minimal variation along Leg 3, and especially above the base of the mixed layer ($\sim 3\text{-}4\text{‰}$). Our isotope mass balance calculations suggest that small mesozooplankton (250-1000 μm) had not incorporated much diazotroph N ($<10\%$) within the euphotic zone, but ingested a larger portion of non-diazotroph particles (e.g., detritus). No other size fraction showed such a consistent trend spanning the basin within this depth range. Mesozooplankton within the 500-1000 μm size fraction followed a pattern similar to the smallest zooplankton, although diazotrophs contribute more N to these animals deeper in

the water column in the central portion of the gyre (~5-10%). Conversely, $\delta^{15}\text{N}$ values for larger zooplankton (>1000 μm) at a depth below the mixed layer suggest a greater vertical range of diazotroph N contribution for these animals. Deeper mesozooplankton (>100m) incorporate diazotroph N, but this signal decreases with depth in all size fractions. Diazotroph N contribution to the largest mesozooplankton size fraction (>4000 μm) was vertically variable up to 400m, but values were generally low (<10%) (Figure 4.8). However, mesozooplankton within the 1000-2000 μm and 2000-4000 μm size classes incorporated a considerable amount of diazotroph N (~5-20%) in the upper 500m, suggesting that these animals are selectively feeding on food sources that are rich in diazotroph N, or have been incorporating diazotroph N for longer periods of time.

Along Leg 3, $\delta^{15}\text{N}_{\text{ZP}}$ for all size fractions other than the smallest zooplankton increase eastward (Figure 4.8). This trend is most noticeable in larger mesozooplankton (>2000 μm) caught below the mixed layer. Interestingly, the weighted mean $\delta^{15}\text{N}_{\text{SP}}$ does not change over the same run, suggesting that mesozooplankton are incorporating less diazotroph N in the eastern portion of the basin relative to the west, despite available diazotroph N in suspended particles (Figure 4.9). These trends could be driven by differences in phytoplankton and/or mesozooplankton community structure across the basin, and/or less diazotroph N incorporation by larger migrating mesozooplankton. For example, Montoya et al. (2007) show evidence that *Trichodesmium* occur more frequently in the western part of the tropical North Atlantic, while unicellular diazotrophs are more abundant in the eastern portion of the basin. These zonal trends may extend northward to our study region (i.e., subtropical North Atlantic). Long-term satellite imaging data of *Trichodesmium* bloom occurrences also show that major blooms, although infrequent, are more prevalent in the north western edge of the North Atlantic gyre, and largely absent from the north eastern part of the basin (Westberry & Siegel 2006).

Vertical patterns in diazotroph N contribution to mesozooplankton could have been driven, in part, by diel vertical migration (DVM). Migrating mesozooplankton typically migrate upwards at dusk to feed in the euphotic zone, and then retreat into cooler, deeper waters at dawn to avoid predators (Zaret & Suffern 1976, Longhurst & Williams 1992, Osgood & Frost 1994, Pearre 2003). DVM has been documented to be a significant contributor to the movement of nutrients (e.g., NH_4^+), POM, and DOM between the euphotic zone and deeper waters below the mixed layer (Dam et al. 1995, Steinberg et al. 2000, Al-Mutairi & Landry 2001, Frangoulis et al. 2005, Hernandez-Leon et al. 2008), but no study to date has assessed the relative contribution of diazotroph POM to migrating mesozooplankton. Similar $\delta^{15}\text{N}$ values for small (250-500 μm) zooplankton between daytime and nighttime collections (Table 4.3) suggest that these mesozooplankton are not actively migrating below the base of the mixed layer. In contrast to the smaller mesozooplankton, larger mesozooplankton (>500 μm) also exhibited higher $\delta^{15}\text{N}$ when collected at night relative during the daytime (Table 4.3 & Figure 4.10), suggesting movement of deeper zooplankton upwards in the water column at night. Other studies have shown size-specific DVM, where larger animals migrated deeper than smaller zooplankton (Rodriguez & Mullin 1986, Madin et al. 2001). Indeed, if we look at depth distributions of $\delta^{15}\text{N}$ between day and night collections, we see a proportionally higher $\delta^{15}\text{N}$ at all depths, which is most pronounced, but not statistically significant, within the 100-200m range (Figure 4.10).

Higher $\delta^{15}\text{N}_{\text{ZP}}$ values of mesozooplankton during night tows suggests that we sampled different mesozooplankton at night, and potentially caught deeper, isotopically heavy mesozooplankton that were migrating into surface waters at night. Higher N_D of larger mesozooplankton (>1000 μm) at depth suggests that these animals are potentially migrating upwards and consuming diazotroph N from either the suspended particle pool

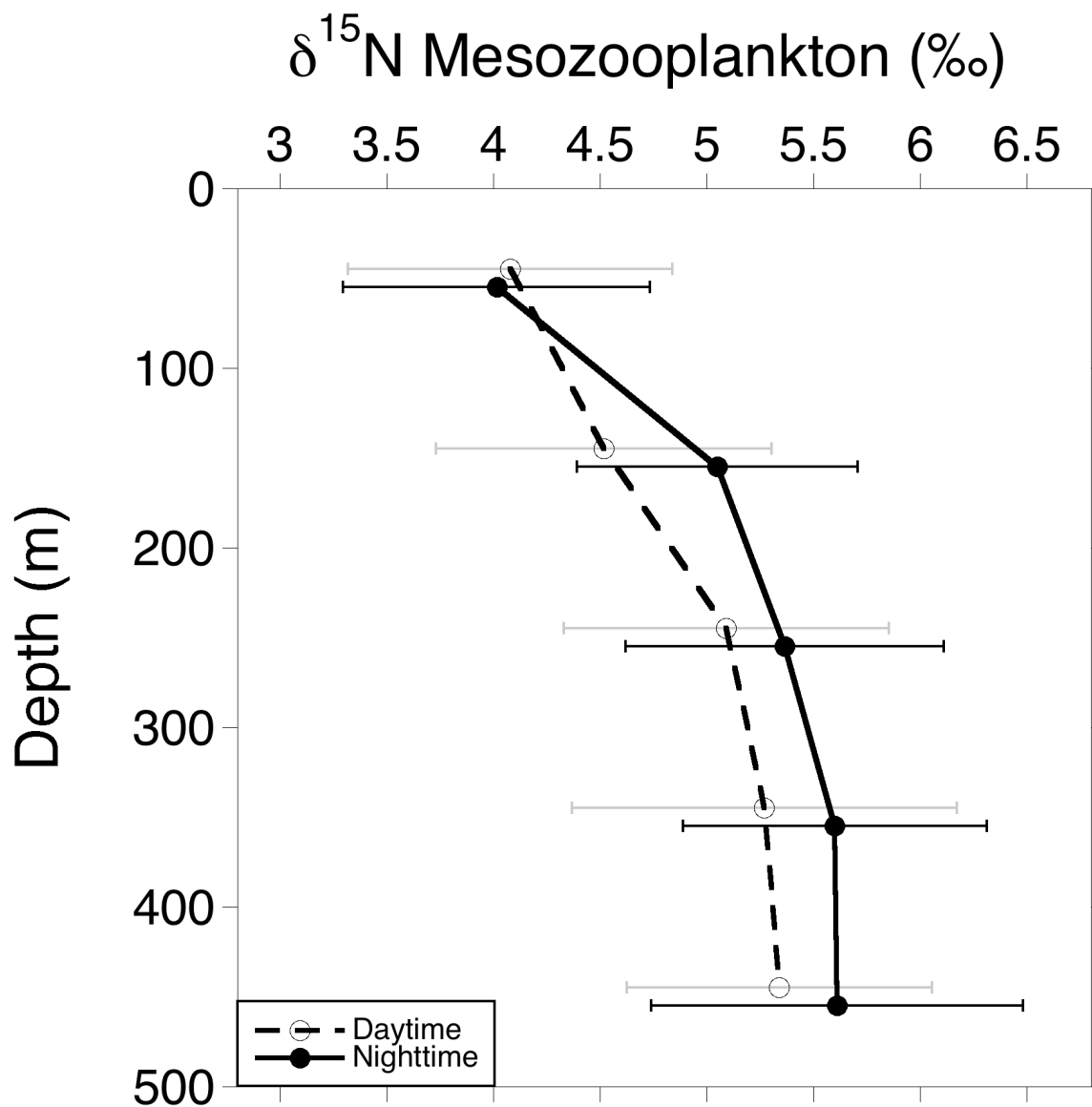


Figure 4.10 - Mean $\delta^{15}\text{N}$ (‰) of mesozooplankton collected at different depths during daytime and nighttime tows along Leg 3 of cruise track SJ0005, a zonal transect spanning the subtropical North Atlantic Ocean at 32°N. Mesozooplankton were collected at 100m intervals, and the circles are plotted in the middle of these intervals. The circles are also offset along the y-axis to show error bars (± 1 S.D.).

and/or smaller mesozooplankton pool. Thus, larger, isotopically heavier mesozooplankton may be ingesting diazotroph N and actively moving it into deeper water. Migrant mesozooplankton diets are heterogeneous, including phytoplankton, micro- and meso-zooplankton, and detritus (e.g., marine snow) (Schnitzer & Steinberg 2002). However, the latter pool may be the most broadly used food source by migrant mesozooplankton. For example, Schnitzer and Steinberg (2002) found that marine snow typically contributed >50% of the gut content for 3 prominent migrant mesozooplankton at BATS. They also found that there was little seasonal variation in the presence of marine snow within the migrants' guts, suggesting that marine snow is an integral part of their diet. Thus, larger migrating mesozooplankton derive their N from various sources that could have accumulated diazotroph N directly or through the microbial loop.

4.4.4 Mechanisms contributing to new N: Lateral and vertical trends

Overall, the mean diazotroph N contribution to suspended particles within the euphotic zone was $30\% \pm 15$ (Leg 2) and $38\% \pm 11$ (Leg 3). Biological mechanisms influencing lower $\delta^{15}\text{N}_{\text{SP}}$ within the mixed layer include: 1) higher proportional contribution of diazotroph biomass, 2) direct diazotroph N release (e.g., DON, NH_4^+) and utilization by other phytoplankton and/or microbial populations, 3) diazotrophs N release through microbial (e.g., viral lysis, DON/ NH_4^+ uptake and utilization via bacteria) and metazoan food web processes (e.g., zooplankton consumption and excretion). Several types of diazotrophs live within the subtropical North Atlantic, such as cyanobacteria (*Trichodesmium* spp.), diazotroph/diatom assemblages (DDAs – *Richelia/Hemiaulus*), and several different groups of picocyanobacteria (e.g., *Crocosphaera* sp., Group As). Both *Trichodesmium* and *Richelia/Hemiaulus* POM are depleted in ^{15}N , averaging between -1 to -2‰ (Carpenter et al. 1999, Montoya et al. 2002). Natural abundance measurements of $\delta^{15}\text{N}$ for unicellular diazotrophs have not been published, but are most likely similar to those of other diazotrophs. Without more information concerning the

concentration and isotopic composition of other organic pools (e.g., DON, DIN), and the types and proportions of diazotrophs present within and below the euphotic zone, it is difficult to assess the efficiency of N transfer of through these systems, especially with regards to the microbial loop. However, trophic transfers between the suspended particle pool and the mesozooplankton may provide information regarding the mechanisms responsible for N movement through the food web.

Crucial questions still remain concerning the dominant mechanism(s) facilitating N input into higher trophic levels by diazotrophs within the world's oceans (Mulholland 2007). These uncertainties reflect our limited knowledge of diazotroph-mesozooplankton interactions and their role in N movement through food webs. For example, although certain mesozooplankton (*Macrosetella* sp.) live on, and occasionally consume, *Trichodesmium* colonies (Oneil et al. 1996, O'Neil 1998, Sheridan et al. 2002, Eberl & Carpenter 2007), there is little evidence to suggest that zooplankton (including *Macrosetella* sp.) prefer to consume *Trichodesmium*. Also, given the potentially harmful array of chemical compounds produced by marine cyanobacteria (Martins et al. 2007), including *Trichodesmium* (Bullard & Hay 2002), cyanobacterial diazotrophs may not be consumed widely by mesozooplankton. Thus, diazotroph N may enter food webs primarily through diazotroph N release and uptake via other phytoplankton, and/or through the microbial loop. Diazotroph N can be released through their metabolic activity (Mulholland et al. 2004, Mulholland et al. 2006, Mulholland 2007), through viral lysis (Hewson et al. 2004), through autocatalyzed, programmed cell death (PCD) (Berman-Frank et al. 2004), or through death and microbial remineralization. Thus, other mechanisms can facilitate diazotroph N movement into higher trophic levels, than through direct consumption of diazotroph POM. Despite the challenge in demonstrating transfer mechanisms of diazotroph N into mesozooplankton, our isotopic data suggest that, although laterally and vertically variable, mesozooplankton incorporate significant amounts of diazotroph N in the STNA. Further work on compound-specific analysis of

mesozooplankton and their food sources may help elucidate the mechanisms and transfer efficiency of N between suspended particles and mesozooplankton, presenting a more detailed picture of diazotroph N movement through oceanic food webs.

4.4.5 N isotope mass balance in the subtropical North Atlantic

Using the natural distribution of N isotopes to trace the inputs of “new” N via biological N₂-fixation in oligotrophic systems requires the isotopic composition of N sources as well as other organic pools. In the North Atlantic, three distinct N sources drive “new” production through deepwater NO₃⁻ upwelling/diffusion, atmospheric deposition (e.g., NO₃⁻, NH₄⁺) and biological N₂-fixation. These N sources also have distinct isotopic signatures: mean deep water δ¹⁵NO₃⁻ is ~4.5‰ (Sigman et al. 1997, Montoya et al. 2002), deposited N has a wider range of δ¹⁵N values ranging from 5 to -14‰ (Cornell et al. 1995), and diazotroph POM typically has a low δ¹⁵N (-1 to -2‰) (Carpenter et al. 1999, McClelland et al. 2003, Capone et al. 2005, Holl et al. 2007).

Animal processes in the upper water column can produce low δ¹⁵N_{SP} relative to deepwater δ¹⁵NO₃⁻ due to isotopic fractionation occurring during metabolism and excretion of isotopically light NH₄⁺ (Checkley & Miller 1989). However, as noted by Montoya et al. (2002), at steady state, animal processes in the upper water column should produce both δ¹⁵N_{SP} and bulk δ¹⁵N_{ZP} equal to or lower than δ¹⁵NO₃⁻, when N₂-fixation is important. Our data for Legs 2 & 3 closely match this pattern, with weighted mean δ¹⁵N_{SP} and δ¹⁵N_{ZP} values below mean deepwater value of δ¹⁵NO₃⁻ values (Figures 4.5 & 4.9). We conclude then, that N₂-fixation is exerting a major influence on upper ocean δ¹⁵N values and its food webs.

Other N sources (e.g., N deposition) could potentially alter the δ¹⁵N of organic matter (OM) in the water column, and affect our isotope mass balance calculations. Input of N through atmospheric deposition may be globally important and may play a significant role in supporting production in the North Atlantic (Cornell et al. 1995, Duce

et al. 2008, Galloway et al. 2008). Reactive N input from the atmosphere may involve either wet deposition via rainwater (e.g., NO_3^- , NH_4^+ , DON), dry deposition of aerosols (including particles), and dissolution of gaseous species (e.g., NH_3) (Baker et al. 2006, Duarte et al. 2006, Baker et al. 2007, Krishnamurthy et al. 2007, Shepon et al. 2007). Atmospheric sources of reactive N (both wet and dry) exhibit a wide range of $\delta^{15}\text{N}$ values (-18‰ to 7‰), but typically have low $\delta^{15}\text{N}$ values (<0‰) in the North Atlantic (Hastings et al. 2003, Baker et al. 2007). N deposition is not uniform across the Atlantic basin, and this variation helps constrain the areas where wet and/or dry N deposition may influence surface production and OM isotopic composition. For example, there is little annual precipitation in the central North Atlantic gyre, where most oceanic precipitation is heavily influenced by the Gulf Stream and generally occurs in the Northwestern part of the basin. Areas with higher precipitation overlap with parts of Leg 2 and 3 of our cruise, and may affect our analysis of diazotroph contribution to organic pools in the upper ocean by altering the isotopic composition of both particles and zooplankton. Precipitation could also influence observed lower surface densities (σ_T) at the northwest and southeast edges of Leg 2 and the western portion of Leg 3 (west of 45°W) (Figures 4.2A & 4.6A). The low average rainfall along the middle stretch of Leg 2 and east of 50°W of Leg 3, suggests that wet N deposition may not be as important in influencing the isotopic composition of organic pools in these regions.

To evaluate the potential influence of rainfall, we first need to determine the concentrations and isotopic values for deposited N species. Hastings et al. (2003) found seasonal variation in both concentration and isotopic composition of rainwater NO_3^- at Bermuda, which they attributed to changes in NO_3^- source during the year (lightning versus fossil fuel emissions). NO_3^- concentration in rainwater ranged from 1.4 to 16.8 μM and $\delta^{15}\text{NO}_3^-$ ranged from -14 to 2‰ over the same period (January 2000-January 2001). For context, they also sampled rainwater collected in areas around Bermuda and found that rainwater $\delta^{15}\text{NO}_3^-$ values were most negative to the north of Bermuda

(~36°N), while values ranged from -4 to >0‰ south and west of Bermuda (Hastings et al. 2003). In the context of our data set, we rarely sampled in regions with extremely negative $\delta^{15}\text{NO}_3^-$ values in rainwater, but $\delta^{15}\text{NO}_3^-$ in rainwater was generally similar to diazotroph $\delta^{15}\text{N}_{\text{PON}}$ in our work area. Given both mean rainfall (via TRMM/GIOVANNI – NASA) along our cruise track and the yearly mean concentrations for NO_3^- collected at Bermuda during January 2000-2001, we estimate that wet N deposition for the period of January-June 2000 could contribute 0.04 and 0.03 $\text{nmol N m}^{-2} \text{ d}^{-1}$, to the regions sampled by Leg 2 and 3 of our cruise, respectively.

Baker et al. (2007) also found low amounts of NH_4^+ in rainwater (~3 μM) along a zonal transect in the North Atlantic basin at 10°N. Given these concentrations, N inputs via NH_4^+ deposition would have been 0.03 and 0.02 $\text{nmol N m}^{-2} \text{ d}^{-1}$ for Leg 2 and 3, respectively, from January-June 2000. Given both of these estimates, total N input (i.e., $\text{NO}_3^- + \text{NH}_4^+$) via wet deposition would be 0.07 and 0.05 $\text{nmol N m}^{-2} \text{ d}^{-1}$ for Leg 2 and 3, respectively, both of which are quite small relative to N_2 -fixation rates measured in the North Atlantic, albeit at lower latitudes (Capone et al. 1997, Capone et al. 2005, Montoya et al. 2007).

To evaluate the potential impact of atmospheric deposition, we can calculate the relative isotopic shift of suspended particles given N inputs and isotopic composition via biological N_2 -fixation and wet N deposition. Isotopically, volume-weighted mean $\delta^{15}\text{NO}_3^-$ found in rainwater during the warm season at BATS was $-1.8\text{‰} \pm 1.7$ (Hastings et al. 2003), which is very similar to diazotroph $\delta^{15}\text{N}_{\text{PON}}$, as mentioned earlier (-2‰) (Carpenter et al. 1999, Montoya et al. 2002, Holl et al. 2007). Given that both N sources are not isotopically distinct, we can simply compare input rates to determine the relative importance of the two sources. For *Trichodesmium* sp., Capone et al. (2005) estimated that average areal N_2 -fixation rate was 239 $\mu\text{mol N m}^{-2} \text{ d}^{-1}$ within the tropical North Atlantic. Given our estimate of mean N deposition ($\text{NO}_3^- + \text{NH}_4^+$) of $0.06 \pm 0.01 \text{ nmol N m}^{-2} \text{ d}^{-1}$, the relative proportion of N from N_2 -fixation is several orders of magnitude

higher than wet N deposition ($((\text{N}_2\text{-fixation rate})/(\text{Wet N deposition rate}) = 2.5 * 10^7)$).

Thus, wet deposition is a minor source of N to our cruise track areas, and probably has little influence on the isotopic composition of organic pools therein.

Dry deposition in the North Atlantic is more difficult to estimate, especially considering the uncertainties inherent in estimating deposition velocities (Baker et al. 2007). Dry deposition can indeed add new N, such as NO_3^- , NH_4^+ and soluble organic nitrogen species to the mixed layer, but may be more important in the eastern portion of the basin due to its proximity to dust from the Sahara. For example, Baker and colleagues (2007) found aerosol N influx to surface waters of the tropical North Atlantic (10°N) to be as high as N_2 -fixation rates, with the greatest contribution occurring in the eastern portion of the tropical North Atlantic ($\sim 20^\circ\text{W}$). Other studies have also reported high dry N deposition in the eastern part of the North Atlantic (Baker et al. 2003, Baker et al. 2006, Duarte et al. 2006), but basin-wide N deposition and isotopic data are not available presently.

Without detailed knowledge of the origin of the aerosols, the underlying chemical reactions producing various NO_x species, or the spatial variation in the inputs and isotopic composition of aerosols in the North Atlantic basin, it is difficult to evaluate the impact of N deposited on the isotopic composition of suspended particles and mesozooplankton along our cruise legs. Geographically, dry N deposits may be negligible due to our cruise's location within the North Atlantic basin (i.e., farther Northwest of major dust inputs from Africa). Dry deposition also typically includes other limiting micronutrients for diazotroph growth (e.g., P, Fe) (Jickells 1999, Jickells et al. 2005, Mahowald et al. 2005, Baker et al. 2006), it is difficult to predict the impact on phytoplankton community structure and $\delta^{15}\text{N}_{\text{POM}}$ based on dry N deposition rates. For example, although Baker et al. (2007) found that N deposition could be quite important relative to N_2 -fixation rates, depth integrated N_2 -fixation rates were positively correlated with P flux into the system via deposition. Diazotroph N_2 -fixation is also co-limited by

Fe and P elsewhere in the Atlantic (Baker et al. 2003, Mills et al. 2004, Baker et al. 2007, Mills et al. 2008). Future experiments should focus on the long-term effects of dust inputs on community structure and production in order to tease these isotope dilemmas apart.

Overall diazotroph N contribution to food webs in the subtropical North Atlantic

To our knowledge, our data set provides the first basin-scale overview of the role of diazotrophy in supporting biological production in the subtropical North Atlantic. Low $\delta^{15}\text{N}_{\text{SP}}$ values dominate the euphotic zone along all of our transects, suggesting significant inputs of new N from diazotrophs throughout our sampling region. Although our data show strong evidence for a significant diazotroph N contribution to suspended particles, it is impossible to resolve finer-scale transfer of N into and between separate organic pools within microbial communities. Oceanic microbial food webs are often quite complex, and N transfer occurs frequently between bacteria and microzooplankton before entering into “classical” food webs that focus on metazoan populations. Compound-specific (AAs) isotopic analysis of DOM and POM may help resolve some of these issues in future studies. However, despite these limitations, we observed trophic interactions between the suspended particle organic pool and size-fractionated mesozooplankton communities.

Despite consistently low $\delta^{15}\text{N}_{\text{SP}}$ within the mixed layer, $\delta^{15}\text{N}_{\text{ZP}}$ values were spatially and vertically variable. Lower $\delta^{15}\text{N}_{\text{ZP}}$ values often coincided with low $\delta^{15}\text{N}_{\text{SP}}$. Diazotroph influence was less pronounced in deeper mesozooplankton populations in the east with respect to the central and western portions of the basin, which may reflect temporal changes in N_2 -fixation (i.e., bloom vs. post-bloom conditions) or basin-wide differences in either/both phytoplankton and zooplankton community structure. Larger mesozooplankton, especially ranging between 1000-4000 μm , incorporated more diazotroph N than any other size fraction through the water column. Larger mesozooplankton (>1000 μm) also seemed to move greater vertical distances within the

upper 500m of the water column, and may exert a stronger influence on diazotroph N movement within the water column relative to smaller mesozooplankton. Although our study shows basin-scale patterns N inputs via biological N₂-fixation on oceanic food webs, future studies should focus on N flows within microbial communities supported by diazotrophs and the potential links transferring diazotroph N to metazoan communities. Future work should also closely examine shifts in food web structure and function associated with nutrient inputs from different N sources, as well as the potential effects of other limiting nutrients (e.g., Fe, P).

CHAPTER 5

TOTAL AND DIAZOTROPH-DERIVED SUSPENDED PARTICLE CONCENTRATION AND MESOZOOPLANKTON BIOMASS IN THE SUBTROPICAL NORTH ATLANTIC OCEAN BASIN

5.1 Introduction

Nutrient availability (NO_3^- , PO_4^{3-} , Fe, etc.) typically plays a dominant role in controlling primary production within the euphotic zone, limiting the total biomass available for consumption and export out of the upper ocean. In oligotrophic oceanic gyres, primary production is dominated by recycled nutrients (e.g., NH_4^+ , DON), and requires allochthonous sources of inorganic nutrients to balance losses due to export of both sinking particulate and dissolved organic matter (POM, DOM, respectively) out of the mixed layer (Dugdale & Goering 1967, Eppley & Peterson 1979). N is typically the limiting nutrient for primary production on biological timescales, and new N is critical in sustaining both primary and secondary production (Ryther & Dunstan 1971, Graziano et al. 1996, Moore et al. 2008). New N is defined as non-recycled N that enters the mixed layer in the form of deep NO_3^- (via diffusion or upwelling), deposition of N through rain and/or atmospheric sources (Cornell et al. 1995, Baker et al. 2007, Duce et al. 2008), or inputs by biological N_2 -fixation (LaRoche & Breitbarth 2005, Mulholland 2007). Assuming steady-state conditions, the input of new N should match the OM flux out of the mixed layer, reflecting the strength of the biological pump in exporting both C and N out of the upper ocean (Eppley & Peterson 1979). Thus, the efficiency by which new N moves into and through oceanic food webs provides direct information on the capacity of the system to remove CO_2 from the atmosphere.

The subtropical/tropical North Atlantic is the site of extensive N_2 -fixation, which plays a crucial role in regional C and N dynamics (Gruber & Sarmiento 1997, Carpenter

et al. 2004, Capone et al. 2005). However, little is known about the movement of that new N into higher trophic levels (e.g., zooplankton, fish). Understanding the movement and accumulation of biomass within the ocean is a crucial component in predicting the impact of new N production on all trophic levels, and specifically addresses questions related to global C and N cycles and oceanic food web structure and function.

Marine mesozooplankton play a crucial role in both OM processing and movement within oceanic food webs, and in global biogeochemical cycling (Roman et al. 2002, Turner 2002, Frangoulis et al. 2005, Hernandez-Leon & Ikeda 2005). Mesozooplankton actively consume POM in the water column (Banse 1995, Roman & Gauzens 1997, Al-Mutairi & Landry 2001, Moller 2005, 2007, Carlotti et al. 2008), and transport OM through release of fecal pellets (Urrere & Knauer 1981, Lampitt et al. 1990, Dagg 1993, Dagg et al. 1997, Lampitt & Antia 1997, Conte et al. 2001, Champalbert et al. 2003, Dagg et al. 2003, Poulsen & Kiorboe 2006, Olli et al. 2007), or through their metabolic activity (e.g., release of CO₂ and DOM) (Steinberg et al. 2000, Al-Mutairi & Landry 2001, Steinberg et al. 2008). They can also alter the size of particles through the physical disruption associated with swimming (Dilling & Alldredge 2000, Goldthwait et al. 2004). Mesozooplankton also represent an important resource for higher trophic levels (e.g., fish, squid, birds) in the water column. Several studies have quantified the basin-scale distribution of mesozooplankton biomass (Isla et al. 2004, Hernandez-Leon & Ikeda 2005), but fewer studies have assessed the proximal N sources supporting mesozooplankton communities (Montoya et al. 2002). Since mesozooplankton play a crucial role in OM movement in the water column, it is crucial to estimate mesozooplankton biomass and influence on biogeochemical cycles, especially in terms of OM flux out of the mixed layer.

Stable isotope techniques have provided opportunities to trace the input and movement of new N into and through oceanic food webs, but the mechanisms driving new N into and through food webs remain poorly understood (Montoya et al. 2002,

McClelland et al. 2003, Reynolds et al. 2007). By using $\delta^{15}\text{N}$ as an in-situ tracer, we can effectively determine if, and to what extent, both suspended particles and mesozooplankton are incorporating new N originating from diazotrophic activity, while also determining the relative importance of mesozooplankton in moving this N through oceanic food webs (Fry & Quinones 1994, Jennings et al. 2008).

Here, we present total and diazotroph-derived new suspended particulate N (PN) and mesozooplankton N (N_{ZOO}) biomass along a cruise in the subtropical North Atlantic Ocean (STNA). To our knowledge, this data set is the first of its kind in that it provides basin-wide estimates of both depth-integrated suspended particle and mesozooplankton biomass and the relative N_{D} contribution to these organic pools. Our data set allows us to: 1) pinpoint geographical and vertical (water column) hotspots of new N within both particle and mesozooplankton organic pools, 2) analyze the efficiency of new N movement through oceanic food webs, and 3) quantify new biomass within multiple organic pools that directly contribute to OM flux in the subtropical North Atlantic.

5.2 Materials and Methods

Seawater and plankton samples were collected on R/V Seward Johnson cruise SJ0005 (April 25 – May 24 2000), from Ft. Pierce, FL to the Canary Islands (Figure 5.1). A CTD -rosette system, equipped with a fluorometer, was used to collect water samples. Suspended particles were collected by gentle pressure filtration of 1.5-18 liters of seawater through pre-combusted (450°C for 2 h) 45-mm GF/F filters that were dried at 60°C and stored over desiccant for analysis ashore. For isotopic and elemental analysis, filters containing particle samples were trimmed to remove the particle-free edge, then cut into quadrants or halves that were pelletized in tin capsules for continuous flow isotope ratio mass spectrometry (CF-IRMS). Seawater nutrient analysis was performed

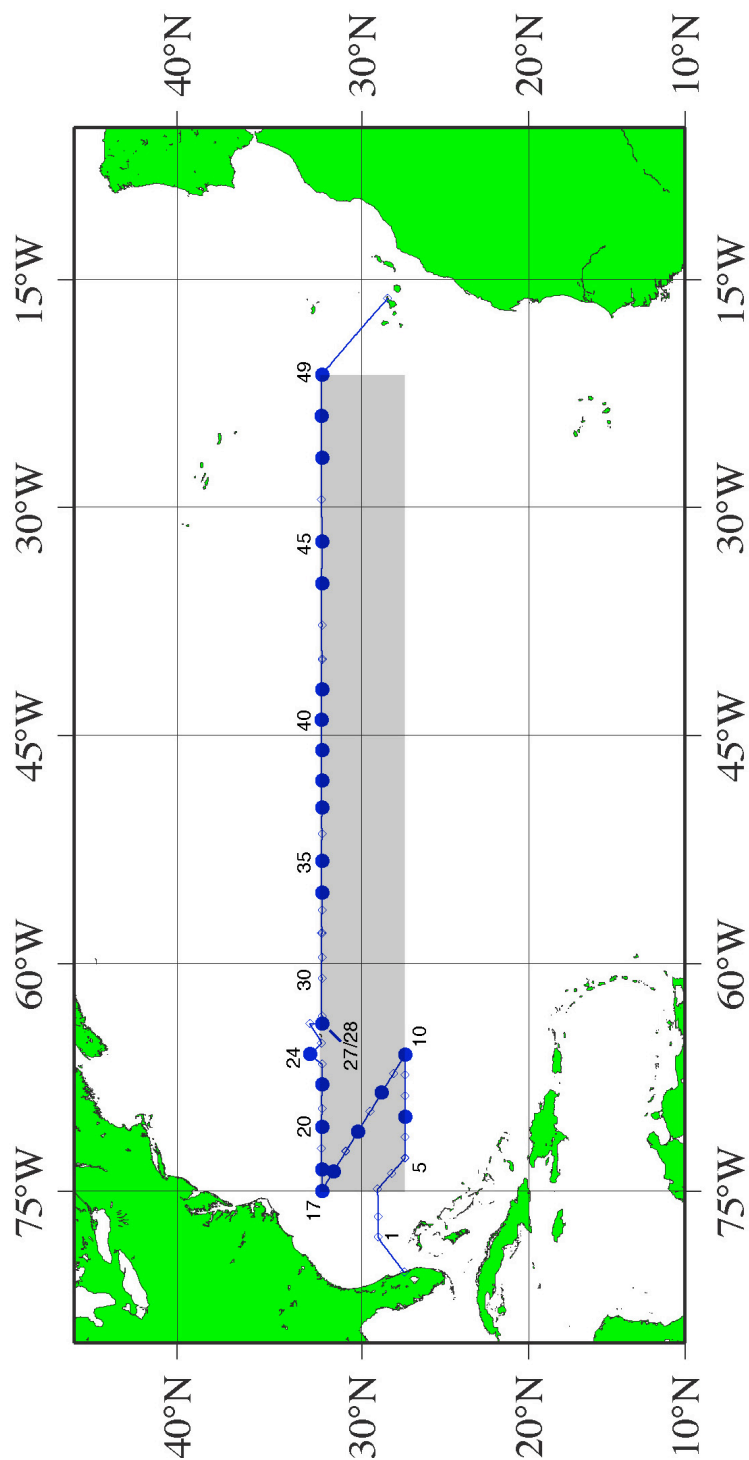


Figure 5.1 - Chart of cruise track SJ0005 comprised of three Legs: Leg 1 travels from Ft. Pierce, FL eastward towards the center of the North Atlantic gyre, Leg 2 turns northwest towards the eastern coast of the US, and Leg 3 turns westward at ~32°N and traverses the basin, terminating eventually in the Canary Islands. Solid circles represent stations where a MOCNESS was deployed and open diamonds represent stations where meter nets were deployed to collect zooplankton. The gray box represents the surface area used to determine total and diazotroph N biomass for this section of the subtropical North Atlantic.

at sea using a Lachat QuickChem 8000 FIA nutrient analyzer.

Mesozooplankton were collected either in diagonal tows of a meter net (333- μm mesh) through the upper 100m of the water column or with a 1-meter MOCNESS (333- μm mesh size) deployed to sample mesozooplankton within 100m depth increments through the upper 500m of the water column. The MOCNESS flowmeter was used to calculate the total volume of seawater filtered through each net, but the volume of seawater filtered through the meter net was not measured. Animals were separated into size fractions by passage through a set of graded Nitex sieves (4000 μm , 2000 μm , 1000 μm , 500 μm , 250 μm) at sea and were then frozen. Once ashore, zooplankton samples were dried at 60°C, ground into a fine powder, weighed for total dry weight (mg), and then sub-sampled and pelletized in tin capsules for isotopic analysis by CF-IRMS. All zooplankton size fractions were weighed after drying to obtain total dry weight (mg) of the zooplankton collected at each station. N and C contents measured by CF-IRMS were used to calculate integrated zooplankton N and C within the water column by trapezoidal integration. Total areal biomass was calculated for each station by summing the product of the average biomass (mg m^{-3}) and depth interval (100m) for all size fractions through the upper water column (final units: mg N m^{-2}).

All natural abundance measurements were made by CF-IRMS using a Micromass Optima interfaced with to an elemental analyzer for online combustion and purification of sample nitrogen and carbon. The CF-IRMS systems used were intercalibrated by running a variety of isotopically characterized organic (peptone, acetanilide, methionine, histidine, and glycine) and inorganic (KNO_3 and NH_4Cl). All $\delta^{15}\text{N}$ values are expressed relative to atmospheric N_2 . Each analytical run included a size series of elemental (acetanilide or methionine) and isotopic (peptone) standards, which provided a check on the stability of the instrument and allowed us to remove the contribution of any analytical blank to our isotopic measurements (Montoya 2008). In almost all cases, the blank was trivially small relative to the samples run and a blank correction was unnecessary. We

conservatively estimate that the overall analytical precision of our isotopic measurements is better than $\pm 0.1\%$.

Stable isotopes data are discussed in detail elsewhere (i.e., Chapter 4).

Diazotroph N contribution was calculated for both suspended particles and mesozooplankton using the isotope mass balance approach of Montoya et al. (2002). Reference $\delta^{15}\text{N}$ values for mesozooplankton included mesozooplankton that were collected in the upper 100m of the water column between 3°N and 3°S , where surface processes should be dominated by deep NO_3^- inputs via equatorial upwelling.

For basin-wide standing stock estimates, mean depth-integrated total and new standing stock (mg N/C m^{-2}) of both suspended particles (upper 200m) and mesozooplankton (upper 200m & 500m) were scaled by total surface area (m^2) of a rectangular area of the STNA defined by stations: 2 (westernmost station), 5-10 (southernmost stations), 17 (northernmost station), and 49 (easternmost station) (Figure 5.1).

5.3 Results

5.3.1 SJ0005 Leg 1 – Stations 2-10

We do not focus on Leg 1, due to spatial gaps in data, but we do estimate average depth-integrated PN and N_{Zoop} concentrations with available data, for comparison with the other Legs.

5.3.2 SJ0005 Leg 2 – Stations 10-17

Leg 2 extended northwestward from Station 10 ($27^\circ 29'\text{N}$, $66^\circ 0.3'\text{W}$) to station 17 ($32^\circ 16'\text{N}$, 75°W) (Figure 5.1). Temperatures in the upper 500m of the water column ranged from $16\text{--}22^\circ\text{C}$, coinciding with σ_t values that ranged from 25.0-26.5 (Figure 4.2A). Both temperature and salinity shoaled west of $70\text{--}75^\circ\text{W}$. The $1\text{-}\mu\text{M NO}_3^-$ contour ranged between 75-200m depth along Leg 2, with considerable spatial variation (Figure

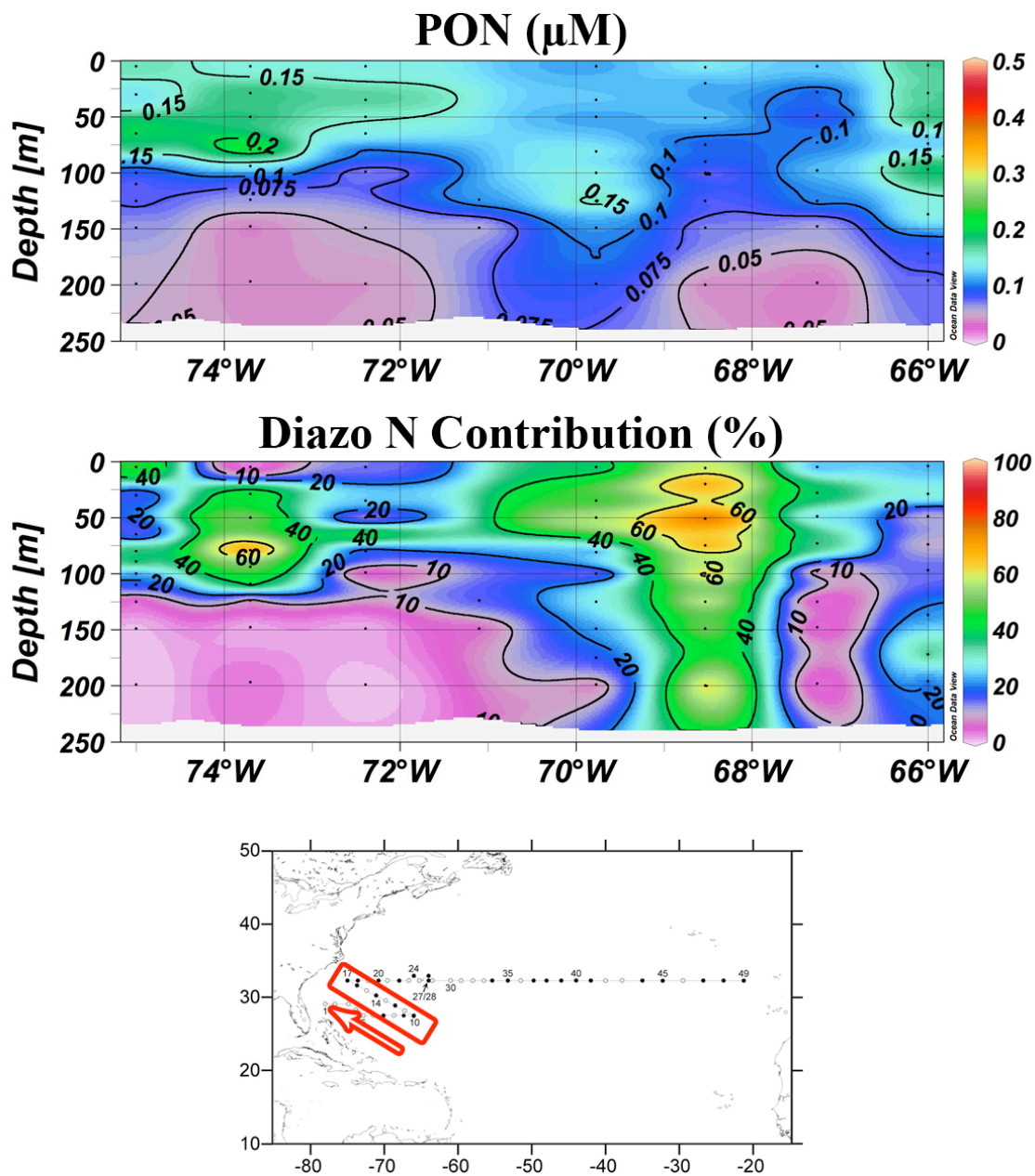


Figure 5.2 - Color contour plot showing PN concentrations (μM N) of suspended particles collected in the upper 250m of the water column along Leg 2 of cruise track SJ0005, a SE to NW transect in the western subtropical North Atlantic Ocean. Figure was prepared using Ocean Data View (Schlitzer 2008).

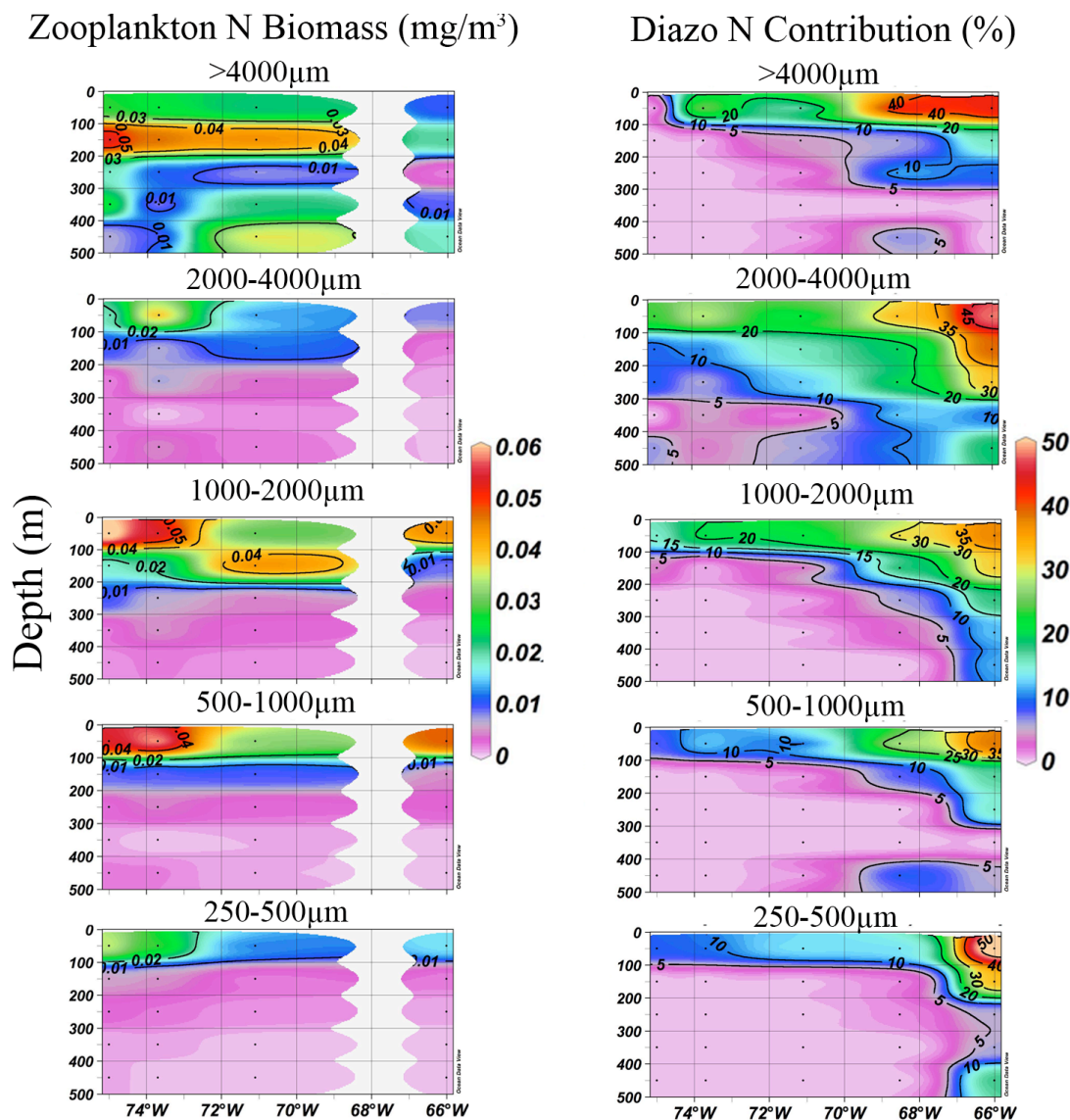


Figure 5.3 – Color contour plot showing mesozooplankton N biomass (mg N m^{-3}) (left) and diazotroph N contribution (right) for different size fractions collected in the upper 500m of the water column along Leg 2 of cruise track SJ0005, a SE to NW transect in the western subtropical North Atlantic Ocean. Figure was prepared using Ocean Data View (Schlitzer 2008).

Table 5.1 - Mean (± 1 SD) size-integrated areal mesozooplankton biomass within each depth range collected along Leg 2 of cruise track SJ0005, a SE to NW transect in the western subtropical North Atlantic Ocean

Average Integrated Zooplankton Biomass (All Size Fractions)			
Depth (m)	<u>Total Biomass (mg/m²)</u>	<u>Nitrogen Biomass (mg/m²)</u>	<u>Carbon Biomass (mg/m²)</u>
0-100	389.1 \pm 318.7	14.9 \pm 4.9	65.1 \pm 21.2
100-200	125.4 \pm 65.4	8.0 \pm 3.2	32.5 \pm 13.0
200-300	31.1 \pm 13.7	2.2 \pm 1.1	8.8 \pm 4.3
300-400	33.7 \pm 14.1	2.0 \pm 1.0	8.8 \pm 4.8
400-500	25.4 \pm 10.8	2.2 \pm 1.3	8.4 \pm 4.4

Table 5.2 - Mean (± 1 SD) depth-integrated areal mesozooplankton biomass of different size fractions collected along Leg 2 of cruise track SJ0005, a SE to NW transect in the western subtropical North Atlantic Ocean

<u>Size Fraction (μm)</u>	<u>Average Integrated Zooplankton Biomass</u>					
	<u>Total Biomass (mg/m^2)</u>		<u>Nitrogen Biomass (mg/m^2)</u>		<u>Carbon Biomass (mg/m^2)</u>	
	<u><200m</u>	<u><500m</u>	<u><200m</u>	<u><500m</u>	<u><200m</u>	<u><500m</u>
250-500	43.0 \pm 18.1	47.1 \pm 20.2	2.6 \pm 1.2	2.8 \pm 1.4	12.0 \pm 5.3	13.1 \pm 5.9
500-1000	62.7 \pm 13.1	68.3 \pm 14.5	4.4 \pm 1.0	4.8 \pm 1.1	19.5 \pm 3.9	21.1 \pm 4.2
1000-2000	105.7 \pm 19.2	118.9 \pm 25.2	7.0 \pm 1.2	7.9 \pm 1.6	29.4 \pm 4.6	33.0 \pm 6.2
2000-4000	48.3 \pm 39.7	56.1 \pm 44.4	2.7 \pm 1.5	3.3 \pm 1.9	11.2 \pm 6.2	13.7 \pm 7.8
>4000	254.9 \pm 264.9	314.5 \pm 268.7	6.2 \pm 2.2	10.6 \pm 3.5	25.6 \pm 8.3	42.8 \pm 13.5

4.2B). Our fluorometric measurements show a clear pigment maximum around the base of the mixed layer, at an average depth of 75m west of 71°W and deepening to ~125m east of 71°W (Figure 4.2B).

Depth-integrated standing stock of PN in the upper 100 m of the water column averaged $191 \pm 42 \text{ mg N m}^{-2}$ along Leg 2. Suspended PN concentrations ranged from 0.03 to 0.24 μM along Leg 2, with the highest concentrations occurring in the mixed layer (upper 100m) (Figure 5.2). PN concentrations were consistently greater than 0.15 μM above 100m, but decreased rapidly with depth and were generally lower than 0.1 μM below 150m. The highest PN concentrations along the transect were located in the upper 100m at stations 10 (27°29'N, 66°0.3'W) and 16 (31°36'N, 73°42'W). We observed higher PN concentrations of 0.12 to 0.19 $\mu\text{M N}$ at station 10, and in the water column at station 16 (0.12-0.19 $\mu\text{M N}$), including the highest value along the transect (0.24 $\mu\text{M N}$).

Mesozooplankton biomass concentrations were greatest in the upper 200m of the water column for all size fractions, with little biomass collected below this depth (Tables 5.1 & 5.2, Figure 5.3). Mesozooplankton within the 250-500 μm , 500-1000 μm , and 1000-2000 μm size fractions were most abundant in the upper 100m of the water column, and the latter two size classes had very high biomass concentrations at both the northwestern ($\sim 0.06 \text{ mg N m}^{-3}$) and southeastern ($\sim 0.04 \text{ mg N m}^{-3}$) edges of Leg 2 (Figure 5.3). The northwestern end of the transect showed the highest biomass values for all the mesozooplankton size classes combined, exhibiting average depth-integrated biomass (upper 200m) of $27.9 \pm 0.1 \text{ mg N m}^{-2}$ between station 16 & 17. The southeastern end of the transect had lower biomass of about half of that amount (15 mg N m^{-2} , station 10 (66°W) (Figure 5.3). Only the largest mesozooplankton ($>4000\mu\text{m}$) showed considerable biomass at depth, with concentrations up to 0.04 mg N m^{-3} between 400-500m at station 14. The biomass of the $>4000\mu\text{m}$ size fraction was greatest between 100-200m ($0.03\text{-}0.05 \text{ mg N m}^{-3}$) on the northwestern section of this transect, from station

14-17 (Figure 5.3). The 1000-2000 μ m size class also had high biomass values at station 14 (~ 0.04 mg N m⁻³) between 100-200m.

Mesozooplankton samples were collected at night (1800-0600) at all stations along Leg 2, so day and night comparisons could not be made.

5.3.3 SJ0005 Leg 3 – Stations 17-49

The third Leg of SJ0005 spanned the subtropical North Atlantic from station 17 (32°16'N, 75°W) to station 49 (32°16'N, 21°16'W) (Figure 5.1). Temperatures in the upper 500m of the water column ranged from 14-22°C, with cooler water shoaling eastward (Figure 4.2A). σ_T values ranged from 25.5 to 28.0, and isopycnals shoaled towards the east, converging on a value of 27.0 in the upper 200m of the water column. As with Leg 2, NO₃⁻ values were below the limit of detection in surface waters (<50m), and the depth of the 1 μ M contour ranged from 100-150m across the transect, deepening steadily from 100m to 150m east of 60°W then shoaling back to 100m at the end of the transect. Fluorometric measurements taken along this transect showed a clear pigment maximum at 75-100m depth across most of the basin, but deepening to between 100-125m in the central North Atlantic between 35-50°W.

Depth-integrated PN in the upper 100 m of the water column averaged 149 ± 64 mg N m⁻². Suspended PN concentration ranged from 0.02 to 0.67 μ M along Leg 3, with the highest values occurring in the mixed layer (Figure 5.4). PN concentrations were consistently greater than 0.075 μ M above 100m, but decreased rapidly with depth and were generally lower than 0.05 μ M below 150m. We found relatively high PN concentrations (>0.02 μ M N) at depths >175 m in the middle of the gyre between stations 35-41 ($\sim 42^\circ$ W- 53° W). The highest PN concentrations found along the transect were located in the upper 100m at stations 22 (32°15.6'N, 67°59'W) and 23 (32°16.2'N, 66°40.2'W), and ranged between 0.23 and 0.67 μ M N. We also observed relatively high

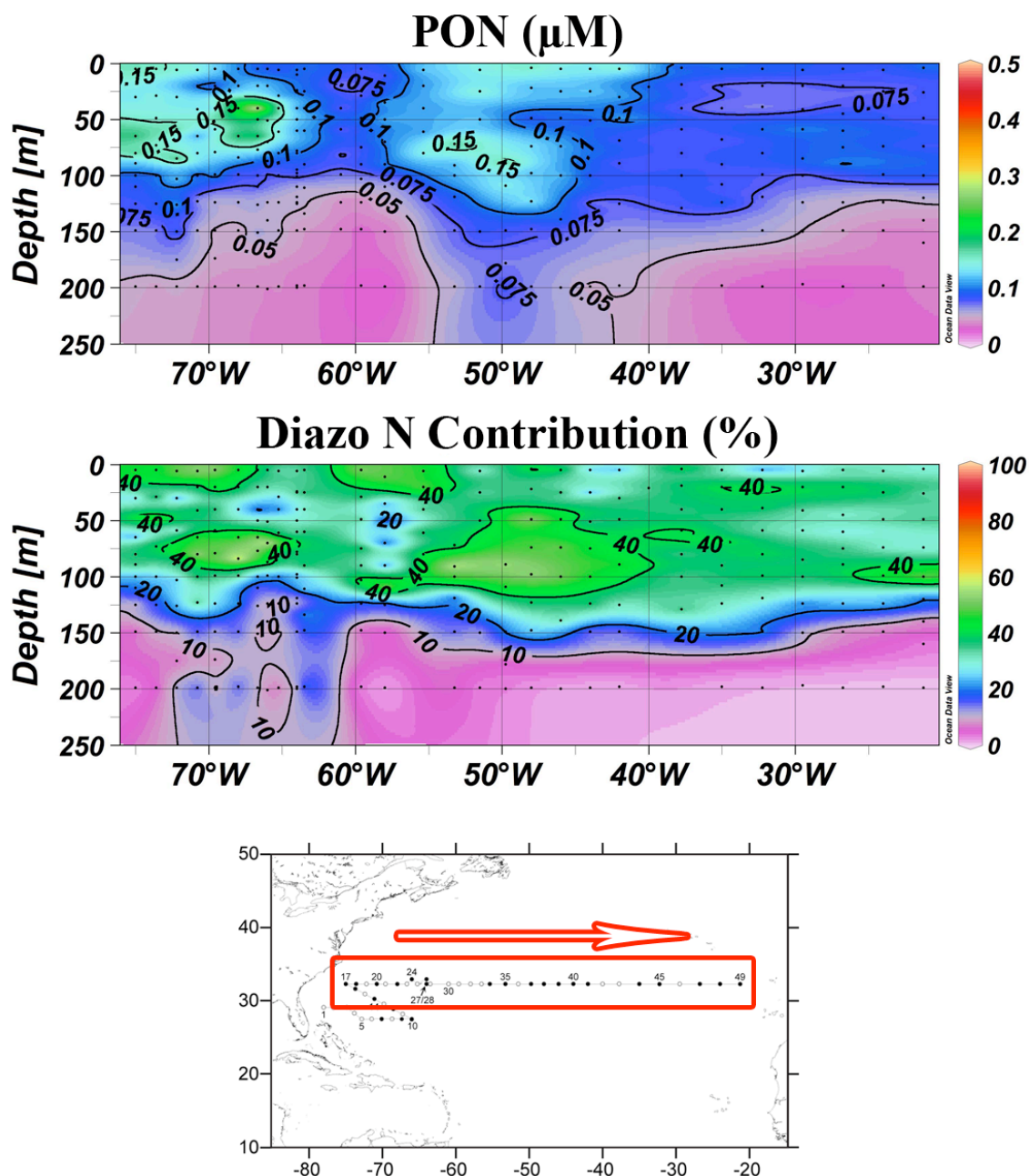


Figure 5.4 - Color contour plots showing PN concentration (μM N) of suspended particles collected in the upper 250m of the water column along Leg 3 of cruise track SJ0005, a zonal transect spanning the subtropical North Atlantic Ocean at 32°N. Figure was prepared using Ocean Data View (Schlitzer 2008).

PN concentrations 0.10 to 0.21 $\mu\text{M N}$ in the upper 100m between stations 34 (32°15.9'N, 55°22.2'W) and 39 (32°15.9'N, 45°59.9'W).

As with Leg 2, mesozooplankton biomass along Leg 3 was highest in the upper 200m of the water column, and N_{ZOO} biomass at depth was size-dependent (Table 5.3 & 5.4, Figure 5.5). The smallest mesozooplankton (250 μm -1000 μm) were generally caught in the upper 200m, with minimal biomass below 200m depth (Figure 5.5). N_{ZOO} biomass in the 1000-2000 μm and 2000-4000 μm size classes was highest within the upper 200m (0.01-0.04 mg N m^{-3}), but exceeded the biomass of smaller zooplankton below 200m (0.005-0.01 mg N m^{-3}). Mesozooplankton within the 2000-4000 μm size fraction deviated from this pattern, exhibiting the lowest biomass values relative to any other zooplankton size fraction collected across the basin. Biomass of the largest zooplankton size class (>4000 μm) was the most variable through the water column, generally having higher biomass values below 200m than in the upper 200m of the water column (Table 5.4).

Along Leg 3, zooplankton biomass was higher when collected at night ($271 \pm 158 \text{ mg dw m}^{-3}$) than during the day ($213 \pm 105 \text{ mg dw m}^{-3}$). Total biomass in the upper 200m was higher at night as well, but was not significantly different from biomass collected during daytime tows ($p > 0.05$). We did, however, observe higher biomass in the mixed layer at night, although this difference did not differ significantly (ANCOVA, F-ratio = 3.6, dF = 4, $p = 0.06$).

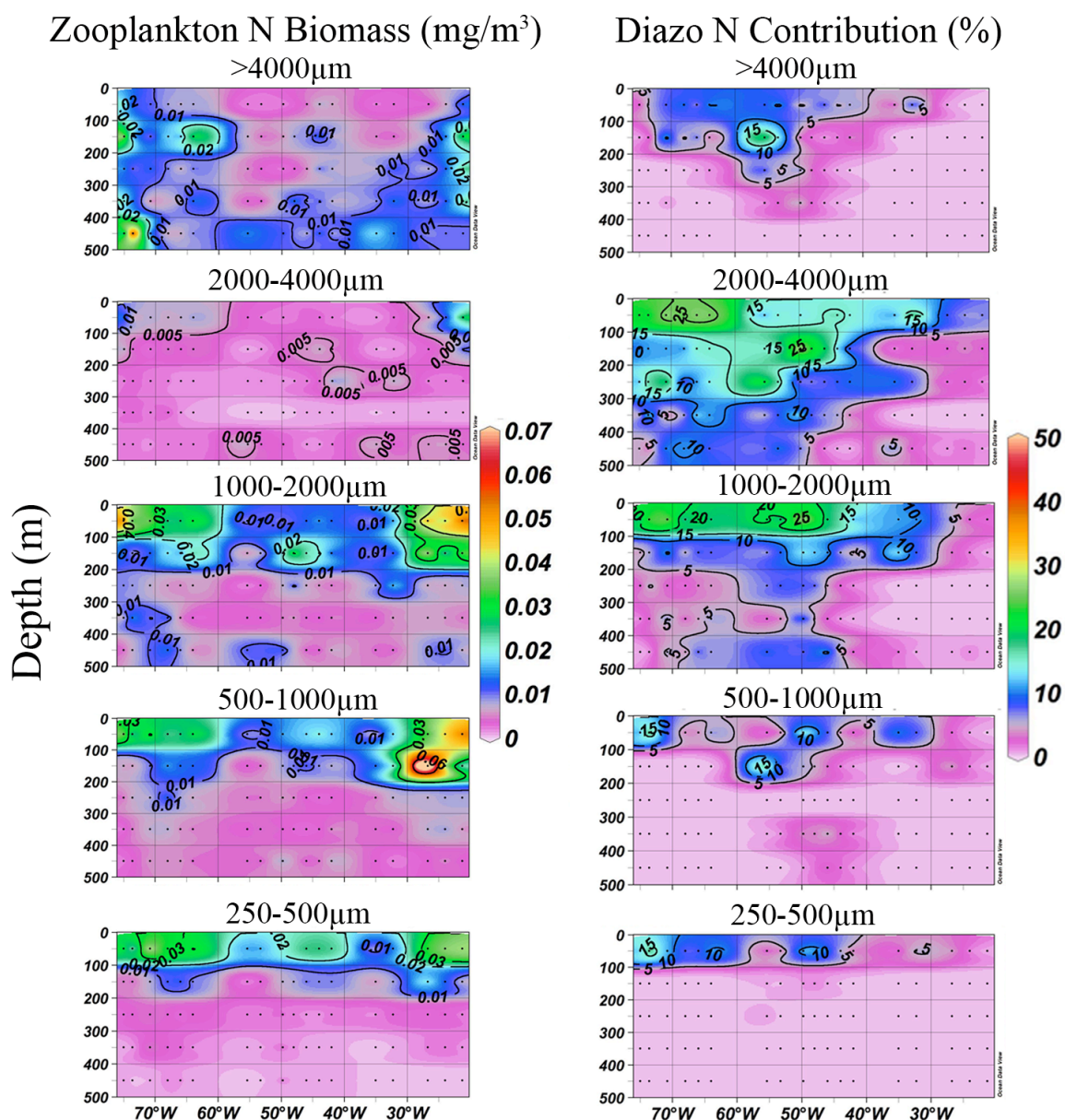


Figure 5.5 - Color contour plots showing mesozooplankton N biomass (mg N m^{-3}) (left) and diazotroph N contribution (right) for different size fractions collected in the upper 500m of the water column Leg 3 of cruise track SJ0005, a zonal transect spanning the subtropical North Atlantic Ocean at 32°N. Figure was prepared using Ocean Data View (Schlitzer 2008).

Table 5.3 - Mean (± 1 SD) size-integrated areal mesozooplankton biomass within each depth range collected along Leg 3 of cruise track SJ0005, a zonal transect spanning the subtropical North Atlantic Ocean at 32°N.

Average Integrated Zooplankton Biomass (All Size Fractions)			
<u>Depth (m)</u>	<u>Total Biomass (mg/m²)</u>	<u>Nitrogen Biomass (mg/m²)</u>	<u>Carbon Biomass (mg/m²)</u>
0-100	146.9 \pm 84.2	8.5 \pm 5.8	36.9 \pm 24.5
100-200	87.5 \pm 65.7	6.1 \pm 5.4	24.2 \pm 20.0
200-300	42.5 \pm 19.0	2.8 \pm 1.5	11.1 \pm 5.6
300-400	32.0 \pm 14.0	2.3 \pm 1.2	9.3 \pm 4.8
400-500	34.9 \pm 25.9	2.8 \pm 2.3	11.4 \pm 10.5

Table 5.4 - Mean (± 1 SD) depth-integrated areal mesozooplankton biomass of different size fractions collected along Leg 3 of cruise track SJ0005, a zonal transect spanning the subtropical North Atlantic Ocean at 32°N.

Average Integrated Zooplankton Biomass						
Size Fraction (μm)	Total Biomass (mg/m^2)		Nitrogen Biomass (mg/m^2)		Carbon Biomass (mg/m^2)	
	<u><200m</u>	<u><500m</u>	<u><200m</u>	<u><500m</u>	<u><200m</u>	<u><500m</u>
250-500	51.7 \pm 20.6	60.1 \pm 24.1	3.3 \pm 1.6	3.8 \pm 1.7	14.4 \pm 7.0	16.7 \pm 8.0
500-1000	55.6 \pm 37.6	77.0 \pm 39.9	3.9 \pm 3.5	5.4 \pm 3.6	16.5 \pm 13.1	23.0 \pm 13.8
1000-2000	69.3 \pm 40.9	95.1 \pm 44.9	4.3 \pm 3.2	6.2 \pm 3.4	17.9 \pm 12.4	25.3 \pm 13.3
2000-4000	17.7 \pm 17.1	27.9 \pm 17.1	1.0 \pm 1.3	1.8 \pm 1.3	4.2 \pm 5.2	7.0 \pm 5.1
>4000	40.1 \pm 46.5	83.8 \pm 65.5	2.1 \pm 2.4	5.3 \pm 4.4	8.1 \pm 9.5	20.9 \pm 17.8

5.4 Discussion

Although new N inputs via biological N₂-fixation support significant primary production in many oceanic environments (Karl et al. 1997, Karl et al. 2002, Capone et al. 2005, LaRoche & Breitbarth 2005), little is known about the movement of this N into higher trophic levels (Montoya et al. 2002, Mulholland 2007). Since mesozooplankton play a crucial role in OM movement into deeper waters (Longhurst et al. 1989, Al-Mutairi & Landry 2001, Steinberg et al. 2002, Frangoulis et al. 2005), it is crucial to quantify their role in diazotroph N incorporation and transport below the mixed layer, which has not been assessed to date. We evaluated the depth-integrated pools of total and new N in suspended particles and mesozooplankton to assess the extent to which diazotrophs support biological production in the upper ocean ($Z < 500\text{m}$). These data help elucidate the extent to which diazotrophs support both primary and secondary production, and the role that N_D plays in both biogeochemical cycling and OM flux through the biological pump.

5.4.1 PN distributions

Depth-integrated total PN have been assessed in the North Atlantic across a wide range of latitudes (between 0°-45°N) (Altabet et al. 1991, Waser et al. 2000, Montoya et al. 2002, Reynolds et al. 2007). Taken together, the available data show both latitudinal and zonal variation in depth-integrated total PN. Waser et al. (2000) collected PN from the euphotic zone along a cruise track (Hudson 1993) from the Canary Islands (~30°N, 21°W) westward to Nova Scotia (43°45'N, 54°19'W) during May-June 1993, which is similar to the timing of SJ0005. They found average depth-integrated PON values of $933 \pm 212 \text{ mg N m}^{-2}$ ($67 \pm 15 \text{ mmol N m}^{-2}$) within the euphotic zone (average depth = $88 \pm 25 \text{ m}$). These averages are much higher than our mean depth-integrated suspended particle biomass along Leg 3, which was $149 \pm 64 \text{ mg N m}^{-2}$ in the upper 100m.

Reynolds et al. (2007) looked at both zonal and meridional patterns of PN concentrations in both the North and South Atlantic. Although they not did sample with high spatial resolution, they found average mixed layer PN stocks of 0.1 $\mu\text{M N}$ in the western gyre (20°N-40°N, 65°W-80°W), 0.3 $\mu\text{M N}$ in the central gyre (7°N-32°N, 30°W-65°W), and 0.2 $\mu\text{M N}$ in the eastern gyre region (7°N-40°N, 5°W-30°W). In comparison, we observed similar PN concentrations averaged in mixed layer in the western portion of the basin ($0.1 \pm 0.14 \mu\text{M N}$), but observed lower PN concentrations in the central ($0.1 \pm 0.04 \mu\text{M N}$) and eastern ($0.09 \pm 0.02 \mu\text{M N}$) subtropical North Atlantic.

Montoya et al. (2002) collected suspended particles along two cruise tracks (SJ9612 & SJ9603) in the western portion of the tropical North Atlantic between 0-28°N, and found average PN concentrations of $682 \pm 402 \text{ mg N m}^{-2}$ for depth-integrated (upper 100m) suspended PN across the basin between 13-16°N. Depth-integrated PN concentration was higher in the western Atlantic ($1016 \pm 563 \text{ mg N m}^{-2}$) than on the eastern side of the basin ($516 \pm 132 \text{ mg N m}^{-2}$) (Landrum et al., *in prep.*), which is consistent with our results of higher average areal PN in the west ($184 \pm 82 \text{ mg N m}^{-2}$) than in the east ($122 \pm 28 \text{ mg N m}^{-2}$). They also observed overall higher depth-integrated total ($682 \pm 402 \text{ mg N m}^{-2}$) PN than we observed along any Leg of our cruise.

5.4.2 N_{ZOO} biomass distributions

Our data show the typical decrease in mesozooplankton biomass with depth (Steinberg et al. 2000, Steinberg et al. 2002, Koppelman et al. 2003, Frangoulis et al. 2005, Fernandez-Alamo & Farber-Lorda 2006). Overall, depth-integrated total N_{ZOO} biomass averaged $15 \pm 9 \text{ mg N m}^{-2}$ above 200m, with lower biomass ($8 \pm 4 \text{ mg N m}^{-2}$) from 200-500m (Figures 5.6 & 5.7). Depth-integrated N_{ZOO} biomass averaged $15.5 \pm 7.9 \text{ mg N m}^{-2}$ and $17.9 \pm 8.7 \text{ mg N m}^{-2}$ along Leg 2 in the upper 200m and 500m, respectively (Figure 5.6). Depth-integrated total N_{ZOO} biomass averaged $15 \pm 10 \text{ mg N m}^{-2}$ in the upper 200m and $22 \pm 11 \text{ mg N m}^{-2}$ in the upper and 500m along Leg 3 (Figure

5.7). A decrease in mesozooplankton N biomass with depth is not surprising since the mixed layer is generally the predominant source of food for mesozooplankton. However, several size fractions were abundant at depth (e.g., animals >4000 μ m on Leg 2), suggesting that these animals either scavenged sinking PN effectively in a food-limited zone (Figures 5.3 & 5.5), or that they actively consumed PN nearer the surface than where they were captured (i.e., diel vertical migration).

In general, mesozooplankton biomass is low in the tropics/subtropics, and increases pole-ward (Hernandez-Leon & Ikeda 2005). Most of the mesozooplankton biomass measurements in the North Atlantic come from sites near the eastern and western ends of the basin (AMT: near eastern end; BATS: near western end). Integrated zooplankton biomass data along both Legs 2 and 3 fall within the range of mesozooplankton biomass reported from oligotrophic areas (Hernandez-Leon & Ikeda 2005), and at BATS (Steinberg et al. 2000, Madin et al. 2001, Steinberg et al. 2001, del Giorgio & Duarte 2002, Roman et al. 2002, Steinberg et al. 2002). Leg 3 of cruise SJ0005 traversed the North Atlantic basin at about the same latitude as both Station S (32°10'N, 64°30'W) and the BATS site (31°50'N 64°10'W), providing a good comparison for our data across the basin. The mean integrated (upper 200m) zooplankton biomass along Leg 3 of our cruise (234 ± 126 mg dw m⁻²) was roughly half the mean zooplankton biomass values seen over a 4-year sampling period at BATS (539 ± 312 mg dw m⁻²) (Madin et al. 2001). Although mesozooplankton biomass varies seasonally, our data are generally lower than measurements at BATS during similar seasons (e.g., April/May 1994-1997). However, depth-integrated mesozooplankton biomass during two BATS cruises (BATS 67 & 68) were similar to values we obtained (142 ± 75 and 186 ± 89 mg dw m⁻², respectively) at two individual sites near the BATS station (~40 km North of BATS) (Madin et al. 2001).

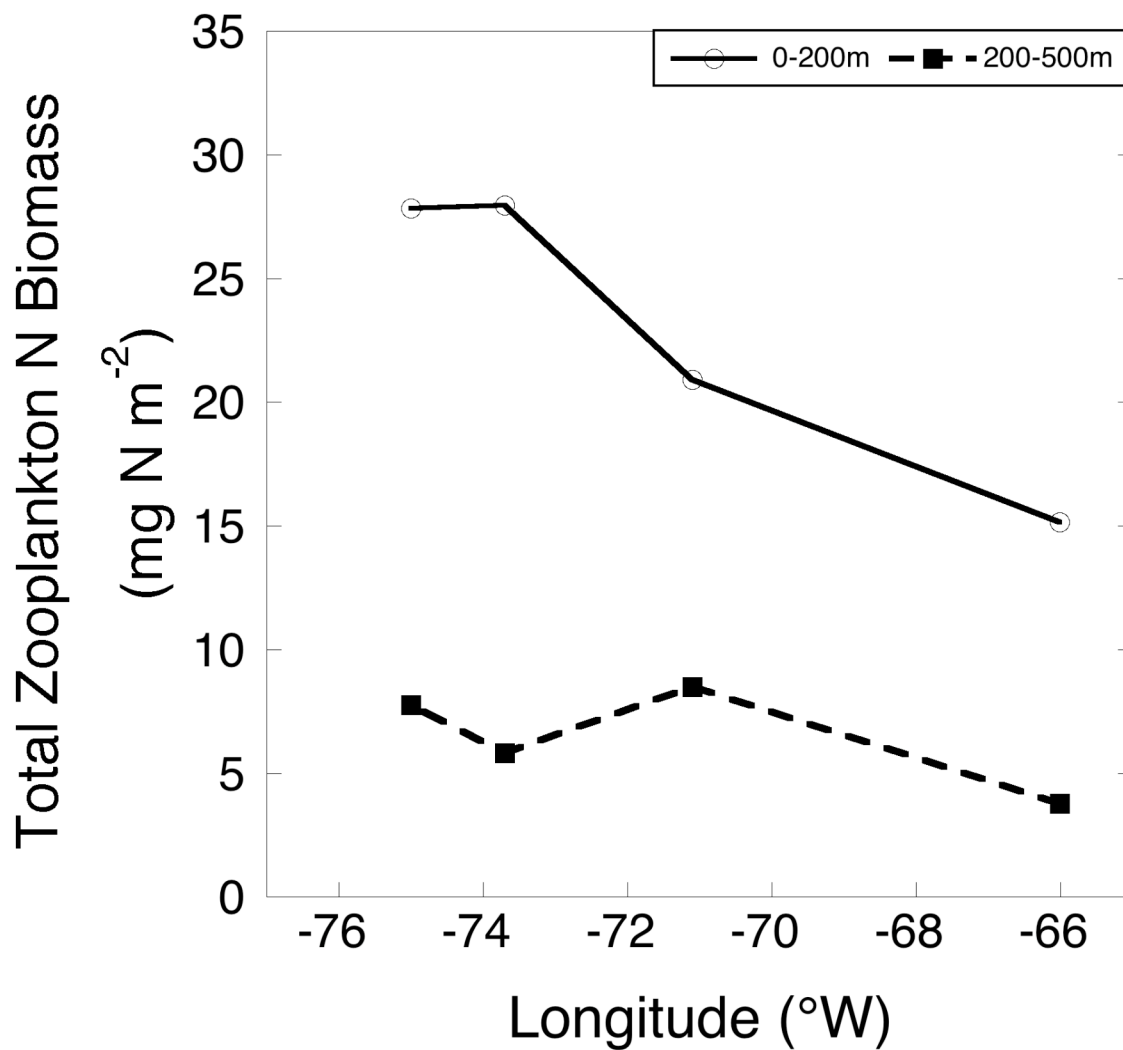


Figure 5.6 - Total mesozooplankton N biomass (mg N m^{-2}) (all size fractions) collected in the upper 200m and from 200-500m in the water column along Leg 2 of cruise track SJ0005, a SE to NW transect in the western subtropical North Atlantic Ocean.

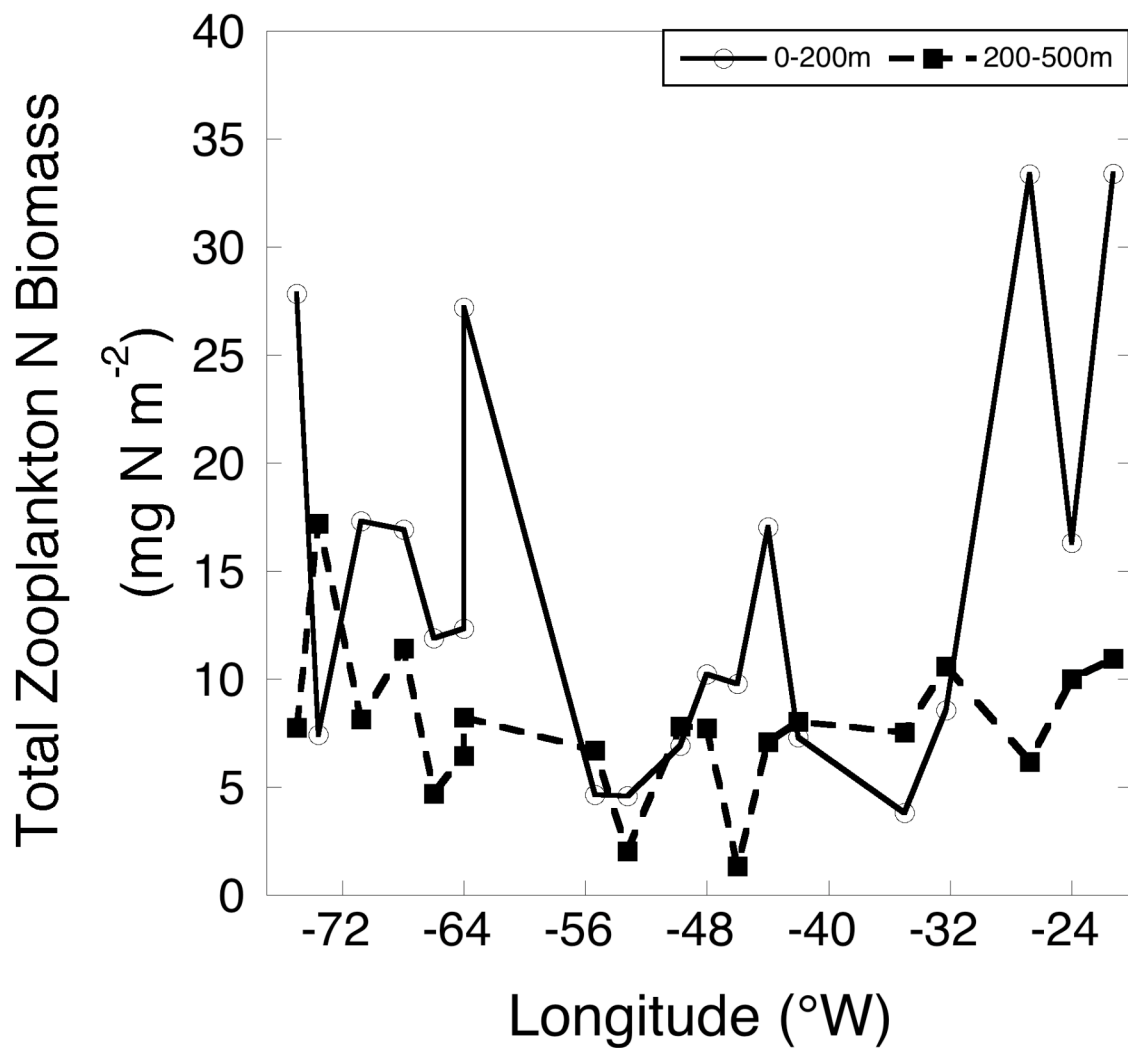


Figure 5.7 - Total mesozooplankton N biomass (mg N m^{-2}) (all size fractions) collected in the upper 200m and from 200-500m in the water column along Leg 3 of cruise track SJ0005, a zonal transect spanning the subtropical North Atlantic Ocean at 32°N.

In contrast, average mesozooplankton biomass collected along the Atlantic Meridional Transect (AMT) in the eastern part of the basin (25°N, 20°W to 40°N, 10°W) was lower ($200 \pm 50 \text{ mg dw m}^{-2}$) than mesozooplankton biomass along the meridional transect of SJ0005 (above) and at the easternmost station along Leg 3 (Station 49, 32°N, -21°W: 413 mg dw m^{-2}). However, higher mesozooplankton biomass values have been recorded at AMT stations in the northeastern corner of the North Atlantic (Maranon et al. 2007). It is difficult to separate seasonal and geographical trends in comparing zooplankton biomass between the two transects, since our cruise does not overlap spatially or temporally with the AMT (Isla et al. 2004).

5.4.3 N_{ZOOP} distributions among size fractions

Generally, mesozooplankton in the 1000-2000µm and >4000µm size classes had higher average N biomass than the mesozooplankton in the 250-500 and 500-1000µm size class (Tables 5.2 & 5.3). This trend was especially strong in the mixed layer along Leg 2 (Table 5.2). The mesozooplankton within the 2000-4000µm size class was much lower than any other size fraction along both legs (but much less abundant along Leg 3), and may include mesozooplankton important for diazotroph N movement through these systems.

Previous studies have documented lower biomass for mesozooplankton in the 2000-5000µm size class than in smaller size fractions. For example, Madin et al. (2001) observed average biomass of 70 -170 mg dw m⁻² (means of day and night samples) for the 2000-5000µm size fraction of mesozooplankton in the upper 200m of the water column at the BATS site between 1994-1998. This value is higher than our average biomass estimates for mesozooplankton in the 2000-4000µm size class (Tables 5.2 & 5.4), especially along Leg 3 ($\sim 18 \pm 18 \text{ mg dw m}^{-2}$). Although our data also show considerably lower biomass for the 2000-4000µm size fraction relative to the other size

fractions, the differences between our cruise and the BATS data could reflect differences in size classes used (i.e., 4000 v. 5000 μ m upper limit).

Other factors, such as net avoidance or ontogenetic/seasonal factors of the mesozooplankton community could also contribute to the low biomass we found in the 2000-4000 μ m size fraction. Net avoidance has been documented in previous studies (Brinton 1967), and this behavior could have driven our low yield of the 2000-4000 μ m size fraction of mesozooplankton. We cannot adequately evaluate this hypothesis given our sampling regime. Seasonal and/or ontogenetic factors could also have played a role since some larger mesozooplankton are known to diapause at depths >500m through May (Johnson et al. 2006, Gislason et al. 2007, Slagstad & Tande 2007). However, since our cruise occurred at the end of the typical time of overwintering mesozooplankton, most of these animals would most likely have been active, and collected within the water column at the time of our cruise.

Alternatively, heavy predation (e.g., fish, squid) could potentially explain lower biomass in the 2000-4000 μ m size fraction. There are many documented cases of higher trophic levels such as fish (Conover et al. 1995, Mianzan et al. 2001, Estrada et al. 2005, Sara & Sara 2007) and squid (Piontkovski et al. 2003), preying on mesozooplankton. Several studies have used isotopes to analyze diet in pelagic fishes (Estrada et al. 2005, MacNeill et al. 2005, Bode et al. 2007), but few (if any) have assessed the contribution of diazotroph N to these consumers, especially in smaller, mesozooplankton-consuming planktivorous organisms (e.g., flying fish). Diazotrophic cyanobacteria have also been shown to harbor an array of potentially harmful chemicals (Hawser et al. 1992), which may disrupt growth and/or reproduction of zooplankton. Thus, lower biomass for this size fraction may indicate a physiological response to diazotrophs. Further analysis of the mechanisms driving lateral and vertical variation in biomass and N_D contribution would be required to fully explore the eventual fate of new production into higher trophic levels with regards to this size class.

5.4.4 N_D contribution to PN

New PN standing stock averaged $71 \pm 36 \text{ mg N m}^{-2}$ ($\sim 30\% N_D$) for the entire cruise, while depth-integrated new PN was slightly higher along Leg 2 ($87 \pm 47 \text{ mg N m}^{-2}$) than on Leg 3 ($66 \pm 32 \text{ mg N m}^{-2}$). High N_D features were quite large along both legs, spanning thousands of kilometers in some cases (Leg 3: Station 31-41). For example, the large feature in the middle of the gyre between 50-100m in the water column along Leg 3 (Figure 5.4) was over 1,650 km long, with distances between stations averaging $166 \pm 28 \text{ km}$. These features also correlated with elevated PN concentrations, suggesting that diazotrophs enhanced the total standing stock of PN in these areas. Particles collected below the mixed layer along Leg 2, at station 12 ($28^\circ 52' \text{N}$, $68^\circ 31' \text{W}$), 13 ($29^\circ 31' \text{N}$, $69^\circ 46' \text{W}$) (Figure 5.2), and at several stations (stations 20-29) west of 50°W along Leg 3 (Figure 5.4) had low concentrations ($0.05\text{-}0.1 \mu\text{M N}$) of PN and contained little diazotroph N ($<10\%$). This suggests that movement of diazotroph N below the mixed layer was minimal at these stations. Some of these stations were also characterized by high N_D contributions to mixed layer particles as well as high N_{ZOO} concentrations (Stations 12, 20-29), while others showed no such association between PN biomass, N_D contributions, and N_{ZOO} concentrations (Stations 16, 34-39).

Variation in deep extension of N_D could have been driven by different transport mechanisms. For example, the higher N_D contribution to suspended particles below the mixed layer at station 12 may reflect export of diazotroph N at this station via mesozooplankton activity (e.g., DVM, fecal pellets). Isotopic evidence suggests that substantial amounts of N_D moved into the mesozooplankton community at station 12 ($>10\%$), with greater diazotroph N incorporation by larger mesozooplankton ($>20\%$) (Figure 5.3). High N_D contribution to the mesozooplankton community also suggests N_D incorporation over longer timescales, given the longer lifetimes of mesozooplankton (i.e., weeks to months) relative to phytoplankton (i.e., days to weeks). We see a similar

isotopic pattern in suspended particle and mesozooplankton at station 16, but lower average PN concentrations ($0.10 \pm 0.03 \mu\text{M N}$), lower N_D contribution to mesozooplankton (10-20%), and no evidence for vertical export of diazotroph N below 100m (Figures 5.2 & 5.3). This suggests that mesozooplankton are also incorporating the diazotroph PN pool, but had not grazed a significant portion of the PN at station 16 (Figure 5.3). Diazotrophs contributed substantially (10-25%) to the PN pool below 100m at several stations along Leg 3 in the western part of the basin. N_D contribution was <10% below 150m, east of station 29 ($32^\circ 16.1' \text{N}$, $63^\circ 29.4' \text{W}$), with no clear contribution to suspended particles in the eastern part of the basin (east of 40°W).

Depth-integrated new PN (via $\delta^{15}\text{N}_{\text{POM}}$) have also been assessed across the North Atlantic across a wide range of latitudes (between 0° - 45°N) (Altabet et al. 1991, Waser et al. 2000, Montoya et al. 2002, Reynolds et al. 2007). Taken together, the available data show both latitudinal and zonal variation in depth-integrated new PN, and provide broader spatial context for our estimates of N_D contribution to suspended particles. Waser et al. (2000) observed considerable N_D contribution for particles along this transect, measuring an average $\delta^{15}\text{N}_{\text{POM}}$ of $3.1 \pm 1.5 \text{ ‰}$, implying an average N_D contribution of $24 \pm 20\%$ based on our isotope mass balance model. These values equate to an average of $199 \pm 151 \text{ mg N m}^{-2}$ of new PN, which is also considerably larger than our estimate ($51 \pm 24 \text{ mg N m}^{-2}$) for the mixed layer.

Reynolds et al. (2007) looked at both zonal and meridional patterns of $\delta^{15}\text{N}_{\text{POM}}$ to determine the role of N_2 -fixation in supporting biomass in both the North and South Atlantic. Along a zonal transect at $\sim 36^\circ \text{N}$ (during May-June 2005), they found similar N_D contribution to suspended particles across in the western and central gyre ($\sim 40\%$), but lower N_D contribution in the eastern region of the gyre (0-20%). We observed consistently high N_D contribution to suspended particles (20-100% - Figure 5.4) along Leg 3, with no decrease in the east. However, higher N_D contribution to suspended particles (20-40%) observed along a section of the AMT track between 20°N and 32°N

and 15°W to 20°W were similar to our values in this area. Reynolds et al (2007) also showed areas of high N_D contribution (50-70%) to suspended particles in the central gyre (30°W-70°W) along a zonal track at 24°N. We similarly found areas of high N_D contribution (~40-50%) in the central gyre. Lower northern (36°N) N_D contribution to suspended particles further suggests that N_D contribution is higher in subtropical latitudes of the central gyre, decreasing northward into more temperate waters (i.e., Waser et al. 2000).

N_D contribution to suspended particles was also greater in the tropical than in the subtropical North Atlantic. Montoya et al. (2002) collected suspended particles on two cruise tracks (SJ9612 & SJ9603) to the tropical North Atlantic between 0-28°N, and observed higher depth-integrated new ($319 \pm 305 \text{ mg N m}^{-2}$) PN in the mixed layer, than we observed along any Leg of our cruise.

These data provide an overview of the distribution of N_D contribution to PN in the North Atlantic. Overall, the highest N_D contribution to suspended particles occurs in the tropical zones of the western and central gyre, with lower N_D contribution in the subtropical and temperate regions (Waser et al. 2000, Reynolds et al. 2007). However, depth-integrated PN concentrations strongly influence the size of the overall pool of N_D available for higher trophic levels. For example, despite relatively lower N_D contribution to particles (24%) collected along the Hudson 1993 track (Waser et al., 2000), depth-integrated new PN was 4 times higher than along Leg 3 of our cruise, reflecting the higher PN concentrations found by Waser et al. (2000). Spatial variation in PN concentrations and $\delta^{15}\text{N}$ in the mixed layer contribute to significant variation in depth-integrated new N_D estimates (Waser et al. 2000, Reynolds et al. 2007). We also observed a clear north-south trend in the Sargasso Sea, where average depth-integrated new PN values were higher along Leg 1 ($83 \pm 30 \text{ mg N m}^{-2}$) than both Leg 2 ($61 \pm 30 \text{ mg N m}^{-2}$) and the western portion (west of 55°W) of Leg 3 ($56 \pm 27 \text{ mg N m}^{-2}$) (Landrum et al., *in*

prep.). However, it is difficult to separate the mechanisms driving these patterns (e.g., higher diazotroph abundances) given our lack of floristic data.

5.4.5 N_D contribution to N_{ZOO}

Overall, depth-integrated diazotroph-derived mesozooplankton N biomass averaged $1.7 \pm 1.6 \text{ mg N m}^{-2}$ above 200m, with lower biomass ($0.13 \pm 0.11 \text{ mg N m}^{-2}$) from 200-500m. Along Leg 2, most of the N_D contribution to N_{ZOO} occurred in the mixed layer for all size fractions (Figures 5.3 & 5.8). Along Leg 2, depth-integrated diazotroph-derived N_{ZOO} biomass averaged $3.4 \pm 2.1 \text{ mg N m}^{-2}$ and $0.07 \pm 0.06 \text{ mg N m}^{-2}$ along Leg 2 in the upper 200m and between 200-500m, respectively (Figure 5.8). Along Leg 3, most of the N_D contribution to N_{ZOO} occurred in the upper 200m for all size fractions (Figures 5.5 & 5.10). Depth-integrated diazotroph N_{ZOO} biomass averaged $1.1 \pm 0.8 \text{ mg N m}^{-2}$ and $0.13 \pm 0.10 \text{ mg N m}^{-2}$ along Leg 3 in the upper 200m and between 200-500m, respectively (Figure 5.10).

We observed lower N_D incorporation by all size fractions below 200m, along both Legs. However, at station 10 along Leg 2, N_D contribution was high to the entire mesozooplankton community in the upper 500m of the water column (Figure 5.3). Higher N_D incorporation in the surface and at depth increased the total depth-integrated diazotroph N_{ZOO} biomass at this station (Figures 5.8 & 5.9). High N_D contribution to deeper mesozooplankton suggests that these organisms were either consuming sinking particles containing N_D at depth, or incorporating N_D through DVM into the mixed layer. Higher N_D contribution to PN below the mixed layer at station 10 also suggests that sinking N_D could have been incorporated by deeper mesozooplankton, but the low biomass of mesozooplankton at depth suggests that the N_D did not promote appreciable accumulation of N_{ZOO} biomass.

The relationship between N_D contribution and N_{ZOO} biomass varied laterally and vertically among mesozooplankton size classes along both Leg 2 and 3 (Figures 5.3 &

5.5). Along Leg 2, although all mesozooplankton size fractions incorporated significant N_D at station 10, certain size fractions represented larger portions of diazotroph N_{ZOO} (Figures 5.3 & 5.9). For example, only the 500-1000 μ m and 1000-2000 μ m size fractions exhibited high N_{ZOO} biomass (0.04-0.05 mg N m⁻³) at station 10 (Figure 5.3). Thus, these size fractions represented the largest portion of diazotroph N_{ZOO} at this station (Figure 5.9). Conversely, the N_{ZOO} biomass for these size fractions was also high at the northwest end of Leg 2 (Station 17), but N_D contribution to N_{ZOO} was lower (10-20%). This produced lower overall depth-integrated diazotroph N_{ZOO} at station 17, where the 1000-2000 μ m size fraction represented the largest pool of N_D for all size fractions (Figure 5.9).

N_D contribution was also high for the 2000-4000 μ m size fraction along Leg 2 (Figure 5.3). Total N_{ZOO} biomass was generally low along this transect, and high N_D did not always coincide with higher N_{ZOO} for this size fraction (Figures 5.3 & 5.9). For example, for this size fraction, we observed high N_{ZOO} biomass (0.02-0.04mg N m⁻³) and lower N_D contribution (20-30%) in the northwest (Station 16) (Figure 5.3). Alternatively, we observed low biomass N_{ZOO} biomass for this size fraction on the southeast end of the transect (Station 10), where N_D contribution was higher (45-50%) (Figure 5.3). Despite lower N_D contribution for this size fraction at station 16, elevated N_{ZOO} biomass values part of the relative diazotroph N_{ZOO} for the mesozooplankton community along Leg 2 (Figure 5.9). N_D contributions to the PN pool could potentially influence this lateral variation. For example, elevated PN concentrations and high N_D to PN at station 16 suggests that more N_D was available for mesozooplankton consumption relative to station 10 (Figure 5.2). Thus, greater N_D availability could have influenced N_D incorporation into N_{ZOO} of the 2000-4000 μ m size fraction at station 16 (Figure 5.9).

Along Leg 3, we found lower N_{ZOO} biomass and higher N_D contribution to mesozooplankton in the central gyre (Figure 5.5). For example, between 30°W- 60°W, N_D contribution to mesozooplankton was typically high (10-30%), but N_{ZOO} biomass

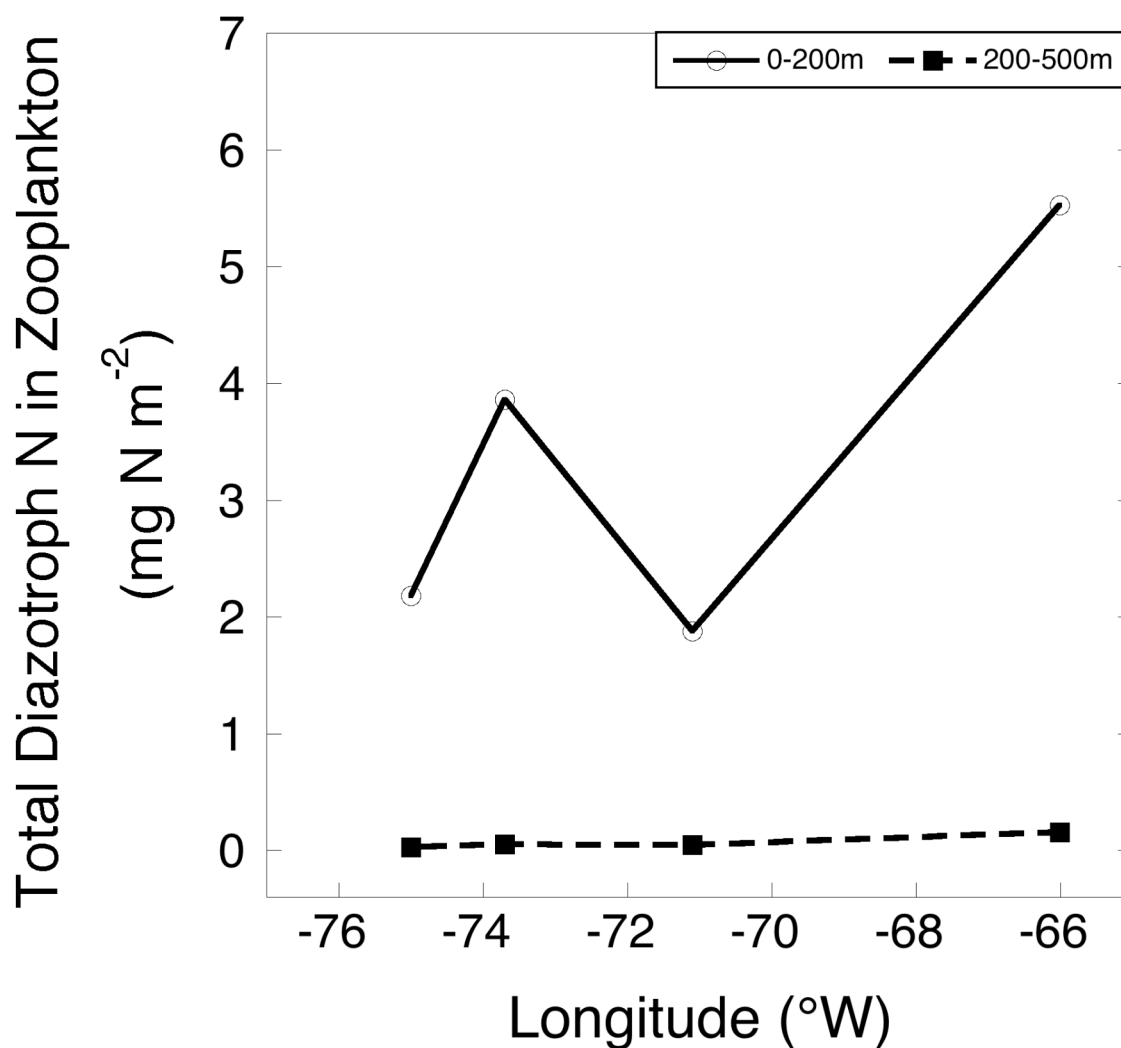


Figure 5.8 - Total diazotroph N biomass (mg N m^{-2}) of mesozooplankton (all size fractions) collected in the upper 200m and from 200-500m in the water column along Leg 2 of cruise track SJ0005, a SE to NW transect in the western subtropical North Atlantic Ocean.

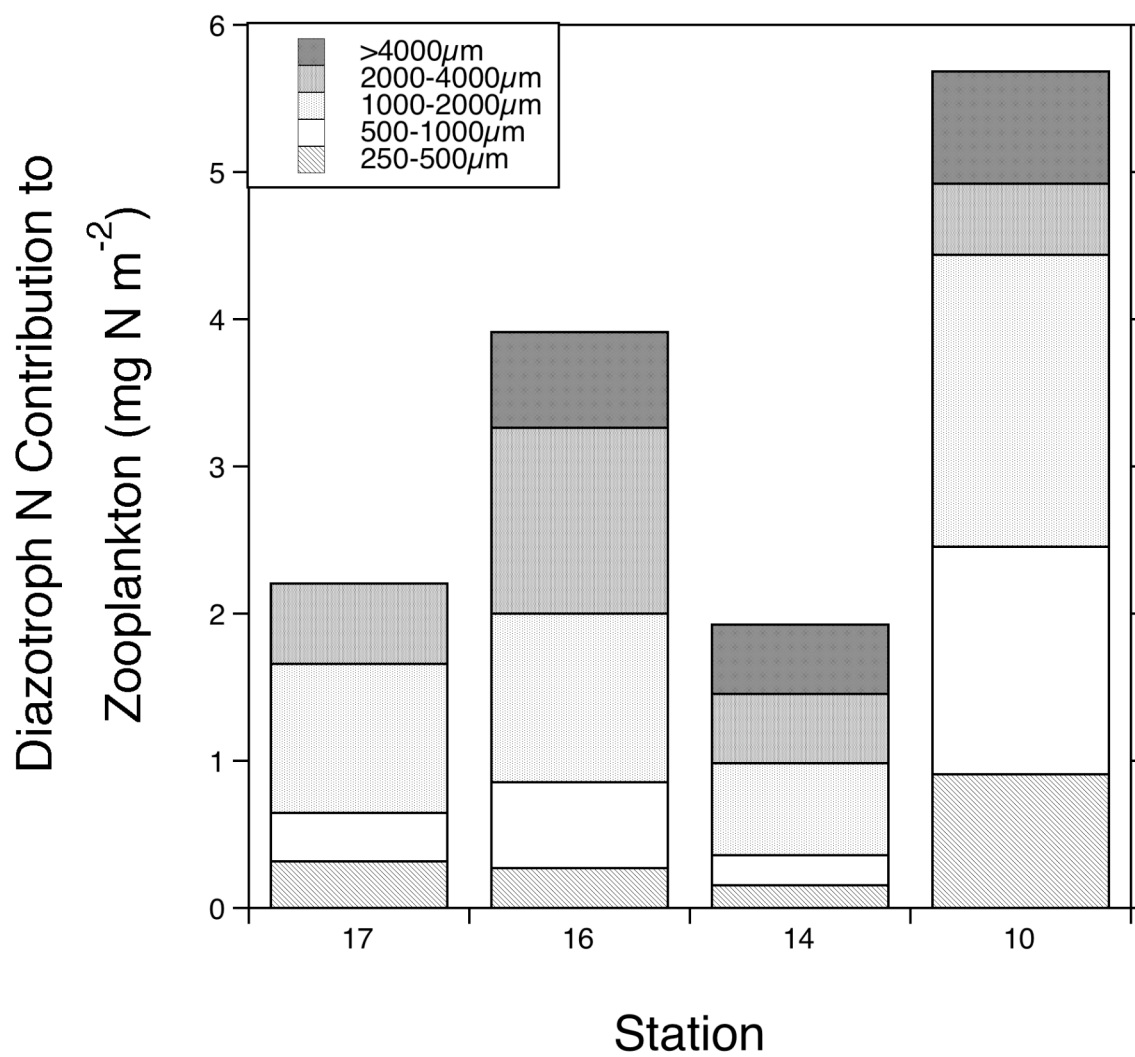


Figure 5.9 - Total diazotroph N biomass (mg N m^{-2}) of mesozooplankton of different size fractions in the upper 500m of the water column along Leg 2 of cruise track SJ0005, a SE to NW transect in the western subtropical North Atlantic Ocean.

was generally lower ($0.01\text{-}0.02\text{ mg N m}^{-3}$) than on either end of the basin ($0.03\text{-}0.05\text{ mg N m}^{-3}$). These trends are most likely driven by a lower assimilation efficiency of organic matter containing diazotroph N, since PN concentrations and N_D contribution were also high in these areas (Figure 5.4). As noted above, we observed high PN concentrations and N_D contribution to particles in the central gyre, suggesting a high concentration of diazotroph N available for consumption in this area. High N_D contribution, and low biomass of mesozooplankton within the same area suggests that mesozooplankton are incorporating N_D , but are not producing substantial total biomass as in the western and eastern ends of the basin (Figures 5.5).

Along Leg 3, only the larger animals ($>1000\mu\text{m}$) showed any vertical variation in N_D contribution, suggesting that larger mesozooplankton were incorporating N_D through vertical migration. Mesozooplankton in the $1000\text{-}2000\mu\text{m}$ and $2000\text{-}4000\mu\text{m}$ size classes also represented a significant fraction of total N_D to N_{ZOO} of the entire mesozooplankton community, which is especially evident in the central and western portions of the basin (Figures 5.10 & 5.11). This further suggests that these larger animals are important components for N_D movement into food webs and through the water column.

We also observed a strong east-west gradient in N_D contribution along Leg 3, which was especially apparent in the three easternmost stations (Stations 47-49). N_D contribution to mesozooplankton was minimal ($<5\%$) for all size fractions east of 30°W , but mesozooplankton biomass was high ($0.03\text{-}0.07\text{mg N m}^{-3}$) relative to biomass in the central and western portions of the basin ($0.01\text{-}0.05\text{ mg N m}^{-3}$). These trends suggest that mesozooplankton N_D incorporation is relatively high in the central and western North Atlantic, while elevated mesozooplankton biomass in the east is driven by incorporation of other N sources. High N_D contribution to suspended particles, low N_D contribution to further suggests that these mesozooplankton are either selectively consuming non-diazotroph N, or inefficiently assimilating diazotroph N.

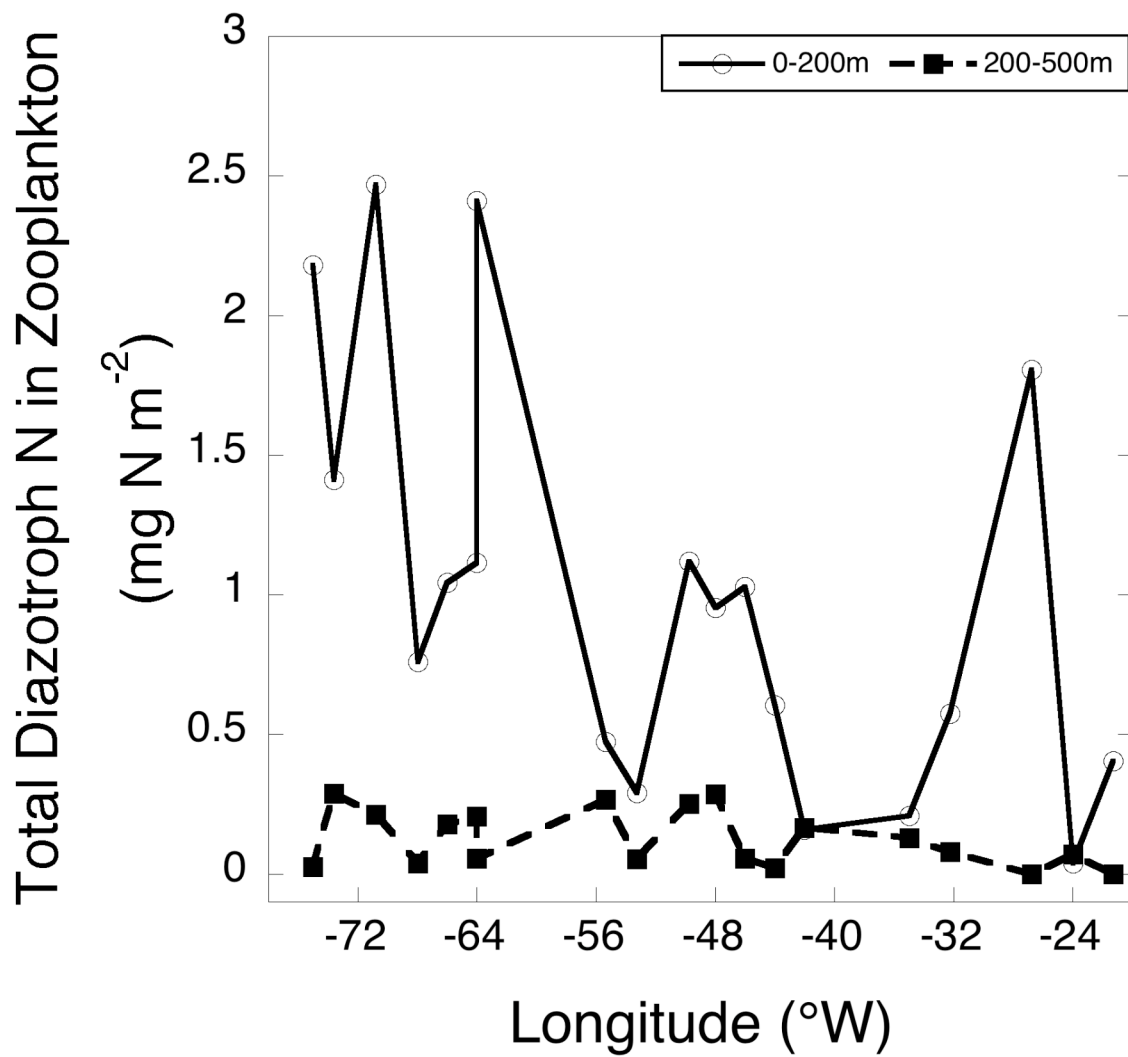


Figure 5.10 - Total diazotroph N biomass (mg N m^{-2}) contributed to mesozooplankton (all size fractions) collected in the upper 200m and from 200-500m in the water column along Leg 3 of cruise track SJ0005, a zonal transect spanning the subtropical North Atlantic Ocean at 32°N.

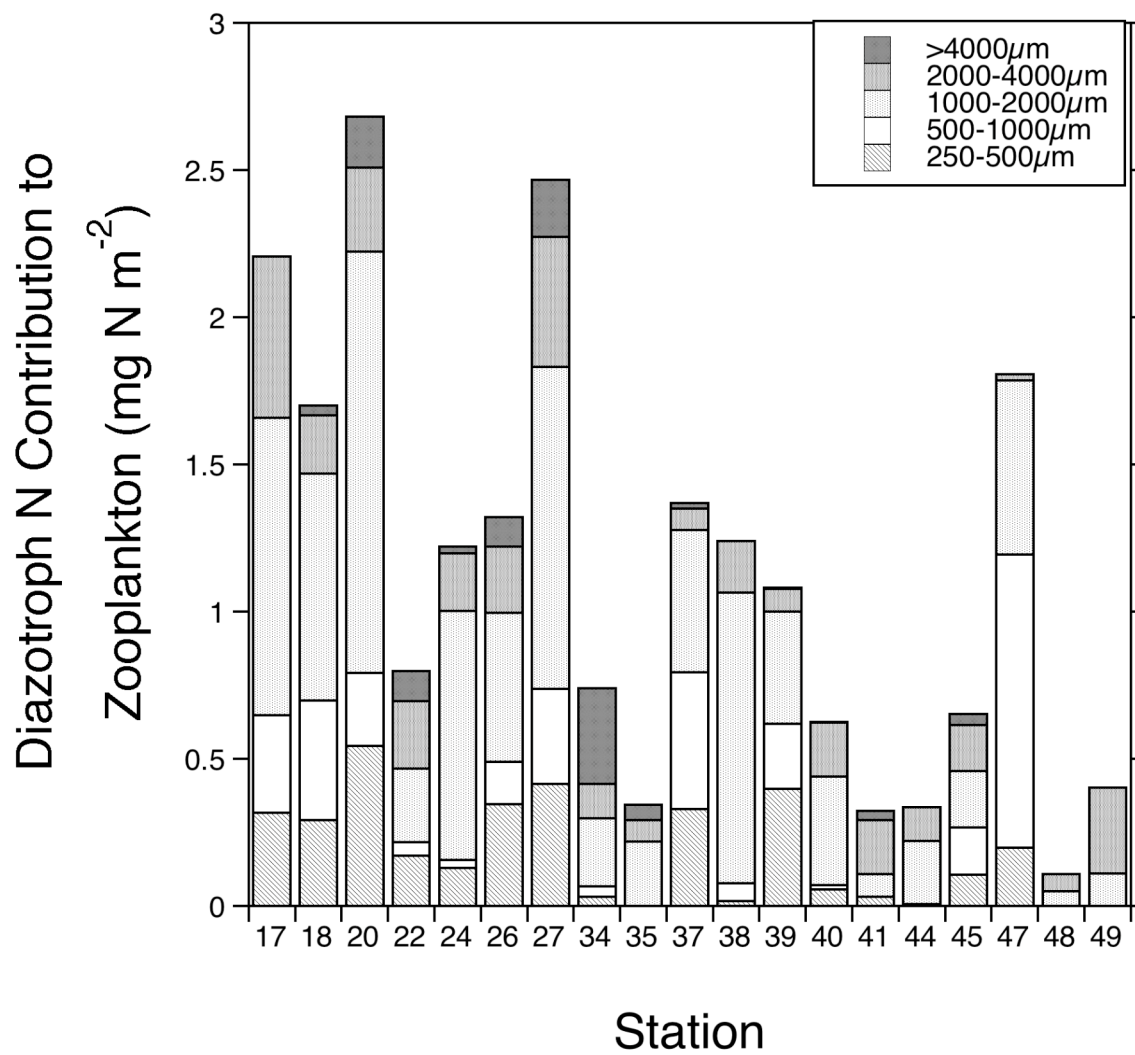


Figure 5.11 - Total diazotroph N biomass (mg N m⁻²) contributed to mesozooplankton of different size fractions in the upper 500m of the water column along Leg 3 of cruise track SJ0005, a zonal transect spanning the subtropical North Atlantic Ocean at 32°N.

Overall, our data suggest that mesozooplankton incorporated N_D along Leg 2 and 3, but that the movement of this N into different size classes is complex and may depend on the taxonomic makeup and structure of the zooplankton community, size-dependent differences in N_D incorporation timescales, or on the availability of N_D . Our data do, however, indicate that diazotroph N contributions to these ecosystems can lead to elevated mesozooplankton N biomass, especially in areas where diazotroph N contributes significantly to both the PN and mesozooplankton pools (e.g., Station 16: Figure 5.2 & 5.3).

5.4.5 Mesozooplankton migration

Mesozooplankton diel vertical migration (DVM) influences global biogeochemical cycling more than any other known migration (Steinberg et al. 2000, Al-Mutairi & Landry 2001, Frangoulis et al. 2005, Hernandez-Leon et al. 2008), but little is known about the N sources supporting migrating zooplankton or the proportion of diazotroph N exported via DVM. As seen along Leg 3, DVM likely influences N_D movement in the water column, especially through migrations of mesozooplankton in the 1000-2000 μ m and 2000-4000 μ m size fractions (Figures 5.5 & 5.11). However, overall low biomass of the 2000-4000 μ m size fraction might potentially limit their impact across the basin.

In order to quantify N_D movement via migrating mesozooplankton, we conservatively estimated migrant biomass as the difference between average night and daytime collections in the upper 200m of the water column along Leg 3. We estimate that migrant biomass averaged 5.4 mg N m⁻², or ~24% of the average total mesozooplankton N biomass collected in the upper 500m of the water column. These values fall within the typical range of estimates of the fraction of the mesozooplankton community that migrates vertically in oceanic systems (15-50%) (Longhurst 1976, Longhurst & Harrison 1988) including BATS (4-70%) (Steinberg et al. 2000, Steinberg

et al. 2002). Our estimate of the absolute quantity of migrating biomass (19 mg C m^{-2}) is low relative to other estimates for the North Atlantic ($5\text{-}480 \text{ mg C m}^{-2}$) (Morales 1999), and represents $\sim 40\%$ of the annual migrating biomass at BATS (Steinberg et al. 2000, Steinberg et al. 2002).

We can combine our estimate of N_{ZOO} biomass that migrates vertically with our isotopic estimate of the contribution of N_D to N_{ZOO} ($\sim 5\%$) to evaluate the role of migration in the vertical flux of diazotroph N. A migrant biomass of 5.4 mg N m^{-2} implies daily movement of new biomass amounting to 0.27 mg N m^{-2} , or 1 mg C m^{-2} (assuming C: N_{ZOO} of 4) into and out of the upper water column. We can then use literature estimates for the relationship between migrant biomass and net C transport (Steinberg et al. 2000) to estimate a net migrant export of new organic matter of $\sim 0.07 \text{ mg C m}^{-2}$ (0.02 mg N m^{-2}) during May 2000. To our knowledge, this is the first estimate of the contribution of vertical migration to export of diazotroph production from the upper water column. These estimates are roughly an order of magnitude lower than previously calculated migrant $\text{CO}_2 + \text{DOC}$ flux rates at BATS (2 mg C m^{-2}).

5.4.6 Spatial variation in N_D trophic transfer efficiency

The new N in PN and N_{ZOO} provides an estimate of the net N_D contribution to biological communities. Our nitrogen isotopic data suggest that diazotrophs contribute substantially to upper ocean primary production, but a smaller fraction of this N supports higher trophic levels. Our results suggest that diazotroph N does not move into higher trophic levels as efficiently as new N derived from other sources (e.g., deep NO_3^-) (Figures 5.12 & 5.13). We calculated trophic transfer efficiency (TTE) as

$$\text{TTE} = \frac{N_{ZOO P-500m}}{PN_{200m}} \times 100 \quad (5.1)$$

where $N_{\text{ZOO}-500\text{m}}$ was the depth and size-integrated N_{ZOO} biomass (mg N m^{-2}) in the upper 500m, and $PN_{200\text{m}}$ was the depth-integrated PN (mg N m^{-2}) in the upper 200m. Similarly, we estimated the transfer efficiency of N_D as

$$\text{TTE}_D = \frac{N_{D,\text{ZOO}-500\text{m}}}{PN_{D,200\text{m}}} \times 100 \quad (5.2)$$

where $N_{D,\text{ZOO}-500\text{m}}$ and $PN_{D,200\text{m}}$ represent the depth integrated biomass of N_D in zooplankton and suspended particles, respectively.

The overall TTE was 12% along the entire cruise. TTE was lower along Leg 2 (9%) than along Leg 3 (12%), with higher TTE between the western (west of 64°W – 13%) and eastern (east of 55°N - 11%) portions of the basin.

Although N_D contribution was high to suspended particles ($\sim 30\%$), we observed much lower N_D to mesozooplankton ($\sim 8\%$). TTE_D was also much lower (2%) than total TTE throughout the cruise due to low N_D to mesozooplankton. This suggests less efficient movement of diazotroph N through these food webs (Figures 5.12 & 5.13). We also observed higher TTE_D along Leg 2 (5%) relative to Leg 3 (2%), which was primarily influenced by high TTE_D at station 10 (7%), at the southeast end of Leg 2. We also observed higher TTE in the western portion of the basin (3%) than in the eastern portion of the basin (1%). Regional differences could have been driven by mesozooplankton particle selection, difficulty assimilating diazotroph POM, and/or differences in the phyto- and zooplankton community structure. Few mesozooplankton are known to consume diazotrophs directly (O'Neil 1998, Eberl & Carpenter 2007), and most diazotroph new N is believed to enter food webs via consumption of phytoplankton utilizing new N released by diazotrophs (Mulholland et al. 1999, Mulholland et al. 2004, Mulholland et al. 2006), through viral lysis of diazotroph cells (Hewson et al. 2004), or through the microbial loop (Sheridan et al. 2002). However, N_D transfer efficiency may depend on the type of diazotroph consumed by mesozooplankton (Montoya et al. 2002).

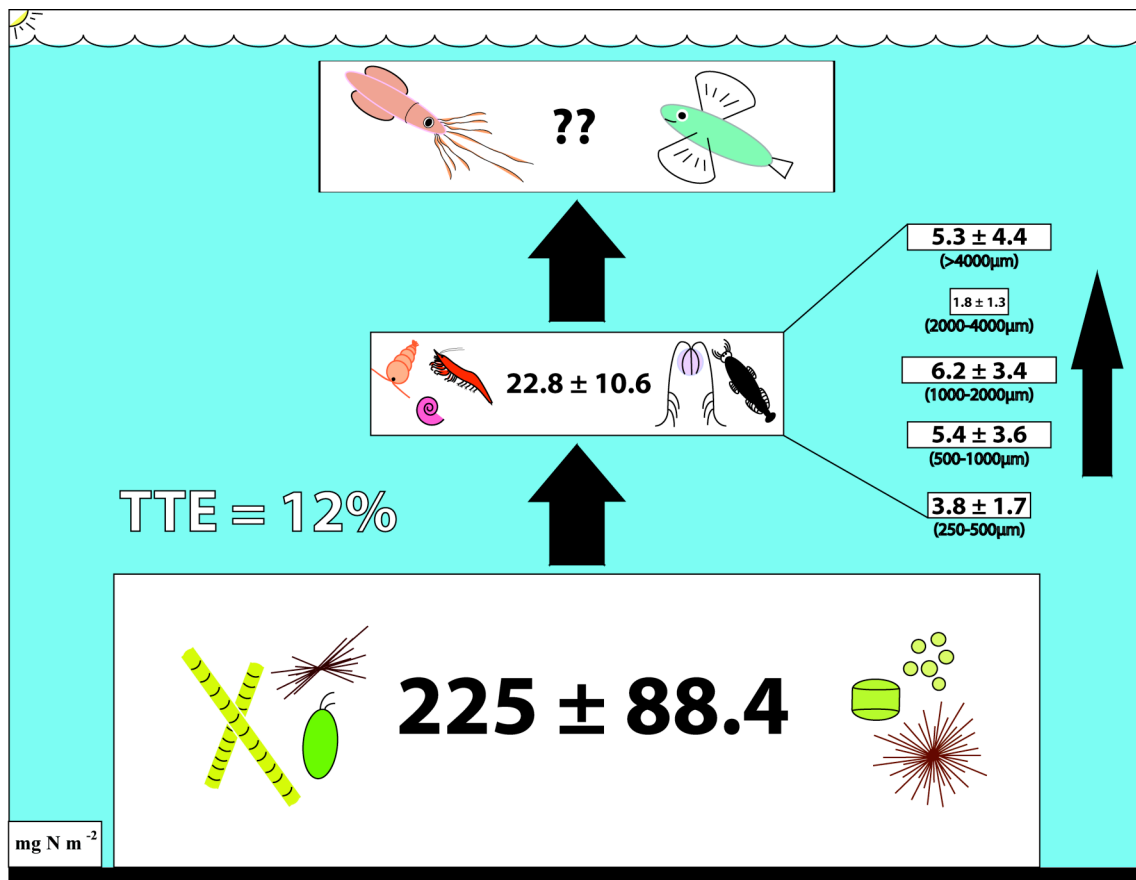


Figure 5.12 - Schematic representation of upper ocean trophic scheme of total N of suspended particles and mesozooplankton. Values in each box are represented by the mean (± 1 SD) depth-integrated N biomass for both suspended particles (upper 200m) and mesozooplankton (upper 500m) along Leg 3 of cruise track SJ0005, a zonal transect spanning the subtropical North Atlantic Ocean at 32°N . TTE represents trophic transfer efficiency of N between particles and mesozooplankton.

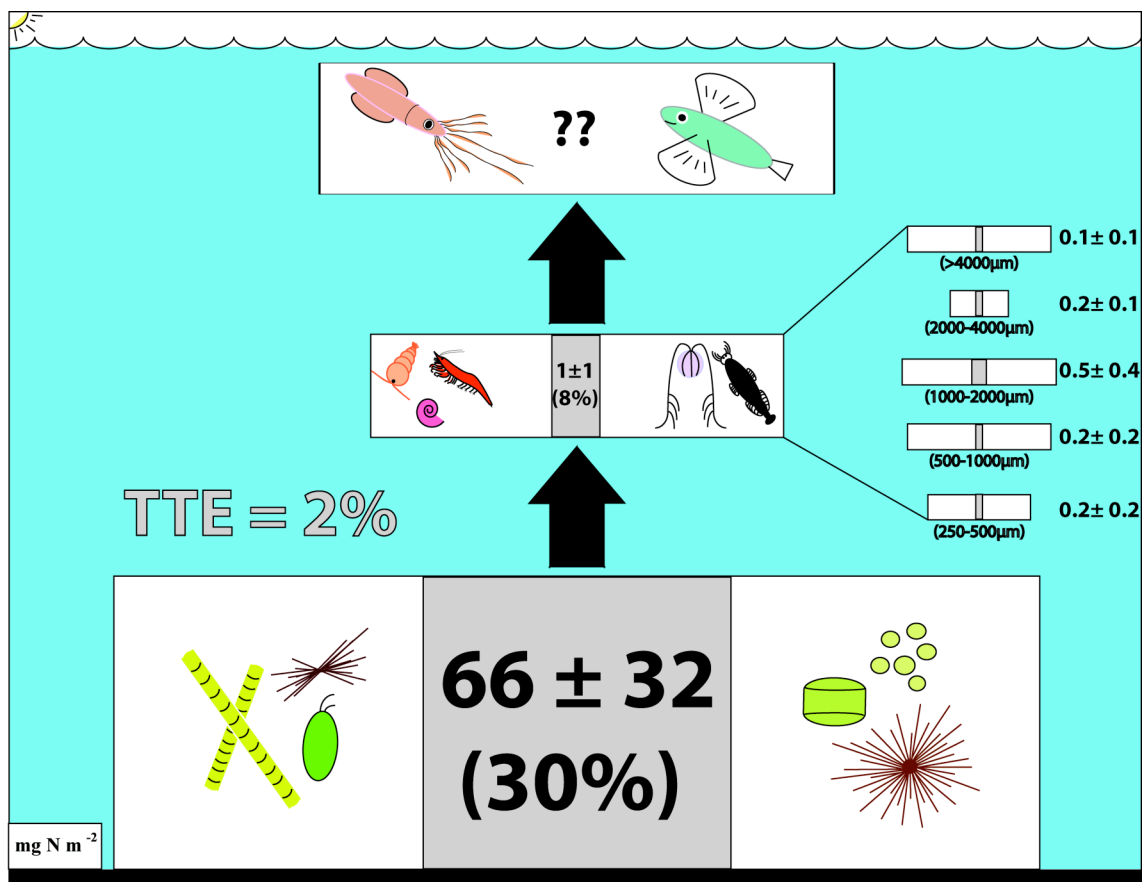


Figure 5.13 - Schematic representation of upper ocean trophic scheme of diazotroph N of suspended particles and mesozooplankton. Values in each box are represented by the mean (± 1 SD) depth-integrated diazotroph N biomass for both suspended particles (upper 200m) and mesozooplankton (upper 500m) along Leg 3 of cruise track SJ0005, a zonal transect spanning the subtropical North Atlantic Ocean at 32°N . TTE represents trophic transfer efficiency of N between particles and mesozooplankton.

For example, Montoya et al. (2002) observed higher N_D contribution to larger mesozooplankton (1000 μ m-4000 μ m) in areas dominated by diazotroph/diatom assemblages (DDAs) (*Richelia/Hemiaulus*), but not in areas with high *Trichodesmium* abundances. They suggested that direct transfer of new N from DDAs to mesozooplankton in these areas were more efficient than N transfer via *Trichodesmium* (e.g., microbial loop). Thus, higher TTE_D at certain stations (e.g., 7% at Station 10) could have been driven, in part, by efficient mesozooplankton incorporation of certain diazotrophs (e.g., DDAs).

A variety of different geochemical techniques, such as mass balances of inorganic species (NO_3^- , PO_4^{2-} , O_2) and drawdown of total inorganic C (NC_T) within the upper ocean (Lee 2001) provide estimates of global and North Atlantic total net community production (NCP = NPP-respiration) that range between 6.2-10.8 Gt C yr⁻¹ and 1.5-4.5 Gt C yr⁻¹, respectively. These estimates suggest that the Atlantic Ocean makes an important contribution to global NCP (Lee 2001, Louanchi & Najjar 2001). Lee et al. (2002) estimated global and regional new C production using observed changes in NC_T and net air-sea CO₂ fluxes (Takahashi et al. 1997) within warm (>20°C) oligotrophic ($NO_3^- < 0.1 \mu\text{mol kg}^{-1}$) waters. They estimated global new C production to be $0.8 \pm 0.3 \text{ Gt C yr}^{-1}$, while the Atlantic Ocean new C production estimates were 0.2 Gt C yr^{-1} from 40°N to 40°S (Lee et al. 2002). Along our cruise, total depth-integrated C biomass for suspended particles (upper 200m) averaged $7.8 \pm 2.7 \text{ Tg C}$, while new C biomass was $2.5 \pm 1.4 \text{ Tg C}$. Total and new depth-integrated (upper 500m) mesozooplankton C biomass averaged $254 \pm 108 \text{ Gg C}$ and $24 \pm 22 \text{ Gg C}$, respectively. Although our cruise sampled only about 10% of the subtropical gyre of the North Atlantic, it is informative to compare our biomass measurements with basin-scale estimates of new production. Our estimates of new PN and zooplankton biomass thus represent between 1 and 4% of the annual new C production estimated by Lee (2002) for the North Atlantic Subtropical Gyre, implying a turnover time for biomass supported by N₂-fixation of days to weeks.

5.4.7 Conclusions

N inputs via biological N_2 -fixation are crucial for supporting oceanic food webs in oligotrophic waters. N_2 -fixation has been previously shown to support substantial primary production, but little is known about its role in supporting higher trophic levels (e.g., mesozooplankton). Mesozooplankton typically play a critical role in the magnitude and efficiency of OM movement throughout the water column, and thus, atmospheric CO_2 sequestration via the biological pump. We show substantial N_D contribution to suspended particles (~30%), which typically coincides with elevated PN concentrations in the mixed layer. We observed several large features with high PN concentrations and N_D contribution, which spanned hundreds to thousands of kilometers across the basin. These data coincide with previous observations of high N_D contribution to suspended particles in the subtropical/central gyre. N_D contribution to suspended particles was also greatest in tropical areas of the central and western gyre, decreasing toward temperate waters. Our estimates for diazotroph new NCP range between 1 to 4% of current NCP estimates in the STNA, implying short turnover times (e.g., ~1 week) for biomass supported by diazotrophs. This implies tight coupling between diazotroph production and export in the STNA. This result helps resolve the potential for N_2 -fixation in removing C_T at the basin scale in oligotrophic oceans, and that diazotroph N export can be sensitive to perturbations on short timescales. Further spatial and temporal sampling of suspended particles in the basin will help resolve diazotroph N contribution to biomass available for consumption and/or flux.

Despite high N_D contribution to the suspended particle pool, N_D contribution to mesozooplankton communities was much lower (8%) and laterally and vertically variable. N_D contribution exceeded 30% for all mesozooplankton size fractions in several areas, but overall TTE_D was ~2.2% (range between Legs 1-3: 1.9-5.1%) from particles to mesozooplankton biomass. We cannot yet assess the mechanisms driving these spatial patterns, and our results highlight the need to focus on determining the proximal

mechanisms driving meridional and zonal trends in TTE_D . We also observed minimal movement of new N to depth via mesozooplankton diazotroph N consumption and export. Our sampling effort provided basin-wide spatial resolution, but failed to record high-resolution temporal shifts in phytoplankton and mesozooplankton community biomass. However, if our results are indicative of typical DVM patterns in the STNA, they suggest that migrating mesozooplankton move a minimal amount of new OM (0.07 mg C m^{-2}) to depth. This flux estimate is more than an order of magnitude lower than other estimates of migrant flux, and other physical flux mechanisms (e.g., diapycnal mixing) driving DOM/POM out of the mixed layer. Future studies should resolve seasonal changes in mesozooplankton total and new biomass, as well as their annual role in DVM driven export in both the interior of the North Atlantic, and in areas exhibiting higher overall migrant and non-migrant biomass.

CHAPTER 6

CONCLUSIONS

6.1 General conclusions

Nitrogen typically limits biological production in oligotrophic oceanic gyres over biologically relevant timescales. The N cycle is inextricably linked to the C cycle, and regulates the movement of OC into the oceans via the biological pump. Stable isotopes provide a strong in-situ tracer for biologically-mediated inputs and movement of N within oceanic ecosystems. Thus, natural distributions of ^{15}N within different organic pools provide a roadmap for N entry and movement throughout oceanic food webs. The $\delta^{15}\text{N}$ of N sources, and the fractionation involved in N transfers between different organic pools of N, are crucial for interpreting ^{15}N distributions in nature. We employed lab-based experiments to elucidate isotopic changes in OM, mediated by decomposition via different heterotrophs, and field-based experiments and observations to determine the mechanisms driving patterns of $\delta^{15}\text{N}$ within food webs of the subtropical North Atlantic Ocean basin.

Particulate organic matter produced by phytoplankton in the euphotic zone is exposed to both microbial and metazoan heterotrophs within the water column. POM processing by these heterotrophs alters the isotopic composition of organic matter, and these alterations provide information about the trophic state of POM. Understanding the proximal mechanisms (e.g., consumption via bacteria, microzooplankton, mesozooplankton, etc.) influencing OM composition is especially important for tracing the source and transformation of sinking POM. In our lab-based experiments, we exposed OM with a known isotopic composition to both microbial communities and shrimp in order to assess the isotopic shifts associated with their consumption of OM. Additionally, we tested the temperature-dependence of microbial decomposition of OM

since. Shrimp tissue was decomposed in both the 4° and 25°C experiments, where N was preferentially degraded with respect to C. We also found that microbial processes tended to enrich OM in ^{15}N , but we didn't see any significant temperature dependence with this trend despite large differences in decomposition rates. This suggests that similar microbial processes influence the $\delta^{15}\text{N}$ of POM regardless of temperature. In addition, future studies should account for this loss of ^{14}N in POM before using these values to infer food web processes and/or reconstruct past climates and nutrient budgets. Our study also provides evidence against earlier hypotheses that suggested vertical patterns of decreasing $\delta^{15}\text{N}$ of sinking POM with depth were driven by microbial processes that preferentially removed ^{15}N . Since compound-specific (AAs) $\delta^{15}\text{N}$ analysis provides more information about the biochemical underpinnings of bulk $\delta^{15}\text{N}$ alterations, future studies should assess the relative isotopic shifts of individual AAs during microbial decomposition of OM.

Metazoans also alter POM through both direct (consumption) and indirect (swimming and/or feeding activity) mechanisms. In our experiments, shrimp (*Palaemonetes* sp.) did not alter the $\delta^{15}\text{N}$ of their food source through digestion, but facilitated higher $\delta^{15}\text{N}$ of their food source via maceration of that OM (e.g., “sloppy feeding”). Our results counter previous studies that show slightly heavier $\delta^{15}\text{N}$ of egested food particles relative to the $\delta^{15}\text{N}$ of their food source, suggesting differences in digestive processes between different groups of mesozooplankton, or little observable fractionation of POM through crustacean digestion. In previous studies, other OM sources (e.g., eggs, “sloppy feeding”) could have altered the isotopic composition of collected fecal pellets. Our experiments were performed using large shrimp that were not gravid, and excreted large, robust fecal pellets that were easily collected and separated from remaining undigested particles. This suggests that there is little, if any, $\delta^{15}\text{N}$ alteration of POM associated with crustacean digestion. However, higher $\delta^{15}\text{N}$ of macerated flake food

suggests that crustaceans can influence the $\delta^{15}\text{N}$ of POM through their feeding processes, independent of digestion.

Our fieldwork in the subtropical North Atlantic aimed to determine the impact of diazotroph N within these ecosystems. Diazotrophs actively fix N_2 in the subtropical North Atlantic gyre, and support primary production. However, to date few studies have assessed the extent to which diazotroph N supports secondary production. In the euphotic zone, weighted mean $\delta^{15}\text{N}_{\text{SP}}$ and $\delta^{15}\text{N}_{\text{ZP}}$ values lower than typical deep $\delta^{15}\text{NO}_3^-$ values ($\sim 4.5\text{‰}$) suggesting that diazotrophs contributed significant N to the food webs. Diazotroph N contribution was generally higher and less spatially variable for suspended particles relative to mesozooplankton. Weighted mean $\delta^{15}\text{N}_{\text{SP}}$ and $\delta^{15}\text{N}_{\text{ZP}}$ values, however, were positively correlated, suggesting a tight coupling between particles and mesozooplankton. Mesozooplankton incorporated diazotroph N either by consuming diazotroph POM directly, or indirectly through N transfers within the microbial loop. At this time it is impossible to assess the dominant pathways for diazotroph N transfer within the suspended particle pool and into the mesozooplankton biomass.

Isotopic evidence suggested that smaller zooplankton were not migrating below 200m and incorporated little diazotroph N in the mixed layer. Smaller mesozooplankton, thus, predominantly consume non-diazotroph particles (e.g., detritus) in the mixed layer without moving into deeper water. Larger mesozooplankton, however, were actively migrating within the upper 500m, presumably consuming diazotroph N upon their ascent into the mixed layer at night. Although migrating mesozooplankton typically transport nutrients, POM and DOM to depth, our study is the first to provide evidence for active movement of diazotroph N to depths below the mixed layer. We also observed higher $\delta^{15}\text{N}_{\text{ZP}}$ in the eastern portion of the basin, despite continuously low $\delta^{15}\text{N}_{\text{SP}}$ values. This suggests that diazotroph N is available, but not highly utilized in eastern food webs. This pattern is most likely driven by differences in the phyto- and zooplankton community structure, and suggests minimal diazotroph N movement into deeper water via DVM.

Areas of high PN concentration and mesozooplankton biomass were often positively correlated with high DNC to those pools. This suggests that diazotrophs actively enhance primary and secondary production in the subtropical North Atlantic, but diazotroph N moved less efficiently into mesozooplankton communities. Diazotroph N trophic transfer efficiency (TTE_D) between PN and mesozooplankton pools ranged from 1.7-4.2% for all stations, which is quite low considering the TTE of bulk particles (12%), and the role diazotrophs play in supporting primary production in this area. We also present the first isotope-based concentration and depth-integrated measurements of both new PN and mesozooplankton biomass in the subtropical North Atlantic gyre. Although our data represent a small portion of estimated NCP for the North Atlantic (~1-4%) (Lee 2001, Lee et al. 2002), they are estimated from a small spatial area (~10% of the North Atlantic). Current estimates of NCP using seasonal and annual drawdown of C_T do not separate influences by different sources of new N driving the C_T drawdown, which is an important factor in predicting future changes in C inventories in nutrient-poor basins. Our estimates only account for new biomass produced via diazotrophs, and not total new biomass with respect to all external N sources (e.g., deep NO_3^-). We also estimated diazotroph N turnover time of days to weeks, suggesting that diazotroph N export is sensitive to perturbations over short timescales. Although we show that wet N deposition was a negligible N input to our sampling area, it proved more difficult to estimate dry N deposition due to a lack of regional N flux data. It is also difficult to predict community responses to overall dry N deposition since many other limiting nutrients (e.g., P, Fe) are supplied concomitant to N, and thus, may enhance N_2 -fixation rather than suppress it (Mills et al. 2004, Mills et al. 2008). However, due to the wide range of $\delta^{15}N$ for both wet and dry N deposits, and growing anthropogenic impact on oceanic basins, future studies must focus their attention on separating the relative contributions of new N via N deposition and biological N_2 -fixation to the upper ocean. Further spatial, temporal and

vertical stable isotope data are also necessary in order to estimate basin-scale new production in these food webs.

6.2 Broader implications and future questions for N cycle studies

Although our data address several aspects of the marine N cycle and the impact of diazotroph contribution to food web structure and function, several important questions still remain unanswered. We still do not know the proximal mechanisms that facilitate N input via diazotrophs into food webs. Few studies have found evidence for direct consumption of diazotrophs via mesozooplankton. O'Neil et al. (1996, 1998) showed that a harpacticoid copepod, *Macrosetella gracilis* can consume and incorporate *Trichodesmium* C into biomass (Oneil & Roman 1994, Oneil et al. 1996). However, gut analyses and $\delta^{13}\text{C}$ distributions within field-collected (off the west coast of Hawaii) copepods, including *M. gracilis*, suggest that copepods are not actively incorporating *Trichodesmium* biomass directly, although their $\delta^{15}\text{N}$ suggested diazotroph N influence (Eberl & Carpenter 2007). Eberl and Carpenter (2007) further hypothesized that *Trichodesmium* may be a better home than food source for *M. gracilis*. *M. gracilis* use *Trichodesmium* as a physical substrate, which is similar to an earlier hypothesis by Judith O'Neil et al. (1998) after they found *M. gracilis* eggs attached to *Trichodesmium* filaments.

Natural abundances of ^{15}N and ^{13}C POM and mesozooplankton found elsewhere (Holl et al. 2007) also suggest *Trichodesmium* incorporation via grazing. *Trichodesmium* abundances and N_2 -fixation rates were highest offshore in the northwest Gulf of Mexico, and $\delta^{15}\text{N}$ values of both POM and smaller mesozooplankton ($<500\mu\text{m}$) were lower relative to stations exhibiting lower *Trichodesmium* abundances. *Trichodesmium* has been shown to exhibit low natural $\delta^{15}\text{N}$ (-0.7 to -0.25‰) and high $\delta^{13}\text{C}$ (-15.2 to -11.9‰) in other regions (Carpenter et al. 1997), making this diazotroph an isotopically distinct phytoplankton for use in isotope tracing studies. Holl et al. (2007) used a two end-

member mixing model to calculate the relative contribution of C to zooplankton (~60%), but these results should be taken with caution, given the potential for error using stable isotopes in systems exhibiting a diverse collection of isotopic end-members. For example, Falkowski et al (1991) showed a wide range of $\delta^{13}\text{C}$ (-5.5‰ to -29.7‰) of several types of phytoplankton, including coccolithophores, dinoflagellates, cryptophytes, and cyanobacteria (Falkowski 1991). They suggested that different carbon fixation pathways (e.g., C3 vs. C4), and the level of C limitation would dictate $\delta^{13}\text{C}$ in phytoplankton, which would alter the overall $\delta^{13}\text{C}$ of the suspended particle pool as well. Thus, without intimate knowledge of the diversity and relative abundance of the phytoplankton communities, it is difficult to assess relative C contribution to mesozooplankton via a single phytoplankton. Also, although the lower $\delta^{15}\text{N}$ values suggest that diazotroph N is an important component for both phytoplankton and mesozooplankton growth, this N can be delivered to other phytoplankton, bacteria, or micro-heterotrophs via other mechanisms (e.g., the microbial loop, diazotroph DON/DIN release).

Sommer et al. (2006) hypothesized that the microbial loop may play a dominant role in diazotroph N transfer between diazotrophs and mesozooplankton. In their mesocosm experiments, *Acartia clausii*, the dominant copepod in Kiel Fjord, avoided the N_2 -fixing cyanobacteria, *Nodularia spumigena*, but consumed other plankton in these incubations. In their mesocosm experiments, copepods exhibited low $\delta^{15}\text{N}$, but did not always suppress *N. spumigena* growth, suggesting that they were not actively feeding on these cyanobacteria. However, copepods did actively feed upon other microzooplankton and phytoplankton (heterotrophic ciliates, dinoflagellates and diatoms), which were proposed as vehicles for diazotroph N transport into copepods. Diazotroph/diatom assemblages (DDAs) may be a good food source for mesozooplankton, but this has not been directly examined either. Interestingly, given the potential for sinking flux out of the water column for some DDAs (Subramaniam et al. 2008) consumption of DDAs via

mesozooplankton may be a crucial link for diazotroph flux into deeper waters. For example, while sampling a DDA bloom in the Amazon River plume, Subramaniam et al., (2008) witnessed a large salp bloom which consumed a large portion of the phytoplankton biomass (>50%) within a single day (Agit Subramaniam, pers. comm.). Although they did not publish grazing rates or isotope data for mesozooplankton, salps often sample POM indiscriminately, and most likely consumed (and exported) a large portion of the DDA biomass in that area. No data presently exists for direct mesozooplankton assimilation of picocyanobacteria, but given their potential for fixing huge quantities of N in oligotrophic systems, they could contribute a considerable amount of N to food webs.

Historically, it has been difficult to identify N pathways through the microbial loop and its link to metazoan populations. When attempting to trace the movement of N, difficulties arise due to the diversity of organisms present in the water column, as well as temporal shifts in community structure and/or selectivity of food sources by metazoans. Furthermore, conclusions drawn about community dynamics are often made by monitoring changes in relative abundances of species within mesocosms, without directly linking consumer with food source(s). Stable isotopes can potentially help resolve some of these issues, but may be limited to specific links within complex food webs. More specifically, there is also a paucity of data that details N transfers within the microbial loop. Azam et al. (1983) highlighted the potential importance of the microbial loop in marine systems, claiming that it was a potential vector for C transfer back into the classical food webs that centered around metazoans grazing on phytoplankton. The “sink vs link” debate has ensued in an attempt to determine the value of the microbial loop as a food source for metazoan populations. The present consensus is that the microbial loop may be more important as a sink, given that studies have shown inefficient movement of bacterial biomass through long protist food chains (Calbet & Landry 2004, Fenchel 2008). However, despite inefficient transfers between bacteria and flagellates,

mesozooplankton often consume organisms along these food chains, short-circuiting the chain by feeding in the middle.

Isotopically, we know little about trophic transfers between microorganisms in oligotrophic systems. Rau et al. (1990) showed that size-fractionated SPOM can indeed exhibit different $\delta^{15}\text{N}$ values, but the transfer mechanisms for these isotopic values remain elusive. Bacterial decomposition will often produce higher $\delta^{15}\text{N}_{\text{POM}}$, which is primarily driven by isotopic fractionation via enzymatic deamination and/or transamination reactions of peptides and amino acids (Macko & Estep 1984, Macko et al. 1991, Macko et al. 1994). Using a multiple-tracer approach, we can devise and carry out shipboard experiments to monitor diazotroph N transfer to various organisms within microbial food webs. Additional tracer techniques would also be easy to implement in large volume $^{15}\text{N}_2$ -fixation incubations both in lab and at sea. Lab-based experiments with culturable diazotrophs (e.g., *Trichodesmium*) or perhaps other more widely consumed phytoplankton, and zooplankton would be essential for developing and fine-tuning execution of these more elaborate experiments.

One field-based approach could be accomplished by collecting seawater at various depths, determine the initial microbial community structure via flow cytometry, and run parallel experiments using $^{15}\text{N}_2$ and $\text{H}^{13}\text{CO}_3^-$ tracers to follow the movement of N and C through the microbial populations. Other tracers (^3H -thymidine, ^{14}C -Leucine) could also be added to estimate active bacterial production. For example, ^3H -thymidine is now typically used to quantify abundances of metabolically active bacteria in environmental samples (Ducklow 1999). Protist grazers retain ^3H -thymidine (and/or leucine) upon bacterial consumption, thereby tracing metabolically active bacterial biomass into these microzooplankton grazers (Zubkov & Tarran 2008). After 24 hours, the seawater should be filtered through nitex mesh of multiple sizes ($<3\mu\text{m}$, $3\text{-}10\mu\text{m}$, $10\text{-}50\mu\text{m}$, $50\text{-}100\mu\text{m}$, $100\text{-}250\mu\text{m}$) in order to separate various populations of bacteria and microzooplankton by size. Multiple replicates of bottle incubations should be performed

to categorize shifts in phytoplankton and microplankton community structure during experiments (via flow cytometry). DNA and RNA extractions, as well as microscopy, could also help assess diazotroph community structure and activity in these microcosms. The subsequent connection between microzooplankton and mesozooplankton communities using these multiple tracer techniques could be easily incorporated into our large volume $^{15}\text{N}_2$ -fixation experiments at sea, providing a powerful combination in elucidating C and N movement. Mesozooplankton could also be added to parallel experiments, in order to trace the movement of our tracers into larger grazers. Several different species of metazoans have already been successfully incorporated in our large-volume incubations at sea during cruises in the tropical North Atlantic (e.g., SJ0609), further suggesting the feasibility of these mesocosm experiments. Finally, diazotrophs (e.g., *Trichodesmium*) could also be added to these experiments, if available from the water column. However, several control incubations, and perhaps incubations of *Trichodesmium* with filtered seawater of the size fractions listed above, would be necessary to separate new N movement through the potentially diverse assemblage of diazotrophs in these incubations.

Is it necessary to understand trophic dynamics at such a complex level? What added information do we gain by looking at specific interactions rather than just grouping organisms into trophic levels and monitoring C and N transfer (as we have done in our field data here)? The simple answer is that predator-prey dynamics in the open ocean are often quite complex both spatially and temporally, and not easily generalized nor quantified through stable isotopic analysis (i.e., isotopic alteration via microbial loop). This complexity can also lead to spatial and temporal variation in food web structure and function, and OM flux throughout the water column. It is often difficult to predict what consumers (i.e., metazoans) choose to incorporate, and when they will choose specific food sources. Other problems, such as omnivory and mixotrophy (e.g., dinoflagellates, algae) blur the potential connections between distinct trophic levels. Marine

mesozooplankton are also often omnivorous, and switch foods seasonally, and on shorter time scales (within days). For example, Leising et al (2005) showed that *Calanus pacificus* often changed its diet unpredictably (weekly samples) while grazing within phytoplankton blooms in Dabob Bay. *C. pacificus* also facilitated growth in other species present (i.e., “apparent negative grazing”), but the mechanisms driving these observations were not separated in their grazing experiments. Leising and colleagues did suggest, however, as others have, that toxic phytoplankton were avoided by these copepods, which supports the growing acceptance that copepods are selective, and certain characteristics of food sources (e.g., harmful metabolites) may influence food choice (Bullard & Hay 2002).

Individual links between consumers and their food source may be especially important for oligotrophic systems where biological production is dominated by N inputs via multiple diazotroph species. For example, Carpenter et al. (1999) followed a bloom of *Hemiaulus hauckii* bloom off the northeast coast of South America, which included coexisting populations of both *H. hauckii* (and its endosymbiotic diazotroph, *Richelia intracellularis*) and *Trichodesmium*. Both diazotrophs were shown to fix N within the water column, and low $\delta^{15}\text{N}$ of both POM and mesozooplankton were attributed to these higher rates (Carpenter et al. 1999). However, although we can quantify the overall impact diazotrophy has to the system, further analysis is required to elucidate the N pathways from each diazotroph into food webs (e.g., direct consumption, N leakage, microbial loop processing). Furthermore, the type of diazotroph may also be important in new N flux out of the water column, be it through direct flux of diazotrophs (Voss et al. 2001, Subramaniam et al. 2008), or mediated by food web processes (Montoya et al. 2002).

Although we have gained a better understanding of C and N flux over the past ~40 years through sediment trap deployments, we still do not know the proximal food web processes that drive vertical patterns of sinking C flux in the oceans. We also do not

know the relative impact various N sources have on C flux into the deep sea (e.g., diazotrophy, eddy-induced NO_3^- upwelling). For example, although *Trichodesmium* can fix N at appreciable rates in the mixed layer, few studies have visually detected these filaments in surface sediment traps. However, low $\delta^{15}\text{N}$ of particles caught in shallow (150m) (Karl et al. 1997, Karl et al. 2002) and deeper (500m) sediment traps (Voss et al. 2001) below areas of high trichome abundances suggests diazotroph N presence in sinking flux. However, we are still unsure about the dominant mechanisms influencing the magnitude of flux with depth (i.e., direct sinking vs. fecal pellets), and the proximal processes reworking POM in transit (i.e., zooplankton vs. microbial decomposition). There are also no data, to my knowledge, observing diazotroph biomass in deeper sediment traps (>500m). Decreasing $\delta^{15}\text{N}$ of sinking particles at the Ocean Flux Program (OFP) site off Bermuda suggested a possible influence of diazotroph N in sinking particles, but this conclusion is very tenuous given our poor understanding of the source and transformation of the POM through the water column. Other studies have shown similar trends in deeper traps, but again, little connection between surface and sinking diazotroph POM can be drawn without a more thorough understanding of particle source and transformation of those particles.

Our data set from the cruise SJ0005 in the subtropical North Atlantic may provide clues to mesozooplankton-driven diazotroph N export out of the mixed layer. Although overall transfer efficiency was low between suspended particles and mesozooplankton, we observed areas where diazotroph N flux could have been facilitated by mesozooplankton consumption and export. Along leg 2 of SJ0005, we observed relatively low $\delta^{15}\text{N}_{\text{SP}}$ values below the euphotic zone at station 12, but relatively high $\delta^{15}\text{N}_{\text{SP}}$ below the euphotic zone at station 11 (Chapter 4, Figure 2). Low $\delta^{15}\text{N}_{\text{ZP}}$ at each of these stations suggested high diazotroph N contribution (>20%) to all size fractions of the mesozooplankton communities, with the highest contribution to larger mesozooplankton at station 11. Rapidly increasing apparent oxygen utilization (AOU)

values with increasing σ_T below the vertical feature at station 11 and 12 also suggest increasing respiration of particulate organic matter (POM) via heterotrophs. Shoaling AOU values at Station 11 reach maximal values ($30 \mu\text{mol l}^{-1}$) while AOU values drop slightly ($26 \mu\text{mol l}^{-1}$) to the northwest at Station 12. Anomalously high $\delta^{15}\text{N}_{\text{SP}}$ values below 150m at Station 11 (6.7‰) also suggest that microbial communities are remineralizing POM at these depths. Microbial respiration of POM often leads to higher $\delta^{15}\text{N}$ of OM (Macko & Estep 1984, Macko et al. 1991, Lehmann et al. 2002), and has been used to explain vertical trends of increasing $\delta^{15}\text{N}_{\text{SP}}$ with increasing depth in the water column (Altabet et al. 1991, Voss et al. 1996, Nakatsuka et al. 1997, Wu et al. 1999b).

We are unsure of the origin of the POM (lateral vs. vertical transport), but I speculate that shoaling AOU values, higher NO_3^- concentrations and higher $\delta^{15}\text{N}_{\text{SP}}$ values below the euphotic zone and lower $\delta^{15}\text{N}_{\text{ZP}}$ values within the mixed layer provides evidence for new N export. A considerable fraction of exported material at station 11 is potentially diazotroph-derived N, considering the high $\delta^{15}\text{N}_{\text{SP}}$ values below 150m. However, low $\delta^{15}\text{N}_{\text{ZP}}$ values of all mesozooplankton size classes in the euphotic zone suggest considerable diazotroph incorporation over weeks to months. Furthermore, lower $\delta^{15}\text{N}_{\text{SP}}$ below the euphotic zone at station 12 relative to station 11 suggests different times of a diazotroph bloom, with the onset of bloom conditions at station 12 and the end of a bloom at station 11. However, these are mere speculations, and would require further measurements (e.g., sinking particles (via sediment trap collection), Chlorophyll a, $\delta^{15}\text{N}_{\text{DON}}$) to resolve the interactions between mesozooplankton and diazotroph N flux.

Although our data answer questions regarding the extent to diazotroph N movement within suspended particles and mesozooplankton in the STNA, many more questions emerge as a result of our findings:

- 1) Does diazotroph N enter higher trophic levels directly through mesozooplankton consumption, or through the microbial loop? Are these trends easily generalized, or species-specific?
- 2) If diazotroph N mainly enters through the microbial loop, can we effectively trace the movement of diazotroph N through these food webs and into higher trophic levels. If so, do certain links translate into higher DNC to mesozooplankton?
- 3) Why is the diazotroph N trophic transfer efficiency (TTE) markedly lower for mesozooplankton over such a broad spatial scale?
- 4) Is TTE between particles and mesozooplankton greater in other basins (e.g., North Pacific)? Are there seasonal differences within the STNA and elsewhere?
- 5) What role does DVM play in transporting diazotroph N to depth?
- 6) What is the overall TTE for the entire system (N_2 input \rightarrow diazotroph PON \rightarrow microzooplankton PON \rightarrow mixotrophs \rightarrow mesozooplankton biomass), and what organic pools preferentially retain diazotroph N (DOM? Smaller plankton not captured on our filters?)?
- 7) How do diazotroph communities respond to other sources of N (e.g., dry and wet deposition), and how does the phytoplankton community shift in response to deposition of limiting nutrients for both diazotrophs (e.g., P, Fe) and non-diazotrophs (N)?

Although these are only a few questions that stem from our research, they are a starting point for future studies. Going forward, we should focus primarily on elucidating the proximal mechanisms of diazotroph N movement through oceanic food webs (e.g., mesozooplankton consumption, microbial interactions), which directly influence food web structure, and ability to export N. Focus should also be placed on characterizing shifts in phytoplankton (and zooplankton) community structure given variable inputs of limiting nutrients that facilitate or minimize diazotroph growth and/or N contribution. Several areas (e.g., Amazon plume, west African coast, STNA, STNP) provide optimal

locations to assess the roles different diazotrophs play in food web dynamics and N movement in the mixed layer and below. Furthermore, future experiments should apply multiple tracer techniques, both in the lab and in the field, in order to trace C and N flow through microbial food webs and into higher trophic levels. (Mariotti et al. 1981, Cifuentes et al. 1989, Horrigan et al. 1990, Hoch et al. 1994, Montoya & McCarthy 1995, Karl et al. 1997, Wu et al. 1997, Brandes et al. 1998, Altabet et al. 1999a, Altabet et al. 1999b, Carpenter et al. 1999, Sigman et al. 1999, Altabet 2001, Casciotti et al. 2003)

REFERENCES

- Adams TS, Sterner RW (2000) The effect of dietary nitrogen content on trophic level N-15 enrichment. *Limnology and Oceanography* 45:601-607
- Al-Mutairi H, Landry MR (2001) Active export of carbon and nitrogen at Station ALOHA by diel migrant zooplankton. *Deep-Sea Research Part II-Topical Studies in Oceanography* 48:2083-2103
- Allredge AL, Gotschalk C (1988) In situ Settling Behavior of Marine Snow. *Limnology and Oceanography* 33:339-351
- Allredge AL, Granata TC, Gotschalk CC, Dickey TD (1990) The Physical Strength of Marine Snow and Its Implications for Particle Disaggregation in the Ocean. *Limnology and Oceanography* 35:1415-1428
- Allredge AL, Silver MW (1988) Characteristics, Dynamics and Significance of Marine Snow. *Progress in Oceanography* 20:41-82
- Altabet MA (1988) Variations in nitrogen isotopic composition between sinking and suspended particles - implications for nitrogen cycling and particle transformation in the open ocean. *Deep-Sea Research Part A-Oceanographic Research Papers* 35:535-554
- Altabet MA (2001) Nitrogen isotopic evidence for micronutrient control of fractional NO₃⁻ utilization in the equatorial Pacific. *Limnology and Oceanography* 46:368-380
- Altabet MA, Deuser WG, Honjo S, Stienen C (1991) Seasonal and depth-related changes in the source of sinking particles in the North Atlantic. *Nature* 354:136-139
- Altabet MA, Francois R (1994) Sedimentary nitrogen isotopic ratio as a recorder for surface ocean nitrate utilization. *Global Biogeochemical Cycles* 8:103-116
- Altabet MA, Francois R, Murray DW, Prell WL (1995) Climate-Related Variations in Denitrification in the Arabian Sea from Sediment N-15/N-14 Ratios. *Nature* 373:506-509

- Altabet MA, Higginson MJ, Murray DW (2002) The effect of millennial-scale changes in Arabian Sea denitrification on atmospheric CO₂. *Nature* 415:159-162
- Altabet MA, McCarthy JJ (1986) Vertical patterns in N-15 natural abundance in PON from the surface waters of warm-core rings. *Journal of Marine Research* 44:185-201
- Altabet MA, Murray DW, Prell WL (1999a) Climatically linked oscillations in Arabian Sea denitrification over the past 1 m.y.: Implications for the marine N cycle. *Paleoceanography* 14:732-743
- Altabet MA, Pilskaln C, Thunell R, Pride C, Sigman D, Chavez F, Francois R (1999b) The nitrogen isotope biogeochemistry of sinking particles from the margin of the Eastern North Pacific. *Deep-Sea Research Part I-Oceanographic Research Papers* 46:655-679
- Altabet MA, Small LF (1990) Nitrogen isotopic ratios in fecal pellets produced by marine zooplankton. *Geochimica Et Cosmochimica Acta* 54:155-163
- Andersson JH, Wijsman JWM, Herman PMJ, Middelburg JJ, Soetaert K, Heip C (2004) Respiration patterns in the deep ocean. *Geophysical Research Letters* 31
- Antia AN, Koeve W, Fischer G, Blanz T, Schulz-Bull D, Scholten J, Neuer S, Kremling K, Kuss J, Peinert R, Hebbeln D, Bathmann U, Conte M, Fehner U, Zeitzschel B (2001) Basin-wide particulate carbon flux in the Atlantic Ocean: Regional export patterns and potential for atmospheric CO₂ sequestration. *Global Biogeochemical Cycles* 15:845-862
- Asper VL, Deuser WG, Knauer GA, Lohrenz SE (1992) Rapid Coupling of Sinking Particle Fluxes between Surface and Deep Ocean Waters. *Nature* 357:670-672
- Azam F (1998) Microbial control of oceanic carbon flux: The plot thickens. *Science* 280:694-696
- Azam F, Worden AZ (2004) Microbes, molecules, and marine ecosystems. *Science* 303:1622-1624
- Bada JL, Schoeninger MJ, Schimmelmann A (1989) Isotopic Fractionation during Peptide-Bond Hydrolysis. *Geochimica Et Cosmochimica Acta* 53:3337-3341

- Baker AR, Jickells TD, Biswas KF, Weston K, French M (2006) Nutrients in atmospheric aerosol particles along the Atlantic Meridional Transect. *Deep-Sea Research Part II-Topical Studies in Oceanography* 53:1706-1719
- Baker AR, Kelly SD, Biswas KF, Witt M, Jickells TD (2003) Atmospheric deposition of nutrients to the Atlantic Ocean. *Geophysical Research Letters* 30
- Baker AR, Weston K, Kelly SD, Voss M, Streu P, Cape JN (2007) Dry and wet deposition of nutrients from the tropical Atlantic atmosphere: Links to primary productivity and nitrogen fixation. *Deep-Sea Research Part I-Oceanographic Research Papers* 54:1704-1720
- Banase K (1995) Zooplankton - Pivotal Role in the Control of Ocean Production. *ICES Journal of Marine Science* 52:265-277
- Battle M, Bender ML, Tans PP, White JWC, Ellis JT, Conway T, Francey RJ (2000) Global carbon sinks and their variability inferred from atmospheric O-2 and delta C-13. *Science* 287:2467-2470
- Benitez-Nelson CR, McGillicuddy DJ (2008) Mesoscale physical-biological-biogeochemical linkages in the open ocean: An introduction to the results of the E-Flux and EDDIES programs - Preface. *Deep-Sea Research Part II-Topical Studies in Oceanography* 55:1133-1138
- Berelson WM (2002) Particle settling rates increase with depth in the ocean. *Deep-Sea Research Part II-Topical Studies in Oceanography* 49:237-251
- Berman-Frank I, Bidle KD, Haramaty L, Falkowski PG (2004) The demise of the marine cyanobacterium, *Trichodesmium* spp., via an autocatalyzed cell death pathway. *Limnology and Oceanography* 49:997-1005
- Bode A, Alvarez-Ossorio MT, Cunha ME, Garrido S, Peleteiro JB, Porteiro C, Valdes L, Varela M (2007) Stable nitrogen isotope studies of the pelagic food web on the Atlantic shelf of the Iberian Peninsula. *Progress in Oceanography* 74:115-131
- Boyd PW, Newton PP (1999) Does planktonic community structure determine downward particulate organic carbon flux in different oceanic provinces? *Deep-Sea Research Part I-Oceanographic Research Papers* 46:63-91

- Boyd PW, Sherry ND, Berges JA, Bishop JKB, Calvert SE, Charette MA, Giovannoni SJ, Goldblatt R, Harrison PJ, Moran SB, Roy S, Soon M, Strom S (1999) Transformations of biogenic particulates from the pelagic to the deep ocean realm. *Deep-Sea Research Part II-Topical Studies in Oceanography* 46:2761-2792
- Brandes JA, Devol AH, Deutsch C (2007) New developments in the marine nitrogen cycle. *Chemical Reviews* 107:577-589
- Brandes JA, Devol AH, Yoshinari T, Jayakumar DA, Naqvi SWA (1998) Isotopic composition of nitrate in the central Arabian Sea and eastern tropical North Pacific: A tracer for mixing and nitrogen cycles. *Limnology and Oceanography* 43:1680-1689
- Breteler W, Grice K, Schouten S, Kloosterhuis HT, Damste JSS (2002) Stable carbon isotope fractionation in the marine copepod *Temora longicornis*: unexpectedly low $\delta^{13}\text{C}$ value of faecal pellets. *Marine Ecology-Progress Series* 240:195-204
- Brinton E (1967) Vertical Migration and Avoidance Capability of Euphausiids in California Current. *Limnology and Oceanography* 12:451-&
- Bullard SB, Hay ME (2002) Palatability of marine macro-holoplankton: Nematocysts, nutritional quality, and chemistry as defenses against consumers. *Limnology and Oceanography* 47:1456-1467
- Burns KA, Greenwood P, Benner R, Brinkman D, Brunskill G, Codi S, Zagorskis I (2004) Organic biomarkers for tracing carbon cycling in the Gulf of Papua (Papua New Guinea). *Continental Shelf Research* 24:2373-2394
- Burns KA, Volkman JK, Cavanagh JA, Brinkman D (2003) Lipids as biomarkers for carbon cycling on the Northwest Shelf of Australia: results from a sediment trap study. *Marine Chemistry* 80:103-128
- Calbet A, Landry MR (2004) Phytoplankton growth, microzooplankton grazing, and carbon cycling in marine systems. *Limnology and Oceanography* 49:51-57
- Capone DG (2001) Marine nitrogen fixation: what's the fuss? *Current Opinion in Microbiology* 4:341-348

- Capone DG, Burns JA, Montoya JP, Subramaniam A, Mahaffey C, Gunderson T, Michaels AF, Carpenter EJ (2005) Nitrogen fixation by *Trichodesmium* spp.: An important source of new nitrogen to the tropical and subtropical North Atlantic Ocean. *Global Biogeochemical Cycles* 19
- Capone DG, Subramaniam A, Montoya JP, Voss M, Humborg C, Johansen AM, Siefert RL, Carpenter EJ (1998) An extensive bloom of the N-2-fixing cyanobacterium *Trichodesmium erythraeum* in the central Arabian Sea. *Marine Ecology-Progress Series* 172:281-292
- Capone DG, Zehr JP, Paerl HW, Bergman B, Carpenter EJ (1997) *Trichodesmium*, a globally significant marine cyanobacterium. *Science* 276:1221-1229
- Carlotti F, Thibault-Botha D, Nowaczyk A, Lefevre D (2008) Zooplankton community structure, biomass and role in carbon fluxes during the second half of a phytoplankton bloom in the eastern sector of the Kerguelen Shelf (January-February 2005). *Deep-Sea Research Part II-Topical Studies in Oceanography* 55:720-733
- Carpenter EJ, Harvey HR, Fry B, Capone DG (1997) Biogeochemical tracers of the marine cyanobacterium *Trichodesmium*. *Deep-Sea Research Part I-Oceanographic Research Papers* 44:27-38
- Carpenter EJ, Montoya JP, Burns J, Mulholland MR, Subramaniam A, Capone DG (1999) Extensive bloom of a N-2-fixing diatom/cyanobacterial association in the tropical Atlantic Ocean. *Marine Ecology-Progress Series* 185:273-283
- Carpenter EJ, Subramaniam A, Capone DG (2004) Biomass and primary productivity of the cyanobacterium *Trichodesmium* spp. in the tropical N Atlantic ocean. *Deep-Sea Research Part I-Oceanographic Research Papers* 51:173-203
- Carr ME, Friedrichs MAM, Schmeltz M, Aita MN, Antoine D, Arrigo KR, Asanuma I, Aumont O, Barber R, Behrenfeld M, Bidigare R, Buitenhuis ET, Campbell J, Ciotti A, Dierssen H, Dowell M, Dunne J, Esaias W, Gentili B, Gregg W, Groom S, Hoepffner N, Ishizaka J, Kameda T, Le Quere C, Lohrenz S, Marra J, Melin F, Moore K, Morel A, Reddy TE, Ryan J, Scardi M, Smyth T, Turpie K, Tilstone G, Waters K, Yamanaka Y (2006) A comparison of global estimates of marine primary production from ocean color. *Deep-Sea Research Part II-Topical Studies in Oceanography* 53:741-770

- Casciotti KL, Sigman DM, Ward BB (2003) Linking diversity and stable isotope fractionation in ammonia-oxidizing bacteria. *Geomicrobiology Journal* 20:335-353
- Cerling TE, Wittemyer G, Rasmussen HB, Vollrath F, Cerling CE, Robinson TJ, Douglas-Hamilton I (2006) Stable isotopes in elephant hair document migration patterns and diet changes. *Proceedings of the National Academy of Sciences of the United States of America* 103:371-373
- Champalbert G, Neveux J, Gaudy R, Le Borgne R (2003) Diel variations of copepod feeding and grazing impact in the high-nutrient, low-chlorophyll zone of the equatorial Pacific Ocean (0 degrees; 3 degrees S, 180 degrees). *Journal of Geophysical Research-Oceans* 108
- Checkley DM, Entzeroth LC (1985) Elemental and Isotopic Fractionation of Carbon and Nitrogen by Marine, Planktonic Copepods and Implications to the Marine Nitrogen-Cycle. *Journal of Plankton Research* 7:553-568
- Checkley DM, Miller CA (1989) Nitrogen Isotope Fractionation by Oceanic Zooplankton. *Deep-Sea Research Part a-Oceanographic Research Papers* 36:1449-1456
- Church MJ, Jenkins BD, Karl DM, Zehr JP (2005) Vertical distributions of nitrogen-fixing phylotypes at Stn ALOHA in the oligotrophic North Pacific Ocean. *Aquatic Microbial Ecology* 38:3-14
- Cifuentes LA, Fogel ML, Pennock JR, Sharp JH (1989) Biogeochemical Factors That Influence the Stable Nitrogen Isotope Ratio of Dissolved Ammonium in the Delaware Estuary. *Geochimica Et Cosmochimica Acta* 53:2713-2721
- Conover RJ, Wilson S, Harding GCH, Vass WP (1995) Climate, Copepods and Cod - Some Thoughts on the Long-Range Prospects for a Sustainable Northern Cod Fishery. *Climate Research* 5:69-82
- Conte MH, Ralph N, Ross EH (2001) Seasonal and interannual variability in deep ocean particle fluxes at the Oceanic Flux Program (OFP)/Bermuda Atlantic Time Series (BATS) site in the western Sargasso Sea near Bermuda. *Deep-Sea Research Part Ii-Topical Studies in Oceanography* 48:1471-1505

- Cornell SE, Jickells TD, Thornton CA (1995) Atmospheric inputs of dissolved organic nitrogen to the oceans. *Nature* 376:243-246
- Dagg M (1993) Sinking Particles as a Possible Source of Nutrition for the Large Calanoid Copepod *Neocalanus-Cristatus* in the Sub-Arctic Pacific-Ocean. *Deep-Sea Research Part I-Oceanographic Research Papers* 40:1431-1445
- Dagg MJ, Frost BW, Newton JA (1997) Vertical migration and feeding behavior of *Calanus pacificus* females during a phytoplankton bloom in Dabob Bay, US. *Limnology and Oceanography* 42:974-980
- Dagg MJ, Urban-Rich J, Peterson JO (2003) The potential contribution of fecal pellets from large copepods to the flux of biogenic silica and particulate organic carbon in the Antarctic Polar Front region near 170 degrees W. *Deep-Sea Research Part II-Topical Studies in Oceanography* 50:675-691
- Dagg MJ, Vidal J, Whitledge TE, Iverson RL, Goering JJ (1982) The Feeding, Respiration, and Excretion of Zooplankton in the Bering Sea During a Spring Bloom. *Deep-Sea Research Part a-Oceanographic Research Papers* 29:45-63
- Dai JH, Sun MY, Culp RA, Noakes JE (2005) Changes in chemical and isotopic signatures of plant materials during degradation: Implication for assessing various organic inputs in estuarine systems. *Geophysical Research Letters* 32
- Dam HG, Zhang XS, Butler M, Roman MR (1995) Mesozooplankton Grazing and Metabolism at the Equator in the Central Pacific - Implications for Carbon and Nitrogen Fluxes. *Deep-Sea Research Part II-Topical Studies in Oceanography* 42:735-756
- Davey M, Tarran GA, Mills MM, Ridame C, Geider RJ, LaRoche J (2008) Nutrient limitation of picophytoplankton photosynthesis and growth in the tropical North Atlantic. *Limnology and Oceanography* 53:1722-1733
- Davis CS, McGillicuddy DJ (2006) Transatlantic abundance of the N-2-fixing colonial cyanobacterium *Trichodesmium*. *Science* 312:1517-1520
- del Giorgio PA, Duarte CM (2002) Respiration in the open ocean. *Nature* 420:379-384

- Deniro MJ, Epstein S (1977) Mechanism of carbon isotope fractionation associated with lipid synthesis. *Science* 197:261-263
- Deniro MJ, Epstein S (1981) Influence of diet on the distribution of nitrogen isotopes in animals. *Geochimica Et Cosmochimica Acta* 45:341-351
- Deuser WG, Jickells TD, King P, Commeau JA (1995) Decadal and annual changes in biogenic opal and carbonate fluxes to the deep Sargasso Sea. *Deep-Sea Research Part I-Oceanographic Research Papers* 42:1923-1932
- Deuser WG, Ross EH (1980) Seasonal change in the flux of organic carbon to the deep Sargasso Sea. *Nature* 283:364-365
- Deuser WG, Ross EH, Anderson RF (1981) Seasonality in the supply of sediment to the deep Sargasso Sea and implications for the rapid transfer of matter to the deep ocean. *Deep-Sea Research Part a-Oceanographic Research Papers* 28:495-505
- Deutsch C, Sarmiento JL, Sigman DM, Gruber N, Dunne JP (2007) Spatial coupling of nitrogen inputs and losses in the ocean. *Nature* 445:163-167
- Dilling L, Alldredge AL (2000) Fragmentation of marine snow by swimming macrozooplankton: A new process impacting carbon cycling in the sea. *Deep-Sea Research Part I-Oceanographic Research Papers* 47:1227-1245
- Dilling L, Brzezinski MA (2004) Quantifying marine snow as a food choice for zooplankton using stable silicon isotope tracers. *Journal of Plankton Research* 26:1105-1114
- Dilling L, Wilson J, Steinberg D, Alldredge A (1998) Feeding by the euphausiid *Euphausia pacifica* and the copepod *Calanus pacificus* on marine snow. *Marine Ecology-Progress Series* 170:189-201
- Ding HB, Sun MY (2005) Biochemical degradation of algal fatty acids in oxic and anoxic sediment-seawater interface systems: effects of structural association and relative roles of aerobic and anaerobic bacteria. *Marine Chemistry* 93:1-19
- Dore JE, Brum JR, Tupas LM, Karl DM (2002) Seasonal and interannual variability in sources of nitrogen supporting export in the oligotrophic subtropical North Pacific Ocean. *Limnology and Oceanography* 47:1595-1607

- Duarte CM, Dachs J, Llabres M, Alonso-Laita P, Gasol JM, Tovar-Sanchez A, Sanudo-Wilhemly S, Agusti S (2006) Aerosol inputs enhance new production in the subtropical northeast Atlantic. *Journal of Geophysical Research-Biogeosciences* 111
- Dubischar CD, Bathmann UV (2002) The occurrence of faecal material in relation to different pelagic systems in the Southern Ocean and its importance for vertical flux. *Deep-Sea Research Part II-Topical Studies in Oceanography* 49:3229-3242
- Duce RA, LaRoche J, Altieri K, Arrigo KR, Baker AR, Capone DG, Cornell S, Dentener F, Galloway J, Ganeshram RS, Geider RJ, Jickells T, Kuypers MM, Langlois R, Liss PS, Liu SM, Middelburg JJ, Moore CM, Nickovic S, Oschlies A, Pedersen T, Prospero J, Schlitzer R, Seitzinger S, Sorensen LL, Uematsu M, Ulloa O, Voss M, Ward B, Zamora L (2008) Impacts of atmospheric anthropogenic nitrogen on the open ocean. *Science* 320:893-897
- Ducklow HW (1999) The bacterial component of the oceanic euphotic zone. *FEMS Microbiology Ecology* 30:1-10
- Dugdale RC (1986) Citation-Classic - Uptake of New and Regenerated Forms of Nitrogen in Primary Productivity. *Current Contents/Agriculture Biology & Environmental Sciences*:14-14
- Dugdale RC, Goering JJ (1967) Uptake of New and Regenerated Forms of Nitrogen in Primary Productivity. *Limnology and Oceanography* 12:196-&
- Eberl R, Carpenter EJ (2007) Association of the copepod *Macrosetella gracilis* with the cyanobacterium *Trichodesmium* spp. in the North Pacific Gyre. *Marine Ecology-Progress Series* 333:205-212
- Emerson CW, Roff JC (1987) Implications of Fecal Pellet Size and Zooplankton Behavior to Estimates of Pelagic-Benthic Carbon Flux. *Marine Ecology-Progress Series* 35:251-257
- Emerson S, Quay P, Karl D, Winn C, Tupas L, Landry M (1997) Experimental determination of the organic carbon flux from open-ocean surface waters. *Nature* 389:951-954

- Emerson S, Stump C, Nicholson D (2008) Net biological oxygen production in the ocean: Remote in situ measurements of O-2 and N-2 in surface waters. *Global Biogeochemical Cycles* 22
- Eppley RW, Peterson BJ (1979) Particulate Organic-Matter Flux and Planktonic New Production in the Deep Ocean. *Nature* 282:677-680
- Estrada JA, Lutcavage M, Thorrold SR (2005) Diet and trophic position of Atlantic bluefin tuna (*Thunnus thynnus*) inferred from stable carbon and nitrogen isotope analysis. *Marine Biology* 147:37-45
- Falcon LI, Carpenter EJ, Cipriano F, Bergman B, Capone DG (2004a) N-2 fixation by unicellular bacterioplankton from the Atlantic and Pacific oceans: Phylogeny and in situ rates. *Applied and Environmental Microbiology* 70:765-770
- Falcon LI, Cipriano F, Chistoserdov AY, Carpenter EJ (2002) Diversity of diazotrophic unicellular cyanobacteria in the tropical North Atlantic Ocean. *Applied and Environmental Microbiology* 68:5760-5764
- Falcon LI, Lindvall S, Bauer K, Bergman B, Carpenter EJ (2004b) Ultrastructure of unicellular N-2 fixing cyanobacteria from the tropical North Atlantic and subtropical North Pacific Oceans. *Journal of Phycology* 40:1074-1078
- Falkowski P, Scholes RJ, Boyle E, Canadell J, Canfield D, Elser J, Gruber N, Hibbard K, Hogberg P, Linder S, Mackenzie FT, Moore B, Pedersen T, Rosenthal Y, Seitzinger S, Smetacek V, Steffen W (2000) The global carbon cycle: A test of our knowledge of earth as a system. *Science* 290:291-296
- Falkowski PG (1991) Species Variability in the Fractionation of C-13 and C-12 by Marine-Phytoplankton. *Journal of Plankton Research* 13:S21-S28
- Falkowski PG, Barber RT, Smetacek V (1998) Biogeochemical controls and feedbacks on ocean primary production. *Science* 281:200-206
- Fantle MS, Dittel AI, Schwalm SM, Epifanio CE, Fogel ML (1999) A food web analysis of the juvenile blue crab, *Callinectes sapidus*, using stable isotopes in whole animals and individual amino acids. *Oecologia* 120:416-426

- Fenchel T (2008) The microbial loop-25 years later. *Journal of Experimental Marine Biology and Ecology* 366:99-103
- Fernandez-Alamo MA, Farber-Lorda J (2006) Zooplankton and the oceanography of the eastern tropical Pacific: A review. *Progress in Oceanography* 69:318-359
- Ferreira V, Graca MAS, de Lima J, Gomes R (2006) Role of physical fragmentation and invertebrate activity in the breakdown rate of leaves. *Archiv Fur Hydrobiologie* 165:493-513
- Foster RA, Subramaniam A, Mahaffey C, Carpenter EJ, Capone DG, Zehr JP (2007) Influence of the Amazon River plume on distributions of free-living and symbiotic cyanobacteria in the western tropical north Atlantic Ocean. *Limnology and Oceanography* 52:517-532
- Francois R, Honjo S, Krishfield R, Manganini S (2002) Factors controlling the flux of organic carbon to the bathypelagic zone of the ocean. *Global Biogeochemical Cycles* 16
- Frangoulis C, Christou ED, Hecq JH (2005) Comparison of marine copepod outfluxes: Nature, rate, fate and role in the carbon and nitrogen cycles. In: *Advances in Marine Biology*, Vol 47, Vol 47, p 253-309
- Freudenthal T, Wagner T, Wenzhofer F, Zabel M, Wefer G (2001) Early diagenesis of organic matter from sediments of the eastern subtropical Atlantic: Evidence from stable nitrogen and carbon isotopes. *Geochimica Et Cosmochimica Acta* 65:1795-1808
- Fry B, Quinones RB (1994) Biomass Spectra and Stable-Isotope Indicators of Trophic Level in Zooplankton of the Northwest Atlantic. *Marine Ecology-Progress Series* 112:201-204
- Fujii M, Ikeda M, Yamanaka Y (2005) Roles of biogeochemical: Processes in the oceanic carbon cycle described with a simple coupled physical-biogeochemical model. *Journal of Oceanography* 61:803-815
- Galimov EM (1981) *The biological fractionation of isotopes*, Vol. Academic Press, INC., London

- Galloway JN, Dentener FJ, Capone DG, Boyer EW, Howarth RW, Seitzinger SP, Asner GP, Cleveland CC, Green PA, Holland EA, Karl DM, Michaels AF, Porter JH, Townsend AR, Vorosmarty CJ (2004) Nitrogen cycles: past, present, and future. *Biogeochemistry* 70:153-226
- Galloway JN, Townsend AR, Erisman JW, Bekunda M, Cai ZC, Freney JR, Martinelli LA, Seitzinger SP, Sutton MA (2008) Transformation of the nitrogen cycle: Recent trends, questions, and potential solutions. *Science* 320:889-892
- Ganeshram RS, Pedersen TF, Calvert SE, Francois R (2002) Reduced nitrogen fixation in the glacial ocean inferred from changes in marine nitrogen and phosphorus inventories. *Nature* 415:156-159
- Gannes LZ, Obrien DM, delRio CM (1997) Stable isotopes in animal ecology: Assumptions, caveats, and a call for more laboratory experiments. *Ecology* 78:1271-1276
- Gaye-Haake B, Lahajnar N, Emeis KC, Unger D, Rixen T, Suthhof A, Ramaswamy V, Schulz H, Paropkari AL, Gupta MVS, Ittekkot V (2005) Stable nitrogen isotopic ratios of sinking particles and sediments from the northern Indian Ocean. *Marine Chemistry* 96:243-255
- Gislason A, Eiane K, Reynisson P (2007) Vertical distribution and mortality of *Calanus finmarchicus* during overwintering in oceanic waters southwest of Iceland. *Marine Biology* 150:1253-1263
- Goldthwait S, Yen J, Brown J, Alldredge A (2004) Quantification of marine snow fragmentation by swimming euphausiids. *Limnology and Oceanography* 49:940-952
- Goldthwait SA, Carlson CA, Henderson GK, Alldredge AL (2005) Effects of physical fragmentation on remineralization of marine snow. *Marine Ecology-Progress Series* 305:59-65
- Gowing MM, Garrison DL, Kunze HB, Winchell CJ (2001) Biological components of Ross Sea short-term particle fluxes in the austral summer of 1995-1996. *Deep-Sea Research Part I-Oceanographic Research Papers* 48:2645-2671
- Graca MAS (2001) The role of invertebrates on leaf litter decomposition in streams - A review. *International Review of Hydrobiology* 86:383-393

- Graziano LM, Geider RJ, Li WKW, Olaizola M (1996) Nitrogen limitation of North Atlantic phytoplankton: Analysis of physiological condition in nutrient enrichment experiments. *Aquatic Microbial Ecology* 11:53-64
- Gruber N, Sarmiento JL (1997) Global patterns of marine nitrogen fixation and denitrification. *Global Biogeochemical Cycles* 11:235-266
- Hall JA, Kalin RM, Larkin MJ, Allen CCR, Harper DB (1999) Variation in stable carbon isotope fractionation during aerobic degradation of phenol and benzoate by contaminant degrading bacteria. *Organic Geochemistry* 30:801-811
- Hansson S, Hobbie JE, Elmgren R, Larsson U, Fry B, Johansson S (1997) The stable nitrogen isotope ratio as a marker of food-web interactions and fish migration. *Ecology* 78:2249-2257
- Hare PE, Fogel ML, Stafford TW, Mitchell AD, Hoering TC (1991) The Isotopic Composition of Carbon and Nitrogen in Individual Amino-Acids Isolated from Modern and Fossil Proteins. *Journal of Archaeological Science* 18:277-292
- Harvey HR, Johnston JR (1995) Lipid-Composition and Flux of Sinking and Size-Fractionated Particles in Chesapeake-Bay. *Organic Geochemistry* 23:751-764
- Harvey HR, Macko SA (1997) Kinetics of phytoplankton decay during simulated sedimentation: changes in lipids under oxic and anoxic conditions. *Organic Geochemistry* 27:129-140
- Harvey HR, Tuttle JH, Bell JT (1995) Kinetics of phytoplankton decay during simulated sedimentation - Changes in biochemical composition and microbial activity under oxic and anoxic conditions. *Geochimica Et Cosmochimica Acta* 59:3367-3377
- Hasegawa T, Koike I, Mukai H (2001) Fate of food nitrogen in marine copepods. *Marine Ecology-Progress Series* 210:167-174
- Hastings MG, Sigman DM, Lipschultz F (2003) Isotopic evidence for source changes of nitrate in rain at Bermuda. *Journal of Geophysical Research-Atmospheres* 108
- Hawser SP, Oneil JM, Roman MR, Codd GA (1992) Toxicity of Blooms of the Cyanobacterium-Trichodesmium to Zooplankton. *Journal of Applied Phycology* 4:79-86

- Hedges JJ, Baldock JA, Gelinas Y, Lee C, Peterson M, Wakeham SG (2001) Evidence for non-selective preservation of organic matter in sinking marine particles. *Nature* 409:801-804
- Hernandez-Leon S, Fraga C, Ikeda T (2008) A global estimation of mesozooplankton ammonium excretion in the open ocean. *Journal of Plankton Research* 30:577-585
- Hernandez-Leon S, Ikeda T (2005) A global assessment of mesozooplankton respiration in the ocean. *Journal of Plankton Research* 27:153-158
- Hernes PJ, Peterson ML, Murray JW, Wakeham SG, Lee C, Hedges JJ (2001) Particulate carbon and nitrogen fluxes and compositions in the central equatorial Pacific. *Deep-Sea Research Part I-Oceanographic Research Papers* 48:1999-2023
- Hewson I, Govil SR, Capone DG, Carpenter EJ, Fuhrman JA (2004) Evidence of *Trichodesmium* viral lysis and potential significance for biogeochemical cycling in the oligotrophic ocean. *Aquatic Microbial Ecology* 36:1-8
- Hobson KA, Alisauskas RT, Clark RG (1993) Stable-Nitrogen Isotope Enrichment in Avian-Tissues Due to Fasting and Nutritional Stress - Implications for Isotopic Analyses of Diet. *Condor* 95:388-394
- Hoch MP, Fogel ML, Kirchman DL (1994) Isotope Fractionation During Ammonium Uptake by Marine Microbial Assemblages. *Geomicrobiology Journal* 12:113-127
- Holl CM, Villareal TA, Payne CD, Clayton TD, Hart C, Montoya JP (2007) *Trichodesmium* in the western Gulf of Mexico: N-15(2)-fixation and natural abundance stable isotope evidence. *Limnology and Oceanography* 52:2249-2259
- Honda MC (2003) Biological pump in northwestern North Pacific. *Journal of Oceanography* 59:671-684
- Honjo S (1996) Fluxes of particles to the interior of the open oceans. In: Ittekkot V, Schafer P, Honjo S, Depetris PJ (eds) *Particle Flux in the Ocean*. John Wiley & Sons, Chichester, p 92-154
- Horrigan SG, Montoya JP, Nevins JL, McCarthy JJ (1990) Natural Isotopic Composition of Dissolved Inorganic Nitrogen in the Chesapeake Bay. *Estuarine Coastal and Shelf Science* 30:393-410

- Houghton RA (2007) Balancing the global carbon budget. *Annual Review of Earth and Planetary Sciences* 35:313-347
- Isla JA, Llope M, Anadon R (2004) Size-fractionated mesozooplankton biomass, metabolism and grazing along a 50 degrees N-30 degrees S transect of the Atlantic Ocean. *Journal of Plankton Research* 26:1301-1313
- Jennings S, Maxwell TAD, Schratzberger M, Milligan SP (2008) Body-size dependent temporal variations in nitrogen stable isotope ratios in food webs. *Marine Ecology-Progress Series* 370:199-206
- Jickells TD (1999) The inputs of dust derived elements to the Sargasso Sea; a synthesis. *Marine Chemistry* 68:5-14
- Jickells TD, An ZS, Andersen KK, Baker AR, Bergametti G, Brooks N, Cao JJ, Boyd PW, Duce RA, Hunter KA, Kawahata H, Kubilay N, laRoche J, Liss PS, Mahowald N, Prospero JM, Ridgwell AJ, Tegen I, Torres R (2005) Global iron connections between desert dust, ocean biogeochemistry, and climate. *Science* 308:67-71
- Johnson C, Pringle J, Chen CS (2006) Transport and retention of dormant copepods in the Gulf of Maine. *Deep-Sea Research Part II-Topical Studies in Oceanography* 53:2520-2536
- Karl D, Letelier R, Tupas L, Dore J, Christian J, Hebel D (1997) The role of nitrogen fixation in biogeochemical cycling in the subtropical North Pacific Ocean. *Nature* 388:533-538
- Karl D, Michaels A, Bergman B, Capone D, Carpenter E, Letelier R, Lipschultz F, Paerl H, Sigman D, Stal L (2002) Dinitrogen fixation in the world's oceans. *Biogeochemistry* 57:47-+
- Karl DM, Letelier RM (2008) Nitrogen fixation-enhanced carbon sequestration in low nitrate, low chlorophyll seascapes. *Marine Ecology-Progress Series* 364:257-268
- Kling GW, Fry B, O'Brien WJ (1992) Stable Isotopes and Planktonic Trophic Structure in Arctic Lakes. *Ecology* 73:561-566

- Knauer GA, Martin JH, Bruland KW (1979) Fluxes of particulate carbon, nitrogen, and phosphorus in the upper water column of the Northeast Pacific. *Deep-Sea Research* 26:97-108
- Koppelman R, Weikert H, Lahajnar N (2003) Vertical distribution of mesozooplankton and its delta N-15 signature at a deep-sea site in the Levantine Sea (eastern Mediterranean) in April 1999. *Journal of Geophysical Research-Oceans* 108
- Krishnamurthy A, Moore JK, Zender CS, Luo C (2007) Effects of atmospheric inorganic nitrogen deposition on ocean biogeochemistry. *Journal of Geophysical Research-Biogeosciences* 112
- Lampitt RS, Antia AN (1997) Particle flux in deep seas: regional characteristics and temporal variability. *Deep-Sea Research Part I-Oceanographic Research Papers* 44:1377-1403
- Lampitt RS, Noji T, Vonbodungen B (1990) What Happens to Zooplankton Fecal Pellets - Implications for Material Flux. *Marine Biology* 104:15-23
- Langlois RJ, Hummer D, LaRoche J (2008) Abundances and distributions of the dominant nifH phylotypes in the Northern Atlantic Ocean. *Applied and Environmental Microbiology* 74:1922-1931
- LaRoche J, Breitbarth E (2005) Importance of the diazotrophs as a source of new nitrogen in the ocean. *Journal of Sea Research* 53:67-91
- Le Fevre J, Legendre L, Rivkin RB (1998) Fluxes of biogenic carbon in the Southern Ocean: roles of large microphagous zooplankton. *Journal of Marine Systems* 17:325-345
- Ledwell JR, Watson AJ, Law CS (1993) Evidence for Slow Mixing across the Pycnocline from an Open-Ocean Tracer-Release Experiment. *Nature* 364:701-703
- Ledwell JR, Watson AJ, Law CS (1998) Mixing of a tracer in the pycnocline. *Journal of Geophysical Research-Oceans* 103:21499-21529
- Lee BG, Fisher NS (1992) Degradation and Elemental Release Rates from Phytoplankton Debris and Their Geochemical Implications. *Limnology and Oceanography* 37:1345-1360

- Lee BG, Fisher NS (1994) Effects of Sinking and Zooplankton Grazing on the Release of Elements from Planktonic Debris. *Marine Ecology-Progress Series* 110:271-281
- Lee C (2002) Particulate organic matter composition and fluxes in the sea. In: Gianguzza A, Pelizzeti E, Sammartano S (eds) *Chemistry of Marine Water and Sediments*. Springer, New York, p 125-146
- Lee C, McKenzie JA, Sturm M (1987) Carbon Isotope Fractionation and Changes in the Flux and Composition of Particulate Matter Resulting from Biological-Activity During a Sediment Trap Experiment in Lake Greifen, Switzerland. *Limnology and Oceanography* 32:83-96
- Lee K (2001) Global net community production estimated from the annual cycle of surface water total dissolved inorganic carbon. *Limnology and Oceanography* 46:1287-1297
- Lee K, Karl DM, Wanninkhof R, Zhang JZ (2002) Global estimates of net carbon production in the nitrate-depleted tropical and subtropical oceans. *Geophysical Research Letters* 29
- Lehmann MF, Bernasconi SM, Barbieri A, McKenzie JA (2002) Preservation of organic matter and alteration of its carbon and nitrogen isotope composition during simulated and in situ early sedimentary diagenesis. *Geochimica Et Cosmochimica Acta* 66:3573-3584
- Lehmann MF, Bernasconi SM, McKenzie JA, Barbieri A, Simona M, Veronesi M (2004) Seasonal variation of the delta C-13 and delta N-15 of particulate and dissolved carbon and nitrogen in Lake Lugano: Constraints on biogeochemical cycling in a eutrophic lake. *Limnology and Oceanography* 49:415-429
- Letelier RM, Karl DM (1996) Role of *Trichodesmium* spp in the productivity of the subtropical North Pacific Ocean. *Marine Ecology-Progress Series* 133:263-273
- Letelier RM, Karl DM (1998) *Trichodesmium* spp. physiology and nutrient fluxes in the North Pacific subtropical gyre. *Aquatic Microbial Ecology* 15:265-276
- Lewis MR, Harrison WG, Oakey NS, Hebert D, Platt T (1986) Vertical Nitrate Fluxes in the Oligotrophic Ocean. *Science* 234:870-873

- Lipschultz F, Bates NR, Carlson CA, Hansell DA (2002) New production in the Sargasso Sea: History and current status. *Global Biogeochemical Cycles* 16
- Liu ZH, Altabet MA, Herbert TD (2005) Glacial-interglacial modulation of eastern tropical North Pacific denitrification over the last 1.8-Myr. *Geophysical Research Letters* 32
- Longhurst A (1976) Vertical Migration. In: Cushing DHaW, J.J. (ed) *The Ecology of Seas*. Blackwell Scientific Publications
- Longhurst A, Sathyendranath S, Platt T, Caverhill C (1995) An Estimate of Global Primary Production in the Ocean from Satellite Radiometer Data. *Journal of Plankton Research* 17:1245-1271
- Longhurst A, Williams R (1992) Carbon Flux by Seasonal Vertical Migrant Copepods Is a Small Number. *Journal of Plankton Research* 14:1495-1509
- Longhurst AR, Bedo A, Harrison WG, Head EJH, Horne EP, Irwin B, Morales C (1989) Nflux - a Test of Vertical Nitrogen Flux by Diel Migrant Biota. *Deep-Sea Research Part a-Oceanographic Research Papers* 36:1705-1719
- Longhurst AR, Harrison WG (1988) Vertical Nitrogen Flux from the Oceanic Photoc Zone by Diel Migrant Zooplankton and Nekton. *Deep-Sea Research Part a-Oceanographic Research Papers* 35:881-889
- Louanchi F, Najjar RG (2000) A global monthly climatology of phosphate, nitrate, and silicate in the upper ocean: Spring-summer export production and shallow remineralization. *Global Biogeochemical Cycles* 14:957-977
- Louanchi F, Najjar RG (2001) Annual cycles of nutrients and oxygen in the upper layers of the North Atlantic Ocean. *Deep-Sea Research Part Ii-Topical Studies in Oceanography* 48:2155-2171
- Lourey MJ, Trull TW, Sigman DM (2003) Sensitivity of delta N-15 of nitrate, surface suspended and deep sinking particulate nitrogen to seasonal nitrate depletion in the Southern Ocean. *Global Biogeochemical Cycles* 17
- Lourey MJ, Trull TW, Tilbrook B (2004) Sensitivity of delta C-13 of Southern Ocean suspended and sinking organic matter to temperature, nutrient utilization, and

atmospheric CO₂. Deep-Sea Research Part I-Oceanographic Research Papers
51:281-305

Lutz M, Dunbar R, Caldeira K (2002) Regional variability in the vertical flux of
particulate organic carbon in the ocean interior. *Global Biogeochemical Cycles* 16

Macaulay MC, Wishner KF, Daly KL (1995) Acoustic Scattering from Zooplankton and
Micronekton in Relation to a Whale Feeding Site near Georges Bank and Cape-
Cod. *Continental Shelf Research* 15:509-537

Mackenzie FT, Lerman A, Andersson AJ (2004) Past and present of sediment and carbon
biogeochemical cycling models. *Biogeosciences* 1:11-32

Macko SA, Engel MH, Qian YR (1994) Early diagenesis and organic matter preservation
- a molecular stable carbon isotope perspective. *Chemical Geology* 114:365-379

Macko SA, Engel MH, Silfer JA (1991) Stable Isotope Effects During the Diagenesis of
Organic-Matter. *Abstracts of Papers of the American Chemical Society* 201:32-
GEOC

Macko SA, Estep MLF (1984) Microbial alteration of stable nitrogen and carbon isotopic
compositions of organic matter. *Organic Geochemistry* 6:787-790

Macko SA, Estep MLF, Engel MH, Hare PE (1986) Kinetic Fractionation of Stable
Nitrogen Isotopes during Amino-Acid Transamination. *Geochimica Et
Cosmochimica Acta* 50:2143-2146

Macko SA, Fogel ML, Hare PE, Hoering TC (1987) Isotopic fractionation of nitrogen
and carbon in the synthesis of amino-acids by microorganisms. *Chemical
Geology* 65:79-92

MacNeill MA, Skomal GB, Fisk AT (2005) Stable isotopes from multiple tissues reveal
diet switching in sharks. *Marine Ecology-Progress Series* 302:199-206

Madin LP, Horgan EF, Steinberg DK (2001) Zooplankton at the Bermuda Atlantic Time-
series Study (BATS) station: diel, seasonal and interannual variation in biomass,
1994-1998. *Deep-Sea Research Part II-Topical Studies in Oceanography* 48:2063-
2082

- Mahaffey C, Michaels AF, Capone DG (2005) The conundrum of marine N₂ fixation. *American Journal of Science* 305:546-595
- Mahaffey C, Williams RG, Wolff GA, Mahowald N, Anderson W, Woodward M (2003) Biogeochemical signatures of nitrogen fixation in the eastern North Atlantic. *Geophysical Research Letters* 30
- Mahowald NM, Baker AR, Bergametti G, Brooks N, Duce RA, Jickells TD, Kubilay N, Prospero JM, Tegen I (2005) Atmospheric global dust cycle and iron inputs to the ocean. *Global Biogeochemical Cycles* 19
- Maranon E, Perez V, Fernandez E, Anadon R, Bode A, Gonzalez N, Huskin I, Isla A, Moran XAG, Mourino B, Quevedo M, Robinson C, Serret P, Teira E, Varela MM, Woodward EMS, Zubkov MV (2007) Planktonic carbon budget in the eastern subtropical North Atlantic. *Aquatic Microbial Ecology* 48:261-275
- Mariotti A, Germon JC, Hubert P, Kaiser P, Letolle R, Tardieux A, Tardieux P (1981) Experimental-Determination of Nitrogen Kinetic Isotope Fractionation - Some Principles - Illustration for the Denitrification and Nitrification Processes. *Plant and Soil* 62:413-430
- Martin AP, Pondaven P (2003) On estimates for the vertical nitrate flux due to eddy pumping. *Journal of Geophysical Research-Oceans* 108
- Martins R, Fernandez N, Beiras R, Vasconcelos V (2007) Toxicity assessment of crude and partially purified extracts of marine *Synechocystis* and *Synechococcus* cyanobacterial strains in marine invertebrates. *Toxicon* 50:791-799
- Mazeas L, Budzinski H, Raymond N (2002) Absence of stable carbon isotope fractionation of saturated and polycyclic aromatic hydrocarbons during aerobic bacterial biodegradation. *Organic Geochemistry* 33:1259-1272
- McCarthy M, Hedges JI, Benner R, Fogel M (2003) Compound-specific delta N-15 measurements of amino acids in dissolved organic matter from the central Pacific Ocean. *Geochimica Et Cosmochimica Acta* 67:A284-A284
- McCarthy MD, Benner R, Lee C, Fogel ML (2007) Amino acid nitrogen isotopic fractionation patterns as indicators of heterotrophy in plankton, particulate, and dissolved organic matter. *Geochimica Et Cosmochimica Acta* 71:4727-4744

- McCarthy MD, Benner R, Lee C, Hedges JI, Fogel ML (2004) Amino acid carbon isotopic fractionation patterns in oceanic dissolved organic matter: an unaltered photoautotrophic source for dissolved organic nitrogen in the ocean? *Marine Chemistry* 92:123-134
- McClelland JW, Holl CM, Montoya JP (2003) Relating low delta N-15 values of zooplankton to N-2-fixation in the tropical North Atlantic: insights provided by stable isotope ratios of amino acids. *Deep-Sea Research Part I-Oceanographic Research Papers* 50:849-861
- McClelland JW, Montoya JP (2002) Trophic relationships and the nitrogen isotopic composition of amino acids in plankton. *Ecology* 83:2173-2180
- McGillicuddy DJ, Anderson LA, Doney SC, Maltrud ME (2003) Eddy-driven sources and sinks of nutrients in the upper ocean: Results from a 0.1 degrees resolution model of the North Atlantic. *Global Biogeochemical Cycles* 17
- McGillicuddy DJ, Robinson AR (1997) Eddy-induced nutrient supply and new production in the Sargasso Sea. *Deep-Sea Research Part I-Oceanographic Research Papers* 44:1427-1450
- McGillicuddy DJ, Robinson AR, Siegel DA, Jannasch HW, Johnson R, Dickey T, McNeil J, Michaels AF, Knap AH (1998) Influence of mesoscale eddies on new production in the Sargasso Sea. *Nature* 394:263-266
- Meckenstock RU, Morasch B, Warthmann R, Schink B, Annweiler E, Michaelis W, Richnow HH (1999) C-13/C-12 isotope fractionation of aromatic hydrocarbons during microbial degradation. *Environmental Microbiology* 1:409-414
- Megens L, Van der Plicht J, De Leeuw JW (1998) Molecular, radioactive and stable carbon isotope characterization of estuarine particulate organic matter. *Radiocarbon* 40:985-990
- Mianzan H, Pajaro M, Colombo GA, Madirolas A (2001) Feeding on survival-food: gelatinous plankton as a source of food for anchovies. *Hydrobiologia* 451:45-53
- Michaels AF, Olson D, Sarmiento JL, Ammerman JW, Fanning K, Jahnke R, Knap AH, Lipschultz F, Prospero JM (1996) Inputs, losses and transformations of nitrogen and phosphorus in the pelagic North Atlantic Ocean. *Biogeochemistry* 35:181-226

- Mills MM, Moore CM, Langlois R, Milne A, Achterberg E, Nachtigall K, Lochte K, Geider RJ, La Roche J (2008) Nitrogen and phosphorus co-limitation of bacterial productivity and growth in the oligotrophic subtropical North Atlantic. *Limnology and Oceanography* 53:824-834
- Mills MM, Ridame C, Davey M, La Roche J, Geider RJ (2004) Iron and phosphorus co-limit nitrogen fixation in the eastern tropical North Atlantic. *Nature* 429:292-294
- Minagawa M, Wada E (1984) Stepwise Enrichment of N-15 Along Food-Chains - Further Evidence and the Relation between Delta-N-15 and Animal Age. *Geochimica Et Cosmochimica Acta* 48:1135-1140
- Mino Y, Saino T, Suzuki K, Maranon E (2002) Isotopic composition of suspended particulate nitrogen (delta N-15(sus)) in surface waters of the Atlantic Ocean from 50 degrees N to 50 degrees S. *Global Biogeochemical Cycles* 16
- Mittelstaedt E (1987) Cyclonic Cold-Core Eddy in the Eastern North-Atlantic .1. Physical Description. *Marine Ecology-Progress Series* 39:145-152
- Moller EF (2005) Sloppy feeding in marine copepods: prey-size-dependent production of dissolved organic carbon. *Journal of Plankton Research* 27:27-35
- Moller EF (2007) Production of dissolved organic carbon by sloppy feeding in the copepods *Acartia tonsa*, *Centropages typicus*, and *Temora longicornis*. *Limnology and Oceanography* 52:79-84
- Montoya JP (2008) Nitrogen stable isotopes in marine environments. In: Capone DG, Carpenter, E.J., Mulholland, M.R., Bronk, D.A. (ed) *Nitrogen in the Marine Environment*. Academic Press, p 1277-1302
- Montoya JP, Carpenter EJ, Capone DG (2002) Nitrogen fixation and nitrogen isotope abundances in zooplankton of the oligotrophic North Atlantic. *Limnology and Oceanography* 47:1617-1628
- Montoya JP, Holl CM, Zehr JP, Hansen A, Villareal TA, Capone DG (2004) High rates of N-2 fixation by unicellular diazotrophs in the oligotrophic Pacific Ocean. *Nature* 430:1027-1031

- Montoya JP, Horrigan SG, McCarthy JJ (1990) Natural abundance of N-15 in particulate nitrogen and zooplankton in the Chesapeake Bay. *Marine Ecology-Progress Series* 65:35-61
- Montoya JP, McCarthy JJ (1995) Isotopic Fractionation During Nitrate Uptake by Phytoplankton Grown in Continuous-Culture. *Journal of Plankton Research* 17:439-464
- Montoya JP, Voss M, Capone DG (2007) Spatial variation in N-2-fixation rate and diazotroph activity in the Tropical Atlantic. *Biogeosciences* 4:369-376
- Montoya JP, Wiebe PH, McCarthy JJ (1992) Natural abundance of N-15 in particulate nitrogen and zooplankton in the Gulf-Stream region and warm-core ring 86a. *Deep-Sea Research Part a-Oceanographic Research Papers* 39:S363-S392
- Moore CM, Mills MM, Langlois R, Milne A, Achterberg EP, La Roche J, Geider RJ (2008) Relative influence of nitrogen and phosphorus availability on phytoplankton physiology and productivity in the oligotrophic sub-tropical North Atlantic Ocean. *Limnology and Oceanography* 53:291-305
- Morales CE (1999) Carbon and nitrogen fluxes in the oceans: the contribution by zooplankton migrants to active transport in the North Atlantic during the Joint Global Ocean Flux Study. *Journal of Plankton Research* 21:1799-1808
- Mourino-Carballido B, Neuer S (2008) Regional Differences in the Role of Eddy Pumping in the North Atlantic Subtropical Gyre HISTORICAL CONUNDRUMS REVISITED. *Oceanography* 21:52-61
- Mulholland MR (2007) The fate of nitrogen fixed by diazotrophs in the ocean. *Biogeosciences* 4:37-51
- Mulholland MR, Bernhardt PW, Heil CA, Bronk DA, O'Neil JM (2006) Nitrogen fixation and release of fixed nitrogen by *Trichodesmium* spp. in the Gulf of Mexico. *Limnology and Oceanography* 51:1762-1776
- Mulholland MR, Bronk DA, Capone DG (2004) Dinitrogen fixation and release of ammonium and dissolved organic nitrogen by *Trichodesmium* IMS101. *Aquatic Microbial Ecology* 37:85-94

- Mulholland MR, Ohki K, Capone DG (1999) Nitrogen utilization and metabolism relative to patterns of N-2 fixation in cultures of *Trichodesmium* NIBB1067. *Journal of Phycology* 35:977-988
- Nakanishi T, Minagawa M (2003) Stable carbon and nitrogen isotopic compositions of sinking particles in the northeast Japan Sea. *Geochemical Journal* 37:261-275
- Nakatsuka T, Handa N, Harada N, Sugimoto T, Imaizumi S (1997) Origin and decomposition of sinking particulate organic matter in the deep water column inferred from the vertical distributions of its δ N-15, δ C-13 and δ C-14. *Deep-Sea Research Part I-Oceanographic Research Papers* 44:1957-1979
- Needoba JA, Sigman DM, Harrison PJ (2004) The mechanism of isotope fractionation during algal nitrate assimilation as illuminated by the N-15/N-14 of intracellular nitrate. *Journal of Phycology* 40:517-522
- Needoba JA, Waser NA, Harrison PJ, Calvert SE (2003) Nitrogen isotope fractionation in 12 species of marine phytoplankton during growth on nitrate. *Marine Ecology-Progress Series* 255:81-91
- Neuer S, Davenport R, Freudenthal T, Wefer G, Llinas O, Rueda MJ, Steinberg DK, Karl DM (2002) Differences in the biological carbon pump at three subtropical ocean sites. *Geophysical Research Letters* 29
- Nguyen RT, Harvey HR (1997) Protein and amino acid cycling during phytoplankton decomposition in oxic and anoxic waters. *Organic Geochemistry* 27:115-128
- O'Neil JM (1998) The colonial cyanobacterium *Trichodesmium* as a physical and nutritional substrate for the harpacticoid copepod *Macrosetella gracilis*. *Journal of Plankton Research* 20:43-59
- Olli K, Wassmann P, Reigstad M, Ratkova TN, Arashkevich E, Pasternak A, Matrai PA, Knulst J, Tranvik L, Klais R, Jacobsen A (2007) The fate of production in the central Arctic Ocean - Top-down regulation by zooplankton expatriates? *Progress in Oceanography* 72:84-113
- Oneil JM, Metzler PM, Glibert PM (1996) Ingestion of N-15(2)-labelled *Trichodesmium* spp and ammonium regeneration by the harpacticoid copepod *Macrosetella gracilis*. *Marine Biology* 125:89-96

- Oneil JM, Roman MR (1994) Ingestion of the Cyanobacterium *Trichodesmium* Spp by Pelagic Harpacticoid Copepods *Macrosetella*, *Miracia* and *Oculostella*. *Hydrobiologia* 293:235-240
- Oschlies A (2002a) Can eddies make ocean deserts bloom? *Global Biogeochemical Cycles* 16
- Oschlies A (2002b) Nutrient supply to the surface waters of the North Atlantic: A model study. *Journal of Geophysical Research-Oceans* 107
- Osgood KE, Frost BW (1994) Ontogenic Diel Vertical Migration Behaviors of the Marine Planktonic Copepods *Calanus-Pacificus* and *Metridia-Lucens*. *Marine Ecology-Progress Series* 104:13-25
- Pearre S (2003) Eat and run? The hunger/satiation hypothesis in vertical migration: history, evidence and consequences. *Biological Reviews* 78:1-79
- Peng TH (2005) Anthropogenic CO₂ in the ocean. *Scientia Marina* 69:85-96
- Peterson BJ (1999) Stable isotopes as tracers of organic matter input and transfer in benthic food webs: A review. *Acta Oecologica-International Journal of Ecology* 20:479-487
- Peterson BJ, Fry B (1987) Stable Isotopes in Ecosystem Studies. *Annual Review of Ecology and Systematics* 18:293-320
- Piao HC, Zhu JM, Liu GS, Liu CQ, Tao FX (2006) Changes of natural C-13 abundance in microbial biomass during litter decomposition. *Applied Soil Ecology* 33:3-9
- Piontkovski S, Williams R, Ignatyev S, Boltachev A, Chesalin M (2003) Structural-functional relationships in the pelagic community of the eastern tropical Atlantic Ocean. *Journal of Plankton Research* 25:1021-1034
- Post DM (2002) Using stable isotopes to estimate trophic position: Models, methods, and assumptions. *Ecology* 83:703-718

- Post DM, Layman CA, Arrington DA, Takimoto G, Quattrochi J, Montana CG (2007) Getting to the fat of the matter: models, methods and assumptions for dealing with lipids in stable isotope analyses. *Oecologia* 152:179-189
- Poulsen LK, Kiorboe T (2006) Vertical flux and degradation rates of copepod fecal pellets in a zooplankton community dominated by small copepods. *Marine Ecology-Progress Series* 323:195-204
- Poulton AJ, Holligan PM, Hickman A, Kim YN, Adey TR, Stinchcombe MC, Holeton C, Root S, Woodward EMS (2006) Phytoplankton carbon fixation, chlorophyll-biomass and diagnostic pigments in the Atlantic Ocean. *Deep-Sea Research Part II-Topical Studies in Oceanography* 53:1593-1610
- Prospero JM, Barrett K, Church T, Dentener F, Duce RA, Galloway JN, Levy H, Moody J, Quinn P (1996) Atmospheric deposition of nutrients to the North Atlantic Basin. *Biogeochemistry* 35:27-73
- Qian Y, Kennicutt MC, Svalberg J, Macko SA, Bidigare RR, Walker J (1996) Suspended particulate organic matter (SPOM) in Gulf of Mexico estuaries: Compound-specific isotope analysis and plant pigment compositions. *Organic Geochemistry* 24:875-888
- Raven JA, Falkowski PG (1999) Oceanic sinks for atmospheric CO₂. *Plant Cell and Environment* 22:741-755
- Reynolds SE, Mather RL, Wolff GA, Williams RG, Landolfi A, Sanders R, Woodward EMS (2007) How widespread and important is N₂ fixation in the north Atlantic ocean? *Global Biogeochemical Cycles* 21
- Rodriguez J, Mullin MM (1986) Diel and Interannual Variation of Size Distribution of Oceanic Zooplanktonic Biomass. *Ecology* 67:215-222
- Roman MR, Adolf HA, Landry MR, Madin LP, Steinberg DK, Zhang X (2002) Estimates of oceanic mesozooplankton production: a comparison using the Bermuda and Hawaii time-series data. *Deep-Sea Research Part II-Topical Studies in Oceanography* 49:175-192
- Roman MR, Gauzens AL (1997) Copepod grazing in the equatorial Pacific. *Limnology and Oceanography* 42:623-634

- Ryther JH, Dunstan WM (1971) Nitrogen, Phosphorus, and Eutrophication in Coastal Marine Environment. *Science* 171:1008-&
- Sabine CL, Feely RA, Gruber N, Key RM, Lee K, Bullister JL, Wanninkhof R, Wong CS, Wallace DWR, Tilbrook B, Millero FJ, Peng TH, Kozyr A, Ono T, Rios AF (2004) The oceanic sink for anthropogenic CO₂. *Science* 305:367-371
- Saino T (1992) N-15 and C-13 Natural Abundance in Suspended Particulate Organic-Matter from a Kuroshio Warm-Core Ring. *Deep-Sea Research Part a-Oceanographic Research Papers* 39:S347-S362
- Saino T, Hattori A (1980) N-15 Natural Abundance in Oceanic Suspended Particulate Matter. *Nature* 283:752-754
- Saino T, Hattori A (1987) Geographical Variation of the Water Column Distribution of Suspended Particulate Organic Nitrogen and Its N-15 Natural Abundance in the Pacific and Its Marginal Seas. *Deep-Sea Research Part a-Oceanographic Research Papers* 34:807-827
- Sara G, Sara R (2007) Feeding habits and trophic levels of bluefin tuna *Thunnus thynnus* of different size classes in the Mediterranean Sea. *Journal of Applied Ichthyology* 23:122-127
- Sarmiento JL, Dunne J, Gnanadesikan A, Key RM, Matsumoto K, Slater R (2002) A new estimate of the CaCO₃ to organic carbon export ratio. *Global Biogeochemical Cycles* 16
- Sarnelle O (1999) Zooplankton effects on vertical particulate flux: Testable models and experimental results. *Limnology and Oceanography* 44:357-370
- Sarthou G, Baker AR, Blain S, Achterberg EP, Boye M, Bowie AR, Croot P, Laan P, de Baar HJW, Jickells TD, Worsfold PJ (2003) Atmospheric iron deposition and sea-surface dissolved iron concentrations in the eastern Atlantic Ocean. *Deep-Sea Research Part I-Oceanographic Research Papers* 50:1339-1352
- Sato M, Sasaki H, Fukuchi M (2002) Stable isotopic compositions of overwintering copepods in the arctic and subarctic waters and implications to the feeding history. *Journal of Marine Systems* 38:165-174

Schlitzer R (2008) Ocean Data View. <http://odv.awi.de>.

Schmidt K, Atkinson A, Stubing D, McClelland JW, Montoya JP, Voss M (2003) Trophic relationships among Southern Ocean copepods and krill: Some uses and limitations of a stable isotope approach. *Limnology and Oceanography* 48:277-289

Schneider B, Schlitzer R, Fischer G, Nothig EM (2003) Depth-dependent elemental compositions of particulate organic matter (POM) in the ocean. *Global Biogeochemical Cycles* 17

Schnetzer A, Steinberg DK (2002) Active transport of particulate organic carbon and nitrogen by vertically migrating zooplankton in the Sargasso Sea. *Marine Ecology-Progress Series* 234:71-84

Shepon A, Gildor H, Labrador LJ, Butler T, Ganzeveld LN, Lawrence MG (2007) Global reactive nitrogen deposition from lightning NO_x. *Journal of Geophysical Research-Atmospheres* 112

Sheridan CC, Steinberg DK, Kling GW (2002) The microbial and metazoan community associated with colonies of *Trichodesmium* spp.,: a quantitative survey. *Journal of Plankton Research* 24:913-922

Sigman DM, Altabet MA, McCorkle DC, Francois R, Fischer G (1999) The delta N-15 of nitrate in the Southern Ocean: Consumption of nitrate in surface waters. *Global Biogeochemical Cycles* 13:1149-1166

Sigman DM, Altabet MA, Michener R, McCorkle DC, Fry B, Holmes RM (1997) Natural abundance-level measurement of the nitrogen isotopic composition of oceanic nitrate: an adaptation of the ammonia diffusion method. *Marine Chemistry* 57:227-242

Silfer JA, Engel MH, Macko SA (1992) Kinetic fractionation of stable carbon and nitrogen isotopes during peptide-bond hydrolysis - Experimental evidence and geochemical implications. *Chemical Geology* 101:211-221

Slagstad D, Tande KS (2007) Structure and resilience of overwintering habitats of *Calanus finmarchicus* in the Eastern Norwegian Sea. *Deep-Sea Research Part II-Topical Studies in Oceanography* 54:2702-2715

- Small LF, Ellis SG (1992) Fecal carbon production by zooplankton in Santa-Monica basin - the effects of body size and carnivorous feeding. *Progress in Oceanography* 30:197-221
- Small LF, Fowler SW, Moore SA, Larosa J (1983) Dissolved and Fecal Pellet Carbon and Nitrogen Release by Zooplankton in Tropical Waters. *Deep-Sea Research Part a-Oceanographic Research Papers* 30:1199-1220
- Small LF, Knauer GA, Tuel MD (1987) The Role of Sinking Fecal Pellets in Stratified Euphotic Zones. *Deep-Sea Research Part a-Oceanographic Research Papers* 34:1705-1712
- Smith SL, Henrichs SM, Rho T (2002) Stable C and N isotopic composition of sinking particles and zooplankton over the southeastern Bering Sea shelf. *Deep-Sea Research Part Ii-Topical Studies in Oceanography* 49:6031-6050
- Sommer F, Hansen T, Sommer U (2006) Transfer of diazotrophic nitrogen to mesozooplankton in Kiel Fjord, Western Baltic Sea: a mesocosm study. *Marine Ecology-Progress Series* 324:105-112
- Steinberg DK, Carlson CA, Bates NR, Goldthwait SA, Madin LP, Michaels AF (2000) Zooplankton vertical migration and the active transport of dissolved organic and inorganic carbon in the Sargasso Sea. *Deep-Sea Research Part I-Oceanographic Research Papers* 47:137-158
- Steinberg DK, Carlson CA, Bates NR, Johnson RJ, Michaels AF, Knap AH (2001) Overview of the US JGOFS Bermuda Atlantic Time-series Study (BATS): a decade-scale look at ocean biology and biogeochemistry. *Deep-Sea Research Part Ii-Topical Studies in Oceanography* 48:1405-1447
- Steinberg DK, Cope JS, Wilson SE, Kobari T (2008) A comparison of mesopelagic mesozooplankton community structure in the subtropical and subarctic North Pacific Ocean. *Deep-Sea Research Part Ii-Topical Studies in Oceanography* 55:1615-1635
- Steinberg DK, Goldthwait SA, Hansell DA (2002) Zooplankton vertical migration and the active transport of dissolved organic and inorganic nitrogen in the Sargasso Sea. *Deep-Sea Research Part I-Oceanographic Research Papers* 49:1445-1461

- Stubing D, Hagen W (2003) Fatty acid biomarker ratios - suitable trophic indicators in Antarctic euphausiids? *Polar Biology* 26:774-782
- Subramaniam A, Brown CW, Hood RR, Carpenter EJ, Capone DG (2002) Detecting *Trichodesmium* blooms in SeaWiFS imagery. *Deep-Sea Research Part II-Topical Studies in Oceanography* 49:107-121
- Subramaniam A, Yager PL, Carpenter EJ, Mahaffey C, Bjorkman K, Cooley S, Kustka AB, Montoya JP, Sanudo-Wilhelmy SA, Shipe R, Capone DG (2008) Amazon River enhances diazotrophy and carbon sequestration in the tropical North Atlantic Ocean. *Proceedings of the National Academy of Sciences of the United States of America* 105:10460-10465
- Sun MY, Zou L, Dai JH, Ding HB, Culp RA, Scranton MI (2004) Molecular carbon isotopic fractionation of algal lipids during decomposition in natural oxic and anoxic seawaters. *Organic Geochemistry* 35:895-908
- Suzuki H, Sasaki H, Fukuchi M (2003) Loss processes of sinking fecal pellets of zooplankton in the mesopelagic layers of the antarctic marginal ice zone. *Journal of Oceanography* 59:809-818
- Takahashi T, Feely RA, Weiss RF, Wanninkhof RH, Chipman DW, Sutherland SC, Takahashi TT (1997) Global air-sea flux of CO₂: An estimate based on measurements of sea-air pCO₂ difference. *Proceedings of the National Academy of Sciences of the United States of America* 94:8292-8299
- Tameler T, Soreide JE, Hop H, Carroll ML (2006) Fractionation of stable isotopes in the Arctic marine copepod *Calanus glacialis*: Effects on the isotopic composition of marine particulate organic matter. *Journal of Experimental Marine Biology and Ecology* 333:231-240
- Thor P, Dam HG, Rogers DR (2003) Fate of organic carbon released from decomposing copepod fecal pellets in relation to bacterial production and ectoenzymatic activity. *Aquatic Microbial Ecology* 33:279-288
- Turner JT (1987) Zooplankton Feeding Ecology - Contents of Fecal Pellets of the Copepod *Centropages-velificatus* from Waters near the Mouth of the Mississippi River. *Biological Bulletin* 173:377-386

- Turner JT (2002) Zooplankton fecal pellets, marine snow and sinking phytoplankton blooms. *Aquatic Microbial Ecology* 27:57-102
- Urrere MA, Knauer GA (1981) Zooplankton fecal pellet fluxes and vertical transport of particulate organic material in the pelagic environment. *Journal of Plankton Research* 3:369-387
- Vitousek PM, Cassman K, Cleveland C, Crews T, Field CB, Grimm NB, Howarth RW, Marino R, Martinelli L, Rastetter EB, Sprent JI (2002a) Towards an ecological understanding of biological nitrogen fixation. *Biogeochemistry* 57:1-45
- Vitousek PM, Hattenschwiler S, Olander L, Allison S (2002b) Nitrogen and nature. *Ambio* 11:97-101
- Voss M (1991) Content of Copepod Fecal Pellets in Relation to Food-Supply in Kiel-Bight and Its Effect on Sedimentation-Rate. *Marine Ecology-Progress Series* 75:217-225
- Voss M, Altabet MA, vonBodungen B (1996) $\delta^{15}\text{N}$ in sedimenting particles as indicator of euphotic-zone processes. *Deep-Sea Research Part I-Oceanographic Research Papers* 43:33-47
- Voss M, Dippner JW, Montoya JP (2001) Nitrogen isotope patterns in the oxygen-deficient waters of the Eastern Tropical North Pacific Ocean. *Deep-Sea Research Part I-Oceanographic Research Papers* 48:1905-1921
- Wada E (1980) Nitrogen isotope fractionation and its significance in biogeochemical processes occurring in marine environments. In: Goldberg ED, Horibe Y, Saruhashi K (eds) *Isotope Marine Chemistry*. Uchida Rokakuho, Tokyo, p 375-398
- Wada E, Hattori A (1976) Natural Abundance of N-15 in Particulate Organic-Matter in North Pacific Ocean. *Geochimica Et Cosmochimica Acta* 40:249-251
- Wada E, Terazaki M, Kabaya Y, Nemoto T (1987) N-15 and C-13 Abundances in the Antarctic Ocean with Emphasis on the Biogeochemical Structure of the Food Web. *Deep-Sea Research Part a-Oceanographic Research Papers* 34:829-841

- Wakeham SG (1995) Lipid biomarkers for heterotrophic alteration of suspended particulate organic matter in oxygenated and anoxic water columns of the ocean. *Deep-Sea Research Part I-Oceanographic Research Papers* 42:1749-1771
- Wakeham SG, Lee C, Hedges JJ, Hernes PJ, Peterson ML (1997) Molecular indicators of diagenetic status in marine organic matter. *Geochimica Et Cosmochimica Acta* 61:5363-5369
- Wakeham SG, Peterson ML, Hedges JJ, Lee C (2002) Lipid biomarker fluxes in the Arabian Sea, with a comparison to the equatorial Pacific Ocean. *Deep-Sea Research Part II-Topical Studies in Oceanography* 49:2265-2301
- Waser NA, Harrison WG, Head EJJ, Nielson B, Lutz VA, Calvert SE (2000) Geographic variations in the nitrogen isotope composition of surface particulate nitrogen and new production across the North Atlantic Ocean. *Deep-Sea Research Part I-Oceanographic Research Papers* 47:1207-1226
- Wassmann P, Ypma JE, Tselepides A (2000) Vertical flux of faecal pellets and microplankton on the shelf of the oligotrophic Cretan Sea (NE Mediterranean Sea). *Progress in Oceanography* 46:241-258
- Wefer G, Fischer G (1993) Seasonal Patterns of Vertical Particle-Flux in Equatorial and Coastal Upwelling Areas of the Eastern Atlantic. *Deep-Sea Research Part I-Oceanographic Research Papers* 40:1613-1645
- Werner I (2000) Faecal pellet production by Arctic under-ice amphipods - transfer of organic matter through the ice/water interface. *Hydrobiologia* 426:89-96
- West JB, Bowen GJ, Cerling TE, Ehleringer JR (2006) Stable isotopes as one of nature's ecological recorders. *Trends in Ecology & Evolution* 21:408-414
- Westberry TK, Siegel DA (2006) Spatial and temporal distribution of *Trichodesmium* blooms in the world's oceans. *Global Biogeochemical Cycles* 20
- Westberry TK, Siegel DA, Subramaniam A (2005) An improved bio-optical model for the remote sensing of *Trichodesmium* spp. blooms. *Journal of Geophysical Research-Oceans* 110
- Wotton RS, Malmqvist B (2001) Feces in aquatic ecosystems. *Bioscience* 51:537-544

- Wu JP, Calvert SE, Wong CS (1997) Nitrogen isotope variations in the subarctic northeast Pacific: Relationships to nitrate utilization and trophic structure. *Deep-Sea Research Part I-Oceanographic Research Papers* 44:287-314
- Wu JP, Calvert SE, Wong CS (1999a) Carbon and nitrogen isotope ratios in sedimenting particulate organic matter at an upwelling site off Vancouver Island. *Estuarine Coastal and Shelf Science* 48:193-203
- Wu JP, Calvert SE, Wong CS, Whitney FA (1999b) Carbon and nitrogen isotopic composition of sedimenting particulate material at Station Papa in the subarctic northeast Pacific. *Deep-Sea Research Part II-Topical Studies in Oceanography* 46:2793-2832
- Yool A, Martin AP, Fernandez C, Clark DR (2007) The significance of nitrification for oceanic new production. *Nature* 447:999-1002
- Zaret TM, Suffern JS (1976) Vertical Migration in Zooplankton as a Predator Avoidance Mechanism. *Limnology and Oceanography* 21:804-813
- Zehr JP, Carpenter EJ, Villareal TA (2000) New perspectives on nitrogen-fixing microorganisms in tropical and subtropical oceans. *Trends in Microbiology* 8:68-73
- Zehr JP, Montoya JP, Jenkins BD, Hewson I, Mondragon E, Short CM, Church MJ, Hansen A, Karl DM (2007) Experiments linking nitrogenase gene expression to nitrogen fixation in the North Pacific subtropical gyre. *Limnology and Oceanography* 52:169-183
- Zehr JP, Ward BB (2002) Nitrogen cycling in the ocean: New perspectives on processes and paradigms. *Applied and Environmental Microbiology* 68:1015-1024
- Zieman JC, Macko SA, Mills AL (1984) Role of seagrasses and mangroves in estuarine food webs - Temporal and spatial changes in stable isotope composition and amino-acid content during decomposition. *Bulletin of Marine Science* 35:380-392
- Zubkov MV, Tarran GA (2008) High bacterivory by the smallest phytoplankton in the North Atlantic Ocean. *Nature* 455:224-U248

VITA

Jason Paul Landrum, son of Paul Dudley and Karen (Johnson) Landrum was born in Gainesville, Florida on March 4, 1979. He graduated from Coral Gables High School in Coral Gables, Florida in 1997. He attended Cornell University in Ithaca, New York, and graduated with a Bachelor of Arts in Earth Sciences in 2001. After graduating from Cornell, he stayed on campus for another year, working as a research technician in an isotope geochemistry laboratory. He matriculated into the School of Biology graduate program at Georgia Institute of Technology as an NSF IGERT Fellow (Aquatic Chemical Signalling) in the Fall of 2002. Under the guidance of Dr. Joseph P. Montoya at Georgia Tech, he used multiple stable isotope techniques, in both lab- and field-based experiments, to study various aspects of the marine N cycle in oligotrophic environments, with specific interest in the movement of diazotroph nitrogen through oceanic food webs.